REGULATION OF CHROMOSOME REPLICATION AND SEGREGATION DURING *Bacillus subtilis* SPORULATION

A Dissertation

by

YI DUAN

Submitted to the Office of Graduate and Professional Studies of
Texas A&M University
in partial fulfillment of the requirements for the degree of

DOCTOR OF PHILOSOPHY

Chair of Committee,	Jennifer Herman
Committee Members,	Geoffrey Kapler
	Hays Rye
	Deborah A. Siegele
Head of Department,	Gregory D. Reinhart

December 2016

Major Subject: Biochemistry

ABSTRACT

Bacteria precisely coordinate DNA replication and chromosome segregation with cell division; accurate regulation of each of these processes is critical to genome inheritance and thus reproductive success. During fast growth, *Bacillus subtilis* carries out multi-fork replication and maintains multiple partial copies of the genome. However, during the developmental process of sporulation, *B. subtilis* shuts down DNA replication initiation and maintains only two copies of the chromosome. SirA (Sporulation inhibitor of replication A), is a protein produced only during sporulation that has been shown to inhibit new rounds of DNA replication by interacting directly with the initiator protein DnaA. Apart from inhibiting replication, I discovered that SirA acts in the same pathway as Soj to facilitate capture of the origin of segregation (*oriC*) in the forespore compartment during sporulation. I identified residues in both SirA and DnaA that are important for mediating the SirA-DnaA interaction and demonstrate that the two functions of SirA (replication inhibition and *oriC* segregation) are genetically separable. My data support the model that SirA interacts with DnaA Domain I to inhibit DNA replication initiation and with DnaA Domain III to promote *oriC* segregation.

ACKNOWLEDGEMENTS

I would like to start by thanking my family members, without their support and understanding, I would not obtain what I have. I want to say thanks to my parents, they raised me up and gave me numerous supports all the time. I particularly would like to say thank you to my wife, she is such a nice and sweet lady. We had to be separated right after our wedding, even with no time for the honeymoon. It was so hard for her to live alone in China as a new bride, but she never complained to me. Instead, she was always considerate and understood my situation, she tried very hard to make me laugh and happy every day. Without her support and consideration, I would not be where I am.

I also appreciate all the help and support from my committee members: Drs Geoffrey Kapler, Hays Rye and Deborah A. Siegele. Thanks for generously providing your time and expertise on guiding me to be a scientist.

I would also like to say thank you to all my friends in the Herman lab. Thank you for treating me as your family members for the past five years. Although my family was thousands of miles away from me, you made me feel less lonely and painful.

I want to say thanks to all members in the Gill lab, Straight lab, Young lab, Zeng lab and Zhang lab. Thank you for providing lots of useful feedback and support. I want to thank all other faculty and staff members in Bio/Bio department, especially Dr. Ayres, Dr. Bryk, Daisy and Rafael. All of you are very nice to me all the time, I really appreciate your effort on helping me doing a better job.

Thanks to all my American friends, especially Anthony and Emily. Thank you for your help on not only the scientific projects but also my life. Thank you for introducing me all the interesting things and helping me know more about American culture. I would like to specially thank Jack, who is not only my undergrad mentee, but

more like my younger brother. Thank you for being such a nice brother, it is my great honor to have you as my buddy.

I also want to say thanks to all my Chinese friends, especially Jinyong, Shuai, Tianhua and Yi Yang in the U.S. and Chang, Chuxiong, Jingbin, Longxiang, Ning, Panpan, Shuqin, Xi, Xin, Xudong and Zhu in China. I enjoyed all the unforgetful time we spent together and I really appreciate you being my friends, sharing my happiness and sorrow.

Finally, I would say thank you to my mentor, Dr. Jennifer Herman. Thank you for introducing me to the fantastic Genetics world and training me to be a geneticist. Thank you for teaching me how to do science and sharing all the life stories. Your love of basic science and critical thinking has been a tremendous influence on me. Thank you for being a great mentor not only in science but also in life.

CONTRIBUTORS AND FUNDING SOURCES

Contributors

The work in this dissertation was supervised and guided by a dissertation committee consisting of Dr. Jennifer Herman [Graduate Advisor and Chair of Committee], Dr. Geoffrey Kapler [Committee Member] and Dr Hays Rye [Committee Member] from the Department of Biochemistry and Biophysics, and Dr. Deborah A. Siegele [Committee Member] from the Department of Biology.

Assays for Chapter II were performed in part by Jack D. Huey of the Department of Biochemistry and Biophysics and were published in 2016. Experiments for Appendix I were conducted in part by Anthony M. Sperber of the Department of Biochemistry and Biophysics and were published in 2016. Strains for Appendix I, IV and V were made in part by Anthony M. Sperber of the Department of Biochemistry and Biophysics. All other work for this dissertation was completed by the student independently.

Funding Sources

The work in this dissertation was funded by the Start-up funding of Dr. Jennifer Herman from the Department of Biochemistry and Biophysics, with the funding number 02-248312. The authors are responsible for the contents in this dissertation. Information in this dissertation does not necessarily represent the official views of the Department of Biochemistry and Biophysics.

TABLE OF CONTENTS

Page

LIST OF FIGURES

FIGURE Page

LIST OF TABLES

CHAPTER I

INTRODUCTION

In both prokaryotes and eukaryotes, successful reproduction requires precise regulation of DNA replication and chromosome segregation. Under conditions of rapid division, many bacteria, including *Bacillus subtilis* and *Escherichia coli*, are unable to finish a complete round of chromosome replication before cell division occurs and therefore must initiate a new round of DNA replication before the first round is complete. This form of growth is very different from eukaryotes, in which chromosome replication and segregation occur in a different phase of the cell cycle than cytokinesis. Bacteria tightly coordinate chromosome segregation with cell division, segregating newly synthesized origins of replication (*oriCs*) toward cell poles (or future cell poles in rapidly growing cells undergoing multifork replication) shortly after initiation (1). The process of *oriC* segregation happens with very high fidelity, even in the absence of known chromosome organizing factors (2, 3). Failure to properly initiate replication or to properly segregate replicated chromosomes has numerous detrimental effect on the cell including abnormal cell growth (4), guillotining and breakage of chromosomes during cell division (5, 6), generation of anucleate cells (7), and cell death (8). Despite the critical nature of genome inheritance to viability, our understanding of the mechanisms underlying chromosome dynamics in bacteria remains incomplete. Fundamental questions related to how bacteria accurately regulate chromosome replication and segregation and, coordinate chromosome dynamics with other essential processes such as cell growth and cell division, remain outstanding. In this thesis, I address these fundamental questions utilizing the well-studied Gram positive bacterial model organism *B. subtilis*.

1.1 *Bacillus subtilis*

Bacillus subtilis is a rod-shaped, non-pathogenic bacterium, which belongs to the endospore-forming phylum Firmicutes. This phylum includes a number of important Gram positive pathogens and commensals, including *Staphylococcus*, *Clostridia*, and *Listeria*, as well as organisms important in food production, such as the *Lactobacillus*. *B. subtilis* is the most characterized Gram positive bacterium, and has served as a model organism for over fifty years. *B. subtilis* is also widely used in industry for the commercial production of enzymes and detergents (9). One of the most widely used *B. subtilis* strains in the laboratory is strain *B. subtilis* 168, a tryptophan auxotroph. The *B. subtilis* 168 strain was isolated by Paul Burkholder and Norman Giles, who used X-rays to mutagenize the Marburg strain (10). Another Marburg strain, NCIB3610, more closely resembles the original wild-type isolates and is more widely used in studies related to multicellular behavior, including biofilm and fruiting body formation, and swarming motility. In contrast, *B. subtilis* 168 is defective in these functions (11), and is thus considered a "domesticated" strain. In this study, we used both strain 168 and another closely related domesticated strain PY79, which has been cured of the conjugative transposon ICEBs1 (12) as well as a prophage called SPβ (13). Compared to the NCIB3610 strain, both *B. subtilis* 168 and PY79 are more competent and thus easier to manipulate genetically. In both of these organisms, the genome can be easily modified with insertions, deletions, and point mutations. *B. subtilis* 168 also has the richest repository of genome-level resources available for any Gram positive bacterium. These resources include a BioCyc database collection (BsubCyc), a barcoded, clean deletion library, and over 250 condition-dependent transcriptomic datasets (14).

1.2 Sporulation

Bacterial cell differentiation is a specialized cellular process that undergone by some bacteria to generate a new cell type that is phenotypically distinct from the parent cell. These changes can be morphological but may also only be physiological and result in the production of a daughter cell with distinct function or roles (15). *B. subtilis* sporulation is a paradigm system for studying cell differentiation in bacteria, including the coordination between gene expression and morphological change.

During vegetative growth, *B. subtilis* replicates DNA, grows, and divides actively, sometimes possessing cells with 2, 4, or even 8 partial copies of the genome (16). When *Bacillus* cells experience nutrient stress, they are capable of entering into a developmental process called sporulation that ultimately results in the production of a metabolically inert, heat and desiccation resistant cell type called a spore (17, 18).

During sporulation, the cell reduces its chromosome copy number to two, as each sporulating cell only needs two copies of the chromosome for spore formation (7). New rounds of DNA replication are prevented by production of a sporulation specific protein called SirA (7). The chromosomes undergoes a dramatic structural change and become stretched across the entire cell in an elongated structure called an axial filament that (19), with the origins of replication anchored to the cell poles (20). After axial filament formation, the sporulating cell forms a septum at one of the cell quarter positions, dividing the cell into a smaller compartment called the forespore and a larger compartment called the mother cell. At the time of polar septum formation, only one quarter of one copy of the chromosome is present in the forespore, creating an initial genetic asymmetry between the mother cell and forespore compartments. Successful spore production requires that *oriC* be located on the forespore side of septum (21). This

positioning somehow allows the remainder of the chromosome to be directionally pumped into the forespore by the FtsK-like DNA translocase, SpoIIIE (22, 23). At this point, the septal peptidoglycan is partially degraded and the membranes present on the mother cell side of the septum start to migrate around the forespore in a process called engulfment. The engulfment stage is completed when the engulfing membrane fuse. At this point, the forespore is bound by two sets of membranes (24). Over time, the peptidoglycan surrounding the forespore is thickened and modified (25), water inside the spore is replaced with dipocolonic acid (SP), and the spore is encapsulated by a protein-based spore coat (26). Eventually the mother cell lyses, releasing the mature endospore into the environment (Fig 1.1)(27-29).

B. subtilis sporulates in response to adverse environmental conditions, especially nutrient deprivation. The spore protects the genome until favorable growth conditions return. The process of spore formation is time-consuming, energy-expensive and becomes irreversible sometime after the completion of polar septum formation even if nutrients become available (30, 31). Therefore, successful sporulation provides *B. subtilis* with a distinct advantage during conditions of environmental stress.

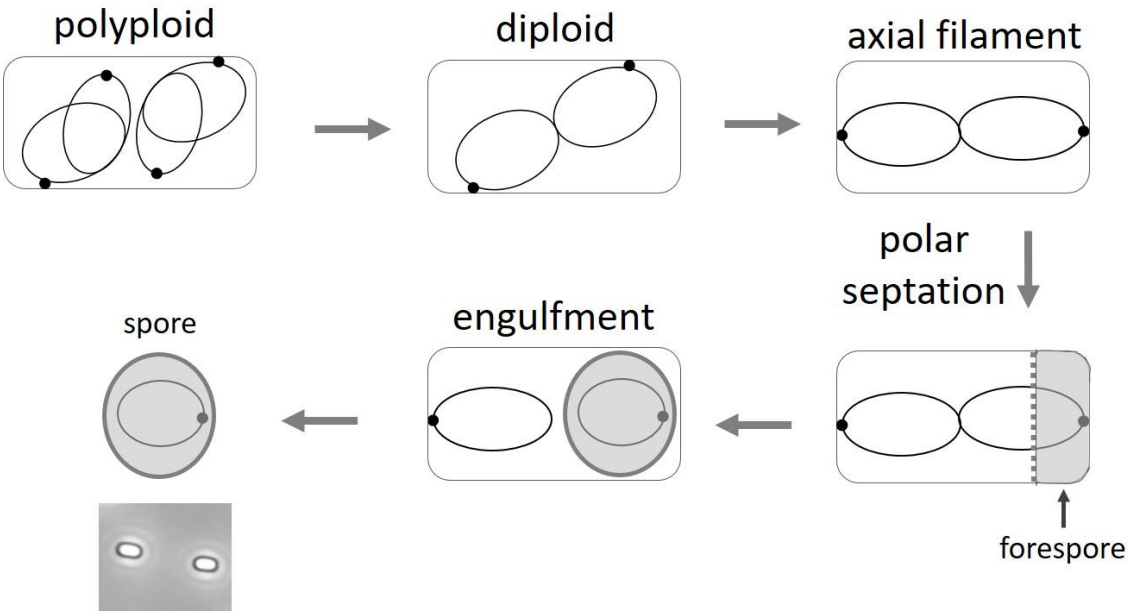

Fig. 1.1. *Bacillus subtilis* sporulation. During sporulation, *B. subtilis* reduces its chromosome copy number to two and stretches the chromosomes along the cell length in an elongated structure called the axial filament. Septation then occurs near one pole, initially capturing only a portion of one chromosome in the forespore compartment. The rest of this chromosome will be pumped into the forespore later by DNA translocase, SpoIIIE. The septum is then degraded, triggering the membrane migration around both sides of the forespore until fuses at the cell pole, releasing the forespore into the mother cell as a protoplast. Finally, peptidoglycan layers and spore coat are formed and when the spore is mature, it is released into the environment following mother cell lysis.

1.2.1 Spo0A

The master regulator of sporulation is a DNA-binding protein called Spo0A. Spo0A is expressed even during vegetative growth, but increases in copy number during stationary phase (32). When conditions become favorable for sporulation, Spo0A is converted into its active phosphorylated form, Spo0A-P (33, 34). Phosphorylation of Spo0A is highly regulated by a complex phosphorelay that integrates environmental signals with the developmental decision to sporulate (35). Spo0A-P can either activate or repress transcription by binding to the so-called *spo0A* box, which has the 7-bp consensus sequence, TGNCGAA (36). *spo0A* boxes are generally found in promoter regions recognized by the vegetative sigma factor σ^A and the stationary phase sigma factor σ^H (37-39). Accumulation of Spo0A-P is correlated with changes in gene expression for more than 500 genes (40), ~25% have been shown to be directly regulated by Spo0A-P binding; one-third of these are positively regulated by Spo0A-P, while the remainder are negatively regulated (36). Spo0A-P activates genes required for downregulation of DNA replication (7), anchoring of *oriC* at the distal cell poles (20) and redistribution of FtsZ from midcell toward the cell pole for polar septum formation (41-43), as well as other sporulation-specific processes (44). In addition to Spo0A-P, the stationary phase sigma factor σ^H is also required for sporulation initiation. σ^H regulates a number of phosphorelay genes including upregulation of *spo0A* itself (32). σ^H also regulates a number of other factors, some of which are important for the later steps of sporulation (45).

1.3 DNA replication

For both prokaryotes and eukaryotes, DNA replication is the basis for biological inheritance and therefore must be carefully regulated to ensure that daughter cells inherit complete copies of the genome (46). During replication, the double stranded DNA is melted. Each original single strand then serves as a template for the production of a new daughter strand, a process referred to as semiconservative replication (47). Cellular proofreading and error-checking mechanisms ensure near perfect fidelity for DNA replication (48). DNA replication, just like the other biological polymerization processes, also includes three steps, initiation, elongation and termination (49).

1.3.1 Replication initiation

In both prokaryotes and eukaryotes, chromosome replication starts at a site called the origin of replication (*oriC*). The origin site needs to be unwound before other components of the replication machinery can be assembled onto the DNA. In both prokaryotes and eukaryotes, initiator proteins are required for this melting process, which is proceeded by the loading of the rest of replisome components including helicase and DNA polymerase (46, 50).

1.3.1.1 Initiation in eukaryotes

Eukaryotic cells, which typically have much larger genomes than their prokaryotic counterparts, have multiple replication origins. To initiate DNA replication, multiple replicative proteins assemble on and then dissociate from these replicative

origins (50). DNA replication is tightly controlled in the context of the cell cycle (51-54). Activation of replication origins occurs as a two-step process during G1 phase (55). First, pre-replication complexes (pre-RC) are formed in a process called licensing. Then, when the appropriate cell cycle cues are received, initiation from pre-RCs begins (56). Tight regulation of assembly and dissociation of pre-RC complexes helps ensure that the initiation of DNA replication only occurs once per cell cycle, and only from designated origins (57-59).

In order to form pre-RC, multiple proteins and/or protein complexes need to be assembled orderly, such as ORC (origin recognition complex), Cdc6 (cell division cycle 6), Cdt1 (chromatin licensing and DNA replication factor 1) and Mcm (minichromosome maintenance proteins)(60). CDK (cyclin-dependent kinase) and DDK (Dbf4-dependent kinase), which phosphorylate the Cdc6 and the Mcm proteins respectively, then activate the pre-RC (52). Phosophorylation leads to the release of Cdc6 and the subsequent formation of the initiation complex, for instance, the interaction between Mcm and Cdc45 (cell division cycle 45)(61). Once formed, the initiation complex leads to the ordered loading of other initiation factors that unwind the DNA and promote the recruitment of DNA polymerases (Fig 1.2)(50).

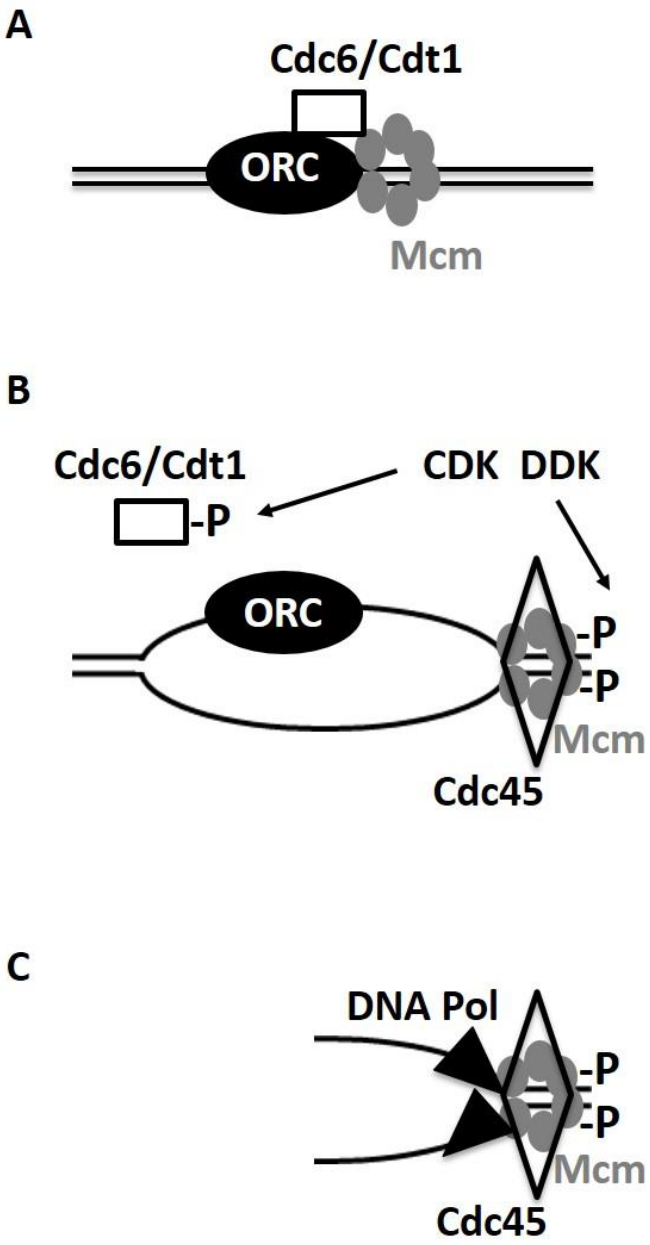

Fig. 1.2. Chromosome replication initiation in budding yeast. (A) Formation of the pre-RC. (B) CDK/DDK-dependent pre-RC activation and origin unwinding. (C) DNA polymerase loading and replication initiating. See text for details.

1.3.1.2 Initiation in prokaryotes

In prokaryotes, chromosomes are generally circular and the origin of replication on the chromosome is called *oriC*. *oriC* is typically AT rich and the length of *oriC* is around 250 base pairs (62). The *oriC* region also possesses multiple sites containing 9-bp motifs called *dnaA* boxes with the consensus sequence 5′-TTATNCACA-3’ (63), which are bound by the initiator protein DnaA (64). During replication initiation, DnaA binds to and oligomerizes at *oriC*, generating conformational changes that result in local unwinding of the AT-rich DNA unwinding element (DUE) followed by assembly of other replication machinery components (63, 65).

In *E. coli*, DUE unwinding is proceeded by recruitment of the helicase loader, DnaC, and loading of the helicase DnaB (66, 67). Helicase loading is followed by the sequential assembly of DnaG primase and the DNA polymerase III holoenzyme on single stranded DNA (68-70).

In *B. subtilis* and other low GC content Gram positive bacteria, different naming conventions are used, and loading of the replicative helicase (DnaC in *B. subtilis*), requires three additional proteins, DnaD, DnaB and DnaI (71). After DnaA binds to *oriC*, DnaD is recruited, followed by the membrane-associated protein DnaB (72). DnaI, also a AAA+ ATPase, then mediates DnaC loading onto the DNA (73). Primase and DNA polymerase are then recruited, leading to the initiation of DNA replication (Fig 1.3).

1.3.1.2.1 DnaA, the bacterial initiator

The initiation protein DnaA is highly conserved in bacteria and has four functional and structural domains (74). The N-terminal domain, Domain I, is known to be important for DnaA self-dimerization and helicase loading, as well as recruitment of other proteins required for initiation (75, 76). Domain I is also critical for interacting with other replication regulators such as DiaA in *E. coli* and SirA in *B. subtilis* (regulators are discussed more below)(77-81). The self-dimerization of DnaA Domain I is necessary for initiating DNA replication because it is essential for the cooperative binding of DnaA at *oriC* that leads to melting of the origin region (82, 83). Domain II is poorly conserved and flexible (84). Domain III carries the AAA+ ATPase motif for ATP binding/hydrolysis and oligomerization of DnaA when it is bound to ATP (74, 85). The C-terminal domain, Domain IV, possesses the helix-turn-helix motif responsible for binding to DNA (Fig 1.4)(65, 74).

In addition to DnaA Domain IV, which harbors the helix-turn-helix motif responsible for direct interaction with DNA, Domain III is also important for DNA binding. In the DNA-free DnaA crystal structure, the orientations of Domain III and Domain IV exhibit a steric clash with DNA when the DNA molecule is modeled into the structure. Therefore, it has been proposed that in the DNA-bound form, DnaA Domain III and Domain IV must exist in a different conformation (65, 86). In its DNA-free form, DnaA Domain IV is only loosely tethered to Domain III, thus it has been suggested that flexibility in this region is important for assembly of the DnaA oligomer on DNA (86).

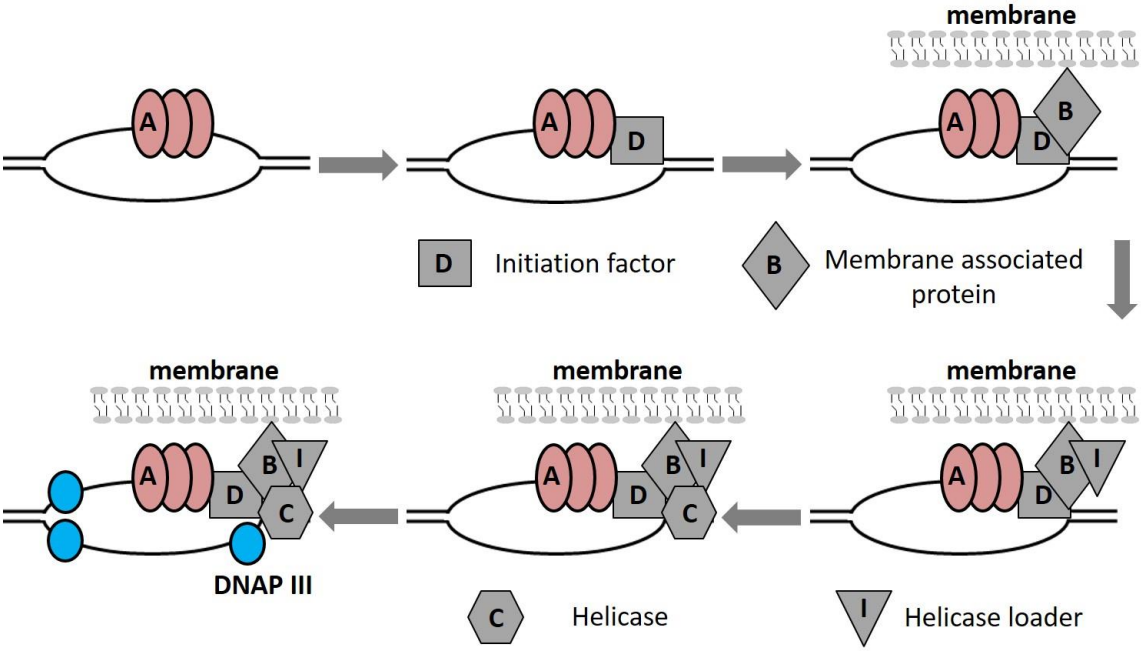

Fig. 1.3. DNA replication initiation in *B. subtilis*. During replication initiation, the initiator protein DnaA binds to *oriC*, forms an oligomer and unwinds the DUE element. For simplicity, the cartoon depicts DnaA on only one strand of DNA. DnaD then binds to DnaA, and is recruited to DnaB at the cytoplasmic membrane. This step is followed by recruitment of the helicase loader (DnaI), helicase (DnaC), primase (not shown) and DNA polymerase III.

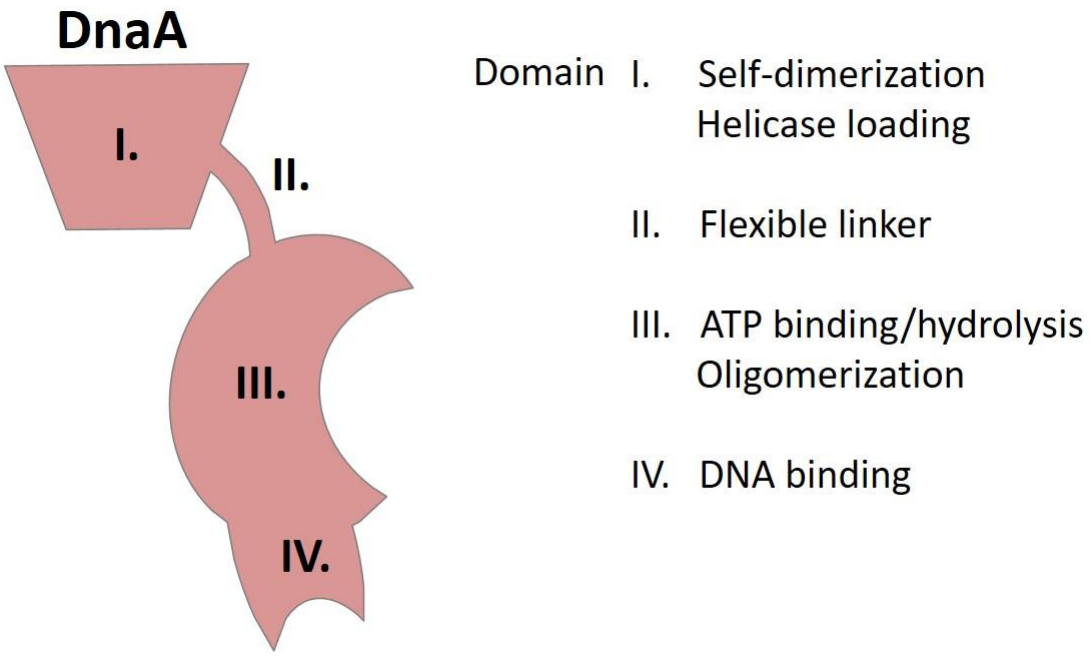

Fig. 1.4. Cartoon representation of DnaA's elongated four domain structure. Domain I is N-terminal while Domain IV is C-terminal.

In bacterial cells, DnaA has two different nucleotide-bound forms: ADP bound DnaA (ADP-DnaA) and ATP bound DnaA (ATP-DnaA). However, only ATP-DnaA is capable of initiating DNA replication (46, 68, 87). During replication, ATP-DnaA binds cooperatively to *dnaA* boxes at *oriC* and forms an ATP-DnaA-*oriC* complex (74, 88). For duplex opening at the AT-rich DNA unwinding element (DUE), enhanced supercoiling is required by DnaA oligomer to bind to DNA (64), which causes a ~28° kink of the local DNA at multiple sites (65), thus promoting unwinding of DUE (63).

In addition to its primary role in replication initiation, DnaA also binds to additional sites around the chromosome, some far distal to *oriC* (89). Many of these secondary sites are in promoter regions, consistent with studies demonstrating that in addition to its role in DNA replication initiation, DnaA can also function as a transcription factor (90, 91). DnaA regulates the transcription of several genes (including its own) by acting as both an activator and a repressor (89-95). DnaA's function as a transcription factor is more active when replication stress is induced by DNA damage, the inhibition of DNA replication elongation, or the inactivation of other replication initiation proteins (89, 91).

1.3.1.2.2 Regulation of initiation

DNA replication is carefully regulated to ensure both daughter cells inherit a copy of the genome. Tight regulation of DNA replication initiation not only determines the overall frequency of DNA synthesis, but also helps to ensure that DNA replication is properly timed during the cell cycle (46, 96). In most bacteria, DNA replication initiation is largely regulated by controlling both the availability and activity of the replication initiation protein DnaA (46, 88, 97).

In *E. coli*, there are at least four regulatory systems to regulate DNA replication initiation (98). *E. coli* methylates DNA at adenine residues at the motif GATC through the activity of the enzyme DNA adenine methylase (Dam)(99). GATC motifs are enriched in the origin-proximal region of the chromosome, and there are eleven GATC sites around the *oriC* region, including one in the promoter region of *dnaA* (100). The newly synthesized DNA strand is unmethylated, thus after initiation, the new *oriC* region is temporarily hemimethylated. The membrane-associated protein SeqA preferentially binds to hemimethylated GATC sites, and temporarily sequesters them from ATP-DnaA binding, thus delaying replication initiation (101-103). Once the strand becomes methylated again, ATP-DnaA can once again compete for binding, thus promoting replication initiation (104, 105). In this way, SeqA and Dam prevent the immediate re-initiation of replication (106, 107). SeqA binding in the *dnaA* promoter region also acts to repress *dnaA* expression further contributing to the delay in initiation (100).

Two additional systems negatively regulate DnaA activity by stimulating ATP hydrolysis of ATP-DnaA (98). The first system is called regulatory inactivation of DnaA (RIDA). RIDA prevents immediate re-initiation by promoting ATP (bound to DnaA) hydrolysis after initiation, yielding ADP-DnaA (108, 109). RIDA activity is dependent on the sliding clamp subunit of DNA polymerase III and an associated protein called Hda (98). Hda possesses a AAA+ ATPase domain and is bound to the clamp in its ADP-bound form (109, 110). Recent studies suggest that Hda-clamp complex interacts with DNA-bound DnaA at Domain I and that the AAA+ ATPase domain of Hda interacts with DnaA Domain III (111-113). The RIDA system is conserved in other Gram negative bacteria as well. In *Caulobacter crescentus*, the Hda ortholog HdaA, has been shown to colocalize with the sliding clamp and inhibit replication (114).

In addition to the RIDA system, the pool of ATP-DnaA available to bind *oriC* is also controlled by titration of ATP-DnaA at a chromosomal locus called *datA* (115-117). The *datA* locus, which resides near *oriC*, contains five *dnaA* boxes (118). Deletion of the *datA* sites does not cause re-initiation of replication, but does give asynchrony phenotype as rifampin-resistant replication initiation (118). In addition to titrating available ATP-DnaA, the *datA* locus contributes to ATP-DnaA hydrolysis in a manner that is still being investigated (119).

DnaA activity is also regulated by positive control mechanisms. The DARS (DnaA re-activating sequence) system has been described to reactivate initiation by stimulating DnaA binding to ATP (120). DARS is a 70-bp DNA fragment containing one *dnaA* box and two *dnaA* box-like sequences which have the opposite orientation as the *dnaA* box (120). In this system, ADP-DnaA binds to DARS and thereby causes disassociation of ADP from DnaA, makes DnaA free to re-associate with ATP (121). Another positive regulator in *E. coli* called DiaA, has been shown to stimulate the cooperative binding of ATP-DnaA on DNA (78, 122). DiaA forms a homotetramer and is able to bind to multiple DnaA molecules simultaneously. DiaA is hypothesized to stimulate conformational changes in DnaA molecule that allow assembly of the ATP-DnaA oligomer on DNA at *oriC* (80). Homologs of *E. coli* DiaA, have been described in several other Gram negative bacteria including *Caulobacter crescentus* and *Helicobacter pylori* (123-126).

Unlike *E. coli*, regulators of DnaA's nucleotide bound state have yet to be identified in *B. subtilis* or other Gram positives. It is possible that at least some of these regulators have yet to be identified. Another hypothesis is that intrinsic differences in the ADP-DnaA exchange rate in Gram positives (at least the ones that have been examined) makes additional factors unnecessary. This hypothesis is based on the observation that in

E. coli, the half-life of ADP-DnaA is ~40 min, whereas the half-life of ADP-DnaA in *B. subtilis* and several other Gram-positive bacteria is ~ 5 min (127). In rapidly growing *B. subtilis*, it is estimated that 90% of DnaA molecules are bound by ATP (85, 128). This high nucleotide exchange rate suggests that DnaA in *B. subtilis* is less likely to be regulated by ATP binding and hydrolysis.

Although sufficient ATP-DnaA levels are required for replication initiation, recent data suggests that increasing ATP-DnaA levels alone cannot account for origin firing and other cues are required (129). In *B. subtilis* and other Gram positive bacteria, other regulators have been described that control DnaA activity through nucleotide-independent mechanisms.

One of the best studied regulators of DnaA activity in *B. subtilis* is YabA. YabA was identified based on its ability to interact with both DnaA and the sliding clamp, DnaN (130). Overproduction of YabA causes decreased replication initiation and a *yabA* mutant overinitiates (131, 132). In vitro, purified YabA alters binding of ATP-DnaA to DNA by inhibiting the cooperativity of DnaA oligomerization, but does not affect either ATP binding or hydrolysis (133). In vivo, YabA associates with DnaA and decreases DnaA occupancy at *oriC* (127, 133). Another initiation protein DnaD, which is essential for helicase loading (72) and thus replication initiation. In vitro, DnaD, like YabA, has also been shown to interfere with the cooperative association of DnaA into its oligomer form, again without affecting ATP binding or hydrolysis (127).

Another protein found to be important in the regulation of DnaA activity in *B. subtilis* is called Soj (ParA). *soj* is located in an operon with the gene encoding DNA-binding protein Spo0J (ParB), which is involved in chromosome condensation in *B.subtilis* (134). ParAB proteins were originally described to be involved in plasmid partitioning (135); however, *parAB* operons are present in bacterial genomes throughout

the eubacteria (136) and have also been implicated in chromosome segregation in several bacteria (136-138).

Genetic and biochemical studies suggest that monomeric Soj acts as a negative regulator of DNA replication initiation, while dimeric Soj permits replication initiation (139-141). Scholefield et al. have shown that Spo0J promotes the conversion of dimeric Soj into monomeric Soj by stimulating Soj's ATPase activity (142). To inhibit replication, Soj interacts with Domain III (127). In vitro, similar to DnaD and YabA (143), Soj has been shown to inhibit DnaA oligomerization without affecting DnaA's ability to bind and hydrolyze ATP (127).

Spo0J and Soj act together to inhibit replication initation. How Spo0J itself is regulated remains an important outstanding question. One possibility is that Spo0J and Soj activity depend on a close association with *oriC* and that movement of Spo0J and/or Soj away from this site could allow enough ATP-DnaA oligomerization to promote loading of other replisome components, or at least DnaA-*oriC* membrane association. Intriguingly, Soj has been shown to interact with MinD at nascent cell division sites (144). Thus, the early steps in the assembly of the cell division complex could serve as a trigger to release the inhibitory hold on DnaA activity. Such a mechanism would also be an elegant way to coordinate the initation of DNA replication with cell division.

1.3.2 Replication elongation and termination

During replication, the origin region is unwound by helicase, a motor protein that is loaded on at the origin region and moves directionally to separate the double-stranded DNA to single-stranded DNA (145). Primase, a DNA-dependent RNA polymerase, next adds small RNA primers to both strands of the DNA template (146). High processivity

DNA polymerase (Pol III in bacteria, Pol δ and Pol ε in eukaryotes) then synthesizing the new daughter strand in the 5' to 3' direction away from the primer using the parent as template during the successive addition of nucleotides (147-149). Since only one primer is added to the leading strand but multiple primers are added to the lagging strand, the leading strand replicates continuously whereas the lagging strand is replicated discontinuously, thus creating Okazaki fragments (150, 151). The RNA primers are degraded and a low processivity DNA polymerase fills in the gaps left behind (152, 153). Finally, the nicks present following the gap-filling step are ligated by DNA ligase (154, 155).

DNA replication terminates when the replication fork is blocked. In order to terminate replication, a termination protein bound at its cognate binding site is required (156, 157). The termination protein is able to physically block the replication fork, and for both *E. coli* and *B. subtilis*, the region where this blockage takes place is called *ter* (158). In bacteria with circular chromosomes, replication initiates at the origin region and creates two replication forks that move bi-directionally. The two replication forks meet each other at *ter*, located on the opposite side of the chromosome as *oriC* (159, 160). In *E. coli*, termination occurs when a protein called Tus binds to termination sequences, preventing the faster replication fork from proceeding (161). This ensures that the slower replication fork reaches the stalled one in the termination region (162). In contrast, eukaryotes initiate replication at multiple sites along the length of a linear chromosome and therefore must also terminate at multiple sites (163, 164).

1.4 Chromosome segregation

For both prokaryotes and eukaryotes, proper chromosome segregation is critical for successful reproduction. After replication, the duplicated chromosomes need to be segregated away from each other and the site of cell division to ensure that each daughter cell will inherit a genome. Not surprisingly, chromosome segregation is a tightly regulated process (16, 165).

1.4.1 Chromosome segregation in eukaryotes

In the S phase of the cell cycle, the two identical sister chromatids (produced after DNA replication) are held together by highly conserved protein complexes called cohesins (166). Cohesins contains two SMCs (structural maintenance of chromosome) called Smc1 and Smc3, and a "kleisin" subunit called Scc1/Mcd1 (167). SMC proteins are found across all domains of life, from bacteria and archaea to yeast and higher eukaryotes (168-170). SMC proteins contain globular N and C-termini seperated by two coiled-coil domains bearing a central hinge domain (Fig 1.5A)(171). The N and C-termini interact with each other, causing the protein to fold over upon itself with a bend at the hinge region. Two subunits then associate at both the hinge region to form a wishbone-shaped structure (Fig 1.5B)(172). Scc1 (the kleisin subunit) interacts with both the C-terminus of Smc1 and the N-terminus of Smc3, acting as a bridge to connect Smc1 and Smc3, thus forming a ring-like structure capable of encircling multiple strands of double stranded DNA (Fig 1.5B)(167).

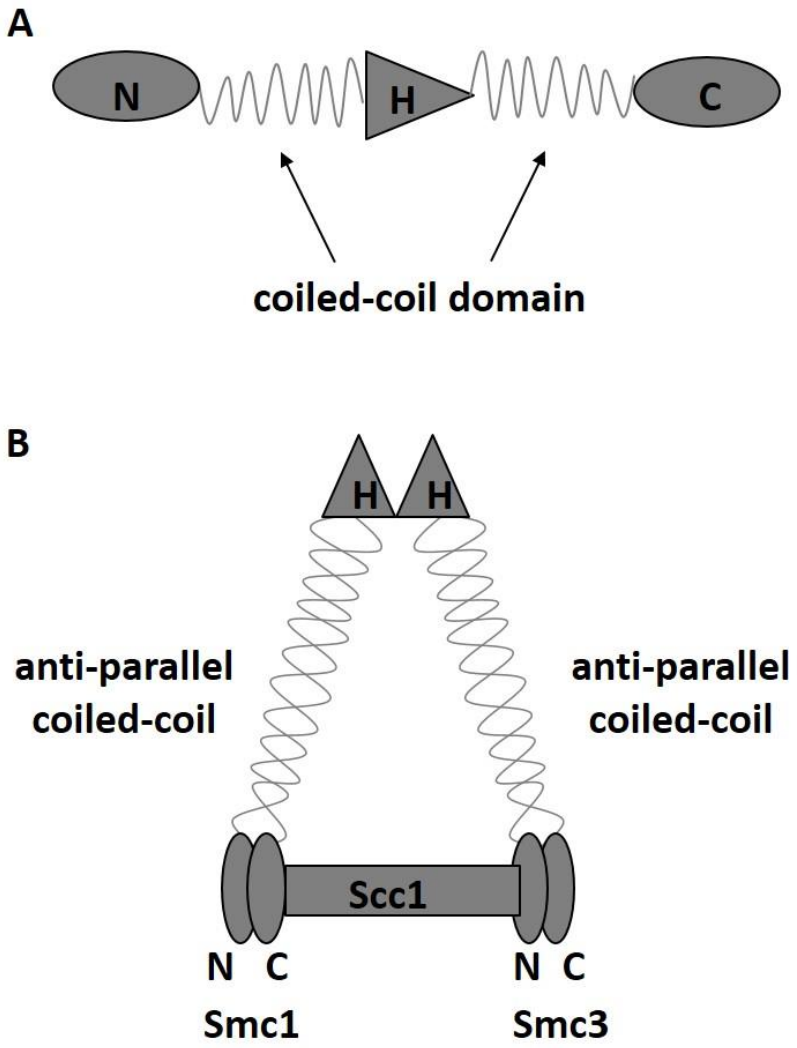

Fig. 1.5. Structure of SMC protein and the cohesin complex. (A) Domain structure of SMC proteins. SMC proteins contain a globular N-terminal domain, coiled-coil domain I, a hinge domain, coiled-coil domain II and a globular C-terminal domain. (B) Structure of the cohesin complex. The N and C-termini of SMC protein associate, causing the SMC protein to fold over on itself. The hinge regions of Smc1 and Smc3 interact with each other to create the SMC dimer. Scc1 interacts with the C-terminus of Smc1 and the N-terminus of Smc3 to form a ring-like structure.

In mitosis, microtubules attach to the kinetochore on the chromatids which are held together by cohesions (173). In budding yeast, each kinetochore only binds to a single microtubule (174). The kinetochore geometry and the error correction system ensure that the sister chromatids attach to microtubules from opposite poles (175, 176). Following attachment, the chromatids are then separated and finally segregate to the cell pole (165). The sister chromatids can then be segregated equally into each daughter cell (177). When all the chromosomes have properly attached to microtubules, the chromatids are ready to fall apart. The anaphase promoting complex, or cyclosome (APC/C)(178), targets the anaphase inhibitor securin for ubiquitnation and degradation by the 26S proteasome (179). Since securin binds to and inhibits the separase (180), this ubiquitination process actually releases the inhibition for separase. Separase is a cysteine protease that cleaves the Scc1 subunit of cohesin, allowing the cohesins to be released from the DNA (Fig 1.6)(181). Once seperated, the chromatids segregate to opposite cell poles (165).

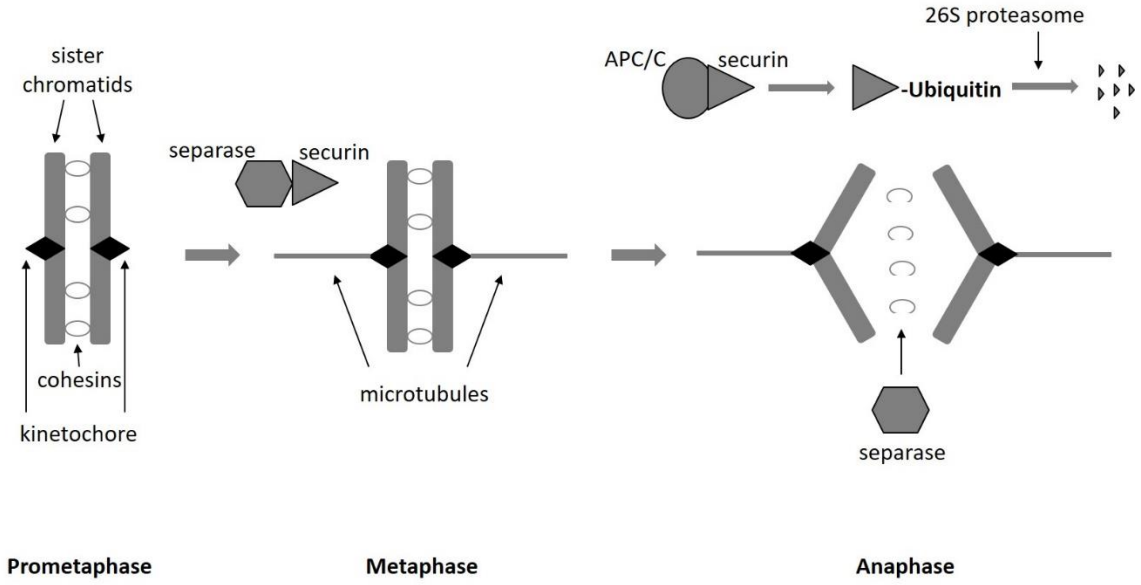

Fig. 1.6. Eukaryotic chromosome segregation during mitosis. In pro-metaphase, the sister chromatids are held together by cohesins. In metaphase, microtubules attach to the kinetochore, only stably associating when the kinteochores of sister chromatids are separately attached to microtubules emanating from opposite cell poles. Separase is still inactivated by securin. In anaphase, APC/C binds to securin, causing it to be ubiquinated and degraded by the 26S proteasome. This leaves separase free to cleave Scc1, releasing DNA held together by the SMC complex. The sister chromatids then separate and segregate to opposite cell poles.

1.4.2 Chromosome segregation in bacteria

Different from eukaryotes, bacteria lack microtubules and appear to rely heavily on chromosome compaction and *oriC* dynamics to help ensure chromosomes are properly segregated to future daughter cells. In all bacteria for which *oriC* dynamics have been examined, newly synthesized replication origins are segregated toward a cell pole (or future cell pole in cells with multi-fork replication) shortly after DNA replication initiation, even while the remainder of the chromosome is being replicated (1). In other words, DNA replication and chromosome segregation are concurrent (182, 183). Three systems, ParAB-*parS*, SMC complexes, and FtsK-like translocation, have been implicated in partitioning bacterial chromosomes to daughter cells (184, 185). The ParAB-*parS* and SMC proteins help ensure efficient *oriC* segregation, especially during conditions of rapid growth when cells have multiple partial copies of the chromosome (16, 186), while FtsK translocase acts preferentially at the terminus of the chromosome to segregate DNA away from the site of cytokinesis or septation.

1.4.2.1 Par proteins

The ParAB-*parS* system is conserved across the members of the eubacteria (136), although, it is notably absent from the model organism *E. coli*. In *B. subtilis*, the Par system is not essential during vegetative growth (139); however, both ParA and ParB play roles in *oriC* segregation during sporulation (see below)(187). In *Vibrio cholerae*, there are two chromosomes, chrI and chrII, each containing *par* loci. ChrII encoded Par system is important for its own segregation, while chrI encoded system is not required for chrI segregation, but instead, moves the origin from the cell pole toward

mid-cell (188). *Caulobacter crescentus* is the only known organism that requires a functional ParAB-*parS* chromosomal system for viability (189).

The *parS* sites on the chromosome were first identified in *B. subtilis* (190). There are eight *parS* sites located around the origin region with the consensus sequence 5′-TGTTNCACGTGAAACA-3′, each with an imperfect 8-bp inverted repeat (190). Chromosomal *parS* sites in other bacteria are very similar to the ones in *B. subtilis*, not only in sequence, but also in *oriC*-proximal location (191-195), strongly suggesting that this location is important for *parS* function. ParB binds to *parS* sites and forms a centromere-like nucleoprotein complex favorable for *oriC* segregation (139, 196), whereas ParA interacts with ParB to help *oriC* partition (197-199).

The exact mechanisms of how ParAB-*parS* system work in different bacteria are still largely unclear, and several sometimes conflicting models have been proposed. In *C. crescentus*, there are two major models describing possible mechanism for ParAB-*parS* dependent segregation of *oriC* (198, 199). The first model is called the “burnt-bridge Brownian ratchet model” (198). This model is partly based on the observation in vitro that ATP-ParA can oligomerize to form a spindle-like structure (198). In vivo, ParA bound to a fluorescent fusion appears to form oscillating clouds near the new cell that coalesce into an elongated structure by high resolution epifluorsecence microscopy. The authors of this study propose that ParB interacts with ParA, stimulating ParA’s ATPase activity and depolymerization. This depolymerization somehow causes ParA to “retract” and “pull” the ParB-*parS*-*oriC* complex towards the new cell pole (198). The other model is called the “DNA-relay model” (199). This model is based on the observation that the chromosome is elastic (200, 201). In this model, the newly synthesized *oriC* is bound by ParB. ParA, which is bound to DNA, can move with the same elasticity as the chromosome, but is constrained to the nucleoid surface and therefore the movement is

different from random diffusion (199). To reach its target at the opposite cell pole, ParB interacts with ParA and stimulates its ATPase activity. This causes ParA dimers to be released from the DNA, where they bind again following dimerization. The ParB-*oriC* complex is biased to move in the same direction as the ParA gradient due to interactions between ParB and ParA. What biases ParA to move toward the new pole is unclear in this model, although the gradient is observed experimentally (199). When the ParB-*parS*-*oriC* complex reaches the pole, it is anchored by a protein called PopZ, thus preventing its diffusion away (198).

In *B. subtilis*, ParA and ParB are more often referred to as Soj and Spo0J, respectively. Both Soj and Spo0J are non-essential, although a *spo0J* mutant produces a small number (1-2%) of anucleate cells (202). Instead of being required for chromosome segregation during vegetative growth (139), *B. subtilis* Soj regulates DNA replication initiation by interacting directly with DnaA (see section above, on regulation of initiation)(140, 143). ATP-Soj binds to DNA as a dimer, and this form permits DNA replication initiation (203). After initiation, Spo0J stimulates the ATPase activity of Soj causing a shift toward the monomer form (142). Monomeric Soj inhibits DnaA activity, by interacting with DnaA Domain III and disrupting DnaA oligomerization (143).

1.4.2.2 SMC complex

SMC proteins are conserved in both prokaryotes and eukaryotes (see text above for details on SMC structure). In bacteria, SMC proteins play important roles in chromosome compaction and segregation (204). In *B. subtilis*, *smc* null mutant is lethal for rapidly growing cells (in rich media at higher temperatures). Although cells are viable when growing at lower temperatures or in minimal media, approximately 10% of

the cells are anucleate, and most cells possess nucleoids of irregular morphology and origin localization (168, 204-206). Similarly, a *C. crescentus smc* mutant is nonviable in rich medium regardless of temperature, and can only grow at lower temperatures in minimal medium. Like *B. subtilis*, abnormal nucleoid morphology and origin localization defect has also been observed in the *C. crescentus smc* mutant; however, very few anucleate cells are produced (207). Instead of SMC, *E. coli* and some of its γ-proteobacterial relatives utilize a functionally equivalent, but evolutionarily distinct protein complex called MukBEF (5). In *E. coli*, *mukBEF* mutants are also temperature sensitive, producing 5% anucleate cells under permissive conditions (208, 209).

Under conditions of rapid growth, *B. subtilis* can possess more than 8 partial copies of the chromosome. Since *smc* null mutant possesses decondensed chromosome, one idea is that the lethality is related to the difficulty in disentangling and partitioning the large mass of chromosomal DNA (168, 210). Consistent with this hypothesis, viability can be restored under non-permissive conditions when cells possess mutations that slow DNA replication (210).

In *B. subtilis*, SMC is enriched around the *oriC* region and this association is mediated by interaction with the ParB-*parS* complex (134, 187). Similarly, in *E. coli*, MukB is shown to generally colocalize with *oriC* (211). Recent data suggest that *E. coli* MukBEF is also briefly associated with the *ter* site of the chromosome, suggesting that MukBEF might also play a role in segregation of the terminus region of the chromosome (212).

Although the mechanisms of how SMC/MukBEF precisely contribute to chromosome segregation remain elusive, there is no doubt that these complexes performs important roles in this process. Moreover, if both SMC and another segregation-important protein complex are impaired, the phenotypes are much more

severe. In *B. subtilis*, *smc parA* double mutant produced more anucleate cells compared to the single mutant (139), while *smc parB* mutant showed a severe *oriC* segregation defect (213). There is likely an intimate relationship between the initiation of replication, *oriC* segregation, and chromosome condensation, as SMC needs to be loaded shortly after new DNA is synthesized, and newly synthesized *oriC* needs to be segregated shortly after initiation; moreover, in *B. subtilis*, ParB regulates aspects of both DnaA replication (142) and apparently, SMC loading at *oriC* (134).

1.4.2.3 FtsK-like DNA translocases

Apart from the two systems mentioned above, the DNA translocase FtsK and its orthologs also play important roles in chromosome decantenation and partitioning in various bacterial species (214, 215). FtsK is not only required for chromosomal dimer resolution during Xer-*dif* recombination, but also for positioning the *dif* site to the cell division site where FtsK acts (214, 216). At midcell, FtsK facilitates the segregation of any chromosomal DNA located in the division plane toward the future daughter cell, thus preventing chromosome guillotining during cell division (217). In addition, FtsK is also present in such bacteria like *Streptomyces coelicolor* and *Borrelia*, which instead of having circular chromosomes, contain linear chromosomes and thus have no need for dimer resolution (218, 219).

B. subtilis possesses two FtsK-like translocases, SftA and SpoIIIE (220, 221). A double knockout of *sftA* and *spoIIIE* is viable, indicating that the genes perform functions that are not essential during normal vegetative growth (222). SpoIIIE was first identified because of its essential role during *B. subtilis* sporulation (6). During sporulation, when the polar septum is formed, initially only a quarter of one

chromosome is trapped into the forespore compartment, the other three quarters remain in the mother cell (see Sporulation, above). SpoIIIE is assembled around DNA transversing the septum (223, 224) and it is responsible for pumping the remainder of the forespore-destined chromosome into the forespore compartment using the energy produced by ATP hydrolysis (225). Burton et al. have shown that the two arms of the chromosome are pumped simultaneously (23), although the exact pumping mechanism remains unknown.

The SpoIIIE recognition site (SRS) is an 8-bp consensus sequence, 5′-GAGAAGGG-3′, and the orientation of this sequence is proposed to affect the directionally of DNA translocation (226). However, the chromosome is ultimately released into the cell compartment possessing *oriC*, and cells that fail to capture *oriC* in the forespore fail to generate spores (21).

1.5 Developmental regulation of DnaA activity and *oriC* segregation during *B. subtilis* sporulation

During *B. subtilis* sporulation, when the chromosome copy number is maintained at two, new rounds of DNA replication are at least partially prevented by SirA (sporulation inhibitor of replication A), another negatively regulator of DnaA (7, 227). *sirA* (formerly called *yneE*) is under the positive control of Spo0A-P and is expressed during the earliest stages of sporulation (36). SirA inhibits new rounds of DNA replication during sporulation by targeting DnaA activity (7, 81). Misexpression of SirA during vegetative growth prevents colony formation on plates and produced anucleate cells in liquid medium, phenocopying depletion of the initiator protein DnaA (7). SirA inhibits DNA replication in a DnaA-dependent manner, as SirA has no effect on the

strain which does not require DnaA to initiate replication (7). Genetic, cell biological, biochemical, and structural studies have shown that SirA targets DnaA Domain I directly to inhibit replication initiation (7, 79, 81).

In bacteria, DNA replication and chromosome segregation occur concurrently (182, 183). In *C. crescentus*, DnaA is able to bind to the centromere region and thereby segregates the chromosome (228). During *B. subtilis* sporulation, Sullivan et al. have shown that a *soj* mutant fails to segregate ~20% *oriC* into the forespore compartment (187). Since Soj is indicated to act as a negative regulator of DnaA activity (127), like SirA, all the above results suggest that SirA may also play an important role in *oriC* segregation during *B. subtilis* sporulation.

In this thesis, I address the mechanism by which SirA inhibits DnaA activity and report a second, genetically distinct function for SirA in ensuring proper *oriC* segregation during *B. subtilis* sporulation.

CHAPTER II

THE DnaA INHIBITOR SirA ACTS IN THE SAME PATHWAY AS Soj (ParA) TO FACILITATE *oriC* SEGREGATION DURING *Bacillus subtilis* SPORULATION*

2.1 Introduction

In all bacteria for which origin of replication (*oriC*) dynamics have been examined, newly synthesized replication origins are segregated toward a cell pole (or future cell pole in cells with multi-fork replication) shortly after DNA replication initiation (3, 16, 182, 183, 213, 229). *oriC* segregation happens with high fidelity and is aided by chromosome condensing and partitioning complexes that include MukBEF, SMC, and ParABS (186, 230). The MukBEF and SMC complexes include condensin proteins that compact the chromosome lengthwise (230), while ParA and ParB orthologs have been found to stabilize the partitioning of both low copy-number plasmids and bacterial chromosomes (137).

In *B. subtilis*, ParA and ParB are most often referred to as Soj and Spo0J, respectively. Spo0J binds to *parS* sites and forms a centromere-like nucleoprotein complex favorable for *oriC* segregation (139, 196). Spo0J-*parS* complexes are also important for SMC enrichment around the *oriC*-proximal region of the chromosome and cohesion of the chromosomal arms following their replication (134, 187, 231). A *spo0J* mutant exhibits a slight increase in the frequency of anucleate cells (202) and is important for *oriC* segregation in the absence of a functional SMC complex (213). Soj,

*Reprinted with permission from "The DnaA inhibitor SirA acts in the same pathway as Soj (ParA) to facilitate oriC segregation during Bacillus subtilis sporulation" by Duan, Y., Huey J.D. and Herman J.K., 2016. Molecular Microbiology, 102(3):530-544. Copyright 2016 by John Wiley & Sons, Inc.

which is encoded in the same operon as Spo0J, is not required for chromosome segregation during vegetative growth (139). Instead, Soj's described function is to regulate DNA replication by interacting directly with the bacterial DNA initiator protein DnaA (140, 143). During replication initiation, DnaA binds to and oligomerizes at *oriC*. Soj binds to DNA as an ATP-dependent dimer, and directly stimulates DnaA to activate DNA replication initiation (203). Following replication initiation, the monomeric form of Soj acts as an inhibitor of initiation by preventing DnaA oligomerization (143). Spo0J promotes Soj's ATPase activity, and thus also appears to function as a negative regulator of replication initiation in vivo (Fig. 2.1)(142).

DNA replication and *oriC* dynamics are also highly regulated during bacterial development. For example, during sporulation, *B. subtilis* reduces its chromosome copy number to two and stretches the chromosomes along the cell length in an *oriC-ter-ter-oriC* arrangement called the axial filament (19, 24). The number of chromosomes in sporulating cells is regulated by nutrient status, a checkpoint protein called Sda (92, 96), and by SirA, a protein expressed early in sporulation that directly targets DnaA activity (7). SirA ensures that new rounds of DNA replication are not initiated, thus preserving a diploidy state in the sporulating cell (7). Once the axial filament forms, septation occurs near one pole, initially capturing only a portion of one chromosome in the future spore (forespore) compartment (138, 187, 232). The remainder of the chromosome is eventually pumped into the forespore, but only if the chromosome's *oriC* region is captured on the forespore side of the polar septum (22). Therefore, the position of *oriC* at the time of polar septation is important for successful sporulation.

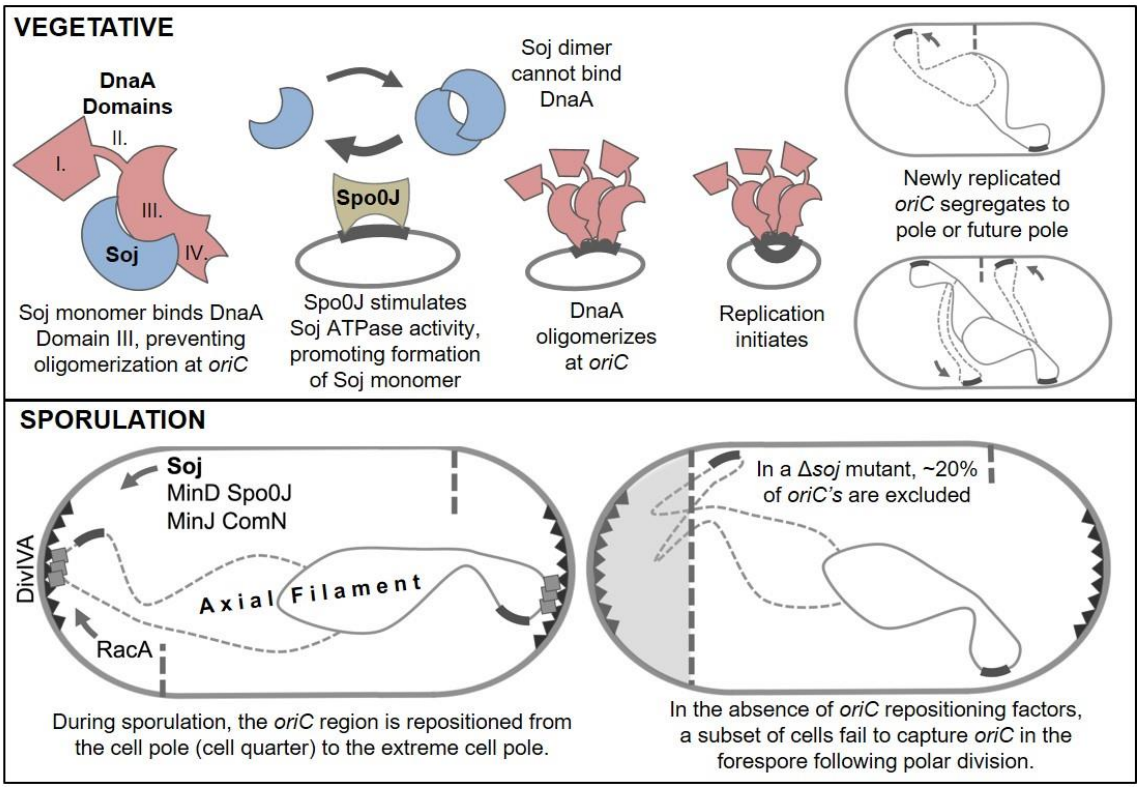

Fig. 2.1. Cartoon representation of chromosome segregation in *B. subtilis*. (Top) Following DNA replication initiation, newly synthesized *oriC*s are repositioned at cell quarters and future cell quarters. Spo0J stimulates formation of Soj monomers, delaying new rounds of DNA replication initiation until an unknown cell cycle cue is received. (Bottom) During sporulation, *oriC* is repositioned from the cell quarter toward the extreme cell pole in a manner that depends on DivIVA (black triangles), RacA (grey squares), MinD, ComN, MinJ, Spo0J, and Soj. In the absence of factors important for *oriC* repositioning during sporulation, a subset of cells fail to capture *oriC* in the forespore compartment following polar septation.

Several proteins have been implicated in *oriC* capture in the forespore (20, 138, 187). Spo0J condenses the *oriC*-proximal region into a centromere-like element favorable for chromosome segregation during both vegetative growth and sporulation (196). Another protein, RacA, contributes by tethering the *oriC*-proximal region to the distal cell pole via interactions with the polar organizing protein DivIVA (Fig 2.1)(20, 138, 233). The DnaA regulator Soj is also important, as a Δ*soj* mutant fails to capture *oriC* in ~20% of sporulating cells (Fig 2.1)(187). Genetic and cell biological data indicate that Soj's importance is amplified in the absence of a functional RacA tethering system, suggesting that these two systems contribute in independent ways (138); the precise role of Soj in *oriC* capture is unknown. Recently, Kloosterman et al. demonstrated that ComN, MinJ, and MinD, proteins that like RacA utilize DivIVA for localization (234-236), also act in the same pathway as Soj to facilitate *oriC* capture (Fig 2.1)(144). The authors propose that during sporulation, a complex of proteins that includes DivIVA, ComN, MinJ, and MinD relocalizes from the cell quarter to the extreme cell pole, and that this relocalization is important for Soj-dependent *oriC* capture (144).

Here we show that the sporulation protein SirA, which also regulates DnaA activity, is also required for high-fidelity *oriC* capture in the forespore (7, 79, 81, 227). More specifically we show that SirA and Soj act in the same pathway to segregate *oriC* in 10% of sporulating cells. Residues in the N-terminus of SirA interact directly with DnaA Domain I to inhibit replication (79), and SirA inhibits new rounds of DNA replication initiation during sporulation (7). Surprisingly, we found that SirA's ability to inhibit DNA replication is not required for its role in *oriC* capture, indicating that these functions are distinct and separable. Using SirA-DnaA gain of interaction screens, we identified additional residues near the C-terminus of SirA and in DnaA Domain III,

which are also important for mediating interaction between the two proteins. Moreover, we isolated one C-terminal substitution in SirA, P141T, which inhibits DNA replication, yet is unable to support SirA-dependent *oriC* capture. These unexpected results suggest that SirA may target two distinct domains of DnaA: Domain I, to inhibit DNA replication, and Domain III to facilitate Soj-dependent *oriC* segregation.

2.2 Materials and methods

2.2.1 General methods

All *B. subtilis* strains were derived from *B. subtilis* 168 or PY79. *E. coli* and *B. subtilis* strains utilized in this study are listed in Table 2.1. Plasmids are listed in Table 2.2. Oligonucleotide primers are listed in Table 2.3. All cloning was carried out in *E. coli* DH5α. *E. coli* strain DHP1 was used for assaying interaction in the B2H. Sporulation was induced by resuspension at 37°C according to the Sterlini-Mandelstam method (237). For microscopy experiments, all samples were grown in 25 ml CH (237) in 250 ml baffled flasks at 37°C in a shaking waterbath set at 280 rpm. For transformation of *E. coli*, antibiotics were included at the following concentrations when indicated: 100 µg/ml ampicillin, and 25 µg/ml kanamycin. For transformation and selection of *B. subtilis*, antibiotics, when required, were included at the following concentrations: 100 µg/ml spectinomycin, 7.5 µg/ml chloramphenicol, 0.8 µg/ml phleomycin, 10 µg/ml tetracycline, 10 µg/ml kanamycin and 1 µg/ml erythromycin with 25 µg/ml lincomycin.

Table 2.1. Strains used in Chapter II.

Strain	Description	Reference
Parental		
B. subtilis PY79	*Bacillus subtilis* laboratory strain	(238)
B. subtilis 168	*Bacillus subtilis* laboratory strain 168 *trpC2*	BGSC (1A866)
E. coli DH5α	*F- endA1 glnV44 thi-1 recA1 relA1 gyrA96 deoR nupG Φ80dlacZΔM15 Δ(lacZYA-argF)U169, hsdR17(r_K^- m_K^+), λ–*	
E. coli DHP1	*F-, cya-99, araD139, galE15, galK16, rpsL1 (Strr), hsdR2, mcrA1,mcrB1;*	Tom Bernhardt
***B. subtilis* PY79**		
BJH015	*spoIIIE36, yycR::*P_{spoIIQ}*-yfp (phleo), amyE::*P_{spoIIQ}*-cfp (cat), sirA::tet, yvbj::sirA (erm)*	This study
BJH090	*spoIIIE36, yycR::*P_{spoIIQ}*-yfp (phleo), amyE::*P_{spoIIQ}*-cfp (cat), sirA::tet*	This study
BJH103	*spoIIIE36, yycR::*P_{spoIIQ}*-yfp (phleo), amyE::*P_{spoIIQ}*-cfp (cat)*	This study
BKE25690	*sda::erm*	BGSC
BYD067	*spoIIIE36, yycR::*P_{spoIIQ}*-yfp (phleo), amyE::*P_{spoIIQ}*-cfp (cat), sirA::*$sirA_{Y51A}$	This study
BYD073	*spoIIIE36, yycR::*P_{spoIIQ}*-yfp (phleo), amyE::*P_{spoIIQ}*-cfp (cat), dnaA::*$dnaA_{F49Y}$	This study
BYD116	*spoIIIE36, yycR::*P_{spoIIQ}*-yfp (phleo), amyE::*P_{spoIIQ}*-cfp (cat), D(soj, spo0J)::spec, pelB::soj- spo0J+ (kan)*	This study
BYD117	*spoIIIE36, yycR::*P_{spoIIQ}*-yfp (phleo), amyE::*P_{spoIIQ}*-cfp (cat), sirA::tet D(soj, spo0J)::spec, pelB::soj- spo0J+ (kan)*	This study
BYD299	*spoIIIE36, yycR::*P_{spoIIQ}*-yfp (phleo), amyE::*P_{spoIIQ}*-cfp (cat), sirA::*$sirA_{P141T}$	This study
BYD302	*spoIIIE36, yycR::*P_{spoIIQ}*-yfp (phleo), amyE::*P_{spoIIQ}*-cfp (cat), sirA::*$sirA_{F14A}$	This study
BYD303	*spoIIIE36, yycR::*P_{spoIIQ}*-yfp (phleo), amyE::*P_{spoIIQ}*-cfp (cat), dnaA::*$dnaA_{A50V}$	This study
BYD306	*spoIIIE36, yycR::*P_{spoIIQ}*-yfp (phleo), amyE::*P_{spoIIQ}*-cfp (cat), sirA::*$sirA_{A111V}$	This study
BYD308	*spoIIIE36, yycR::*P_{spoIIQ}*-yfp (phleo), amyE::*P_{spoIIQ}*-cfp (cat), sirA::*$sirA_{E144A}$	This study

Table 2.1. Continued.

Strain	Description	Reference
BYD310	*spoIIIE36, yycR::*P$_{spoIIQ}$*-yfp (phleo), amyE::*P$_{spoIIQ}$*-cfp (cat), sirA::sirA*$_{S123C}$	This study
BYD470	*spoIIIE36, yycR::*P$_{spoIIQ}$*-yfp (phleo), amyE::*P$_{spoIIQ}$*-cfp (cat), D(soj, spo0J)::spec, pelB::soj- spo0J+ (kan), sda::erm*	This study
BYD471	*spoIIIE36, yycR::*P$_{spoIIQ}$*-yfp (phleo), amyE::*P$_{spoIIQ}$*-cfp (cat), D(soj, spo0J)::spec, pelB::soj- spo0J+ (kan), sirA::tet, sda::erm*	This study
BYD472	*spoIIIE36, yycR::*P$_{spoIIQ}$*-yfp (phleo), amyE::*P$_{spoIIQ}$*-cfp (cat), sirA::tet, sda::erm*	This study
BYD498	*spoIIIE36, yycR::*P$_{spoIIQ}$*-yfp (phleo), amyE::*P$_{spoIIQ}$*-cfp (cat), sirA::sirA*$_{T113M}$	This study
BYD499	*spoIIIE36, yycR::*P$_{spoIIQ}$*-yfp (phleo), amyE::*P$_{spoIIQ}$*-cfp (cat), sirA::sirA*$_{V118M}$	This study
BYD500	*spoIIIE36, yycR::*P$_{spoIIQ}$*-yfp (phleo), amyE::*P$_{spoIIQ}$*-cfp (cat), sirA::sirA*$_{K121N}$	This study
BYD533	*spoIIIE36, yycR::*P$_{spoIIQ}$*-yfp (phleo), amyE::*P$_{spoIIQ}$*-cfp (cat), sirA::sirA*$_{I103V}$	This study
***B. subtilis* 168**		
BAM075	*amyE::*P$_{hy}$ *(spec)*	This study
BYD036	*amyE::*P$_{hy}$*-sirA (spec)*	This study
BYD283	*amyE::*P$_{hy}$*-sirA*$_{P141T}$ *(spec)*	This study
BYD285	*amyE::*P$_{hy}$*-sirA*$_{Q30L}$ *(spec)*	This study
BYD286	*amyE::P*$_{hy}$*-sirA*$_{Q41H}$ *(spec)*	This study
BYD287	*amyE::P*$_{hy}$*-sirA*$_{L69F}$ *(spec)*	This study
BYD288	*amyE::P*$_{hy}$*-sirA*$_{A111V}$ *(spec)*	This study
BYD291	*amyE::P*$_{hy}$*-sirA*$_{I83K}$ *(spec)*	This study
BYD292	*amyE::P*$_{hy}$*-sirA*$_{E144A}$ *(spec)*	This study
BYD293	*amyE::P*$_{hy}$*-sirA*$_{R64P}$ *(spec)*	This study
BYD294	*amyE::P*$_{hy}$*-sirA*$_{F115Y}$ *(spec)*	This study
BYD295	*amyE::P*$_{hy}$*-sirA*$_{S123C}$ *(spec)*	This study
BYD296	*amyE::P*$_{hy}$*-sirA*$_{P124L}$ *(spec)*	This study
BYD297	*amyE::P*$_{hy}$*-sirA*$_{S106P}$ *(spec)*	This study
BYD298	*amyE::P*$_{hy}$*-sirA*$_{L28P}$ *(spec)*	This study
BYD462	*amyE::P*$_{hy}$*-sirA*$_{F14A}$ *(spec)*	This study
BYD463	*amyE::P*$_{hy}$*-sirA*$_{Y51A}$ *(spec)*	This study

Table 2.1. Continued.

Strain	Description	Reference
BYD464	*amyE::*P_{hy}*-sirA (spec), dnaA∴dnaA*$_{F49Y}$	This study
BYD465	*amyE::*P_{hy}*-sirA (spec), dnaA∴dnaA*$_{A50V}$	This study
BYD549	*amyE::*P_{hy}*-sirA*$_{I103V}$ *(spec)*	This study
BYD550	*amyE::*P_{hy}*-sirA*$_{T113M}$ *(spec)*	This study
BYD551	*amyE::*P_{hy}*-sirA*$_{V118M}$ *(spec)*	This study
BYD552	*amyE::*P_{hy}*-sirA*$_{K121N}$ *(spec)*	This study
BYD574	*amyE::*P_{hy}*-sirA (spec), D(soj, spo0J)::cat, pelB::soj- spo0J+ (kan)*	This study
BYD575	*amyE::*P_{hy} *(spec), D(soj, spo0J)::cat, pelB::soj-spo0J+ (kan)*	This study
***E. coli* DHP1**		
CYD050	*dnaA-T25 (kan), sirA-T18 (amp)*	This study
CYD051	*dnaA-T25 (kan), sirA*$_{Y51A}$*-T18 (amp)*	This study
CYD053	*dnaA*$_{F49Y}$*-T25 (kan), sirA-T18 (amp)*	This study
CYD055	*dnaA*$_{A50V}$*-T25 (kan), sirA-T18 (amp)*	This study
CYD060	*dnaA-T25 (kan), empty-T18 (amp)*	This study
CYD061	*empty-T25 (kan), sirA-T18 (amp)*	This study
CYD062	*empty-T25 (kan), sirA*$_{Y51A}$*-T18 (amp)*	This study
CYD064	*dnaA*$_{F49Y}$*-T25 (kan), empty-T18 (amp)*	This study
CYD066	*dnaA*$_{A50V}$*-T25 (kan), empty-T18 (amp)*	This study
CYD168	*dnaA*$_{A50V}$*-T25 (kan), sirA*$_{I103V}$*-T18 (amp)*	This study
CYD169	*dnaA*$_{A50V}$*-T25 (kan), sirA*$_{T113M}$*-T18 (amp)*	This study
CYD172	*dnaA*$_{A50V}$*-T25 (kan), sirA*$_{V118M}$*-T18 (amp)*	This study
CYD173	*dnaA*$_{A50V}$*-T25 (kan), sirA*$_{K121N}$*-T18 (amp)*	This study
CYD175	*dnaAA50V-T25 (kan), sirA*$_{P141T}$*-T18 (amp)*	This study
CYD286	*T25-soj (kan), sirA-T18 (amp)*	This study
CYD306	*T25-soj (kan), empty-T18 (amp)*	This study
CYD307	*T25-empty (kan), sirA-T18 (amp)*	This study
CYD602	*dnaA*$_{T116N}$*-T25 (kan), sirA*$_{Y51A}$*-T18 (amp)*	This study
CYD605	*dnaA*$_{F120S}$*-T25 (kan), sirA*$_{Y51A}$*-T18 (amp)*	This study
CYD608	*dnaA*$_{I122T}$*-T25 (kan), sirA*$_{Y51A}$*-T18 (amp)*	This study
CYD611	*dnaA*$_{H130D}$*-T25 (kan), sirA*$_{Y51A}$*-T18 (amp)*	This study
CYD626	*dnaA*$_{V136A}$*-T25 (kan), sirA*$_{Y51A}$*-T18 (amp)*	This study
CYD629	*dnaA*$_{K197N}$*-T25 (kan), sirA*$_{Y51A}$*-T18 (amp)*	This study
CYD632	*dnaA*$_{D215V}$*-T25 (kan), sirA*$_{Y51A}$*-T18 (amp)*	This study
CYD635	*dnaA*$_{P255L}$*-T25 (kan), sirA*$_{Y51A}$*-T18 (amp)*	This study
CYD638	*dnaA*$_{G268R}$*-T25 (kan), sirA*$_{Y51A}$*-T18 (amp)*	This study
CYD711	*T25-soj (kan), sirA*$_{P141T}$*-T18 (amp)*	This study

Table 2.1. Continued.

Strain	Description	Reference
CYD715	*T25-soj (kan), sirA$_{T113M}$-T18 (amp)*	This study
CYD716	*T25-soj (kan), sirA$_{V118M}$-T18 (amp)*	This study
CYD717	*T25-soj (kan), sirA$_{K121N}$-T18 (amp)*	This study
CYD718	*T25-empty (kan), sirA$_{P141T}$-T18 (amp)*	This study
CYD722	*T25-empty (kan), sirA$_{T113M}$-T18 (amp)*	This study
CYD723	*T25-empty (kan), sirA$_{V118M}$-T18 (amp)*	This study
CYD724	*T25-empty (kan), sirA$_{K121N}$-T18 (amp)*	This study
CYD736	*T25-soj (kan), sirA$_{E144A}$-T18 (amp)*	This study
CYD737	*T25-empty (kan), sirA$_{E144A}$-T18 (amp)*	This study
CYD742	*T25-soj (kan), sirA$_{A111V}$-T18 (amp)*	This study
CYD743	*T25-empty (kan), sirA$_{A111V}$-T18 (amp)*	This study
CYD765	*T25-soj (kan), sirA$_{S123C}$-T18 (amp)*	This study
CYD770	*T25-empty (kan), sirA$_{S123C}$-T18 (amp)*	This study
CYD823	*dnaA-T25 (kan), sirA$_{F14A}$-T18 (amp)*	This study
CYD824	*empty-T25 (kan), sirA$_{F14A}$-T18 (amp)*	This study
CYD1050	*T25-soj (kan), sirA$_{I103V}$-T18 (amp)*	This study
CYD1055	*T25-empty (kan), sirA$_{I103V}$-T18 (amp)*	This study

Table 2.2. Plasmids used in Chapter II.

Plasmid	Description	Reference
pCH363	*empty-T18 (amp)*	Tom Bernhardt
pDR111	*amyE::P_{hy}-empty (spec)*	David Z. Rudner
pKNT25	*empty-T25 (kan)*	Tom Bernhardt
pKT25	*T25-empty (kan)*	Tom Bernhardt
pminiMAD	*ori^{BsTs} (amp)(erm)*	(239)
pYD009	*sirA-T18 (amp)*	This study
pYD011	*dnaA-T25 (kan)*	This study
pYD040	*dnaA$_{F49Y}$-T25 (kan)*	This study
pYD042	*dnaA$_{A50V}$-T25 (kan)*	This study
pYD059	*sirA$_{Y51A}$-T18 (amp)*	This study
pYD081	*pminiMAD-dnaA$_{F49Y}$ (amp)*	This study
pYD096	*T25-soj (kan)*	This study
pYD101	*pminiMAD-sirA$_{Y51A}$ (amp)*	This study
pYD102	*amyE::P_{hy}-sirA (amp)*	This study
pYD125	*amyE::P_{hy}-sirA$_{P141T}$ (amp)*	This study
pYD126	*amyE::P_{hy}-sirA$_{Q30L}$ (amp)*	This study
pYD127	*amyE::P_{hy}-sirA$_{I83K}$ (amp)*	This study
pYD128	*pminiMAD-sirA$_{P141T}$ (amp)*	This study
pYD129	*pminiMAD-sirA$_{F14A}$ (amp)*	This study
pYD130	*pminiMAD-dnaA$_{A50V}$ (amp)*	This study
pYD131	*amyE::P_{hy}-sirA$_{Q41H}$ (amp)*	This study
pYD132	*sirA$_{E144A}$-T18 (amp)*	This study
pYD133	*amyE::P_{hy}-sirA$_{E144A}$ (amp)*	This study
pYD134	*amyE::P_{hy}-sirA$_{L69F}$ (amp)*	This study
pYD135	*amyE::P_{hy}-sirA$_{A111V}$ (amp)*	This study
pYD136	*amyE::P_{hy}-sirA$_{R64P}$ (amp)*	This study
pYD137	*pminiMAD-sirA$_{E144A}$ (amp)*	This study
pYD138	*pminiMAD-sirA$_{S123C}$ (amp)*	This study
pYD139	*sirA$_{S123C}$-T18 (amp)*	This study
pYD140	*amyE::P_{hy}-sirA$_{S123C}$ (amp)*	This study
pYD141	*amyE::P_{hy}-sirA$_{P124L}$ (amp)*	This study
pYD142	*amyE::P_{hy}-sirA$_{S106P}$ (amp)*	This study
pYD143	*amyE::P_{hy}-sirA$_{L28P}$ (amp)*	This study
pYD146	*sirA$_{A111V}$-T18 (amp)*	This study
pYD165	*pminiMAD-sirA$_{A111V}$ (amp)*	This study
pYD166	*pminiMAD-sirA$_{I103V}$ (amp)*	This study
pYD167	*pminiMAD-sirA$_{T113M}$ (amp)*	This study
pYD168	*pminiMAD-sirA$_{V118M}$ (amp)*	This study
pYD169	*pminiMAD-sirA$_{K121N}$ (amp)*	This study

Table 2.2. Continued.

Plasmid	Description	Reference
pYD170	*amyE::P_{hy}-sirA$_{F115Y}$ (amp)*	This study
pYD171	*amyE::P_{hy}-sirA$_{F14A}$ (amp)*	This study
pYD172	*amyE::P_{hy}-sirA$_{Y51A}$ (amp)*	This study
pYD173	*sirA$_{I103V}$-T18 (amp)*	This study
pYD174	*sirA$_{T113M}$-T18 (amp)*	This study
pYD175	*sirA$_{V118M}$-T18 (amp)*	This study
pYD176	*sirA$_{K121N}$-T18 (amp)*	This study
pYD177	*sirA$_{P141T}$-T18 (amp)*	This study
pYD178	*dnaA$_{T116N}$-T25 (kan)*	This study
pYD179	*dnaA$_{F120S}$-T25 (kan)*	This study
pYD180	*dnaA$_{I122T}$-T25 (kan)*	This study
pYD181	*dnaA$_{H130D}$-T25 (kan)*	This study
pYD182	*dnaA$_{V136A}$-T25 (kan)*	This study
pYD183	*dnaA$_{K197N}$-T25 (kan)*	This study
pYD184	*dnaA$_{D215V}$-T25 (kan)*	This study
pYD185	*dnaA$_{P255L}$-T25 (kan)*	This study
pYD186	*dnaA$_{G268R}$-T25 (kan)*	This study
pYD187	*sirA$_{F14A}$-T18 (amp)*	This study

Table 2.3. Oligonucleotides used in Chapter II.

Oligo	**Sequence 5' to 3'**
OJH083	ATGACAGAGAAACAGATTCAAGCTATTACACAACCAATCCCGA
OYD006	CATTGCATGCGTAACACACAGGAAACAGCTATGGAACGTCACTACTATACG
OYD007	GCATGGATCCGAACCGCTACCGACAAAATTTCTTTCTTTCAC
OYD011	GCATGGTACCGAACCGCTACCTTTAAGCTGTTCTTTAATTTCTTT
OYD035	GCATGGATCCGTAACACACAGGAAACAGCTATGGAAAATATATTAGACCTGTG
OYD043	CAATCACGGCTCCCAATGAATATGCCAGAGACTGGCTGGAGTCC
OYD045	TCACGGCTCCCAATGAATTTGTCAGAGACTGGCTGGAGTCCAG
OYD046	AAGCTTGCATGCCTGCAGGT
OYD047	GGTCGGCGGCGTTTGCGTAAC
OYD059	CAGCCAGTCTCTGGCATATTCATTGGGAGCCGTGATTGTTAATG
OYD061	CTGGACTCCAGCCAGTCTCTGACAAATTCATTGGGAGCCGTGA
OYD070	GTGTGGAATTGTGAGCGGATAAC
OYD116	CATTGGACAAGCCTTGAAAAGCAG
OYD117	GTAATCTCCCGAAGCCACAATTTC
OYD122	GCATGGATCCCGGCTTTTTTTAGTATCCACAG
OYD123	GCATGAATTCGTTTGTAAATTTCTCAGAAGACAG
OYD214	TCGGGATTGGTTGTGTAATAGCTTGAATCTGTTTCTCTGTCAT
OYD215	GCATGGATCCTCAATGGACCGTTTTGAGAAAC
OYD216	GCATGAATTCAGGTTTCATTCCCATTTGCATC
OYD254	GCATGGATCCGGGCAGCGGTGTGGGAAAAATCATAGCAATTAC
OYD255	GCATGAATTCTTAGCCATTCGCAGCCACTTCC
OYD276	AGCAATTACGAACCAAAAAGTCGGGGTCGGCAAAACAACGA
OYD277	TCGTTGTTTTGCCGACCCCGACTTTTTGGTTCGTAATTGCT
OYD280	GGTTCTGCTGGTAGATATTGCTCCGCAGGGAAATGCGACAA
OYD281	TTGTCGCATTTCCCTGCGGAGCAATATCTACCAGCAGAACC
OYD296	CCATTATGTAATAGATCATAATCC
OYD297	GACAACTCTGATTAATGCTCC
OYD302	ATCATAATCTTTACGTATTATTTCG
OYD305	GGCTTCGGGAGATTACGAGGTAGAAACGATATTCTTTGAAG
OYD306	CTTCAAAGAATATCGTTTCTACCTCGTAATCTCCCGAAGCC
OYD310	TATGCTCAATCCAAAATATAATTTTGATACTTTTGTCATCG
OYD311	CGATGACAAAAGTATCAAAATTATATTTTGGATTGAGCATA

Table 2.3. Continued.

Oligo	Sequence 5' to 3'
OYD312	AAAATATACTTTTGATACTTCTGTCATCGGATCTGGAAACC
OYD313	GGTTTCCAGATCCGATGACAGAAGTATCAAAAGTATATTTT
OYD314	TACTTTTGATACTTTTGTCACCGGATCTGGAAACCGATTTG
OYD315	CAAATCGGTTTCCAGATCCGGTGACAAAAGTATCAAAAGTA
OYD316	GATCTGGAAACCGATTTGCAGATGCTGCTTCCCTCGCAGTA
OYD317	TACTGCGAGGGAAGCAGCATCTGCAAATCGGTTTCCAGATC
OYD326	TGATGTGCTTTTGATAGATGTTATTCAATTTTTAGCGGGGA
OYD327	TCCCCGCTAAAAATTGAATAACATCTATCAAAAGCACATCA
OYD328	TGCGCTCACGTTTTGAATGGAGACTTATTACAGATATCACA
OYD329	TGTGATATCTGTAATAAGTCTCCATTCAAAACGTGAGCGCA
OYD330	AACTCTATCCGAGATAATAATGCCGTCGACTTCCGCAATCG
OYD331	CGATTGCGGAAGTCGACGGCATTATTATCTCGGATAGAGTT
OYD354	CTGTTCAGCGCATTGCGCAC
OYD362	ATGCAAGCTTACATAAGGAGGAACTACTATGGAACGTCACTAC TATACG
OYD363	AGCTGCTAGCTTAGACAAAATTTCTTTCTTTCAC
OYD364	GCATGCATGCGTAACACACAGGAAA
OYD365	GCATGGATCCGAACCGCTACCGA
OYD366	CGTACCTGATCAAAGAGGAAGCTGCCAATCACTATTTCGGCC
OYD367	GGCCGAAATAGTGATTGGCAGCTTCCTCTTTGATCAGGTACG
OYD368	GCATGGATCCATGGAACGTCACTACTATACG
OYD369	GCATGAATTCCTGCAAATTGTCATGGCGAAC
OYD376	AGCGTTACGGATGGCTAAATACGGTGAAAGAAAGAAATTTT
OYD377	AAAATTTCTTTCTTTCACCGTATTTAGCCATCCGTAACGCT
OYD380	GGTTATGTTTGAGCTGTTTCTAGACTATCATTGGACAAGCC
OYD381	GGCTTGTCCAATGATAGTCTAGAAACAGCTCAAACATAACC
OYD382	GCTGGATTATATTTATAGAAAAGCTTTGCCGAAAGCAAAAG
OYD383	CTTTTGCTTTCGGCAAAGCTTTTCTATAAATATAATCCAGC
OYD384	AGCTGCTAGCTTAGACAAAATTTCTTGCTTTCAC
OYD387	ATGCGTCGACACATAAGGAGGAACTACTATGGAACGTCACTAC TATACG
OYD388	AGCTGCATGCTTAGACAAAATTTCTTTCTTTCAC
OYD389	ACAAGCCTTGAAAAGCAGCACTATGAAATGACAGAGAAACA
OYD390	TGTTTCTCTGTCATTTCATAGTGCTGCTTTTCAAGGCTTGT
OYD391	ATGGCTAAATCCGGTGAAAGCAAGAAATTTTGTCTAAAACC
OYD392	GGTTTTAGACAAAATTTCTTGCTTTCACCGGATTTAGCCAT
OYD397	TTACGAGGCAGAAACGATATACTTTGAAGTGTTAAGAAAAG
OYD398	CTTTTCTTAACACTTCAAAGTATATCGTTTCTGCCTCGTAA
OYD399	TTGAAGTGTTAAGAAAAGTATGCCCTTGCTTTTTAGCAATG

Table 2.3. Continued.

Oligo	**Sequence 5’ to 3’**
OYD400	CATTGCTAAAAAGCAAGGGCATACTTTTCTTAACACTTCAA
OYD401	AGTGTTAAGAAAAGTAAGCCTTTGCTTTTTAGCAATGGATT
OYD402	AATCCATTGCTAAAAAGCAAAGGCTTACTTTTCTTAACACT
OYD403	ACATGATAGAAATTGTGGCTCCGGGAGATTACGAGGCAGAA
OYD404	TTCTGCCTCGTAATCTCCCGGAGCCACAATTTCTATCATGT
OYD405	GGAATCGGTTATGTTTGAGCCGTTTCAAGACTATCATTGGA
OYD406	TCCAATGATAGTCTTGAAACGGCTCAAACATAACCGATTCC
OYD491	TGAAGGAGCACATGATAGAAGTTGTGGCTTCGGGAGATTAC
OYD492	GGGAGATTACGAGGCAGAAATGATATTCTTTGAAGTGTTAA
OYD493	TTAACACTTCAAAGAATATCATTTCTGCCTCGTAATCTCCC
OYD494	CAGAAACGATATTCTTTGAAATGTTAAGAAAAGTAAGCCCT
OYD495	AGGGCTTACTTTTCTTAACATTTCAAAGAATATCGTTTCTG
OYD496	TTCTTTGAAGTGTTAAGAAATGTAAGCCCTTGCTTTTTAGC
OYD497	GCTAAAAAGCAAGGGCTTACATTTCTTAACACTTCAAAGAA
OYD498	GTAATCTCCCGAAGCCACAACTTCTATCATGTGCTCCTTCA
OYD517	CCGGCCGCCAAAGGAAATTCTGACACTTGAAGACAGATTGC
OYD518	GCAATCTGTCTTCAAGTGTCAGAATTTCCTTTGGCGGCCGG
OYD526	GCATGGATCCGAACCGCTACCGACAAAATTTCTTGCTTTCAC
OYD527	ACATGCTGCTTCCCTCGCAGGAGCGGAAGCGCCCGCGAAAG
OYD528	CTTTCGCGGGCGCTTCCGCTCCTGCGAGGGAAGCAGCATGT

2.2.2 Microscopy

All samples were grown in CH media overnight at room temperature to mid-exponential, back-diluted to OD_{600}=0.008 in 25 ml CH, and grown at 37°C in a shaking waterbath set at 280 rpm for 1.5 hrs. When indicated, 1 mM IPTG was added, and cells were grown for an additional 1.5 hrs. All cells were in mid-exponential growth when images were captured. To capture images, 1 ml of cells were pelleted at 6,010 x g for 1 min in a tabletop microfuge at room temperature. The supernatant was removed by aspiration and the pellet resuspended in ~10 ul PBS containing FM4-64 membrane stain (3 µg/ml)(Life Technologies) and DAPI DNA stain (2 µg/ml)(Molecular Probes). Cells were mounted on glass slides with polylysine treated coverslips immediately before imaging. Fluorescence microscopy was performed with a Nikon Ti-E microscope equipped with a CFI Plan Apo lambda DM 100X objective, and Prior Scientific Lumen 200 Illumination system, C-FL UV-2E/C DAPI, C-FL GFP HC HISN Zero Shift, C-FL YFP HC HISN Zero Shift, and C-FL Cyan GFP, filter cubes, and a CoolSNAP HQ2 monochrome camera. All images were captured with NIS Elements Advanced Research (version 4.10), and processed with NIS Elements and ImageJ64 (240).

2.2.3 Quantitative forespore chromosome trapping assay

Assays were carried out as previously described (187). An *oriC*-proximal reporter (-7° *yycR*::P_{spoIIQ}-*yfp*) and a right-arm reporter (28° *amyE*::P_{spoIIQ}-*cfp*) were used to assess chromosome organization. Cells were collected and membranes were stained with TMA-DPH (0.02 mM) as described in microscopy. YFP, CFP, and TMA-DPH images were captured 2.5 hrs after cells were resuspended and grown in sporulation

media (237) at 37°C in a shaking waterbath set at 280 rpm. Images from a minimum of four biological replicates were captured for each strain. To quantitate the number of cells with the forespore reporters trapped in the forespore, the CFP, YFP, and TMA images were pseudocolored and overlaid. Forespores containing detectable signal from YFP, CFP, or both from at least four independent fields (n>500 cells per trial) were counted manually for each biological replicate, adjusting brightness to ensure that even cells with faint signal were counted. Forespores failing to capture either reporter were generally <1% and were not included in the counts for -7° reporter excluded. The average percentage and standard deviation of forespores with CFP signal only (indicating that the -7° *oriC*-proximal reporter was not captured in the forespore) were plotted using Microsoft Excel. The statistical significance between samples (P-value) was determined using an unpaired Student's t-test.

2.2.4 Bacterial two-hybrid assay (B2H), general methods

Bacterial two hybrids were performed essentially as described (241) with the following modifications: cloning was carried out in the presence of 0.2% glucose (w/v) in addition to antibiotics. *E. coli* strain DHP1 harboring the relevant pairwise interactions were grown to exponential phase in LB with 0.2% glucose (w/v), ampicillin (50 μg/ml), and kanamycin (25 μg/ml). Samples were normalized by OD_{600} and five μl of each culture spotted on M9-glucose minimal media plates containing 250 μM isopropyl-β-D-thiogalactopyranoside (IPTG), 40 μg/ml 5-bromo-4-chloro-3-indolyl-β-D-galactopyranoside (X-Gal), ampicillin (50 μg/ml), and kanamycin (25 μg/ml). Plates were incubated at room temperature in the dark for 50 to 70 hrs prior to image capture.

2.2.5 Screen for SirA variants that exhibited a loss of interaction with Soj

The loss-of-interaction screen was performed by B2H assay (see above). Soj was fused to C-terminus of the *cyaA* T25 domain (T25-Soj). SirA was fused to N-terminus of the *cyaA* T18 domain (SirA-T18). *E. coli* strain DHP1 was co-transformed with a plasmid encoding wild-type T25-Soj and a ligation reaction between a mutagenized pool of *sirA* PCR products digested with SphI and BamHI and pCH363 cut with SphI and BamHI (to generate SirA-T18 fusions). The *sirA* gene was mutagenized by PCR using the Genemorph II random DNA mutagenesis kit (Agilent Technologies). The co-transformations were plated on LB solid media (1.5% bacto-agar (w/v)) supplemented with 0.2% glucose (w/v), ampicillin (50 μg/ml), and kanamycin (25 μg/ml). To screen for loss-of-interaction variants, ~2,000 colonies were patched onto M9-glucose minimal media plates supplemented with IPTG (250 μM), X-Gal (40 μg/ml), ampicillin (50 μg/ml), and kanamycin (25 μg/ml). Patches that appeared white were rescreened on M9-glucose minimal media plates containing IPTG (250 μM), X-Gal (40 μg/ml), ampicillin (50 μg/ml), and kanamycin (25 μg/ml) to reduce the number of false negatives. Approximately 12% of the clones screened showed a loss of interaction between SirA and Soj. PCR with primers OYD70 and OYD354 was used to eliminate loss-of-interaction candidates that lacked a *sirA* insert of the appropriate size in the SirA-T18 plasmid, reducing the number of candidates to 42. These candidates were sequenced to eliminate candidates possessing premature stop codons or multiple mutations, reducing the number of candidates to 13. To exclude SirA variants that might be misfolded, each candidate allele was PCR amplified with OYD362 and OYD363, cloned into the HindIII/NheI site of an inducible misexpression vector and growth was assessed as described.

2.2.6 Screen for SirA variants that exhibit a gain of interaction with DnaA$_{A50V}$

The gain-of-interaction screen was performed by first co-transforming *E. coli* strain DHP1 with a plasmid encoding DnaA$_{A50V}$-T25 and a pool of mutagenized *sirA*-T18 ligation products. The *sirA* gene was mutagenized by PCR using the Genemorph II random DNA mutagenesis kit (Agilent Technologies). Co-transformation was selected for on LB plates supplemented with 0.2% glucose (w/v), ampicillin (50 μg/ml), and kanamycin (25 μg/ml). Gain-of-interaction variants were identified by screening on M9-glucose minimal media plates supplemented with IPTG (250 μM), X-Gal (40 μg/ml), ampicillin (50 μg/ml), and kanamycin (25 μg/ml). Plasmids encoding candidates were used as the template to amplify *sirA* region using OYD70 and OYD354, and each PCR product was sequenced by using OYD116 and OYD117 to determine the identity of the associated mutations.

2.2.7 Screen for DnaA variants that exhibit a gain of interaction with SirA$_{Y51A}$

The gain-of-interaction screen was performed by first co-transforming cells with a plasmid encoding SirA$_{Y51A}$-T18 and a pool of mutagenized *dnaA*-T25 ligation products. The co-transformations were plated on LB plates supplemented with 0.2% glucose (w/v), ampicillin (50 μg/ml), and kanamycin (25 μg/ml) and gain-of-interaction variants were identified by screening patches on M9-glucose minimal media plates supplemented with IPTG (250 μM), X-Gal (40 μg/ml), ampicillin (50 μg/ml), and kanamycin (25 μg/ml). Plasmids encoding gain-of-interaction candidates were used as the template to amplify *dnaA* using OYD46 and OYD47. Each PCR product was sequenced in both directions using OYD296 and OYD297.

2.2.8 Allelic replacement of wild-type *sirA* with *sirA* mutants

The *sirA* mutants were generated through allelic replacement. Briefly, each mutant gene was generated using overlap extension PCR and cloned into the vector pminiMAD, a plasmid harboring a temperature sensitive origin of replication. Each plasmid was then transformed into *B. subtilis* 168 and single-crossover integration was selected by plating cells at 37°C in the presence of erythromycin (1 µg/ml) and lincomycin (25 µg/ml). Six independent colonies were inoculated into six independent 3 ml LB cultures and grown overnight at room temperature in a rotary drum set at 60 rpm. The next day, the cultures were back-diluted 150X in fresh LB, and grown 8 hrs at room temperature. 100 µl of a 10^{-5} dilution of each culture was plated on 6 independent LB plates, and incubated overnight at 37°C. Ten single colonies from each plate were patched on LB plate and LB plate supplemented with erythromycin (1 µg/ml) and lincomycin (25 µg/ml). After streaking for isolated colonies, genomic DNA was collected from several antibiotic sensitive colonies obtained from each independent culture. The *sirA* region was then PCR-amplified (primer pair OYD006 and OYD007) and strains carrying the desired mutation were identified by sequencing with primer OYD116 and OYD117.

2.2.9 Plate growth assay

B. subtilis strains were streaked on LB plates containing 100 µg/ml spectinomycin and 1 mM IPTG when indicated. The plates were incubated at 37°C overnight and images were captured on a ScanJet G4050 flatbed scanner (Hewlett Packard) set on medium format mode.

2.2.10 Western blot analysis

To test the stability of SirA variants by western blot analysis, 2 ml cell pellets were collected 2 hrs after resuspension in sporulation media (237) and frozen at -80°C until processing. Lysates were generated by resuspending each pellet in 50 µl lysis buffer [20 mM Tris pH 7.5, 10 mM EDTA, 1 mg/ml lysozyme, 10 µg/ml DNase I, 100 µg/ml RNase A, 1mM PMSF] and incubated 15 min at room temperature. Fifty µl of 2X sample buffer [0.25 M Tris pH 6.8, 4% SDS, 20% glycerol, 10 mM EDTA] containing 10% 2-mercaptoethanol was added and samples were boiled for 5 min. Lysate loads were normalized by OD_{600} values obtained at the time of cell harvest (normalized to OD_{600} = 1). Five µl of each cell lysate was loaded, and proteins were separated on a 4-20% Tris-HCl gradient gels (Lonza). Proteins were transferred to nitrocellulose membrane (Pall) for 1 hr at 60 V on an ice bath. Membranes were blocked in PBS [pH 7.4] containing 0.05% Tween-20 and 5% non-fat milk powder (w/v). Membranes were incubated overnight at 4°C with a 1:1,000 dilution of α-SirA peptide antibody (CSKRYGWLNPVKERN, Genscript) in PBS [pH 7.4] containing 0.05% Tween-20 and 5% non-fat milk powder (w/v) and washed. The membranes were then incubated with 1:10,000 dilutions of horseradish peroxidase-conjugated goat anti-rabbit immunoglobulin G secondary antibody (Bio-Rad) in PBS [pH 7.4] containing 0.05% Tween-20 and 5% non-fat milk powder (w/v) for 1 hr at room temperature. After washing, blots were incubated with SuperSignal West Femto Chemiluminescent substrate (Thermo) prior to capture in an Amersham Imager 600 (GE Healthcare). All western blots were performed on a minimum of three biological and experimental replicates. Densitometric analysis of the levels compared to the wild-type controls were

performed with ImageJ (240). Levels of SirA were always within 2-fold of wild-type for all of the strains examined.

2.3 Results

2.3.1 A Δ*sirA* mutant has an *oriC* segregation defect during sporulation

Soj interacts directly with DnaA Domain III (140, 143) and is required for the high fidelity capture of *oriC* in the forespore compartment (187). SirA also interacts with DnaA (7, 79) and a Δ*sirA* mutant is reported to have a defect in organization of the axial filament during sporulation (7). Since Soj and SirA both regulate DnaA activity directly, we hypothesized that SirA and Soj might both act through a DnaA-dependent pathway to facilitate *oriC* segregation during sporulation. To test this idea, we determined the location of *oriC* in a Δ*sirA* mutant using a single cell chromosome organization assay that provides a readout of regions of DNA captured or "trapped" in the forespore compartment during sporulation (187). We found that 10% of cells in the Δ*sirA* mutant population failed to trap the *oriC*-proximal reporter (Fig 2.2). Introducing P_{sirA}-*sirA* back into the chromosome at an ectopic locus in the Δ*sirA* mutant restored *oriC* trapping to levels indistinguishable from wildtype ($P>0.5$), indicating that the defect could be specifically attributed to the loss of *sirA* (Fig 2.2). In comparison, a Δ*soj* mutant failed to capture an *oriC*-proximal reporter (integrated at -7°) in 19% of sporulating cells, while wildtype failed in less than 1% of cells (Fig. 2.2), similar to prior reports (187). A Δ*soj* Δ*sirA* double mutant phenocopied the Δ*soj* mutant, consistent with SirA acting in the same pathway as Soj to facilitate *oriC* capture. The nine percent difference between the *Δsoj* and Δ*sirA* mutants was reproducible ($P<0.001$), indicating that Soj also contributes

to the capture of *oriC*s in a SirA-independent manner. The *oriC* capture defect in the Δ*soj* and Δ*soj* Δ*sirA* double mutants was reduced to 10% when the gene for the DNA replication checkpoint protein, Sda, was also deleted (Fig 2.2). In contrast, deletion of *sda* in the Δ*sirA* mutant did not further enhance *oriC* capture in a statistically significant way (P>0.05)(Fig 2.2); at the same time we do not exclude the possibility that the slight enhancement of *oriC* capture seen in the Δ*sirA* Δ*sda* mutant compared to the Δ*sirA* mutant represents a real biological difference. Synthesis of Sda delays sporulation in cells that are actively initiating DNA replication (140). Therefore, these results suggest that the fate of the nine percent of *oriC*s that depend on Soj but not SirA may relate to the replication status of this subset of cells, although we did not investigate this observation further.

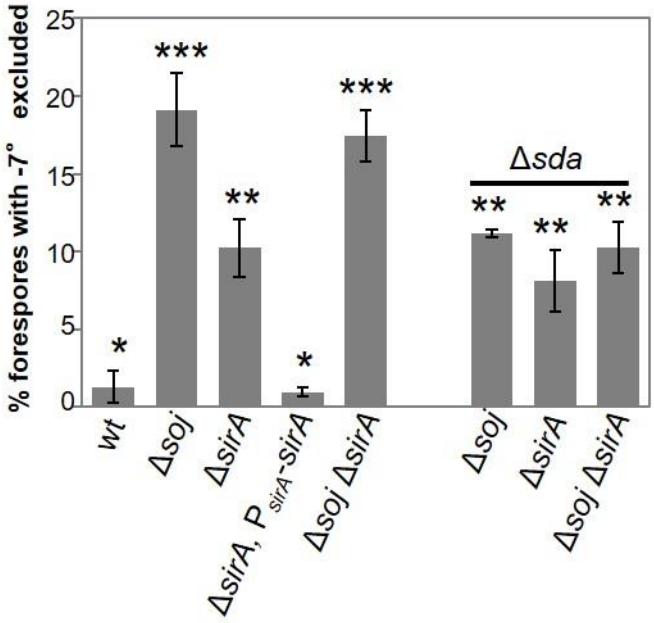

Fig. 2.2. SirA and Soj act in the same pathway to segregate *oriC* during sporulation. Single cell analysis indicating the average percentage of forespores that fail to capture the origin reporter (-7°) in the forespore during sporulation. Wildtype (BJH103), Δ*soj* (BYD116), Δ*sirA* (BJH090), Δ*sirA*, P_{sirA}-*sirA* (BJH015), Δ*soj* Δ*sirA* (BYD117), Δ*soj* Δ*sda* (BYD470), Δ*sirA* Δ*sda* (BYD472) and Δ*soj* Δ*sirA* Δ*sda* (BYD471). A minimum of 500 cells from each of four biological replicates was counted for each strain (total n >2000 average). Error bars indicate standard deviation from the average of the four trials. The asterisks indicate pairwise comparisons that were statistically indistinguishable (P>0.05, students t-test).

2.3.2 A wild-type interaction between SirA and Soj is not required for SirA-dependent *oriC* capture

Our data indicate that SirA and Soj act in the same pathway to facilitate *oriC* segregation in 10% of cells (Fig 2.2). To assess if SirA might interact directly with Soj to facilitate *oriC* segregation, we performed a bacterial two-hybrid (B2H) assay. A positive interaction was observed between SirA-T18 and T25-Soj that was absent in the negative controls (Fig 2.3A). To test if the interaction between SirA and Soj was important for *oriC* capture in vivo, we first screened for SirA variants that exhibited a loss of interaction with Soj. To obtain such variants, we introduced a mutagenized pool of *sirA* PCR products into a B2H plasmid to generate a SirA-T18 pool, and transformed this plasmid pool into *E. coli* reporter cells harboring the B2H partner plasmid, T25-Soj. Next we screened for SirA variants that showed loss of interaction with Soj in the B2H assay. *sirA* alleles that appeared full-length in a PCR test were sequenced, and alleles encoding premature stop codons or multiple mutations were eliminated, leaving 13 candidates (Table 2.4).

SirA is natively expressed only during sporulation and misexpression (forcing expression during vegetative growth by placing under the control of an IPTG-inducible promoter on the chromosome) inhibits DnaA activity and prevents colony formation on plates (7), a phenotype that is not dependent on Soj (Fig 2.4). Therefore, we screened for properly folded proteins using misexpression. Seven of the loss-of-interaction mutants did not inhibit DnaA activity, as judged by growth on media containing inducer (Table 2.4) and were excluded from further analysis since we were unable to assess if they were properly folded. The remaining six mutants phenocopied the wild-type *sirA* vegetative misexpression phenotype (Table 2.4), suggesting the proteins were not misfolded.

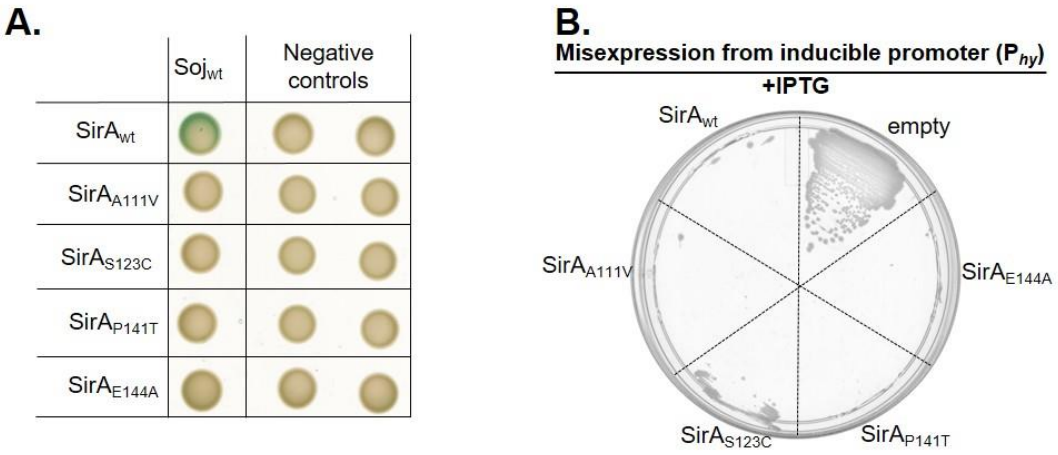

Fig. 2.3. Identification and characterization of SirA variants that exhibit loss of interaction with Soj. (A) B2H between Soj and SirA (CYD286) or Soj and each of the following SirA variants: SirA$_{A111V}$ (CYD742), SirA$_{S123C}$ (CYD765), SirA$_{P141T}$ (CYD711), SirA$_{E144A}$ (CYD736). Negative controls: empty partner vector with wild-type SirA or the indicated SirA variant (column 1) or Soj with the empty partner vector (column 2). (B) Growth of strains harboring P$_{hy}$-*sirA* (BYD036), P$_{hy}$-*sirA$_{A111V}$* (BYD288), P$_{hy}$-*sirA$_{S123C}$* (BYD295), P$_{hy}$-*sirA$_{P141T}$* (BYD283), P$_{hy}$-*sirA$_{E144A}$* (BYD292) or P$_{hy}$-*empty* (BAM075) following misexpression. (C) Western blot analysis using α-SirA antibody on samples taken 2 hrs after sporulation by resuspension. Wildtype (BJH103), Δ*sirA* (BJH090), *sirA$_{A111V}$* (BYD306), *sirA$_{S123C}$* (BYD310), *sirA$_{P141T}$* (BYD299), *sirA$_{E144A}$* (BYD308). (D) The same misexpression strains listed in B were grown in CH liquid media 1.5 hrs after the addition of 1mM IPTG. Cell membranes were stained with FM4-64 (pseudocolored pink) and DNA with DAPI (pseudocolored green). White arrowheads indicate example anucleate cells. (E) Single cell analysis indicating the average percentage of forespores that fail to capture the origin reporter (-7°) in the forespore during sporulation using the same strains listed in C. A minimum of 500 cells from each of four biological replicates was counted for each strain (total n >2000 average). Error bars indicate standard deviation from the average of the four trials. The wildtype and delta *sirA* data from Fig 2.2 were re-plotted to aid comparison. Only the Δ*sirA* mutant and *sirA$_{P141T}$* differ significantly from wildtype.

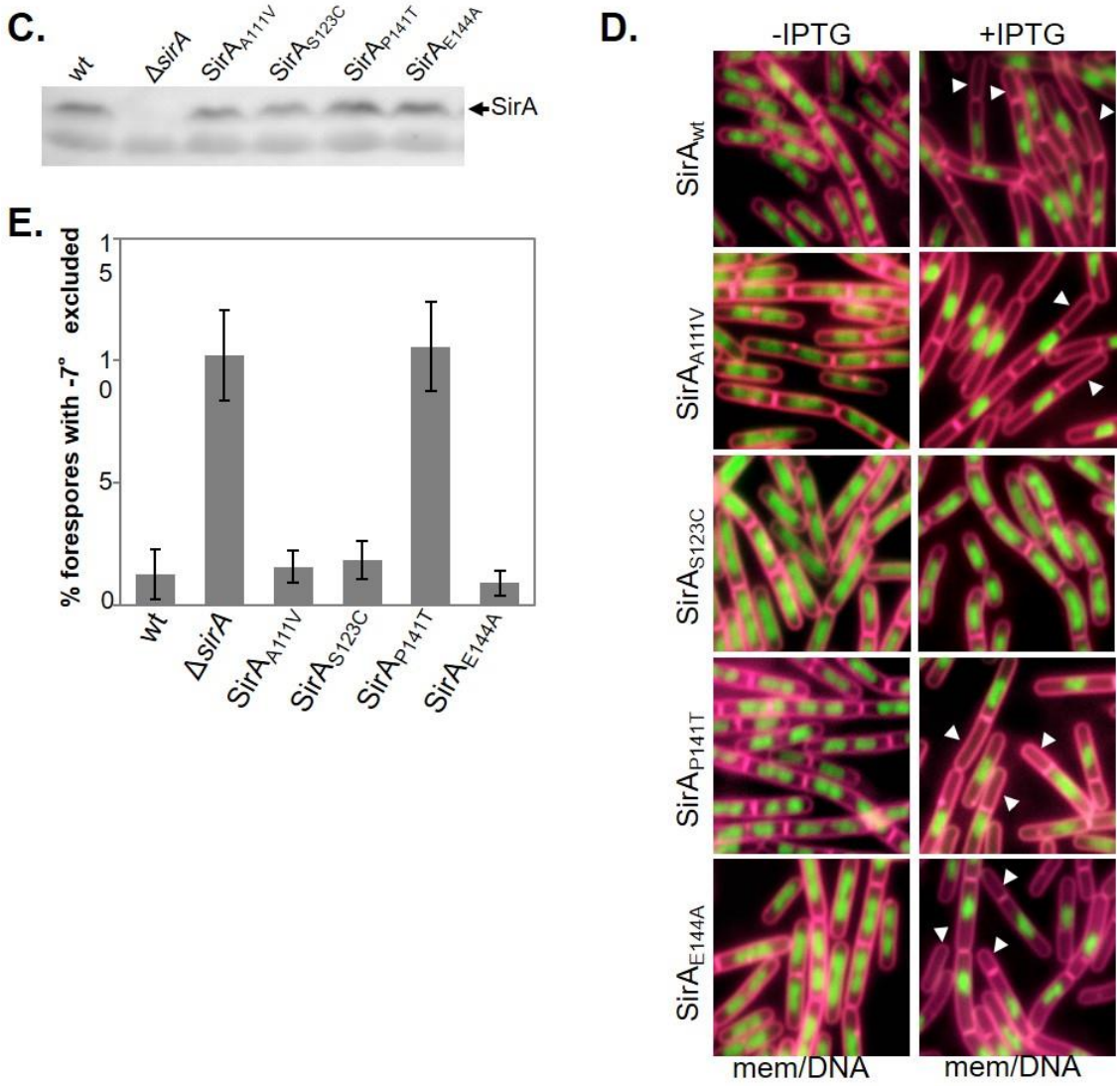

Fig. 2.3. Continued

Table 2.4. Identification of SirA variants that do not interact with Soj in B2H. Growth refers to the resistance (R), or sensitivity (S) of the cells to SirA-mediated growth inhibition following misexpression from an IPTG inducible promoter (P_{hy}). Each of the misexpression constructs was integrated in single copy at the *amyE* locus.

SirA variants exhibiting loss of interaction with Soj		
sirA	**Variant**	**Growth**
CTG→CCG	L28P	R
CGG→CCG	R64P	R
TTA→TTC	L69F	R
ATA→AAA	I83K	R
TCG→CCG	S106P	R
TTC→TAC	F115Y	R
CCT→CTT	P124L	R
CAA→CTA	Q30L	S
CAG→CAC	Q41H	S
GCA→GTA	A111V	S
AGC→TGC	S123C	S
CCG→ACG	P141T	S
GAA→GCA	E144A	S

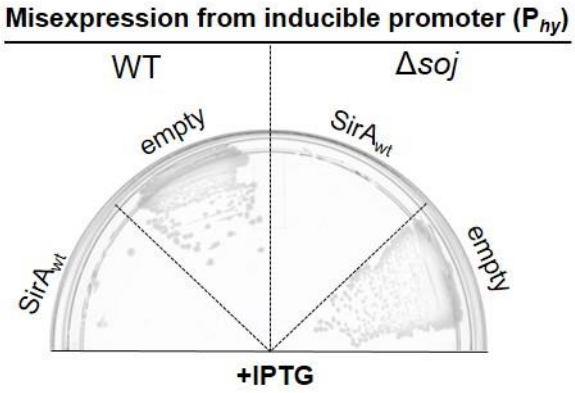

Fig. 2.4. Soj is not required for SirA to prevent colony formation on the plate. Cells harboring one copy of P_{hy}-*sirA* (BYD036) or the P_{hy} promoter without an insert (BAM075) in a wild-type background or a Δ*soj* background (BYD574 and BYD575, respectively) were streaked on an LB plate supplemented with 100 µg/ml spectinomycin and 1 mM IPTG. Cells were grown at 37°C overnight before image capture.

Next we performed the chromosome organization assay on strains harboring $SirA_{A111V,}$ $SirA_{S123C,}$ $SirA_{P141T}$, or $SirA_{E144A}$. These variants were initially chosen because they showed loss-of-interaction with Soj (Fig 2.3A), prevented growth on plates when misexpressed (Fig 2.3B), clustered in residues distal to the described DnaA-SirA interaction interface implicated in regulation of DnaA (Fig 2.5), and exhibited comparable levels of SirA protein compared to wildtype when expressed from the native locus (Fig 2.3C). When we investigated the membrane and nucleoid phenotypes associated with vegetative misexpression, $SirA_{A111V,}$ $SirA_{P141T}$, and $SirA_{E144A}$ appeared indistinguishable from the control strain misexpressing wild-type SirA, including the generation of anucleate cells (Fig 2.3D). However, $SirA_{S123C}$ displayed no obvious signs of inhibited DNA replication, and instead exhibited slightly curved cells or cell poles (Fig 2.3D). After 150 min induction, cells expressing $SirA_{S123C}$ exhibited hooked poles, bent filaments, and signs of lysis (Fig 2.6). The nucleoids in these cells showed no obvious indications of replication inhibition, suggesting the mechanism leading to cell killing in this strain is distinct from the other three loss-of-interaction variants.

Cells expressing $SirA_{A111V,}$ $SirA_{S123C}$, and $SirA_{E144A}$ in place of wild-type SirA captured the *oriC* reporter at levels statistically indistinguishable from wildtype (Fig 2.3E). In contrast, the $SirA_{P141T}$ variant phenocopied the Δ*sirA* mutant, failing to capture *oriC* in 10% of sporulating cells (Fig 2.3E). From these data we conclude that a wild-type interaction between SirA and Soj is not required for SirA-dependent *oriC* capture and that $SirA_{P141T}$ appears to be critical for wild-type SirA activity. Moreover, since $SirA_{P141T}$ can still inhibit DNA replication (Table 2.4, Fig 2.3B and 2.3D), these results suggest that the *oriC* capture function of SirA comprises a genetically separable and distinct activity.

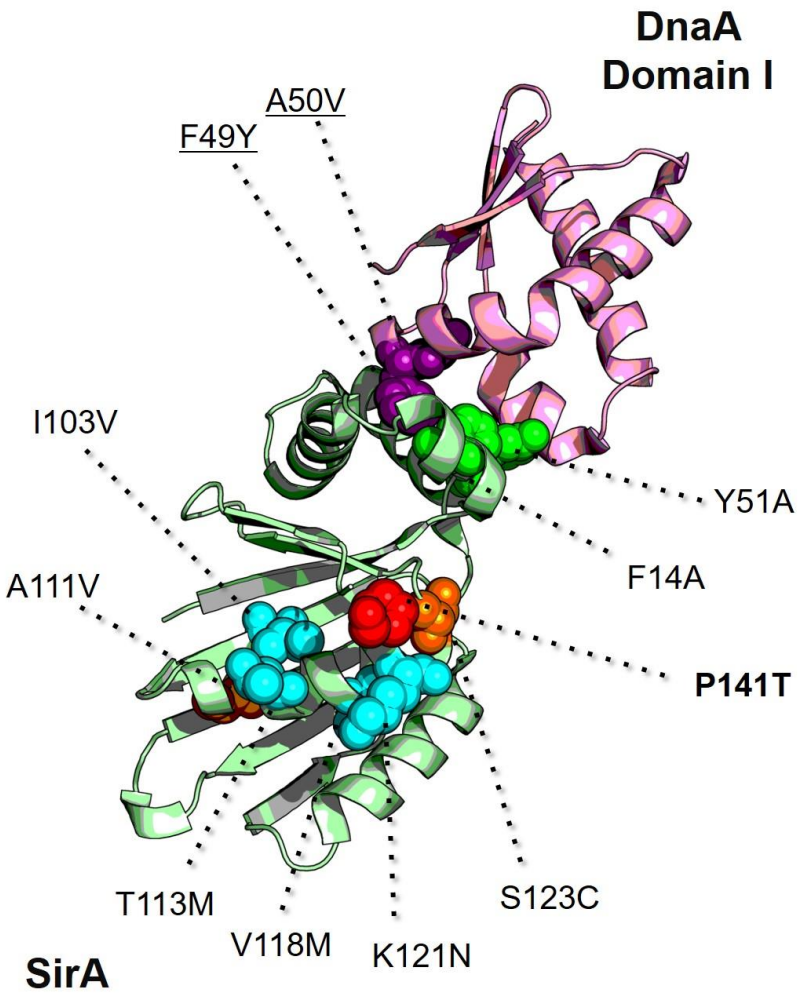

Fig. 2.5. SirA-DnaA Domain I crystal structure. Structure from PDB: 4TPS (79). *B. subtilis* DnaA Domain I (pink) and *B. subtilis* SirA (light green). The location of $SirA_{P141T}$ which exhibits gain of interaction with $DnaA_{A50V}$ and loss of interaction with Soj (red). Location of other SirA variants that exhibit loss-of-interaction with Soj (orange). Location of SirA variants (except $SirA_{P141T}$) that exhibit gain of interaction with $DnaA_{A50V}$ (cyan). The location of the $SirA_{E144A}$ substitution is not shown because it is absent in the structure. Location of substitutions exhibiting loss of interaction with wild-type DnaA (bright green). Location of DnaA substitutions that exhibit loss of interaction with wild-type SirA (purple).

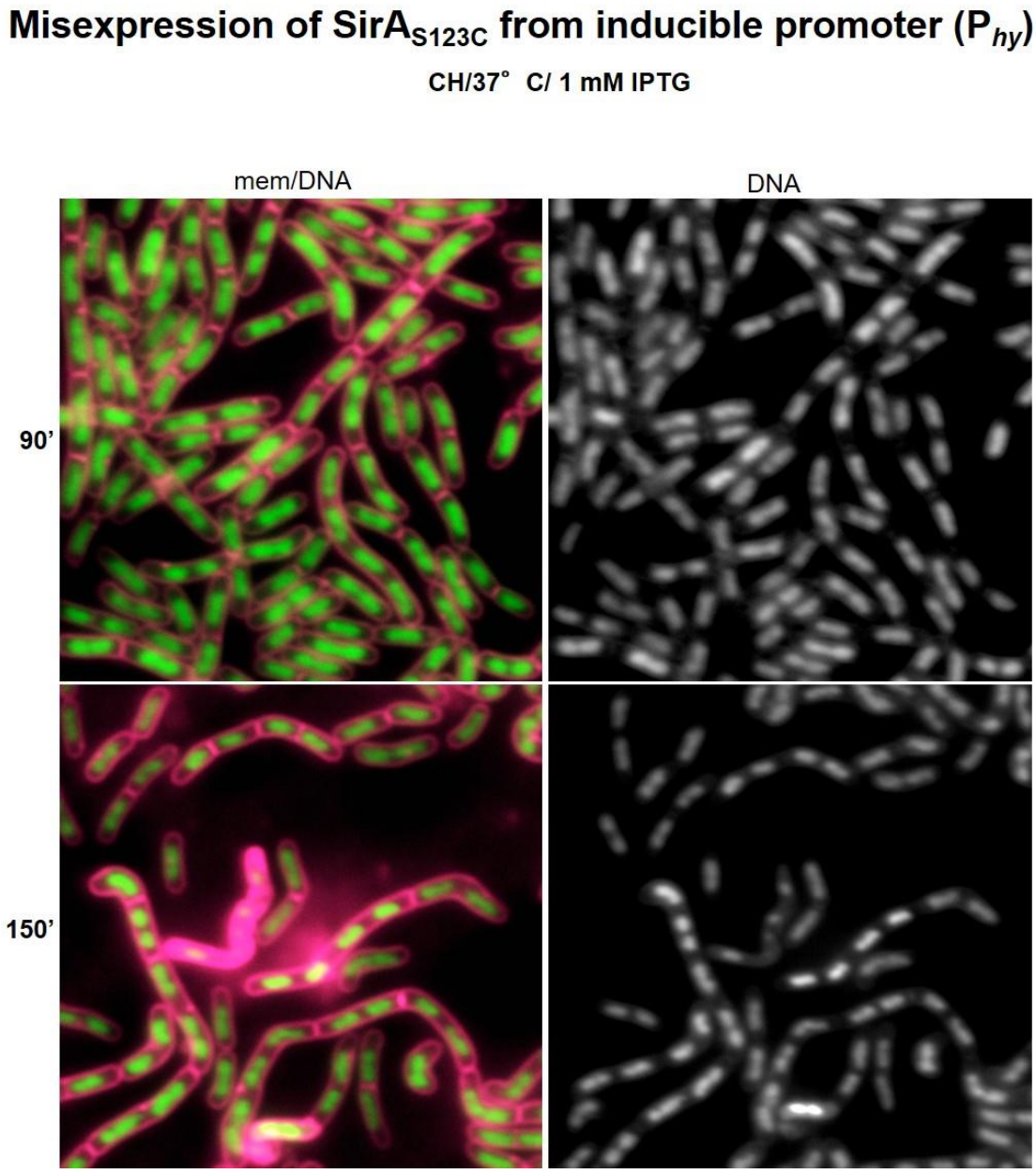

Fig. 2.6. Misexpression of SirA$_{S123C}$ in liquid culture. Cells harboring one copy of P$_{hy}$-*sirA$_{S123C}$* (BYD295) strains grown in CH liquid media for 1.5 hrs (top) and 2.5 hrs (bottom) after the addition of 1mM IPTG. Cell membranes were stained with FM4-64 (pseudocolored pink) and DNA with DAPI (pseudocolored green).

2.3.3 SirA facilitates *oriC* capture independent of its ability to inhibit DNA replication

To further test the hypothesis that SirA's ability to inhibit DnaA activity was independent from SirA's observed role in *oriC* segregation, we generated two *sirA* variants, $SirA_{F14A}$ and $SirA_{Y51A}$, which are defective in their ability to inhibit DnaA. $SirA_{F14A}$ has an amino acid substitution at the described interaction interface between SirA and DnaA and was previously shown to be defective in the ability to inhibit DnaA activity in vivo (79). Since $SirA_{Y51}$ is also located at the SirA-DnaA interaction interface (79), we predicted a substitution in Y51 would also result in a loss-of-function phenotype. Compared to wild-type SirA, both $SirA_{F14A}$ and $SirA_{Y51A}$ showed reduced interaction with full-length DnaA in a B2H assay (Fig 2.7A). In addition, cells misexpressing $SirA_{F14A}$ or $SirA_{Y51A}$ during vegetative growth grew well on plates (Fig 2.7B) and did not generate anucleates in liquid culture (Fig 2.7C). These results indicate that $SirA_{F14A}$ and $SirA_{Y51A}$ are perturbed in their ability to inhibit DNA replication.

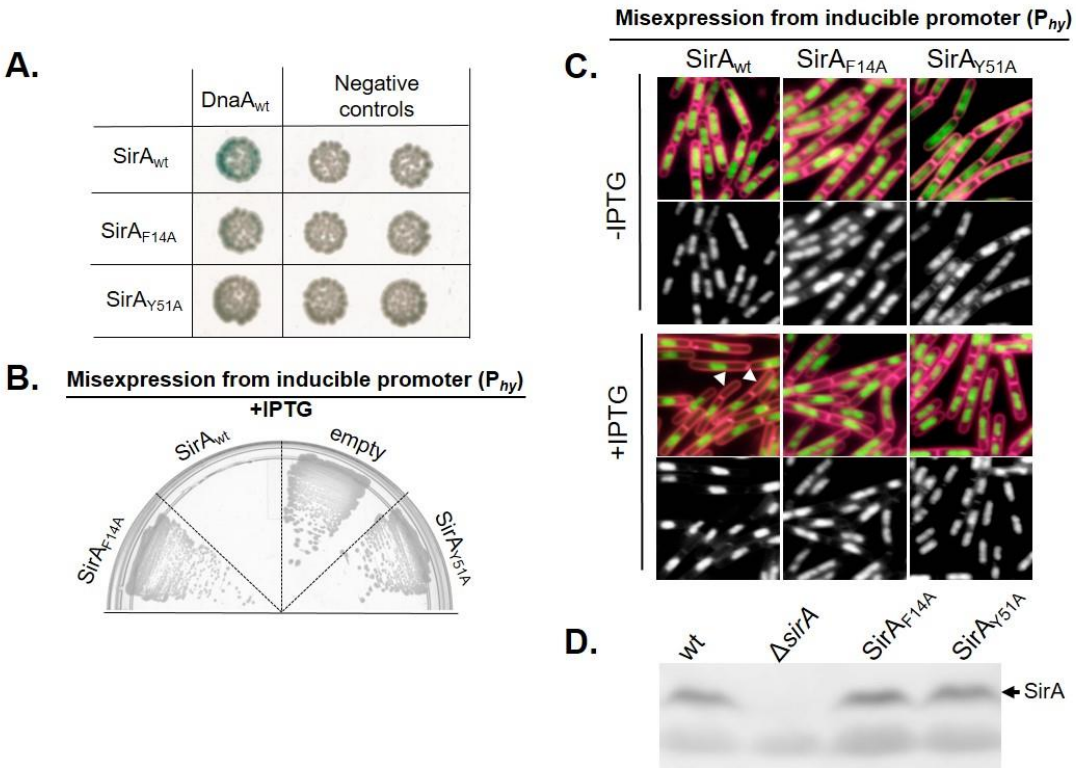

Fig. 2.7. SirA$_{F14A}$ and SirA$_{Y51A}$ exhibit reduced capacities to inhibit DNA replication. (A) B2H assay between DnaA and SirA (CYD050), DnaA and SirA$_{F14A}$ (CYD823), and DnaA and SirA$_{Y51A}$ (CYD051). Negative controls: empty partner vector with wild-type SirA or the indicated SirA variant (column 1) or DnaA with the empty partner vector (column 2). (B) Growth of strains harboring P$_{hy}$-*sirA* (BYD036), P$_{hy}$-*sirA$_{F14A}$* (BYD462), P$_{hy}$-*sirA$_{Y51A}$* (BYD463) or P$_{hy}$-*empty* (BAM075) following misexpression. (C) The same misexpression strains grown in CH liquid media 1.5 hrs after the addition of 1mM IPTG. Cell membranes were stained with FM4-64 (pseudocolored pink) and DNA with DAPI (pseudocolored green). White arrowheads indicate example anucleate cells. (D) Western blot analysis using α-SirA antibody on samples taken 2 hrs after sporulation by resuspension. Wildtype (BJH103), Δ*sirA* (BJH090), *sirA$_{F14A}$* (BYD302), *sirA$_{Y51A}$* (BYD067).

Based on the observation that the DNA replication and *oriC* capture phenotypes were uncoupled in cells expressing $SirA_{P141T}$, we hypothesized that $SirA_{F14A}$ and $SirA_{Y51A}$ would still be able to facilitate *oriC* capture. To test this hypothesis, we replaced native *sirA* with alleles encoding either $SirA_{F14A}$ or $SirA_{Y51A}$ at the native locus. Western blot analysis indicated that variants were stable and expressed at levels indistinguishable from those in wildtype (Fig 2.7D). Next, we tested the ability of the variants to facilitate *oriC* capture in the single cell trapping assay (187). The $SirA_{Y51A}$ variant supported *oriC* capture at levels statistically indistinguishable from wildtype ($P>0.05$)(Fig 2.8). The $SirA_{F14A}$ variant produced a more intermediate phenotype, although it supported capture of the *oriC*-proximal reporter at levels more similar to wildtype than the Δ*sirA* mutant (4% vs. 10%)(Fig 2.8). These results further suggest that SirA's role in *oriC* capture can be uncoupled from its ability to inhibit DNA replication initiation.

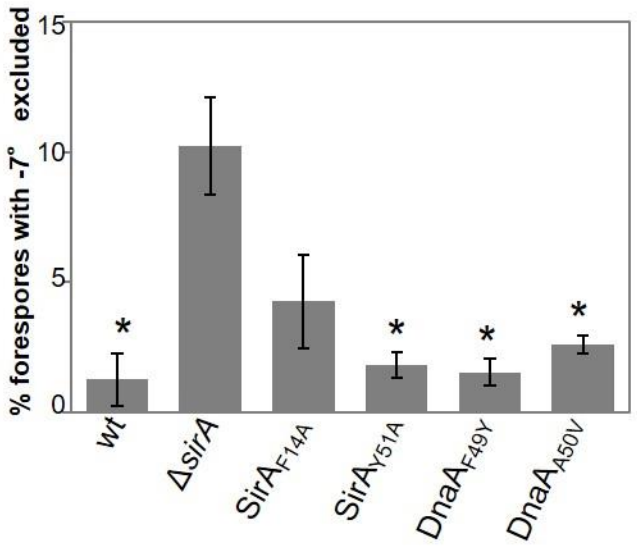

Fig. 2.8. SirA facilitates *oriC* capture independent of its ability to inhibit DNA replication. Single cell analysis indicating the average percentage of forespores that fail to capture the origin reporter (-7°) in the forespore during sporulation. Wildtype (BJH103), Δ*sirA* (BJH090), $sirA_{F14A}$ (BYD302), $sirA_{Y51A}$ (BYD067), $dnaA_{F49Y}$ (BYD073), $dnaA_{A50V}$ (BYD303). A minimum of 500 cells from each of four biological replicates was counted for each strain (total n >2000 average). Error bars indicate standard deviation from the average of the four trials. The data for wild-type and Δ*sirA* are identical to those in Fig 2.2. The asterisks indicate pairwise comparisons that were statistically indistinguishable (P>0.05, students t-test).

Although cells misexpressing $SirA_{Y51A}$ and $SirA_{F14A}$ during vegetative growth exhibited phenotypes consistent with a reduced ability to inhibit DnaA-dependent replication initiation (Fig 2.7B and 2.7C), it is possible the variants retained sufficient activity to inhibit DNA replication initiation during sporulation. Therefore, we extended our analysis to test *oriC* capture in cells harboring variants of DnaA ($DnaA_{F49Y}$ and $DnaA_{A50V}$) previously shown to be insensitive to SirA misexpression (81). We replaced wild-type *dnaA* with alleles encoding $DnaA_{F49Y}$ and $DnaA_{A50V}$ (markerless replacement of the wild-type gene at the native locus) and tested the ability of cells to resist the effects of SirA misexpression. Cells possessing either $DnaA_{F49Y}$ or $DnaA_{A50V}$ grew indistinguishably from wildtype during vegetative growth (Fig 2.9A) and possessed wild-type nucleoid morphology before SirA induction (Fig 2.9B), indicating that the variants were functional with respect to supporting DNA replication initiation in vivo. Both DnaA variants were also resistant to misexpression of SirA as judged by both growth on plates (Fig 2.9A) and nucleoid morphology (Fig 2.9B). These results confirm prior findings that cells utilizing $DnaA_{F49Y}$ or $DnaA_{A50V}$ are indeed resistant to SirA's ability to inhibit DNA replication initiation (81). Moreover, the variants did not detectably interact with wild-type SirA in a B2H assay (Fig 2.9C), consistent with the loss-of-interaction observed in a yeast two-hybrid assay (81).

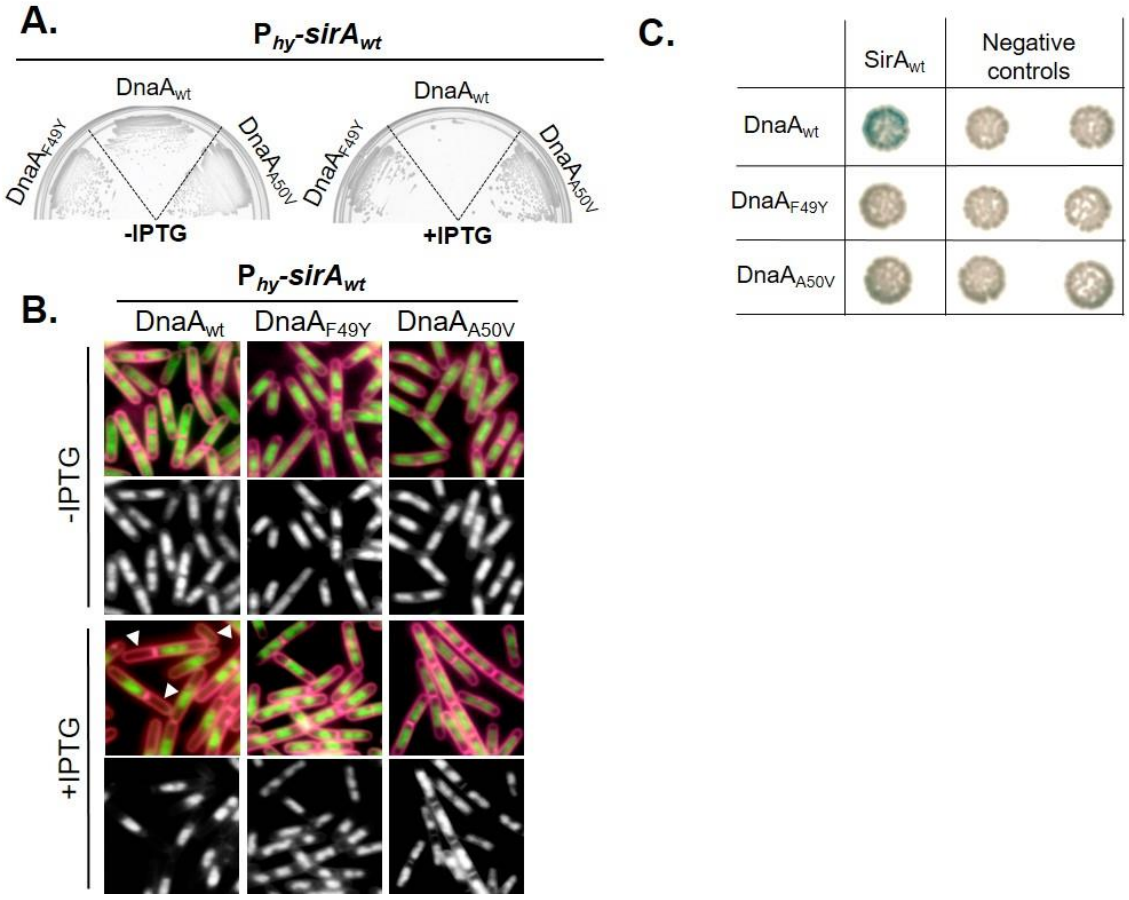

Fig. 2.9. $DnaA_{F49Y}$ and $DnaA_{A50V}$ are insensitive to SirA. (A) Growth of strains harboring P_{hy}-*sirA* in backgrounds encoding wild-type *dnaA* (BYD036), *dnaA*$_{F49Y}$ (BYD464) or *dnaA*$_{A50V}$ (BYD465) following misexpression. (B) The same misexpression strains grown in CH liquid media 1.5 hrs after the addition of 1mM IPTG. Cell membranes were stained with FM4-64 (pseudocolored pink) and DNA with DAPI (pseudocolored green). White arrowheads indicate example anucleate cells. (C) B2H assay between SirA and DnaA (CYD050), SirA and $DnaA_{F49Y}$ (CYD053), and SirA and $DnaA_{A50V}$ (CYD055). Negative controls: empty partner vector with wild-type DnaA or the indicated DnaA variant (column 1) or SirA with the empty partner vector (column 2).

To test if cells utilizing $DnaA_{F49Y}$ or $DnaA_{A50V}$ were compromised in *oriC* segregation, we performed the chromosome organization assay in strain backgrounds harboring alleles encoding either $DnaA_{F49Y}$ or $DnaA_{A50V}$ in place of wild-type *dnaA* at the native locus. Both $DnaA_{F49Y}$ and $DnaA_{A50V}$ supported capture of the *oriC*-proximal reporter at levels statistically indistinguishable from wild-type DnaA ($P>0.05$)(Fig 2.8). These results further support the conclusion that SirA's role in *oriC* capture is not dependent on its ability to inhibit DNA replication through its interactions with DnaA Domain I. At the same time, we do not exclude the possibility that SirA promotes *oriC* segregation through another DnaA-dependent mechanism.

2.3.4 Residues near the C-terminus of SirA and in DnaA Domain III promote interaction between the two proteins

Our data suggest that the DnaA Domain I interaction is not required for *oriC* segregation, and we identified one variant, $SirA_{P141T}$, that supported DNA replication but not *oriC* segregation. Since this substitution occurred in the extreme C-terminus of SirA in a region distal to the described SirA-DnaA interaction interface (Fig 2.5), we hypothesized that this second region of SirA might interact with a distinct region of DnaA to promote *oriC* segregation. We were unable to assess the possibility of a second interaction interface using known data, as the SirA-DnaA co-crystal structure could only be obtained using only DnaA Domain I (79). Moreover, the suppressor selection utilized to identify DnaA residues important for interaction relied upon the ability of SirA to inhibit DNA replication (81), which our data indicate is a genetically separable activity. Therefore, we designed two genetic screens to identify SirA and DnaA residues that contribute to interaction between the two full-length proteins.

To identify residues of DnaA important for interaction with SirA, we performed a gain-of-interaction screen based on the observation that $SirA_{Y51A}$ and wild-type DnaA do not detectably interact in the B2H assay (Fig 2.7A). We mutagenized *dnaA* and screened for DnaA variants that showed restored interaction with $SirA_{Y51A}$ (Table 2.5 and Fig 2.10). Unexpectedly, each of the nine variants we identified, $DnaA_{T116N}$, $DnaA_{F120S}$, $DnaA_{I122T}$, $DnaA_{H130D}$, $DnaA_{V136A}$, $DnaA_{K197N}$, $DnaA_{D215V,}$ $DnaA_{P255L,}$ and $DnaA_{G268R}$ possessed substitutions in DnaA Domain III (Table 2.5 and Fig 2.11), a region outside of the known SirA-DnaA interaction interface (79). Of note, $DnaA_{F120}$, $DnaA_{I122}$, and $DnaA_{H130}$ cluster to a region of DnaA Domain III previously implicated in the toxicity bypass associated with induced expression of Soj_{G12V}, a constitutive monomer of Soj that also shows gain of interaction with wild-type DnaA (143). These results could suggest SirA and Soj are capable of targeting the same region of DnaA, although we do not exclude other possibilities.

In a complementary approach, we took advantage of the fact that wild-type SirA and $DnaA_{A50V}$ do not interact in the B2H assay (Fig 2.9C) to identify regions of SirA important for SirA-DnaA interaction. We mutagenized *sirA* and screened for SirA variants that restored interaction with $DnaA_{A50V}$ (Table 2.5 and Fig 2.10). Surprisingly, all of the gain-of-interaction variants we identified ($SirA_{I103V}$, $SirA_{T113M,}$ $SirA_{V118M}$, $SirA_{K121N}$, and $SirA_{P141T}$) mapped to a region of SirA distal to the characterized SirA-DnaA Domain I binding interface (Table 2.5 and Fig 2.5). Taken together, the location of the variants identified in the two gain-of-interaction screens are consistent with the idea that residues in SirA's C-terminus interact directly with DnaA Domain III.

Table 2.5. Residues outside the characterized SirA-DnaA interface promote interaction. Identification of DnaA and SirA variants that result in gain of interaction with $SirA_{Y51A}$ and $DnaA_{A50V}$, respectively, in a B2H assay.

DnaA variants exhibiting gain of interaction with $SirA_{Y51A}$	
dnaA	**Variant**
ACT→AAT	T116N
TTT→TCT	F120S
ATC→ACC	I122T
CAT→GAT	H130D
GTA→GGA	V136A
AAA→AAT	K197N
GAT→GTT	D215V
CCG→CTG	P255L
GGA→AGA	G268R
SirA variants exhibiting gain of interaction with $DnaA_{A50V}$	
sirA	**Variant**
ATT→GTT	I103V
ACG→ATG	T113M
GTG→ATG	V118M
AAA→AAT	K121N
CCG→ACG	P141T

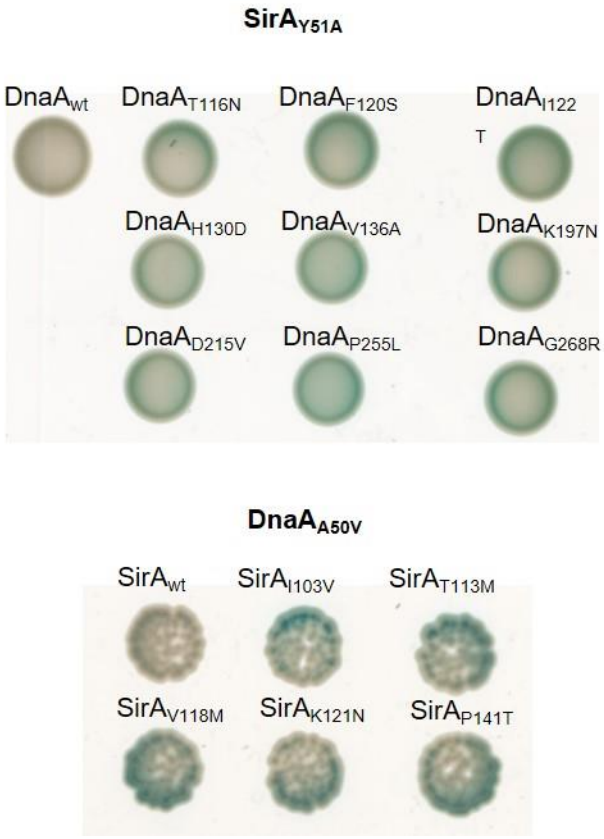

Fig. 2.10. Residues outside the characterized SirA-DnaA interface promote interaction between the two proteins. B2H assay between SirA$_{Y51A}$ and wild-type DnaA (CYD051), or SirA$_{Y51A}$ and each of the following DnaA variants: DnaA$_{T116N}$ (CYD602), DnaA$_{F120S}$ (CYD605), DnaA$_{I122T}$ (CYD608), DnaA$_{H130D}$ (CYD611), DnaA$_{V136A}$ (CYD626), DnaA$_{K197N}$ (CYD629), DnaA$_{D215V}$ (CYD632), DnaA$_{P255L}$ (CYD635), DnaA$_{G268R}$ (CYD638). (B) B2H assay between DnaA$_{A50V}$ and wild-type SirA (CYD055), and DnaA$_{A50V}$ and each of the following SirA variants: SirA$_{I103V}$ (CYD168), SirA$_{T113M}$ (CYD169), SirA$_{V118M}$ (CYD172), SirA$_{K121N}$ (CYD173), SirA$_{P141T}$ (CYD175).

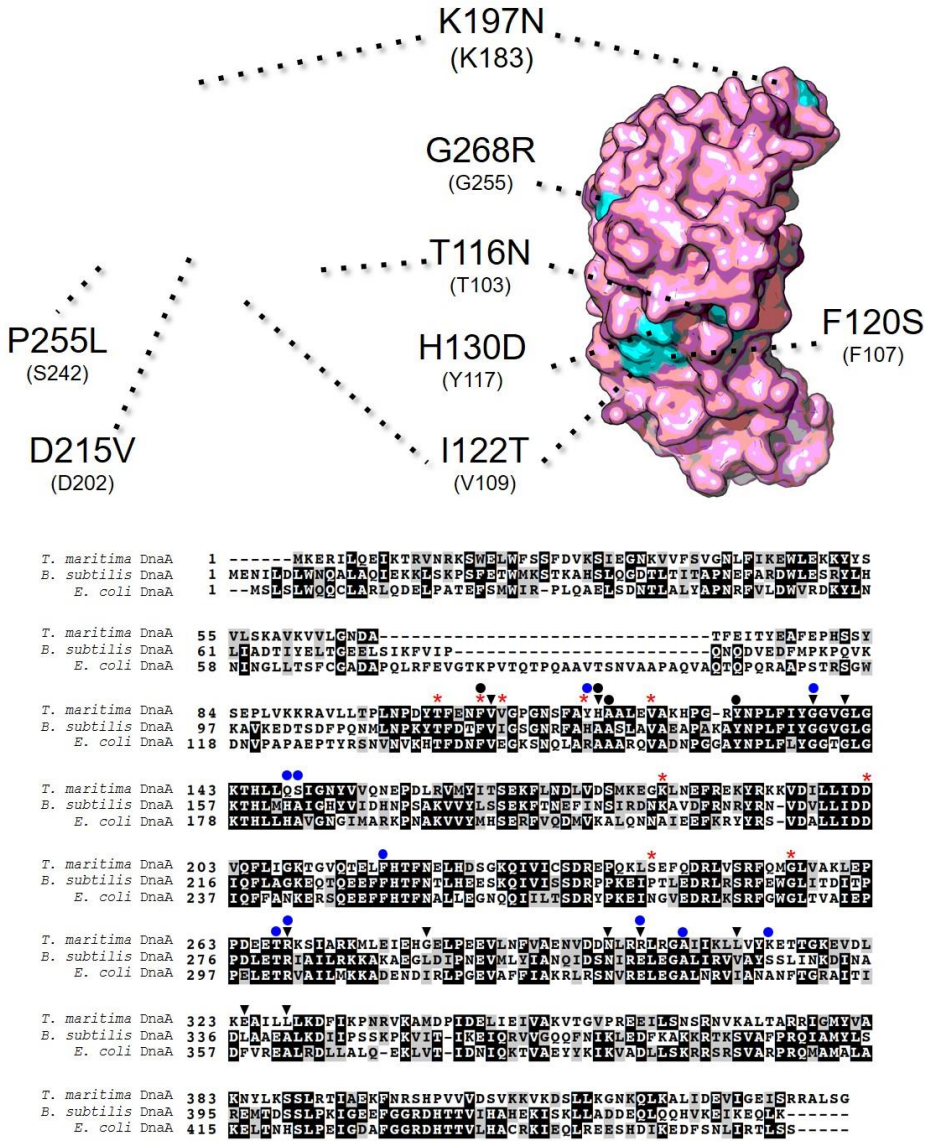

Fig. 2.11. DnaA Domain III crystal structure. Structure from PDB: 2Z4S (242). *T. maritima* DnaA Domain III (pink). The location of DnaA substitutions that exhibit gain of interaction with $SirA_{Y51A}$ are shown in cyan on the structure and indicated on the sequence alignment by red asterisks. The location of residue changes that confer resistance to Soj_{G12V} misexpression are indicated with filled black triangles on the sequence alignment. The location of residue changes that confer resistance to YabA misexpression are indicated with filled blue circles. The location of residues implicated in DnaD interaction are indicated with filled black circles.

Of note, $SirA_{P141T}$ was also identified in the SirA-Soj loss-of-interaction screen (Table 2.4 and Fig. 2.3), and each of the SirA-$DnaA_{A50V}$ gain-of-interaction variants identified also exhibited a loss of interaction with Soj in a B2H assay (Fig 2.12A). Moreover, with the exception of $SirA_{P141T}$ (Fig 2.3E) and $SirA_{T113M}$ (which were statistically different from wildtype, $P<0.05$), each of the variants fully supported wild-type capture of *oriC* (Fig 2.12B). None of the variants prevented colony formation on plates when misexpressed, suggesting they did not inhibit DNA replication (Fig 2.12C). These data further support the conclusion that SirA's roles in DNA replication and *oriC* segregation are functionally distinct.

In bacteria, DNA replication generally takes place at a single *oriC* and is followed by rapid segregation of the newly replicated origin toward the cell pole (or future cell pole)(Fig 2.1). The ParABS system, found in a wide-range of both Gram positive and Gram negative bacteria (136), has been implicated in the segregation of chromosomes following replication (243). However, in *B. subtilis*, cells without Soj (ParA) have no detectable defect in chromosome segregation during vegetative growth (139) and a majority (>98%) of cells lacking Spo0J (ParB) still effectively partition chromosomes between daughter cells (202). Spo0J becomes critical when chromosome condensation is severely impacted by the absence of a functional SMC complex (168), yet the SMC complex is itself only essential during conditions of fast growth (168, 206), and even an *smc spo0J* double mutant is still viable under slow growth conditions (168). Thus, although Spo0J and SMC are clearly important for fidelity, additional mechanisms likely exist to facilitate chromosome segregation.

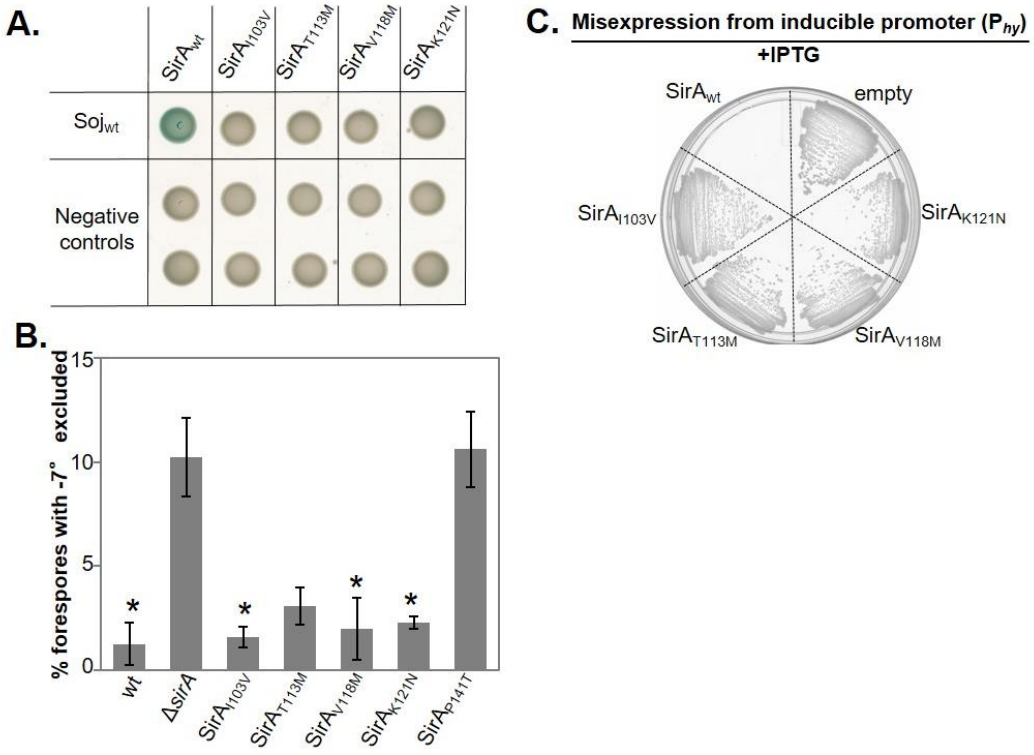

Fig. 2.12. Variants with mutations in residues outside the characterized SirA-DnaA interface can still segregate *oriC* but cannot inhibit DNA replication. (A) B2H assay between Soj and SirA (CYD286), and Soj and each of the following SirA variants: $SirA_{I103V}$ (CYD1050), $SirA_{T113M}$ (CYD715), $SirA_{V118M}$ (CYD716), $SirA_{K121N}$ (CYD717). Negative controls: empty partner vector with wild-type SirA or the indicated SirA variant (top row) or wild-type Soj with the empty partner vector (bottom row). (B) Single cell analysis indicating the average percentage of forespores that fail to capture the origin reporter (-7°) in the forespore during sporulation. Wildtype (BJH103), Δ*sirA* (BJH090), $sirA_{I103V}$ (BYD533), $sirA_{T113M}$ (BYD498), $sirA_{V118M}$ (BYD499), $sirA_{K121N}$ (BYD500). A minimum of 2,000 cells from four biological replicates were counted for each strain. The asterisks indicate pairwise comparisons that were statistically indistinguishable (P>0.05, students t-test). The difference between wildtype and $sirA_{T113M}$ was significant (P=0.04). Error bars indicate standard deviation from the average of the four trials. The data for wildtype, Δ*sirA*, and $sirA_{P141T}$ are the same as Figure 2.3. (C) Growth of strains harboring P_{hy}-*sirA* (BYD036), P_{hy}-$sirA_{I103V}$ (BYD549), P_{hy}-$sirA_{T113M}$ (BYD550), P_{hy}-$sirA_{V118M}$ (BYD551), P_{hy}-$sirA_{K121N}$ (BYD552) or P_{hy}-*empty* (BAM075) following misexpression.

2.4 Discussion

Recent evidence indicates that in *B. subtilis*, Soj's major function is to regulate DNA replication initiation by interacting directly with DnaA (140, 143). More specifically, a Soj monomer interacts directly with DnaA Domain III to inhibit DnaA oligomerization until the appropriate cell cycle cue is received for initiation (143). Spo0J participates in this regulation by stimulating Soj's ATPase activity, thus converting Soj from a dimer to a monomer (Fig 2.1, vegetative)(142). During sporulation, Soj is also important for ensuring that the replication origins of ~20% of sporulating cells are captured in the forespore compartment (187). It is not known if Soj's *oriC* capture function depends on its ability to regulate DnaA activity, however we observed that about half of the forespores that fail to capture *oriC* in a Δ*soj* mutant can be rescued by deleting *sda* (the percentage of *oriC*s out of forespore decreases from ~20% to ~10%)(Fig 2.2). Since Sda executes the sporulation block imposed on actively initiating cells (96), this result hints that the *oriC* capture defect may relate to the association of DnaA with *oriC.*

There is some precedence for DnaA affecting *oriC* positioning. In *Caulobacter crescentus*, which requires a functioning ParABS system for *oriC* segregation (199, 244), DnaA has been shown to promote *oriC* segregation independent of its role in initiating DNA replication (228). This finding raises the interesting possibility that other bacteria might also utilize initiator proteins to facilitate chromosome segregation. How might this occur? One possibility, which is supported by a growing body of data, is that regulators of DNA replication are spatially coupled to proteins that mark the boundaries of cell poles (and future cell poles) such as DivIVA (245, 246) and MinD (247).

Consistent with this hypothesis, Soj is capable of localizing at/near septa in a manner that depends on MinD (140, 248).

Restricting replication initiation to the boundaries of poles and future poles would be an efficient way to facilitate *oriC* segregation during vegetative growth (Fig 2.1), but it would also pose a new problem for sporulating *B. subtilis*; during sporulation, the cell quarters become the sites where polar division occurs, so positioning of *oriC* at these sites could drastically decrease the probability of *oriC* being captured on the forespore side of the septum. RacA presumably decreases this probability by anchoring the centromere-like element generated by Spo0J bound at *parS* sites at the extreme cell pole in a DivIVA-dependent manner (20, 138, 233). Additionally, MinD was recently shown to act upstream of Soj in *oriC* capture (144). Interestingly, GFP-MinD shows a significant redistribution from the cell quarter toward a subpolar position during sporulation, and the authors of this study propose that MinD is part of a larger polar segregation complex (which includes Soj), that facilitates redistribution of *oriC* from the cell quarter toward the extreme cell pole (Fig 2.1)(144).

In the present study, our goal was to further investigate the relationship between *oriC* segregation and the activity of the DnaA inhibitor SirA (7, 79, 81). We found that in addition to inhibiting DNA replication, SirA is also important for chromosome segregation during sporulation. More specifically, we found that 10% of sporulating cells require SirA to capture *oriC* in the forespore (Fig 2.2). Epistasis experiments indicate that SirA acts in the same pathway as Soj to facilitate *oriC* segregation (Fig 2.2). Intriguingly, Soj and SirA interact in a B2H assay (Fig 2.3A and 2.12A); however, since most of the SirA-Soj loss-of-interaction variants remain functional with respect to facilitating *oriC* capture (Fig 2.3E and 2.12B), the physiological relevance of this interaction is currently unclear. The G12V substitution in Soj that exhibits gain of

interaction with DnaA (140) occurs at the interface of a Soj dimer and prevents dimer formation (142). Therefore, one speculation is that if SirA and Soj target the same surface on DnaA Domain III (this remains to be determined, see below), Soj and SirA may be capable of forming a heterodimer.

One of the most significant findings in this study is the observation that SirA's ability to inhibit DNA replication through contacts with DnaA Domain I appears to be completely distinct from SirA's role in *oriC* segregation. DnaA variants insensitive to SirA's replication inhibiting activity ($DnaA_{F49Y}$ or $DnaA_{A50V}$) and several SirA variants perturbed in their ability to inhibit DNA replication ($SirA_{Y51A}$, $SirA_{I103V}$, $SirA_{V118M}$, and $SirA_{K121N}$), each exhibit wild-type *oriC* capture phenotypes (Fig 2.8 and Fig 2.12B). Reciprocally, we identified one SirA variant ($SirA_{P141T}$) that inhibits DNA replication, yet is unable to support *oriC* capture. Functional analyses of several SirA-DnaA gain-of-interaction variants further suggest that the *oriC* capture function of SirA is mediated through a previously uncharacterized interaction between SirA and DnaA Domain III. Interestingly, we did not identify even a single compensatory substitution that restored interaction at the known interface between in SirA and DnaA Domain I in either of the gain of interaction screens, suggesting the requisite substitutions are rare or may require more than one amino acid change. In addition, although we think it is unlikely since SirA does not interact with wild-type *E. coli* DnaA (81), we also cannot exclude the possibility that the gain of interactions we observe are mediated through one or more *E. coli* proteins acquiring the capacity to bridge the interaction between SirA and DnaA in the B2H.

In the absence of structural data, we are unable to confidently assess if SirA might have the capability to interact with DnaA Domain I and Domain III simultaneously, or if such an interaction would be mutually exclusive (either DnaA

Domain I or Domain III). We favor the second model, as all but one of the SirA-DnaA gain-of-interaction variants we identified support *oriC* capture (Fig 2.12B), but no longer prevent growth following misexpression (Fig 2.12C). We hypothesize that these SirA variants do not kill because they have an increased propensity to interact with Domain III over Domain I.

Several of the substitutions in DnaA Domain III that show gain of interaction with SirA (specifically $DnaA_{F120S}$, $DnaA_{I122T}$, and $DnaA_{H130D}$) map to a surface previously shown to suppress the toxicity associated with overexpression of Soj_{G12V}, a monomeric variant of Soj (Fig 2.11)(143). Interestingly, Soj_{G12V} also shows gain of interaction with DnaA (140). Substitutions obtained in residues in this region of DnaA (A132 and A131) also exhibited overreplication phenotypes that could act as general suppressors of replication inhibition, thus this region of DnaA was not considered a likely location for direct interaction with Soj (143). Residues in this region of DnaA have also been implicated as possible sites of interaction with YabA and DnaD (Fig 2.9)(127, 249), two other DnaA regulators that can also inhibit DnaA oligomerization (127, 250). It is feasible that if Soj targets this surface of DnaA, then substitutions that change the Soj-DnaA interaction might also affect DnaD and YabA binding, leading to overreplication.

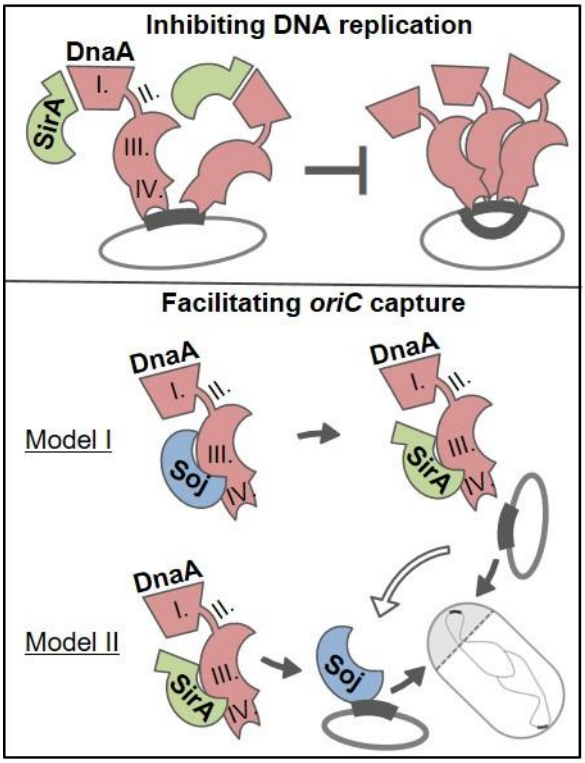

Fig. 2.13. Models for SirA activity. SirA inhibits DNA replication through interactions with DnaA Domain I; this activity is not required for *oriC* capture. SirA targets DnaA Domain III to maintain *oriC* in a state favorable for repositioning. In Model I, Soj acts upstream of SirA, generating a conformation of DnaA favorable for SirA association. The association of SirA with DnaA Domain III then permits *oriC* repositioning. In Model II, Soj acts downstream of SirA to facilitate *oriC* capture. Model I does not exclude the possibility that Soj may also be required to facilitate *oriC* capture through an independent, downstream mechanism (open arrow).

If SirA targets the same surface of DnaA Domain III as Soj, then why would both SirA and Soj be required to reposition *oriC* toward the extreme cell pole during sporulation (Fig 2.13)? Current data does not reveal if SirA acts upstream, downstream, or in parallel with Soj in *oriC* capture. We hypothesize that at some point prior to polar division, Soj is no longer able to perform its function in inhibiting new rounds of DNA replication, perhaps because it is repositioned toward the distal pole via interactions with MinD (144) or because Spo0J is no longer available to stimulate formation of the Soj monomer. In this capacity, SirA could functionally replace Soj (Fig 2.13), interacting with DnaA Domain III and thereby inhibiting oligomerization at *oriC* (Fig 2.13). SirA could also prevent DnaA from associating with the membrane-associated initiation proteins DnaD/B, thus keeping *oriC* free to segregate. The additional requirement of Soj for *oriC* capture could also suggest that Soj is required to create a conformation of DnaA favorable for SirA to bind DnaA Domain III (Fig 2.13, Model I), and/or that Soj acts downstream of SirA to facilitate *oriC* repositioning through an independent mechanism (Fig 2.13, Model I and II). Regardless of the mechanism, we propose that in this capacity, SirA's function is to ensure that the 10% of cells that would otherwise fail to capture *oriC* are able to do so. This 10% decrease may seem small, however since *oriC* capture is critical for successful sporulation (22), having such failsafe mechanisms in place would result in a significant fitness advantage in the face of selective pressures like desiccation.

It is intriguing that Soj and SirA, two different proteins involved in *oriC* positioning, also directly regulate aspects of initiator function. Jacob and Brenner, in their discussion of the replicon model for DNA replication in bacteria, alluded to the possibility of such a connection more than 50 years ago. "In bacteria, a simple and precise system insuring both the regulation of chromosome duplication and the

distribution of the two formed chromosomes to the two daughter cells could result from a connection between the chromosome and the bacterial surface; the initiator, for instance, being attached to some specific structure of the cell surface" (251). Although some details of their model turned out to be wrong (for example, elongation between anchored origins does not account for the rapid segregation of chromosomes following initiation), the core idea that interactions among the initiator, the chromosome, and the membrane could help partition chromosomes still remains a valid model. Such a model explains not only the robustness of chromosome segregation observed in model systems, but also hints at how chromosome partitioning may have evolved in early forms of life proliferating through vesiculation and blebbing of membranes (252).

CHAPTER III

SirA INHIBITS DNA REPLICATION INITIATION BY INTERACTING WITH DnaA DOMAIN I DURING *Bacillus subtilis* SPORULATION

3.1 Introduction

In bacteria, the initiator protein DnaA is precisely regulated to tightly control DNA replication initiation and consequently, genome inheritance (46, 97, 253). DnaA is essential, highly conserved, and possesses four functional domains (74). Domain I, which is close to the N-terminus, has been to shown to be important for DnaA self-dimerization (76) and helicase loading (75), as well as interaction with several regulators of DNA replication, including DiaA in *Escherichia coli* (78, 80) and HobA in *Helicobactor pylori* (126). Domain II is a non-essential flexible linker and is poorly conserved (84), although some data suggest it may stimulate helicase loading in *E. coli* (254). Domain III is the largest domain and possesses an AAA+ ATPase region (74), that is critical for ATP binding and hydrolysis as well as DnaA oligomerization (85, 86). Domain IV, which is located at the C-terminus, possesses the helix-turn-helix motif that mediates DNA binding (65).

During replication initiation, DnaA binds to and oligomerizes at the origin region and unwinds it, allowing other replisome components, such as helicase and DNA polymerase, to be loaded (63, 65). In *E. coli*, the replicative helicase DnaB is loaded to the unwound origin region with the help of the helicase loader DnaC (68-70); in *B. subtilis*, which follows different naming conventions for some of the replication proteins, three additional proteins, DnaD, DnaB and DnaI, are also needed in order to load the replicative helicase DnaC (72, 73). After DnaA-dependent *oriC* unwinding, DnaD is

recruited to DnaA, followed by the membrane-associated protein DnaB (72). The addition of DnaB to the complex leads to recruitment of the helicase loader DnaI, which then facilitates loading of the replicative helicase DnaC and DNA polymerase III (Fig 1.3)(73).

During rapid growth, *B. subtilis* can initiate a new round of DNA replication before completing the prior rounds of synthesis, resulting in cells with 2, 4, or even 8 copies of *oriC* (16). However, during sporulation, only two copies of the genome are required, and mechanisms exist to shut down new rounds of DNA replication (24). Three independent mechanisms have been shown to contribute to the regulation of DNA replication during sporulation. First, new rounds of replication are prevented in response to an entry into stationary phase (32). Second, the global sporulation response regulator, Spo0A, has been shown to repress the expression of *dnaA*, *dnaN* and *dnaG*, genes that encode replisome components (36). Finally, a sporulation specific protein, SirA (Sporulation inhibitor of replication A) is synthesized, maintaining sporulating cells in a diploid state by interacting directly with the initiation protein DnaA (7, 79, 81). A Δ*sirA* mutant shows an over-replication phenotype during sporulation, sometimes resulting in production of so-called "twins" in which a single mother cell generates two spores (7). The twin spores are defective in germination, indicating that over-replication is detrimental for the sporulating cell (92, 255).

SirA, which is the main focus of this dissertation, has been shown to inhibit DNA replication initiation by interacting with DnaA (7, 81). At the time this study was initiated, very little was known about how SirA inhibited DnaA function. To better characterize SirA's mechanism of action, conditions to overexpress a soluble form of SirA were screened. Although no conditions were found to solubilize SirA, co-expression of SirA with DnaA, but not DnaD or DnaB resulted in an altered degradation

pattern during expression testing. Bacterial two-hybrid (B2H) interaction screening indicated that if SirA interacts with DnaD or DnaB, then such interactions are below the threshold of detection for the assay.

To identify possible functional targets associated with SirA misexpression during vegetative growth, suppressors resistant to SirA-mediated inhibition of DNA replication were isolated. All of the isolated suppressors identified, both spontaneous and following NTG-mediated mutagenesis, generated one of four substitutions in DnaA Domain I: $DnaA_{N47D}$, $DnaA_{F49Y}$, $DnaA_{A50T}$ and $DnaA_{A50V}$. These results suggested that DnaA is likely the only target required for SirA-mediated inhibition of DNA replication, and implicated DnaA Domain I as the possible interaction interface for SirA. In 2011, Rahn-Lee et al. published a study showing that DnaA Domain I is sufficient for SirA interaction in yeast two-hybrid (Y2H)(81). These authors also showed that a positive interaction between SirA and *E. coli* $DnaA_{V47A}$ (but not wild-type *E. coli* DnaA) was detected by Y2H (81). To test if SirA would target DnaA activity in a heterologous system, an *E. coli*-based plasmid maintenance assay was developed. The results suggest that SirA can target *E. coli* $DnaA_{V47A}$ activity, even though *E. coli* lacks DnaD and DnaB, consistent with the idea that SirA acts to inhibit DNA replication primarily through targeting of DnaA. In 2014, Jameson et al. solved a structure of SirA in complex with DnaA Domain I (79). The results of this study corroborated the genetic results obtained by both Rahn-Lee et al and our group indicating that SirA interacts directly with DnaA Domain I.

3.2 Materials and methods

3.2.1 General methods

All *B. subtilis* strains were derived from *B. subtilis* 168. *E. coli* and *B. subtilis* strains utilized in this study are listed in Table 3.1. Plasmids are listed in Table 3.2. Oligonucleotide primers are listed in Table 3.3.

All cloning was carried out in *E. coli* DH5α. *E. coli* strain DHP1 was used for assaying interaction in the B2H. For transformation of *E. coli*, antibiotics were included at the following concentrations when indicated: 100 µg/ml ampicillin, and 25 µg/ml kanamycin. For transformation and selection of *B. subtilis*, antibiotics, when required, were included at the following concentrations: 100 µg/ml spectinomycin, 0.8 µg/ml phleomycin, and 1 µg/ml erythromycin with 25 µg/ml lincomycin (MLS).

Table 3.1. Strains used in Chapter III.

Strain	Description	Reference
Parental		
B. subtilis 168	*Bacillus subtilis* laboratory strain 168 *trpC2*	BGSC (1A866)
B. megaterium WH320	*Host strain for B. megaterium protein expression system*	MoBiTec
E. coli DH5α	*F- endA1 glnV44 thi-1 recA1 relA1 gyrA96 deoR nupG Φ80dlacZΔM15 Δ(lacZYA-argF)U169, hsdR17(r_K^- m_K^+), λ–*	
E. coli DHP1	*F-, cya-99, araD139, galE15, galK16, rpsL1 (Strr), hsdR2, mcrA1,mcrB1;*	Tom Bernhardt
E. coli BL21 (DE3)	F– *ompT gal dcm lon hsdS$_B$*($r_B^-m_B^-$) [*malB*$^+$]$_{K\text{-}12}$(λ^S) λ(DE3 [*lacI lacUV5-T7p07 ind1 sam7 nin5*])	
E. coli BL21 (DE3) pLysS	F– *ompT gal dcm lon hsdS$_B$*($r_B^-m_B^-$) [*malB*$^+$]$_{K\text{-}12}$(λ^S) λ(DE3 [*lacI lacUV5-T7p07 ind1 sam7 nin5*]) pLysS[*T7p20 ori*$_{p15A}$](Cm^R)	
E. coli MG1655	K-12 F– λ– *ilvG– rfb-50 rph-1*	
E. coli MS3898	*asnB32 relA1 spoT1 thi-1 ilv-192 zia::pKN500 (pKN500=mini-R1)* *dnaA mad-2 (F-) recA1 (imm434)*	Jon M. Kaguni
***B. subtilis* 168**		
BYD027	*amyE::*P$_{hy}$*-sirA (spec), yhdG::*P$_{hy}$*-sirA (phleo), sacA::*P$_{hy}$*-lacZ (erm)*	This study
DHP1		
CYD050	*dnaA-T25 (kan), sirA-T18 (amp)*	This study
CYD052	*dnaA$_{N47D}$-T25 (kan), sirA-T18 (amp)*	This study
CYD053	*dnaA$_{F49Y}$-T25 (kan), sirA-T18 (amp)*	This study
CYD054	*dnaA$_{A50T}$-T25 (kan), sirA-T18 (amp)*	This study
CYD055	*dnaA$_{A50V}$-T25 (kan), sirA-T18 (amp)*	This study
CYD060	*dnaA-T25 (kan), empty-T18 (amp)*	This study
CYD061	*empty-T25 (kan), sirA-T18 (amp)*	This study
CYD063	*dnaA$_{N47D}$-T25 (kan), empty-T18 (amp)*	This study
CYD065	*dnaA$_{A50T}$-T25 (kan), empty-T18 (amp)*	This study
CYD066	*dnaA$_{A50V}$-T25 (kan), empty-T18 (amp)*	This study
CYD092	*dnaA$_{S23A}$-T25 (kan), sirA-T18 (amp)*	This study
CYD093	*dnaA$_{E25A}$-T25 (kan), sirA-T18 (amp)*	This study
CYD094	*dnaA$_{W27A}$-T25 (kan), sirA-T18 (amp)*	This study
CYD095	*dnaA$_{W53A}$-T25 (kan), sirA-T18 (amp)*	This study
CYD098	*dnaA$_{S23A}$-T25 (kan), empty-T18 (amp)*	This study

Table 3.1. Continued.

Strain	Description	Reference
CYD099	*dnaA$_{E25A}$-T25 (kan), empty-T18 (amp)*	This study
CYD100	*dnaA$_{W27A}$-T25 (kan), empty-T18 (amp)*	This study
CYD101	*dnaA$_{W53A}$-T25 (kan), empty-T18 (amp)*	This study
CYD123	*dnaA$_{F24A}$-T25 (kan), sirA-T18 (amp)*	This study
CYD124	*dnaA$_{T26S}$-T25 (kan), sirA-T18 (amp)*	This study
CYD125	*dnaA$_{E48R}$-T25 (kan), sirA-T18 (amp)*	This study
CYD126	*dnaA$_{R51L}$-T25 (kan), sirA-T18 (amp)*	This study
CYD127	*dnaA$_{D52N}$-T25 (kan), sirA-T18 (amp)*	This study
CYD131	*sirA-T25 (kan), empty-T18 (amp)*	This study
CYD137	*dnaA$_{F24A}$-T25 (kan), empty-T18 (amp)*	This study
CYD138	*dnaA$_{T26S}$-T25 (kan), empty-T18 (amp)*	This study
CYD139	*dnaA$_{E48R}$-T25 (kan), empty-T18 (amp)*	This study
CYD140	*dnaA$_{R51L}$-T25 (kan), empty-T18 (amp)*	This study
CYD141	*dnaA$_{D52N}$-T25 (kan), empty-T18 (amp)*	This study
CYD492	*sirA-T25 (kan), T18-dnaD (amp)*	This study
CYD499	*sirA-T25 (kan), dnaB-T18 (amp)*	This study
CYD537	*empty-T25 (kan), dnaB-T18 (amp)*	This study
CYD595	*empty-T25 (kan), T18-dnaD (amp)*	This study
CYD686	*sirA-T25 (kan), T18-empty (amp)*	This study
MG1655		
CJW089	*sirA-pBAD24 (amp)*	David Z. Rudner
MS3898		
CYD227	*pBR322 in MS3898*	This study
CYD228	*pRB100 in MS3898*	This study
CYD229	*pYD192 in MS3898*	This study
CYD237	*pYD193 in MS3898*	This study
CYD238	*pYD194 in MS3898*	This study
CYD239	*pYD195 in MS3898*	This study
CYD267	*pYD196 in MS3898*	This study
CYD268	*pYD197 in MS3898*	This study
CYD269	*pYD198 in MS3898*	This study

Table 3.2. Plasmids used in Chapter III.

Plasmid	**Description**	**Reference**
pACYC184	*non-oriC plasmid (cat)*	Jon M. Kaguni
pBR322	*non-dnaA plasmid (amp)*	Jon M. Kaguni
pCM959-Cm^R	*E. coli oriC-pACYC184 (cat)*	Jon M. Kaguni
pJW029	*sirA-pBAD24 (amp)*	David Z. Rudner
pKM328	*dnaA-His6-sirA-pET DUET (amp)*	David Z. Rudner
pLM022	*sirA-His6-pET24b+ (kan)*	David Z. Rudner
pLM023	*His6-sirA-pRsetA (kan)*	David Z. Rudner
pRB100	*E. coli dnaA-pBR322 (amp)*	Jon M. Kaguni
pYD025	*dnaB-His6-sirA-pET DUET (amp)*	This study
pYD026	*dnaD-His6-sirA-pET DUET (amp)*	This study
pYD030	*sirA-His6-pMM1522 (amp)*	This study
pYD052	*His6-SUMO-sirA-pTB146 (amp)* *(sirA from B. megaterium)*	This study
pYD053	*His6-SUMO-sirA-pTB146 (amp)* *(sirA from B. licheniformis)*	This study
pYD054	*His6-SUMO-sirA-pTB146 (amp)* *(sirA from B. amyloliquefaciens)*	This study
pYD192	*E. coli $dnaA_{V47A}$-pBR322 (amp)*	This study
pYD193	*sirA-pBR322 (amp)*	This study
pYD194	*E. coli dnaA-sirA-pBR322 (amp)*	This study
pYD195	*E. coli $dnaA_{V47A}$-sirA-pBR322 (amp)*	This study
pYD196	*$sirA_{Y51A}$-pBR322 (amp)*	This study
pYD197	*E. coli dnaA-$sirA_{Y51A}$-pBR322 (amp)*	This study
pYD198	*E. coli $dnaA_{V47A}$-$sirA_{Y51A}$-pBR322 (amp)*	This study

Table 3.3. Oligonucleotides used in Chapter III.

Oligo	**Sequence 5' to 3'**
OJH083	ATGACAGAGAAACAGATTCAAGCTATTACACAACCAATCCCG A
OJH165	TATACATATGGCTGACTATTGGAAAGAT
OJH166	TCGAGGGTACCGACTTAATAGGCAGAGTATTTTTTCA
OJH167	TATACATATGAAAAAACAGCAATTTATTGATA
OJH168	TCGAGGGTACCGACTTATTGTTCAAGCCAATTGTAAAA
OJH169	GATCCGAATTCGATGGAACGTCACTACTATACG
OJH170	AGCTTGTCGACCTGTTAGACAAAATTTCTTTCTTTCAC
OYD054	GGGAAATGTACAATGGAACGTCACTACTATACG
OYD055	GCCGGCATGCGGGACAAAATTTCTTTCTTTCAC
OYD075	AAAAAGCTCTTCCGGTGTGAGAACGTATGAAGTATATTT
OYD076	TTTTTCTCGAGTTACACAAATTTTCTTGTTTTCACAG
OYD077	AAAAAGCTCTTCCGGTATGGAACGCCATTATTATACGTATT
OYD078	TTTTTCTCGAGTTATACAAAATTTCTTTCTTTCACAGG
OYD079	AAAAAGCTCTTCCGGTATGGAACGTCATTACTATACACAC
OYD080	TTTTTCTCGAGTTAGACAAAATTTCTTTCTCTGACC
OYD159	CTTGTCCCGTACCCAATCGAGGGCAAAACGGTTTGGCGCGTA C
OYD160	GTACGCGCCAAACCGTTTTGCCCTCGATTGGGTACGGGACAA G
OYD193	CATTGCTGCAGGCATCGTGG
OYD194	AGGTTTACGATGACAATGTTCTG
OYD195	CACCGCATGCAGCAGGTGAG
OYD214	TCGGGATTGGTTGTGTAATAGCTTGAATCTGTTTCTCTGTCAT
OYD238	GATCCATATGGGATTTGTCCTACTCAGGAG
OYD251	GATCGCTCTTCCAGCTGACGTCTAAGAAACCATTATTAT

3.2.2 Protein overexpression in *E. coli*

10 ng of plasmid was transformed into 100 µl *E. coli* BL21 (DE3) chemical competent cells (treated by RbCl, see details below) and plated on an LB-Lennox agar plate with proper antibiotics. Fresh colonies were used to inoculate 25 ml of Cinnabar media (Teknova) in a 250 ml baffled flask with appropriate antibiotic, and culture was placed in shaking waterbath set at 280 rpm and 30°C. Cells were grown to an OD_{600} of 5, at which time 100 µl of uninduced cell pellet was collected by centrifugation at 6,010 x g for 1 min at room temperature. The supernatant was removed by aspiration and the pellet placed at -80°C until processing. Protein expression was induced for 5 hrs following the addition of 1 mM IPTG. To test for induction, 100 µl of cells were collected as described above. To analyze induction, pellets were resuspended in 50 µl SDS sample buffer and samples were boiled for 10 min prior to loading on a 4-20% Tris-Glycine protein gel (BioRad). Samples were normalized to each other by OD_{600} values. For solubility test, cultures were pelleted in a 50 ml falcon tube at 2,576 x g for 10 min at room temperature. Pellets were resuspended in 5 ml lysis buffer [50 mM Tris-HCl pH 8.0, 300 mM NaCl, 10 mM imidazole, 200 µg/ml lysozyme, 10 µg/ml DNase, 10 µl protease inhibitor cocktail P8465 (sigma)] and the cells were lysed by using a French press. Cell debris as well as insoluble proteins were separated from the soluble proteins by spinning down at 13,000 x g for 30 min at 4°C. The supernatant (containing soluble proteins) were transferred to a new 50 ml falcon tube and the pellets were resuspended in 10 ml SDS sample buffer. 50 µl of the supernatant was mixed with 50 µl 2X SDS sample buffer and boiled for 10 min. 100 µl of the resuspended pellet was also boiled for 10 min. Samples were normalized to each other by OD_{600} values. Protein gels were ran at 80 V for 30 min at room temperature, followed by 200 V for 30 min at room

temperature. Gels were stained with coomassie blue for 2 hrs at room temperature and destained with 10% acetic acid, 50% methanol and 40% dH_2O at room temperature overnight.

3.2.3 Protein purification by Nickel column affinity chromatography

Protein expression and cell lysis are almost the same as above except for the modifications below: plasmids were transformed into *E. coli* BL21 (DE3) pLysS cells; the cells were grown with proper antibiotics and 0.1% glucose; cell pellets were resuspended in 30 ml lysis buffer [50 mM Tris-HCl pH 8.0, 300 mM KCl, 10% glycerol, 20 mM imidazole, 10 µg/ml DNase, 10 µl protease inhibitor cocktail P8465 (sigma)].

The soluble part (supernatant) is then purified by Nickel column affinity chromatography. 1 ml Ni-NTA Agarose beads (0.5 ml bed volume) were equilibrated by lysis buffer and then the supernatant was loaded on the column. Flow-through was stored in a 50 ml falcon tube for later use. Column was then washed with 10 ml wash buffer (the same as lysis buffer) and then eluted eight times with 250 µl elution buffer [50 mM Tris-HCl pH 8.0, 300 mM KCl, 10% glycerol, 250 mM imidazole]. All the samples were normalized by OD_{600} prior to loading on the gel.

3.2.4 In vitro protein synthesis

Reactions were carried out according to manufacturer instructions using 1µg PCR product as template. The PCR product template for the expression of N-terminal 6X His tagged SirA was amplified by using pLM023 as the template and OJH140/OJH142 as the primers. The PCR product template for the expression of C-

terminal 6X His tagged SirA was amplified by using pLM022 as the template and OJH140/OJH141 as the primers. For the Qiagen EasyXpress Protein Synthesis Kit, 1 µg template, 17.5 µl *E. coli* extract and 20 µl EasyXpress Reaction Buffer were mixed, adding RNase-free water to the total volume of 50 µl. The reaction was incubated at 37°C for 1 hr and then centrifuged at 21,130 x g for 5 min at room temperature. The supernatant was transferred to another tube, adding 50 µl of 2X SDS sample buffer and boiled for 10 min prior to loading on the gel. The pellet was resuspended in 100 µl 1X SDS sample buffer and boiled for 10 min prior to loading. For the NEB PURExpress® *In Vitro* Protein Synthesis Kit, 1 µg template, 10 µl solution A and 7.5 µl solution B were mixed, adding nuclease-free water to the total volume of 25 µl. The mixture was incubated at 37°C for 2 hrs and centrifuged at 21,130 x g for 5 min at room temperature. The supernatant was transferred to another tube and 25 µl of 2X SDS sample buffer was added. The sample was boiled for 10 min prior to loading on the gel; the pellet was resuspended in 50 µl 1X SDS sample buffer and boiled for 10 min prior to loading.

3.2.5 Protoplasting *Bacillus megaterium*

One freshly streaked single colony was inoculated in 5 ml LB-Lennox medium and grown at 37°C to mid-exponential phase. Cells were pelleted at 2,576 x g for 10 min at room temperature and washed twice with 1X SMM buffer [500mM sucrose, 20mM maleic acid, 20mM magnesium chloride, pH 6.5]. Pellets were resuspended in 500 µl 1X SMM buffer containing 500 µg/ml lysozyme, gently shaked for 30 min at room temperature until 90% of the cells have protoplasted. Cells were then spun down at 2,576 x g for 10 min at room temperature, aliquoted in 500 µl and stored at -80°C until use.

3.2.6 Transformation of *B. megaterium* protoplasts

500 µl of protoplast suspension (see above) was thawed on ice and 5 µg plasmid was added. 1.5 ml of 1X SMM buffer containing 40% (w/v) PEG6000 was then added and the protoplasts were incubated for 2 min at room temperature. 5 ml 1X SMM buffer was added and the protoplasts were gently mixed. Protoplasts were harvested by centrifugation at 1,300 x g for 10 min at room temperature. The supernatant was discarded and the pellets were resuspended in 500 µl 1X SMM buffer, and gently agitated at 37°C for 1.5 hrs. 200 µl cells were then added into 2.5 ml CR5-top agar [300mM sucrose, 30mM 3-morpholinopropane-1-sulfonic acid (MOPS), 16.5mM NaOH pH 7.3; 15mM potassium sulfate, 50mM magnesium chloride, 20mM calcium chloride, 0.4mM monopotassium phosphate, 50mM proline, 1% glucose; 0.2 mg/ml casamino acids, 10 mg/ml yeast extract, 0.4% agar], gently mixed and poured onto a prewarmed LB-Lennox agar plate supplemented with 10 µg/ml tetracycline. Plates were incubated at 37°C overnight and colonies that arose were re-streaked on a fresh LB-Lennox agar plate supplemented with 10 µg/ml tetracycline.

3.2.7 Protein overexpression in *B. megaterium*

One freshly streaked single colony was inoculated in 5 ml LB-Lennox medium supplemented with 10 µg/ml tetracycline, and grown at 37°C to mid-exponential phase. The culture was back-diluted to OD_{600} = 0.02 in 25 ml LB-Lennox medium supplemented with 10 µg/ml tetracycline in a 250 ml baffled flask, and grown at 37°C in a shaking waterbath set at 280 rpm to OD_{600} = 0.3. 1 ml uninduced sample was collected by centrifugation at 6,010 x g for 1 min at room temperature. Xylose was added to the

culture to a final concentration of 0.5% (w/v) to induce protein expression. Cultures were grown at 37°C until OD_{600} = 1.5. 1 ml sample was pelleted at the same way as described above. Pellets for both uninduced and induced samples were resuspended in 50 µl lysis buffer [20 mM Tris pH 7.5, 1 mg/ml lysozyme, 10 µg/ml DNase I, 100 µg/ml RNase A, 1 mM phenylmethylsulfonyl fluoride (PMSF)] and incubated for 15 min at room temperature. 50 µl 2X SDS sample buffer was added, boiled for 10 min prior to loading. Lysate loads were normalized by OD_{600} values obtained at the time of cell harvest.

3.2.8 Western blot analysis

Protein samples were prepared as described in the above paragraphs. Western blots were performed essentially the same as described in Materials and Methods in Chapter II. 5 µl of each sample was loaded on a 4-20% Tris-HCl gradient gels (BioRad). Proteins were transferred to nitrocellulose membrane (Pall) for 1 hr at 60 V on an ice bath. Membranes were blocked in PBS [pH 7.4] containing 0.05% Tween-20 and 5% non-fat milk powder (w/v). Membranes were incubated overnight at 4°C with a 1:1,000 dilution of α-SirA peptide antibody (CSKRYGWLNPVKERN, Genscript) in PBS [pH 7.4] containing 0.05% Tween-20 and 5% non-fat milk powder (w/v) and washed. The membranes were then incubated with a 1:10,000 dilution of horseradish peroxidase-conjugated goat anti-rabbit immunoglobulin G secondary antibody (Bio-Rad) in PBS [pH 7.4] containing 0.05% Tween-20 and 5% non-fat milk powder (w/v) for 1 hr at room temperature. After washing, blots were incubated with SuperSignal West Femto Chemiluminescent substrate (Thermo) prior to capture in an Amersham Imager 600 (GE Healthcare).

3.2.9 Spontaneous suppressor selection

Six independent single colonies of BYD027 (2X P_{hy}-*sirA*, P_{hy}-*lacZ*) were used to inoculate six independent 5 ml LB-Lennox cultures. The cultures were grown for 6 hrs at 37°C and 0.3 µl of each culture was diluted in 100 µl LB and plated on an LB-Lennox agar plate containing 100 µg/ml spectinomycin and 1 mM IPTG. After overnight growth at 37°C, suppressor colonies that arose were patched on LB-Lennox agar plates supplemented with 100 µg/ml spectinomycin as well as LB-Lennox agar plates supplemented with 100 µg/ml spectinomycin, 1mM IPTG, and 40 µg/ml 5-bromo-4-chloro-3-indolyl-β-D-galactopyranoside (X-Gal). The patches were then grown at 37°C overnight. Only patches that appeared blue on the X-Gal plate were selected for further analysis; this screen eliminated mutants unable to derepress P_{hy} in the presence of IPTG, specifically LacI dominant mutants (256). In addition, each P_{hy}-*sirA* construct (there were two copies in the genome of the strain used for suppressor selection, see above) was transformed into a wild-type background to ensure that the original expression construct remained fully functional with respect to preventing cell growth on LB-Lennox agar plates supplemented with the relevant antibiotic and 1mM IPTG. The *dnaA* region of each suppressor strain was amplified from genomic DNA using OYD122 and OYD13. The PCR product was sequenced in the forward and reverse direction using OYD296 and OYD297.

3.2.10 Suppressor selection by NTG mutagenesis

A single colony of BYD027 (2X P_{hy}-*sirA*, P_{hy}-*lacZ*) was inoculated in 5 ml LB-Lennox medium at 37°C to mid-exponential phase, back-diluted to OD_{600} = 0.01 in 25

ml LB-Lennox medium in 250 ml baffled flasks, and grown at 37°C in a shaking waterbath set at 280 rpm to OD_{600} = 1. Cells were pelleted at 2,576 x g for 5 min at room temperature and washed one time with SC buffer [150mM NaCl, 10mM NaCitrate]. Pellets were resuspended with 10 ml SC buffer containing one of the following concentrations of N-Methyl-N-nitro-N-nitrosoguanidine (NTG): 1 µg/ml, 5 µg/ml or 10 µg/ml. The cell suspensions were then incubated at 37°C for 10 min. After incubation, the cells were pelleted at 2,576 x g for 5 min at room temperature and washed twice with LB-Lennox medium. Pellets were then resuspended with 25 ml LB-Lennox medium containing 15% glycerol, aliquoted and stored at -80°C. To obtain suppressors resistant to SirA misexpression during vegetative growth, 1 µl of the NTG treated cells were plated on LB-Lennox agar plate supplemented with 100 µg/ml spectinomycin and 1mM IPTG. Further analysis proceeded as described under the section on spontaneous suppressor selection.

3.2.11 Bacterial two-hybrid assay (B2H), general methods

Bacterial two hybrids were performed essentially as described (241) with the following modifications: cloning was carried out in the presence of 0.2% glucose (w/v) in addition to the appropriate antibiotics. *E. coli* strain DHP1 harboring the relevant pairwise interactions were grown to exponential phase in LB-Lennox media supplemented with 0.2% glucose (w/v), ampicillin (50 µg/ml), and kanamycin (25 µg/ml). Samples were normalized by OD_{600} and five µl of each culture spotted on M9-glucose minimal media plates containing 250µM IPTG, 40 µg/ml X-Gal, ampicillin (50 µg/ml), and kanamycin (25 µg/ml). Plates were incubated at room temperature in the dark for 50 to 70 hrs prior to image capture.

3.2.12 Plasmid maintenance assay

1 ng of pBR322 (or pRB100, or pYD192, see Table 3.1, Table 3.2 and the legend of Table 3.4) was transformed into RbCl competent *E. coli* strain CYD199 (see below)(76) and plated on LB-Lennox agar plates supplemented with 100 μg/ml ampicillin. The plate was incubated overnight at 37°C. Single colonies from each plate were isolated, generating CYD227 and other relevant strains. Each of these strains was made RbCl competent (see below), aliquoted, and frozen at -80°C for future transformations. To test for maintenance of the *oriC*-containing plasmid, 100 ng of pCM959-Cm^R (*oriC* plasmid) was then transformed into the RbCl competent CYD227 and other relevant strains, followed by plating on LB-Lennox agar plates supplemented with ampicillin (100 μg/ml) and chloramphenicol (30 μg/ml). Plates were incubated at 37°C for 48 hrs, and the number of colonies on each plate was enumerated. In order to be able to directly compare them, 1 ng of pACYC184 (non-*oriC* plasmid) was transformed into the same competent cells as mentioned above, to know the relative competence for each strain.

3.2.13 Making RbCl *E. coli* competent cells

One freshly streaked single colony was inoculated in 5 ml LB-Lennox medium supplemented with proper antibiotics, grown at 37°C to mid-exponential phase. This culture was diluted an OD_{600} = 0.01 in 50 ml LB-Lennox medium supplemented with proper antibiotics in a 250 ml baffled flasks, and grown at 37°C in a shaking waterbath set at 280 rpm to OD_{600} = 0.5. The culture was collected in a 50 ml falcon tube and placed on ice for 15 min. Cells were pelleted by centrifugation at at 2,576 x g for 10 min

at 4°C, and the supernatant was discarded. Pellets were resuspended in 5 ml of cold TFB I [30mM potassium acetate, 100 mM rubidium chloride, 10 mM $CaCl_2$, 50 mM $MnCl_2$, 15% glycerol, pH 5.8] and placed on ice for 15 min. Cells were pelleted again at 2,576 x g for 10 min at 4°C. The supernatant was discarded whereas the pellet was resuspended in 1 ml of cold TFB II [10mM 3-morpholinopropane-1-sulfonic acid (MOPS), 10 mM rubidium chloride, 75 mM $CaCl_2$, 15% glycerol, pH 6.5] and placed on ice for 30 min. Cells were aliquoted and stored at -80°C until use.

3.2.14 Microscopy

1 ng of pJW029 (*sirA-pBAD24*) was transformed into *E. coli* MG1655 cells and plated on LB-Lennox agar (1.5% w/v) plates containing 100 µg/ml ampicillin to make CJW089. For microscopy experiments, a single colony of CJW089 was inoculated in 25 ml LB-Lennox medium with 100 µg/ml ampicillin in a 250 ml baffled flasks and placed in a shaking waterbath set at.37°C and 280 rpm. At low OD_{600} (~0.04), 0.2% arabinose was added to the induced cultures. Images were captured 2 hrs post-induction. 1 ml culture was pelleted by centrifugation at 6,010 x g for 1 min at room temperature, then pellets were resuspended in ~5 µl DAPI (2 µg/ml) before mounting on glass slides with polylysine-treated coverslips.

3.3 Results

3.3.1 SirA is insoluble when overexpressed in *E. coli*

In an effort to obtain purified SirA for biochemical assays and structural studies, we attempted to define conditions to obtain a soluble form of SirA protein. *sirA* was cloned into pET overexpression vectors containing either N or C-terminal 6X His tags as well as an N-terminal His-SUMO tag. For each expression construct, two different rich media (LB-Lennox and Cinnabar) were tried at three different growth temperatures (37°C, 30°C and 22°C), and samples were fractionated into a soluble (S) and pellet (P) fraction as described above. Under all of the conditions tested, SirA was expressed, but found exclusively in the insoluble, pellet fraction under our standard lysis conditions (see materials and methods). The 30°C induction in Cinnabar media is shown as a representative result in Fig 3.1. SirA was also found exclusively in the insoluble fraction when expressed using two-different commercial in vitro transcription and translation systems (Fig 3.2). In some cases, homologs of a protein can be expressed in a soluble state. Therefore, we also attempted to express SirA homologs from several other *Bacillus* species fused to an N-terminal His-SUMO tag. Each of the homologs was also found in the insoluble fraction following the cell lysis step (Fig 3.3).

E. coli is not always an optimal system to overexpress soluble proteins. Several Gram positive protein overexpression systems exist, including one for *B. megaterium*, a species closely related to *B. subtilis* (257). Using the *B. megaterium* overexpression system developed by MoBiTec, we attempted to overexpress a C-terminal 6X His-tagged version of SirA (see Materials and Methods for details). Using this system, SirA was expressed, but was once again found in the insoluble fraction (Fig 3.4).

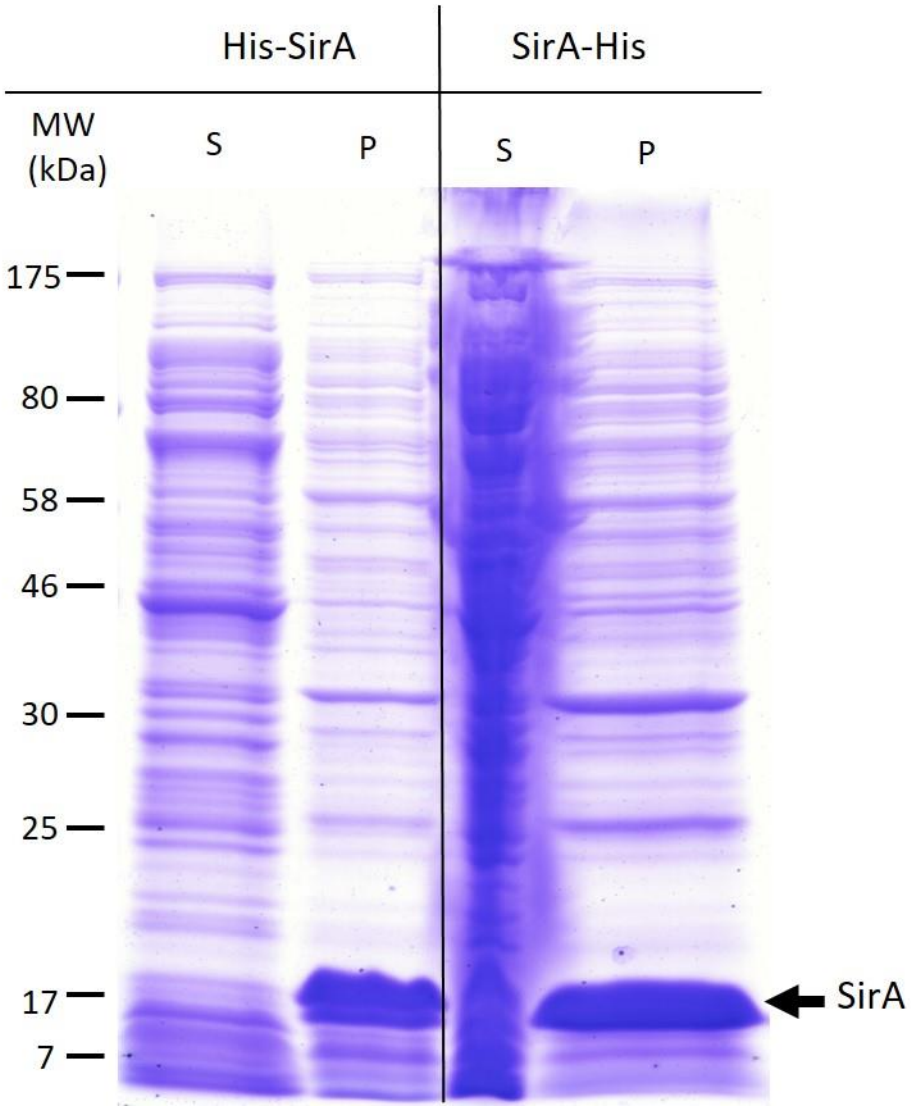

Fig. 3.1. SirA overexpressed in *E. coli* in Cinnabar media. The expected molecular weight of His-tagged SirA is ~18 kDa. pLM023 (His-SirA) or pLM022 (SirA-His) was transformed into *E. coli* BL21 (DE3) competent cells and grown in Cinnabar media as described in materials and methods. After fractionation, the supernatant (S) and pellet (P) fractions were analyzed by SDS-PAGE.

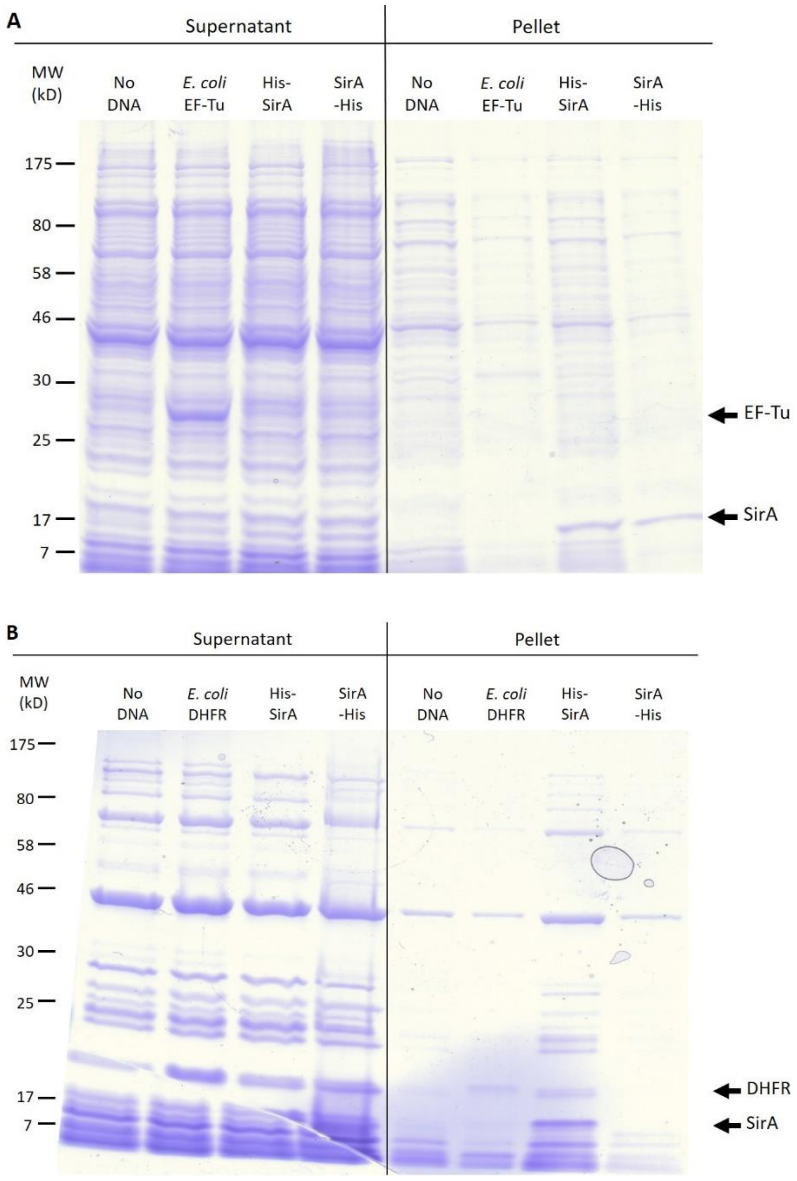

Fig. 3.2. SirA expressed in cell-free transcription and translation system. PCR product amplified using pLM023 (His-SirA) or pLM022 (SirA-His) as template was used as template to synthesize protein. After synthesis, samples were centrifuged to separate the supernatant (S) and the pellet (P) fractions. (A) Expression performed using the EasyXpress Protein Synthesis Kit" (Qiagen). Plasmid encoding *E. coli* EF-Tu was used as the positive control. (B) Expression performed using PURExpress® *In Vitro* Protein Synthesis Kit (New England BioLabs). Plasmid encoding *E. coli* DHFR was used as the positive control.

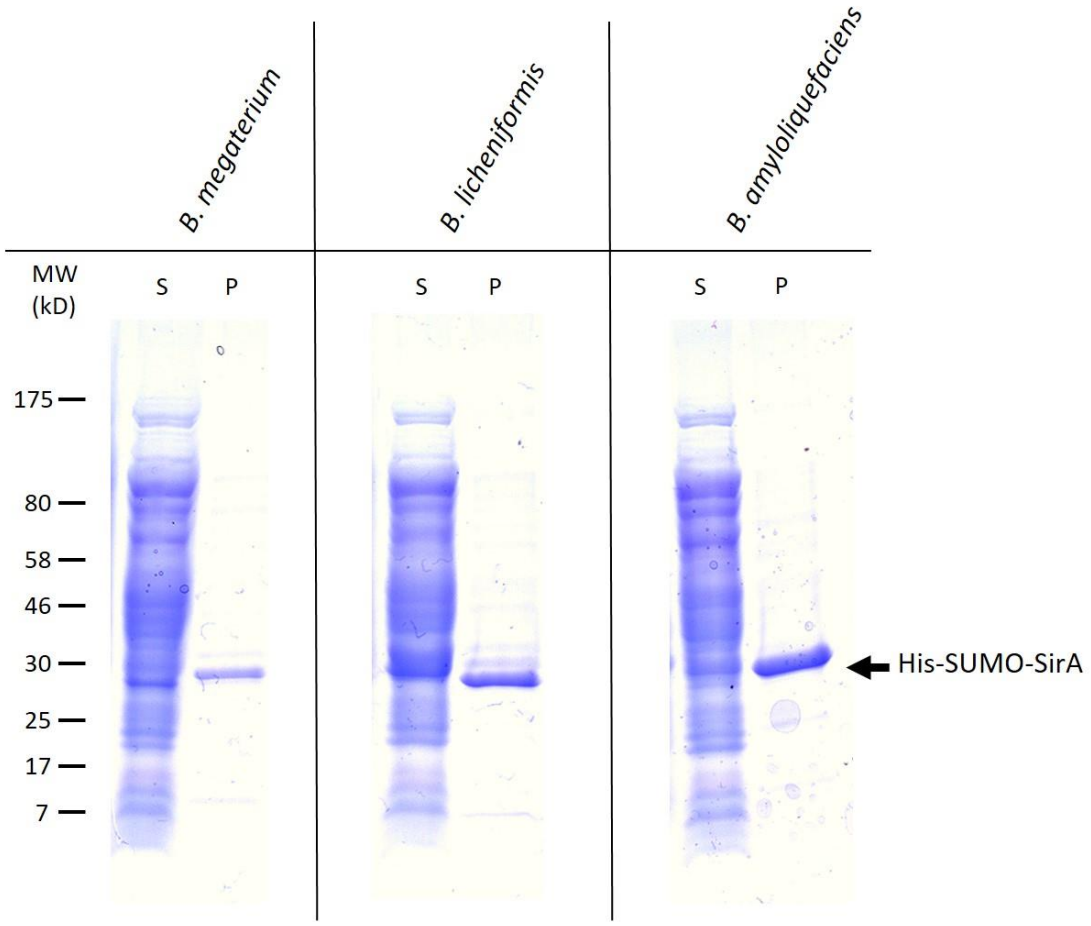

Fig. 3.3. SirA from other *Bacillus* species overexpressed in *E. coli*. Expected size of the His-Sumo-SirA proteins is ~30 kDa. pYD052 (His-SUMO-SirA from *B. megaterium*), pYD053 (His-SUMO-SirA from *B. licheniformis*) or pYD054 (His-SUMO-SirA from *B. amyloliquefaciens*) were transformed into *E. coli* BL21 (DE3) competent cells and grown in the Cinnabar media to an OD600 of ~5. Induction was for 5 hrs with 1 mM IPTG. Samples were then collected, lysed and fractionated. After centrifugation, supernatant (S) and pellet (P) fractions were each loaded on the gel.

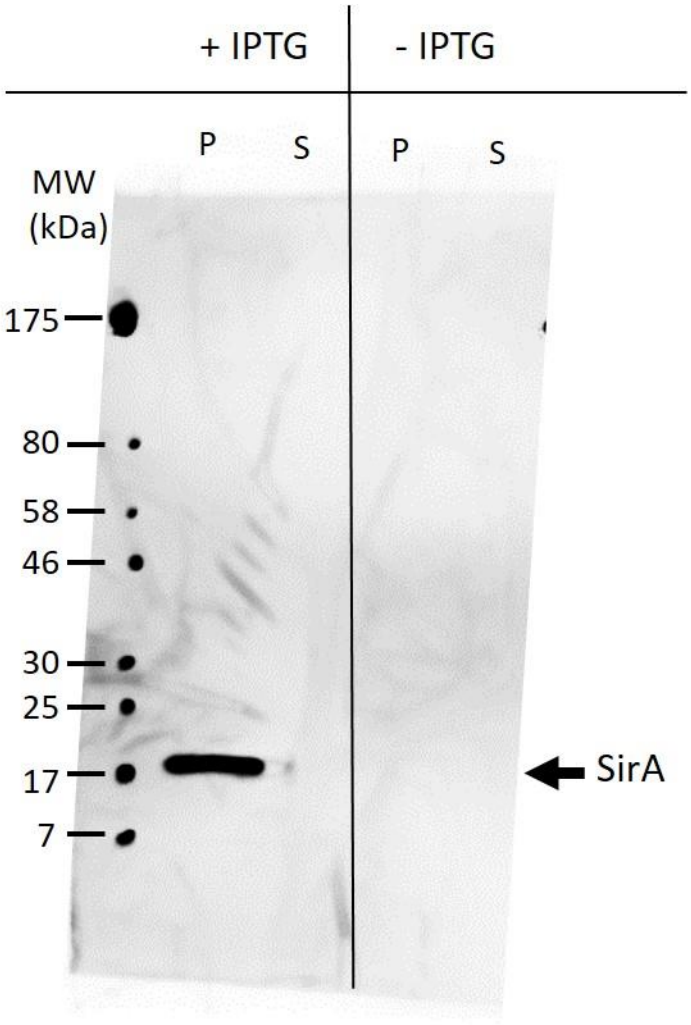

Fig. 3.4. SirA overexpression in *B. megaterium.* Expected size of the SirA-His proteins is as indicated. pYD030 (SirA-His plasmid used in *B. megaterium* overexpression system) was transformed into *B. megaterium* protoplasts and grew in LB-Lennox media. When indicated, 1mM IPTG was used to induce protein expression. Samples were then collected and lysed. After centrifugation, supernatant and pellet were each loaded on the gel. “S” stands for “supernatant” and “P” stands for “pellet”.

Since conditions to obtain soluble protein following overexpression were not successful, we attempted to refold the protein obtained from the pellet fractions using sequential 1.0 M dialysis step-downs. SirA in the pellet fraction was solubilized by the addition of 8.0 M urea. SirA remained in solution until the step-down from 6.0 M to 5.0 M urea, at which point the protein rapidly precipitated from solution.

Sometimes proteins that are normally found in complexes are stabilized or solubilized when they are co-expressed or co-purified in the presence of native binding partners. Since SirA was previously shown to interact directly with DnaA (7, 81), we co-expressed SirA with DnaA. In addition, co-expression of SirA with either DnaD or DnaB (two other proteins required for initiation in *B. subtilis*) was also tested. As shown in Fig 3.5, SirA was found in the pellet fraction in each of the conditions tested (Fig 3.5). Interestingly, when SirA was co-expressed with untagged DnaA, two bands were present in the expected 17 kDa range (Fig 3.5A), while only one band was present when SirA was co-expressed with either untagged DnaB (Fig 3.5B) or untagged DnaD (Fig 3.5C). To test if the lower band was truncated SirA, we performed western blot analysis using both an anti-SirA C-terminal specific peptide antibody (CSKRYGWLNPVKERN, Genscript) and anti-His primary antibody (Sigma). Both the upper and lower bands cross-reacted with SirA using the anti-His antibody (Fig 3.6A), indicating that both bands contained the N-terminus of His-SirA. However, the the top band but not the bottom band was not with a peptide antibody that detects only the extreme C-terminus of SirA (Fig 3.6B), suggesting the higher mobility protein had been proteolytically cleaved near the C-terminus. These results suggested that DnaA-interaction made SirA more susceptible to proteolytic cleavage, possibly due to conformational changes induced by DnaA binding.

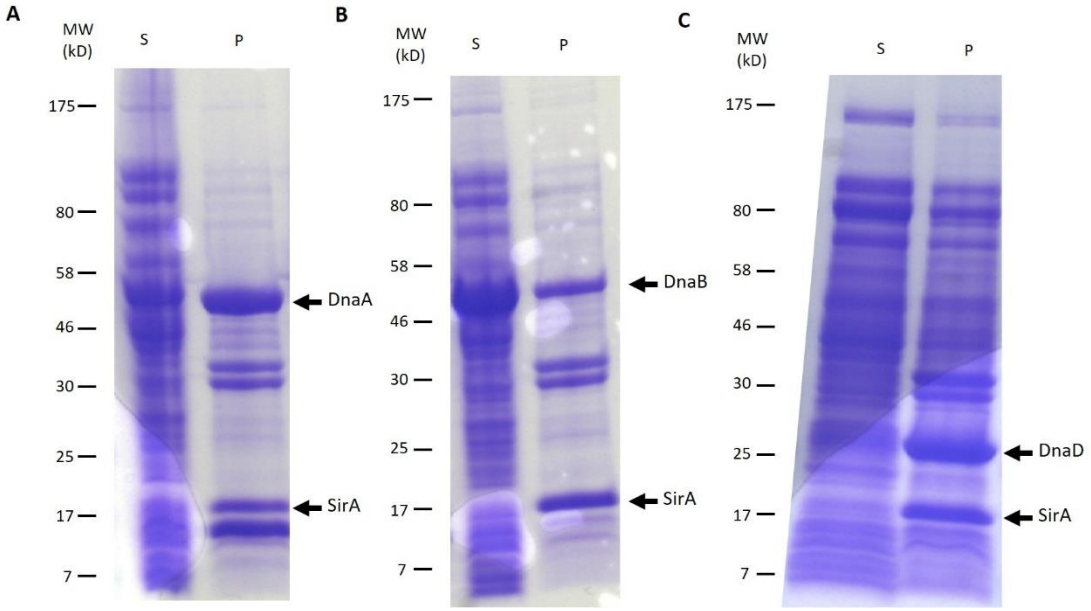

Fig. 3.5. *B. subtilis* SirA co-expressed with other replication initiation proteins. pKM328 (His-SirA, together with *B. subtilis* DnaA, on pDUET vector) (A), pYD025 (His-SirA, together with *B. subtilis* DnaB, on pDUET vector) (B) or pYD026 (His-SirA, together with *B. subtilis* DnaD, on pDUET vector) (C) was transformed into *E. coli* BL21 (DE3) competent cells and grew in the Cinnabar media. Samples were then collected, lysed, and fractionated. Normalized loads of the supernatant (S) and pellet (P) fractions were run on a 4-20% gradient gel (BioRad).

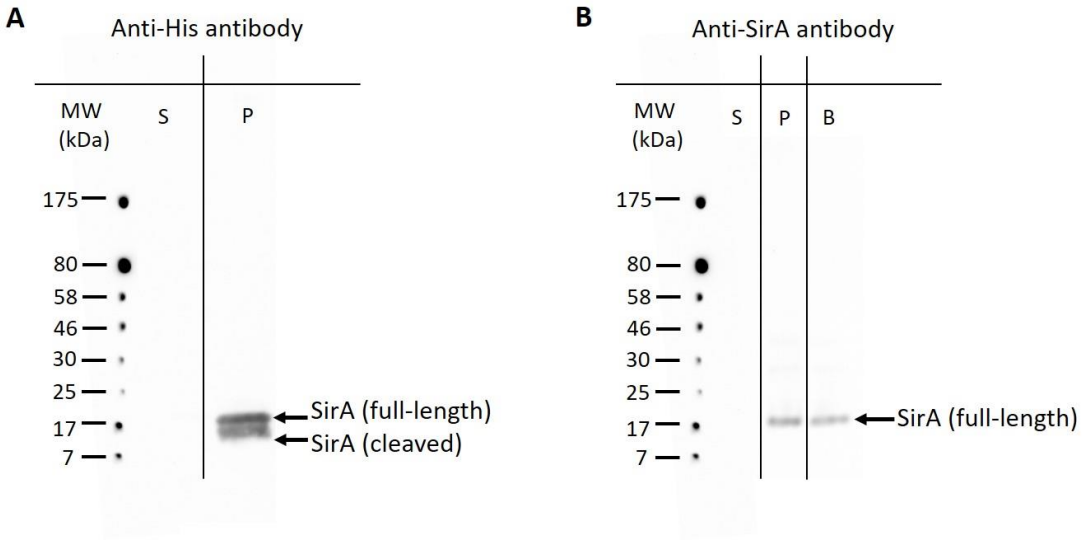

Fig. 3.6. C-terminal SirA is cleaved when co-expressed with *B. subtilis* DnaA. (A) The same samples shown in Fig 3.5A were used to perform western blot with the N-terminal recognizing anti-His antibody (Sigma). Supernatant (S) and pellet (P) fractions are shown. (B) The same samples shown in Fig 3.5A were used to perform western blot with the C-terminus recognizing anti-SirA peptide antibody. The lane labeled "B" is the pellet from cells co-expressing SirA with DnaB, shown for comparison.

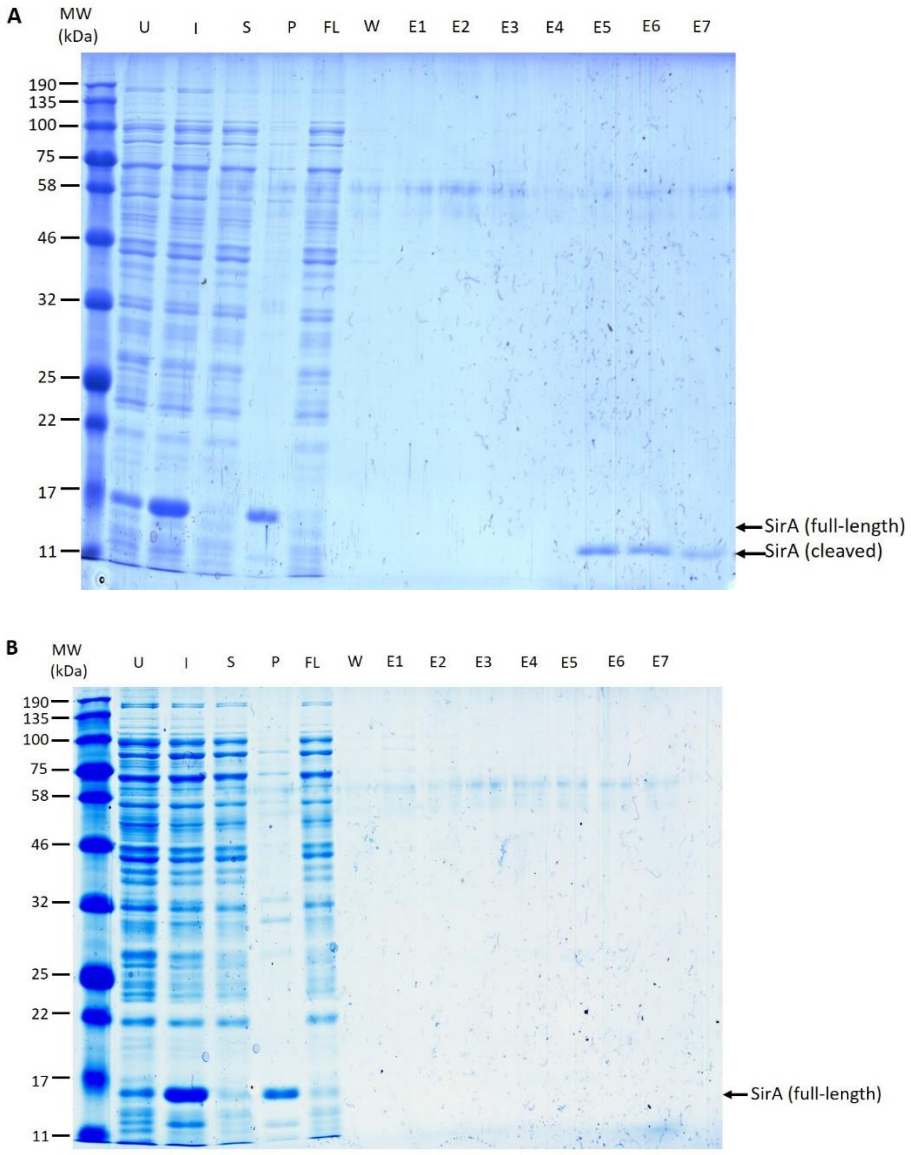

Fig. 3.7. A soluble form of C-terminal cleaved SirA can be enriched following Nickel affinity chromatography of the soluble overexpression fraction. pLM023 (His-SirA) (A) or pLM022 (SirA-His) (B) was transformed into *E. coli* BL21 (DE3) competent cells and grown in Cinnabar media. Samples were collected and fractionated as described in materials and methods. On this gel, lysates from uninduced sample (U) and induced sample (I) are shown, followed by the supernatant (S) and the pellet (P) after lysis and centrifugation. The flow-through (FL), washing sample (W) and multiple elution samples (E1 to E7) during purification were loaded next.

Interestingly, even though overexpressed His-SirA appears to fractionate exclusively to the insoluble fraction based on coomassie staining (Fig 3.1), if the soluble fraction is collected and subjected to Nickel affinity chromatography, a cleaved, but soluble form of His-SirA can be enriched for and eluted (Fig 3.7A). The cleavage must occur near the C-terminus, as the His-tag in this construct is N-terminal. In addition, the C-terminal His-tagged construct did not have this cleaved product (Fig 3.7B). These results suggest that the aggregation of full-length SirA may be mediated through self-interactions occurring near SirA's C-terminus.

3.3.2 SirA does not interact with DnaD or DnaB in bacterial two-hybrid assay

In *B. subtilis*, binding of DnaA at *oriC* is followed by recruitment of DnaD, and the subsequent association of a pre-initiation complex with the membrane through interactions with the membrane-associated protein DnaB (72). Assembly of this complex precedes loading of the helicase (DnaC) and DNA polymerase III (71). Inactivation of either DnaD or DnaB phenocopies inactivation of DnaA, with cells failing to initiate DNA replication (258). During sporulation, SirA inhibits the initiation of DNA replication (7), at least partially by targeting DnaA Domain I (Chapter II)(this study)(79, 81); we also showed that SirA has a second, distinct function in promoting the segregation of *oriC* from the cell quarter to the distal cell pole during sporulation (See Chapter II)(77). Based on this data, we hypothesized that one way SirA might function in *oriC* segregation is to disrupt or prevent interactions between the DnaA-*oriC* complex and the membrane, for example by preventing an interaction between DnaA and DnaD, or DnaD and DnaB. In this way, SirA could function to keep *oriC* free for segregation toward the distal pole (see Fig 2.2 and Fig 2.13)(77). SirA could disrupt/prevent

interactions with the membrane by binding to DnaA and preventing its association with DnaD. Alternatively, SirA could interact with DnaD and/or DnaB directly. To test if SirA interacts directly with either DnaD or DnaB, bacterial two-hybrid assays were performed. As shown in Fig 3.8, no interaction greater than that observed in the negative controls was not detected between with SirA and either DnaD or DnaB. Since DnaB is a membrane-associated protein and membrane associated proteins often give high background in B2H assays, the assay was repeated with DnaB truncations lacking a transmembrane domain; however, the interaction remained negative (data not shown). Based on this data, it was concluded that DnaD and DnaB either do not interact directly with SirA, or that the interaction is below the threshold of detection for the assay.

3.3.3 DnaA Domain I is important for SirA function in vivo

SirA was previously shown to interact with DnaA directly (7). Based on this observation, Rahn-Lee et al. directly mutagenized *dnaA* and identified four DnaA variants, $DnaA_{N47D}$, $DnaA_{F49Y}$, $DnaA_{A50T}$ and $DnaA_{A50V}$, which supported cell viability, but were insensitive to SirA-mediated killing following misexpression (81). These variants were also determined to result in loss of interaction with wild-type SirA in a yeast two-hybrid assay (81). In a concurrent study, we sought to identify spontaneous suppressor mutations that resulted in resistance to SirA-mediated killing. Cells harboring two copies of the IPTG-inducible SirA misexpression construct were plated on media containing IPTG, and resulting suppressors were screened to ensure that the misexpression constructs remained functional (see Materials and Methods for details). Thirty different SirA-resistant mutants were identified in this screen. Sequencing of the *dnaA* region in each mutant revealed one of four substitutions: $DnaA_{N47D}$, $DnaA_{F49Y}$,

$DnaA_{A50T}$ and $DnaA_{A50V}$, invariant to those identified in the study utilizing random mutagenesis of *dnaA*. Each of these substitutions was sufficient to confer resistance to SirA in a clean genetic background. These results suggested that SirA likely inhibits DNA replication through direct interactions with DnaA Domain I. Increasing the mutation rate by exposing cells to the mutagen NTG did not result in the identification of additional variants, strongly suggesting that the results of both initial screens were saturating.

3.3.4 DnaA Domain I is important for SirA interaction in B2H

In two independent studies, one utilizing random mutagenesis of *dnaA* and one looking for spontaneous mutants, *B. subtilis* DnaA N47, F49 and A50 were implicated in resistance to SirA's killing phenotype. Rahn–lee et al showed that $DnaA_{N47D}$, $DnaA_{F49Y}$, $DnaA_{A50T}$ and $DnaA_{A50V}$ resulted in loss of interaction with wild-type SirA in a yeast two-hybrid assay (81). We independently determined that $DnaA_{N47D}$, $DnaA_{F49Y}$, $DnaA_{A50T}$ and $DnaA_{A50V}$ resulted in loss of interaction with wild-type SirA in a B2H assay (Fig 3.9).

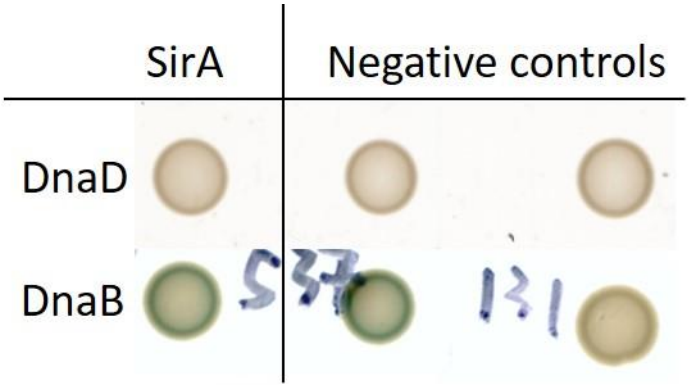

Fig. 3.8. SirA does not interact with DnaD and DnaB in a B2H assay. B2H between SirA and DnaD (CYD492), or DnaB (CYD499) are shown on the left. Negative controls are on the right: empty partner vector with wild-type DnaD (CYD595) or DnaB (CYD537) (middle column) or SirA with the empty partner vector (CYD686 or CYD131) (right column).

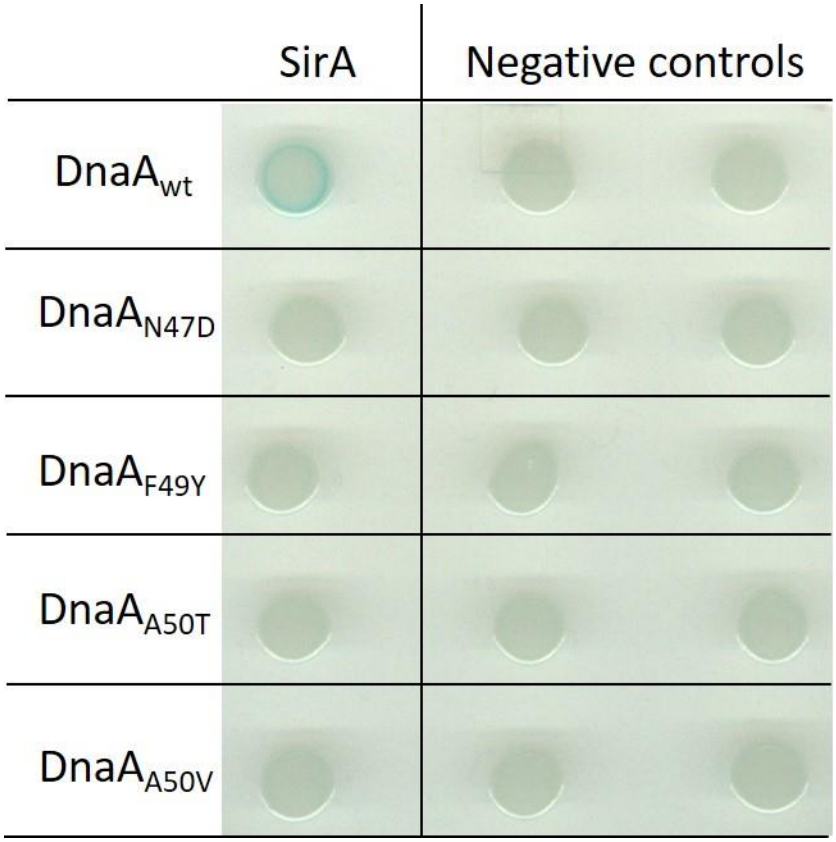

Fig. 3.9. SirA does not interact with DnaA variants containing point mutations in domain I. B2H between SirA and wild-type DnaA (CYD050), DnaA$_{N47D}$ (CYD052), DnaA$_{F49Y}$ (CYD053), DnaA$_{A50T}$ (CYD054) or DnaA$_{A50V}$ (CYD055) are shown on the left. Negative controls are on the right: empty partner vector with wild-type DnaA (CYD060), DnaA$_{N47D}$ (CYD063), DnaA$_{F49Y}$ (CYD064), DnaA$_{A50T}$ (CYD065) or DnaA$_{A50V}$ (CYD066) (middle column) or SirA with the empty partner vector (CYD061) (right column).

Interestingly, *B. subtilis* DnaA F49, which is the equivalent of *E. coli* DnaA F46 was previously shown to be important for interaction between DnaA and DiaA, a positive regulator of DnaA in *E. coli* (122). Based on this observation, we hypothesized that *E. coli* DiaA and SirA might interact in a similar way with DnaA, but with opposite activities (positive and negative regulation, respectively). The crystal structures of *E. coli* DiaA and DnaA domain I have been solved (PDB ID: 2YVA and 2E0G, respectively)(75, 80). Using NMR to further study the DiaA-DnaA interaction (122), Keyamura et al. found that DiaA likely makes contacts with *E. coli* DnaA E21, W25 and W50 (S23, W27 and W53 in *B. subtilis*, respectively)(Fig 3.10, Fig 3.11)(122). Additional residues in this region of DnaA were also hypothesized to be important for the *E. coli* DnaA-DiaA interaction. We hypothesized that if SirA interacts with DnaA similar to DiaA, then substitutions in equivalent residues in *B. subtilis* DnaA might result in a change in interaction between SirA and DnaA. To test this hypothesis, each of the above-mentioned residues (S23, W27 and W53) as well as the ones around the potential interaction interface was replaced with Alanine. All but one of the variants showed loss-of-interaction with SirA by B2H. These results further suggest that SirA interacts directly with DnaA Domain I, and suggest that SirA and DiaA may interface with DnaA in similar ways (Fig 3.9, Fig 3.12).

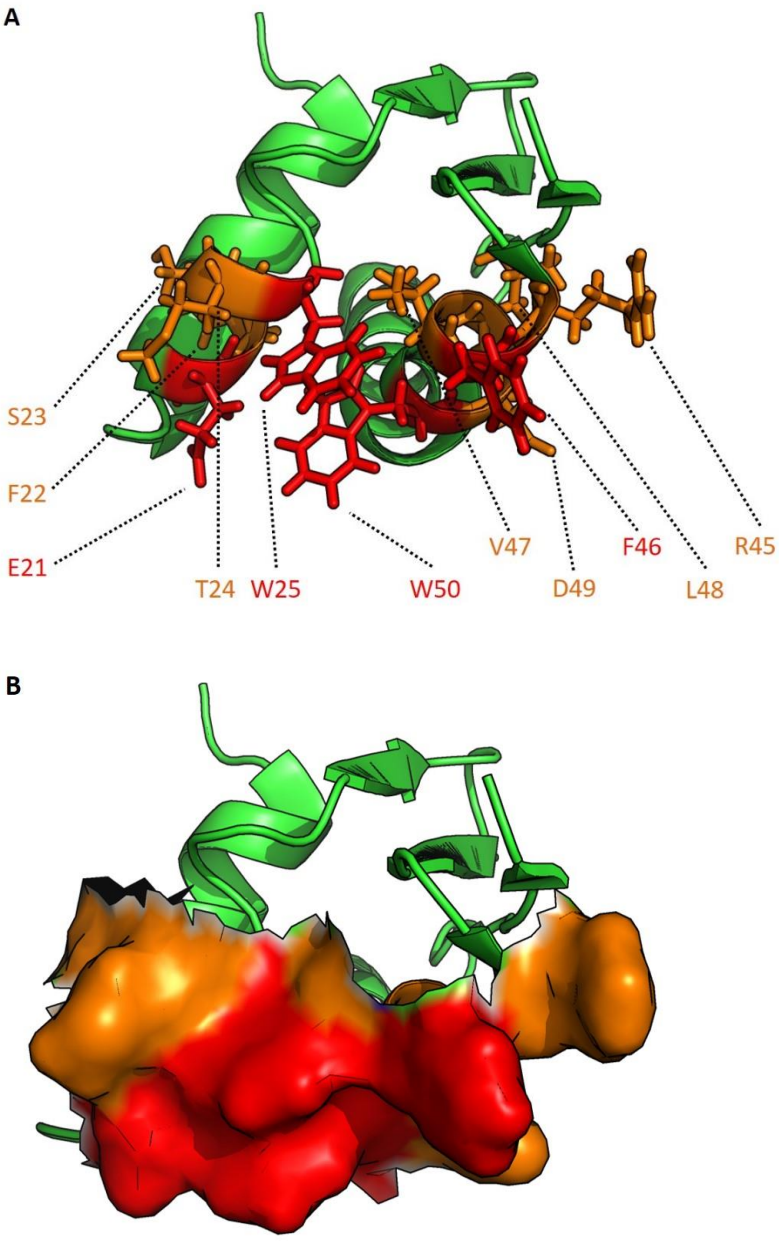

Fig. 3.10. *E. coli* DnaA Domain I structure. *E. coli* DnaA Domain I structure (PDB ID: 2E0G)(75), showing only residues 1-80. Residues labeled in red have been shown to be important for *E. coli* DnaA-DiaA interaction (122). Residues labeled in orange are hypothesized to be important for DiaA interaction. Relevant residues shown as sticks (A) or through surface modeling (B) for comparison.

Fig. 3.11. Alignment between *E. coli* DnaA and *B. sub* DnaA. Red asterisks indicate residues that have been shown to be important for *E. coli* DnaA-DiaA interaction (122); orange arrows point to the residues that are hypothesized to be important for DiaA interaction.

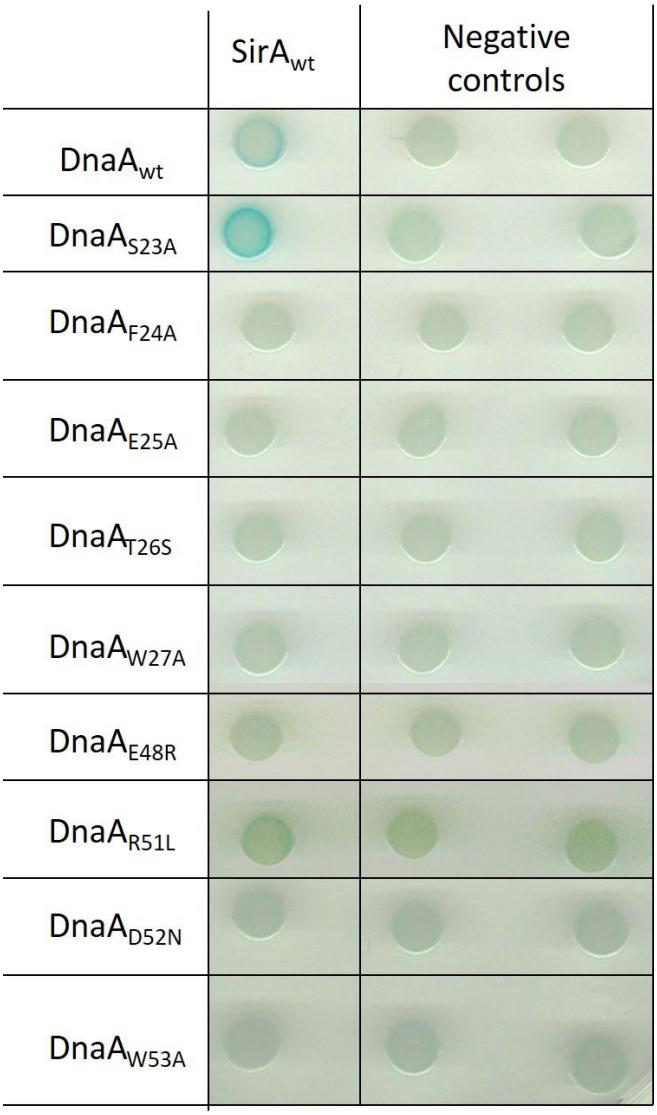

Fig. 3.12. DnaA Domain I is important for SirA interaction. B2H between SirA and wild-type *B. subtilis* DnaA (CYD050), DnaA$_{S23A}$ (CYD092), DnaA$_{F24A}$ (CYD123), DnaA$_{E25A}$ (CYD093), DnaA$_{T26S}$ (CYD124), DnaA$_{W27A}$ (CYD094), DnaA$_{E48R}$ (CYD125), DnaA$_{R51L}$ (CYD126), DnaA$_{D52N}$ (CYD127) and DnaA$_{W53A}$ (CYD095). Negative controls: empty partner vector with wild-type DnaA (CYD060), DnaA$_{S23A}$ (CYD098), DnaA$_{F24A}$ (CYD137), DnaA$_{E25A}$ (CYD099), DnaA$_{T26S}$ (CYD138), DnaA$_{W27A}$ (CYD100), DnaA$_{E48R}$ (CYD139), DnaA$_{R51L}$ (CYD140), DnaA$_{D52N}$ (CYD141) and DnaA$_{W53A}$ (CYD101)(left column) or SirA with the empty partner vector (right column)

Attempts to replace wild-type *dnaA* with *dnaA* mutants encoding any of the Alanine substitutions were unsuccessful, suggesting that the proteins do not support viability in vivo. This result is consistent with the fact that none of the variants were obtained in the SirA-resistant suppressor selections. Since the substitutions did not support viability in vivo, we were unable to determine if the proteins were folded stably expressed and folded correctly. However, *B. subtilis* $DnaA_{S23A}$ showed gain-of-interaction with SirA in a B2H assay, suggesting it is at least folded. Interestingly, in *E. coli*, the equivalent substitution ($DnaA_{E21A}$) results in a loss of interaction with DiaA (122). These contrasting behaviors following substitution at this region of DnaA may provide insight regarding how DiaA and SirA are able to respectively function as positive and negative regulators of DnaA activity.

3.3.5 SirA can affect *E. coli* $DnaA_{V47A}$ function in vivo

When expressed in *E. coli* from a high or medium copy number plasmid, SirA has no detectable effect on *E. coli* DNA replication as judged by DAPI staining of the nucleoid (Fig 3.13). Rahn-Lee et al. showed that wild-type SirA does not interact with wild-type *E. coli* DnaA in a yeast two-hybrid assay (81). Interestingly, *E. coli* DnaA V47 is A50 in *B. subtilis*. I and others have found that in *B. subtilis*, a $DnaA_{A50V}$ variant is resistant to SirA (see the text above and Fig 2.9A, B)(77, 81) and *B. subtilis* $DnaA_{A50V}$ does not interact with SirA in a B2H assay (Fig 2.9C, Fig 3.9)(77). These results suggest that having an Adenine at this position might be important for interaction. Consistent with this idea, the *E. coli* $DnaA_{V47A}$ variant shows interaction with SirA in a yeast two-hybrid assay (81). Based on these data, we hypothesized that *E. coli* expressing $DnaA_{V47A}$ might render *E. coli* sensitive to SirA expression. To test this hypothesis, I attempted to replace wild-type *dnaA* with *dnaA*$_{V47A}$ on the *E. coli* chromosome.

Repeated attempts to generate the mutant were unsuccessful, possibly due to inviability of the resultant strain.

To circumscribe this problem, we adapted an established plasmid maintenance assay. This assay tests the ability of a plasmid-encoded copy of *dnaA* to support replication of a separate DnaA-dependent plasmid (76). The assay utilizes an *E. coli* strain that does not require DnaA for chromosomal replication, thus uncoupling the host strain viability from DnaA activity (76). In the assay, *E. coli dnaA* or the *dnaA* mutant being tested is present on a DnaA-independent replicating plasmid encoding ampicillin resistance (amp^R). A second DnaA-dependent plasmid (*oriC* plasmid) encoding chloramphenicol resistance (cat^R) is used to assess if the DnaA being made is functional. If the *dnaA* on the amp^R plasmid is functional, then the *oriC* plasmid will be replicated, resulting in chloramphenicol-resistant transformants. The results are shown in Table 3.4.

Although all the strains were made competent in the same time by using the same batch of media and buffer, it is still possible that different strain background may have difference in competence. In order to be able to directly compare the results shown in Table 3.4 and draw conclusions, we used another plasmid which replication is independent of DnaA as the control. The plasmid was transformed into each strain (the same as the ones in Table 3.4) and the number of colonies were counted and reported in Table 3.5.

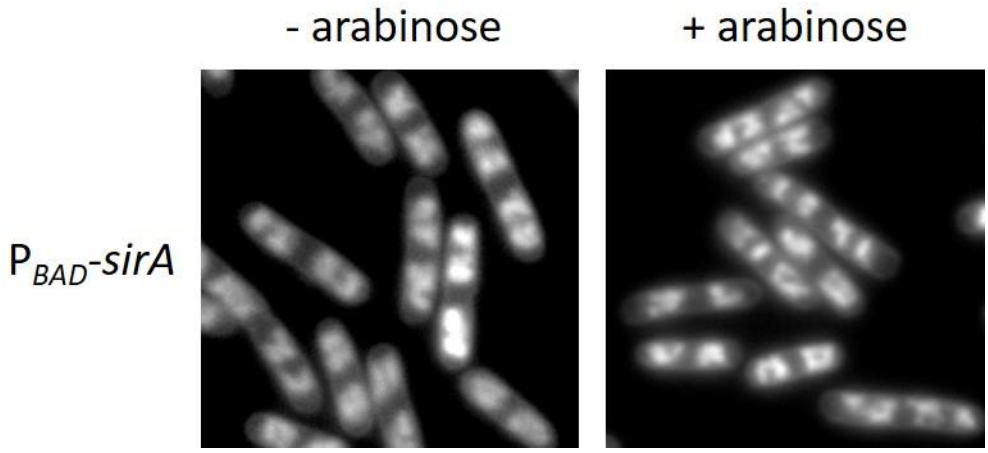

Fig. 3.13. SirA overexpression does not obviously inhibit wild-type *E. coli* DNA replication, based on nucleoid morphology. MG1655 harboring P$_{BAD}$-*sirA* (CJW089) was grown in LB-Lennox media supplemented with 100 µg/ml ampicillin at 37°C to mid-exponential and back-diluted in the same media to an OD_{600} of ~0.04. When indicated, 0.2% arabinose was added to induce protein expression. Cells were grown for 2 hrs at 37°C before image capture. DNA was stained with DAPI (2 µg/ml). All images were scaled identically.

Table 3.4. *E. coli*-based plasmid maintenance assay. In this assay, the *E. coli* strain utilized replicates DNA independent of DnaA. The DnaA variant being tested is encoded on an amp^R plasmid that also replicates independent of DnaA. The cat^R plasmid utilizes DnaA for its replication. Recovery of transformants indicates that the cat^R plasmid was replicated. 100 ng of pCM959-Cm^R (*oriC* plasmid) was transformed into CYD227 (empty + empty), CYD228 (empty + $DnaA_{wt}$), CYD229 (empty + $DnaA_{V47A}$), CYD237 ($SirA_{wt}$ + empty), CYD238 ($SirA_{wt}$ + $DnaA_{wt}$), CYD239 ($SirA_{wt}$ + $DnaA_{V47A}$), CYD267 ($SirA_{Y51A}$ + empty), CYD268 ($SirA_{Y51A}$ + $DnaA_{wt}$) or CYD269 ($SirA_{Y51A}$ + $DnaA_{V47A}$), and cells were selected on LB-Lennox agar plates containing both ampicillin and chloramphenicol. The values indicate the average number of colonies obtained in three independent transformations followed by the standard deviation.

	Empty vector	$SirA_{wt}$	$SirA_{Y51A}$
Empty vector (amp^R)	0	0	0
$DnaA_{wt}$ (amp^R)	92±3	46±4	47±4
$DnaA_{V47A}$ (amp^R)	91±4	0	23±3

Table 3.5. Control for the plasmid maintenance assay. The cat^R plasmid does not require DnaA for its replication, thus is used as a control to test the competence difference between each strain. Transformants indicates that the cat^R plasmid was replicated. 1 ng of pACYC184 (DnaA-independent plasmid) was transformed into the same strains as shown in Table 3.4, and cells were selected on LB-Lennox agar plates containing both ampicillin and chloramphenicol. The values indicate the average number of colonies obtained in three independent transformations followed by the standard deviation.

	Empty vector	$SirA_{wt}$	$SirA_{Y51A}$
Empty vector (amp^R)	226±19	227±7	211±11
$DnaA_{wt}$ (amp^R)	521±14	530±22	525±18
$DnaA_{V47A}$ (amp^R)	560±15	509±14	512±11

Using this assay, we determined that both wild-type DnaA and $DnaA_{V47A}$ supported DNA replication, as evidenced by the recovery of similar numbers of cat^R transformants (Table 3.4). Constitutively expressed *sirA* or the *sirA* mutant was then cloned onto the DnaA dependent plasmid, and once again cat^R transformants were selected for. As shown in Table 3.4, transformants were readily obtained for cells expressing wild-type DnaA, but not the $DnaA_{V47A}$ variant. Notably, there were reproducibly approximately 2-fold fewer colonies for even wild-type DnaA compared to the control lacking SirA (actually it is 4-fold fewer considering the competence difference between each strain, see above and Table 3.5), suggesting that SirA may have some limited capacity to inhibit even wild-type *E. coli* DnaA activity. These results also suggest that SirA is capable of more strongly inhibiting $DnaA_{V47A}$ activity. Next we hypothesized that $SirA_{Y51A}$, a variant with reduced ability to inhibit DNA replication (Fig 2.7)(77), would also show reduced ability to inhibit *E. coli* DnaA-dependent replication in plasmid maintenance assay. Consistent with idea, introduction of $SirA_{Y51A}$ did result in the recovery of cat^R transformants (about 2X reduced compared to the control strain lacking SirA)(Table 3.4). In total, these results suggest that the mechanism by which SirA inhibits DnaA-dependent DNA replication does not absolutely require any *Bacillus* specific factors, further implicating DnaA as the primary target of SirA function.

3.4 Discussion

3.4.1 SirA is insoluble when overexpressed in *E. coli*

To our knowledge, the only overexpression condition known to produce soluble SirA is co-expression of SirA with *B. subtilis* DnaA Domain I (79). While this form was useful in obtaining structural information, it was not useful in biochemical assays since the complex could not be reversed (79). The reasons underlying SirA's poor solubility are unclear from the structure itself. The protein is globular and relatively small (~18 kDa), with no sequences suggestive of membrane association. It is striking that a C-terminally cleaved form of SirA appears to be soluble (Fig 3.7).

One interpretation of this result is that SirA is capable of self-association through interactions requiring the extreme C-terminus. In the crystal structure, amino acid assignments could only be made up until residue P141. The remaining seven amino acids, VKERNFV were disordered (79). The self-association we observed following SirA expression could be disordered aggregation, or it could be assembly of some sort of higher-order oligomer. These ideas could be tested using a number of in vitro methods. For example, overexpression of SirA variants with C-terminal truncations would be expected to increase SirA's solubility. Such a result could have a number of implications for our current model explaining how SirA functions both to inhibit DnaA activity and to promote *oriC* segregation. The DnaA gain of interaction substitutions identified in Chapter II (Table 2.5)(77) occur exclusively in the C-terminus of SirA. If these variants are less able to self-associate, then it could shift the population of SirA toward a more monomeric form that is better able to interact with DnaA Domain I. If it is true, this could have also resulted in the gain of interaction read-out in the B2H assay. This

hypothesis could be tested by assaying the SirA gain of interaction variants for increased solubility following protein overexpression. Similarly, the DnaA Domain III variants identified in in the gain of interaction screen could have resulted from DnaA being less able to oligomerize, thus favoring its interaction with SirA (Chapter II, Table 2.5)(77) could also be variants shifted toward a more monomeric version of DnaA. Future experiments will be aimed at characterizing the variants using biochemical methods.

3.4.2 DnaA Domain I is important for SirA interaction and killing activity

We performed suppressor selections following SirA expression both by using the mutagen NTG and selecting for spontaneous mutations. We obtained the same four variants ($DnaA_{N47D}$, $DnaA_{F49Y}$, $DnaA_{A50T}$ and $DnaA_{A50V}$) obtained by others who directly mutagenized *dnaA* and introduced the alleles into the *B. subtilis* chromosome (81). These results suggest that DnaA Domain I may be the only target for SirA to inhibit DNA replication initiation. We also identified additional loss-of-interaction variants possessed substitutions on DnaA Domain I (Fig 3.12), further supporting the conclusion that DnaA Domain I is the primary, if not sole target required by SirA to perform its function in DNA replication inhibition. However, it is also possible that mutations in other SirA targets (either in other *dnaA* or in other gene products) might result in cellular lethality, thus precluding their identification through suppressor selection.

3.4.3 SirA can inhibit DnaA function without any *B. subtilis* specific factors

SirA inhibits DNA replication by interacting with DnaA Domain I, and the N47, F49 and A50 residues in *B. subtilis* DnaA are important for SirA-DnaA interaction (This study)(81). Moreover, we showed that SirA can affect *E. coli* $DnaA_{V47A}$ function, further suggesting that the Alanine at position 47 (position 50 in *B. subtilis*) is important for SirA to efficiently target DnaA activity. Importantly, this result also indicates that SirA does not require any *Bacillus* specific factors to inhibit DnaA's activity in vivo. Consistent with this observation, no interaction was detected between SirA and the initiation factors DnaD and DnaB by B2H analysis (Fig 3.8). At the same time, these negative results do not exclude the possibility that in vivo, SirA could affect its role in *oriC* segregation by preventing association of a DnaA-*oriC* complex with the membrane, perhaps by preventing association of DnaA with DnaD and/or DnaB.

It has been shown that in *E. coli*, DnaA Domain I is important for DnaA self-dimerization, which is essential for its cooperative oligomerization on DNA (76, 83). Although DnaA Domain I is not required for *B. subtilis* DnaA self-oligomerization in vitro (143), it is still possible that DnaA Domain I function contributes to DnaA oligomerization and/or DNA binding in vivo. Since we've shown that SirA targets DnaA Domain I to inhibit DNA replication initiation, it is possible that this inhibition is due to the disruption of DnaA self-dimerization. To test this idea, the ability of DnaA to form a homodimer through Domain I could be tested in vivo using a modified λcI repression assay (259). If it did, the effect of SirA on formation of this complex could be assessed. This hypothesis could also be tested in vitro if soluble SirA can be obtained.

DnaA Domain I has also been shown to be important for helicase loading in *E. coli* (260, 261). In *B. subtilis*, DnaD and DnaB are also required (71). However, these

results do not exclude the possibility that DnaA Domain I is separately important for helicase loading in *B. subtilis*. In addition, *E. coli* $DnaA_{E21}$ (which is $DnaA_{S23}$ in *B. subtilis*) has been shown to be important for *E. coli* helicase loading, possibly by directly interacting with the helicase (75). We observed that *B. subtilis* $DnaA_{S23}$ is also important for SirA interaction (Fig 3.12). Therefore, it is also possible that SirA may inhibit DNA replication by disrupting helicase loading. We think SirA is unlikely to regulate ATP binding/hydrolysis of DnaA, due to the high nucleotide exchange rate in *B. subtilis* (127). Future experiments aimed at purifying a soluble version of SirA will allow further testing of this and other hypotheses.

CHAPTER IV

CONCLUSIONS AND FUTURE DIRECTIONS

In bacteria, chromosome replication and segregation are tightly regulated to ensure that each future daughter cell will inherit at least one copy of the genome (16). Despite the significance of genome inheritance, very little is known about how bacterial cells coordinate DNA replication and segregation with cell growth and division. The work presented in this dissertation provides significant insight into two fundamental questions: how is DNA replication regulated, and how are the replicated chromosomes segregated?

Previous results have shown that a sporulation specific protein SirA (Sporulation inhibitor of replication A) inhibits DNA replication initiation during *Bacillus subtilis* sporulation by directly interacting with the initiator protein DnaA (7, 81). In bacteria, DNA replication initiation and origin segregation are closely coordinated (182, 183). Results in Chapter II suggest that in addition to inhibiting DNA replication, SirA also plays an important role in ensuring proper *oriC* segregation during sporulation. The data suggest that SirA facilitates *oriC* capture by acting in the same pathway as another DnaA regulator critical for *oriC* partitioning, Soj (140, 143, 187). One of the most important conclusions in Chapter II is that SirA's ability to inhibit DNA replication initiation is distinct from its role in origin segregation. Results in Chapter II suggest that *oriC* segregation may be intimately linked to interactions between DnaA and *oriC*. The intimate relationship between DNA replication initiation and chromosome segregation is highlighted by the identification of yet another factor (SirA) that not only regulates DnaA activity, but also plays a role in *oriC* segregation. In Chapter III, additional experiments were performed to better understand how SirA inhibits DNA replication at

the molecular level. Results in Chapter III show that DnaA Domain I is important for SirA interaction, and that this interaction is required for SirA to inhibit DNA replication initiation. Furthermore, by performing genetic screens, the interaction interface between SirA and DnaA are determined, further supporting the information provided by the co-crystal structure between SirA and *B. subtilis* DnaA Domain I (79). Finally, results in Chapter III indicate that SirA can inhibit replication in a manner that does not require any *B. subtilis* specific factors. These results suggest that SirA does not require other proteins, such as DnaD or DnaB to direct replication inhibition.

4.1 SirA acts in the same pathway as Soj to facilitate *oriC* capture during *B. subtilis* sporulation

Soj has been shown to be important for *oriC* segregation during *B. subtilis* sporulation, as a *soj* mutant fails to capture *oriC* in ~20% of sporulating cells (187). Results in Chapter II are consistent with this published result, with the further observation that the segregation defect could be reduced to ~10% if the gene for the replication checkpoint protein Sda was also deleted (Fig 2.2). Since Soj has been shown to be able to inhibit DNA replication (140, 143) and Sda executes the sporulation block imposed on actively initiating cells (96), these results hint that half of the *oriC* capture defect in observed in the Δ*soj* mutant may relate to Soj's ability to inhibit DNA replication. Interestingly, results in Chapter II also show that a similar number of origins in the Δ*sirA* mutant (~10%) do not capture *oriC* in the forespore (Fig 2.2). Since Soj and SirA appear to act in the same pathway to facilitate *oriC* capture, I propose that this remaining 10% of origins requires the activity of both Soj and SirA. Currently there is no evidence to indicate whether SirA acts upstream, downstream, or in parallel with Soj

to support *oriC* partitioning. One possibility is that SirA interacts with DnaA to release *oriC* from a membrane-associated pre-replication complex, and that Soj acts downstream of SirA to segregate the free *oriC* toward the distal cell pole (Fig 2.13). One possible mechanism to explain how Soj might perform this function is proposed by Kloosterman et al. (144). In this paper, the authors showed that the MinD/MinJ/ComN protein complex is relocalized from the cell quarter position to the distal cell cell pole through interactions with DivIVA. Soj (which interacts with MinD) may promote *oriC* segregation through its interactions with Spo0J (which binds near *oriC*) and MinD. Further experiments will be required to provide more information regarding the mechanism.

Another interesting question is why only 10% of cells fail to capture *oriC* in the Δ*sirA* mutant? One speculation, which is outlined in Fig 4.1, is that in a mixed population of fast growing cells, only a subset are preparing to initiate replication. In *B. subtilis*, initiation occurs at the membrane and requires the formation of a complex which I generically call a pre-replication complex (71), similar to terminology proposed for *E. coli* (66). Replication only initiates when the proper cell cycle cue is received. At some point early in sporulation, the signal to initiate replication is shut down, and *oriC* needs to be segregated to the distal cell pole. In my model, *oriC*s not attached to the membrane (90%) are able to segregate; however, origins associated with the membrane that have not had the chance to initiate become stuck. In this model, one of SirA's primary functions is not to inhibit new rounds of replication, as has been proposed (7), but rather to disrupt interactions between DnaA and *oriC* so that *oriC* is free to be segregated by Soj. Cells lacking *sirA* are unable to segregate those *oriC*s stuck on the membrane, thus resulting in the ~10% *oriC* capture defect observed in Chapter II (Fig 2.2, Fig 4.1). Alternatively, if expressed early enough with respect to when the pre-

replication complex would be formed, SirA could prevent DnaA from ever engaging *oriC*. Further biochemical assays could be done to test some of these ideas (see below).

4.2 SirA's replication inhibition mechanism might be conserved in other bacterial species

Both the prior results and the results presented in Chapter III indicate that SirA inhibits DNA replication initiation by directly interacting with DnaA Domain I (7, 79, 81). In addition, results in Chapter III suggest that SirA can inhibit DnaA activity without needing any *B. subtilis* specific factors (such as *B. subtilis* DnaD and/or DnaB) (Table 3.4). Since DnaA Domain I is important for DnaA self-dimerization and helicase loading (76, 83), it is possible that SirA inhibits replication by disrupting one or both of these processes. In *E. coli*, DnaA self-dimerization through Domain I is required for cooperative DnaA oligomerization (82, 83). To test if SirA is able to disrupt DnaA self-dimerization, λcI repression assay (259) could be performed to detect DnaA dimerization status in the absence and presence of SirA. Another possibility is that SirA affects helicase loading and results in replication inhibition. In *E. coli*, $DnaA_{E21}$ ($DnaA_{S23}$ in *B. subtilis*) is important for helicase loading (75). Interestingly, results in Chapter III shows that this residue is also important for SirA interaction in *B. subtilis*. The ability to obtain soluble SirA (see discussion below) would be useful to test some of these hypotheses.

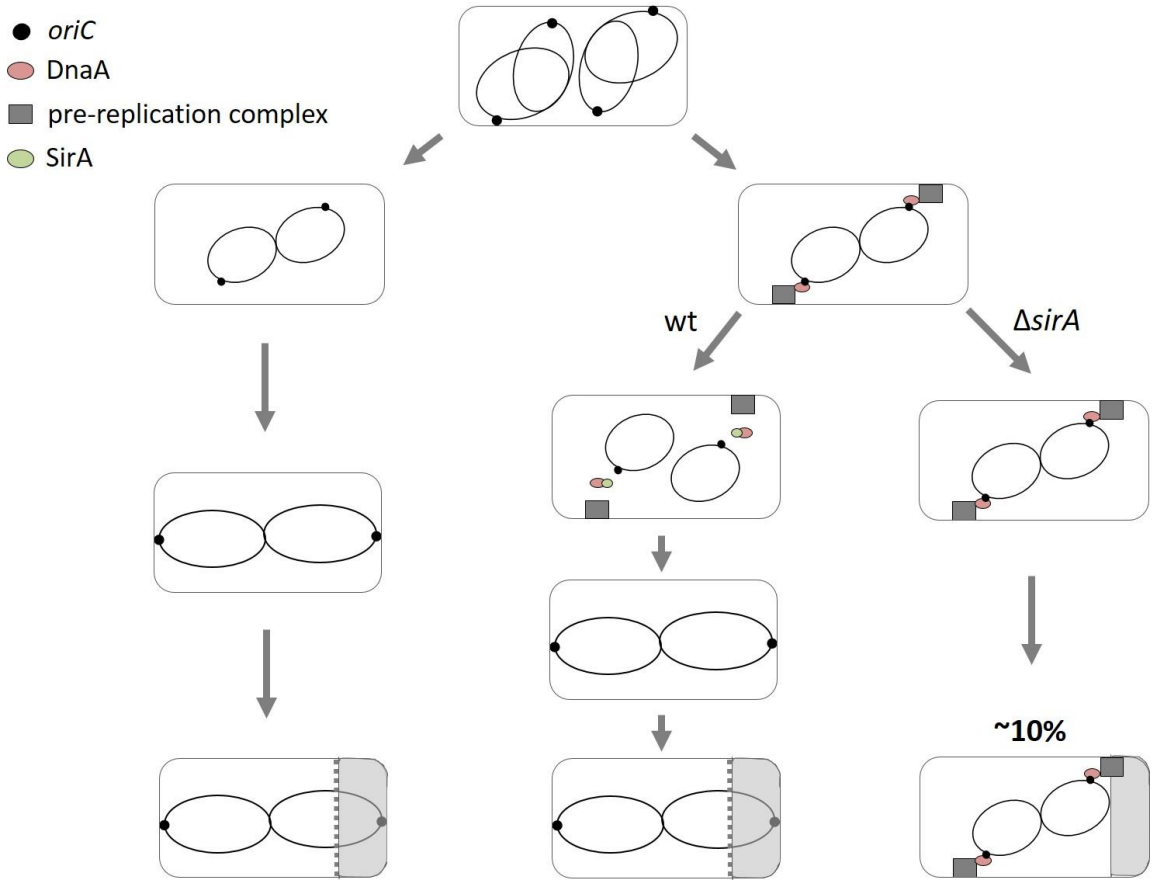

Fig. 4.1. Model for SirA's role in *oriC* segregation during *B. subtilis* sporulation. In a mixed population of fast growing cells, only a subset of cells (~10%) have formed pre-replication complexes at the cell membrane. During *B. subtilis* sporulation, those *oriC*s not attached to the membrane are freely segregated to the cell pole (left panel). Those cells that have engaged the *oriC* in pre-replication complexes become stuck at the membrane as the signal for new rounds of initiation has been shut down. In wild-type cells, SirA interacts with DnaA and releases *oriC* from pre-replication complex, allowing it to be segregated to the cell pole (middle panel). In cells lacking *sirA*, stuck *oriC*s cannot be segregated to the cell pole, thus contributing to the ~10% *oriC* defect observed in the single cell chromosome organization assay (right panel).

So far, the only condition for producing soluble SirA in *E. coli* protein overexpression system is to co-express SirA with *B. subtilis* DnaA Domain I (79). In Chapter III, preliminary evidence is presented that SirA may be capable of self-association through interactions mediated by its C-terminus. More specifically, it has been observed that if the extreme C-terminus of SirA is cleaved, the protein becomes soluble (Fig 3.6, Fig 3.7). To further test this idea, engineered C-terminal truncations of SirA could be overexpressed and tested for solubility.

4.3 SirA's role in *oriC* capture can be uncoupled from its ability to inhibit DNA replication initiation

Results in Chapter II have shown that two DnaA variants which are insensitive to SirA's killing activity ($DnaA_{F49Y}$, $DnaA_{A50V}$), and several SirA variants that are defective in their ability to inhibit DNA replication ($SirA_{Y51A}$, $SirA_{I103V}$, $SirA_{V118M}$, and $SirA_{K121N}$), all captured *oriC* at levels similar to wildtype (Fig 2.8, Fig 2.12). These observations lead to one of the most significant conclusions in Chapter II: SirA's functions in DNA replication and *oriC* segregation represent distinct functions of the protein. Similar to SirA, Soj also functions both as an inhibitor of DnaA (140, 143), and to promote *oriC* capture during sporulation (Fig 2.2)(187). In *Caulobacter crescentus*, the conserved initiation protein DnaA has been shown to be important for chromosome segregation independent of its role in DNA replication (228). Since replication initiation and *oriC* segregation are closely coordinated in bacteria (182, 183), it could be reasonably speculated that bacteria utilize replication initiation proteins to facilitate chromosome segregation. This idea is supported by a growing number of results that the replication regulators are spatially coupled to proteins that marked the boundaries of the

cell poles where the *oriC* is positioned (245-247). A similar idea was proposed more than fifty years ago when it was proposed that the precise regulation of chromosome replication and segregation could result from a connection between the chromosome and the cell surface (262). Results in Chapter II have provided further supports to this idea. Linking the *oriC* to the membrane (possibly through interactions with initators) could help explain the robustness of chromosome partitioning observed in current model systems, even those lacking all known partitioning systems (2, 3, 16, 190). Furthermore, if the sites of attachment were somehow coordinated with cell growth, this model could explain how early forms of life, proliferating through vesiculation (252) may have segregated their genetic material.

REFERENCES

1. Gordon GS & Wright A (2000) DNA segregation in bacteria. *Annual Review of Microbiology* 54(1):681-708.

2. Glaser P, Sharpe ME, Raether B, Perego M, Ohlsen K *et al.* (1997) Dynamic, mitotic-like behavior of a bacterial protein required for accurate chromosome partitioning. *Genes & Development* 11(9):1160-1168.

3. Lewis PJ & Errington J (1997) Direct evidence for active segregation of *oriC* regions of the *Bacillus subtilis* chromosome and co-localization with the Spo0J partitioning protein. *Molecular Microbiology* 25(5):945-954.

4. Jaffé A, D'Ari R, & Norris V (1986) SOS-independent coupling between DNA replication and cell division in *Escherichia coli. Journal of Bacteriology* 165(1):66-71.

5. Niki H, Jaffé A, Imamura R, Ogura T, & Hiraga S (1991) The new gene *mukB* codes for a 177 kd protein with coiled-coil domains involved in chromosome partitioning of *E. coli*. *The EMBO Journal* 10(1):183-193.

6. Wu L & Errington J (1994) *Bacillus subtilis* SpoIIIE protein required for DNA segregation during asymmetric cell division. *Science* 264(5158):572-575.

7. Wagner JK, Marquis KA, & Rudner DZ (2009) SirA enforces diploidy by inhibiting the replication initiator DnaA during spore formation in *Bacillus subtilis. Molecular Microbiology* 73(5):963-974.

8. Drlica K, Malik M, Kerns RJ, & Zhao X (2008) Quinolone-mediated bacterial death. *Antimicrobial Agents and Chemotherapy* 52(2):385-392.

9. van Dijl J & Hecker M (2013) *Bacillus subtilis*: from soil bacterium to super-secreting cell factory. *Microbial Cell Factories* 12(1):1-6.

10. Burkholder PR & Giles NH, Jr. (1947) Induced biochemical mutations in *Bacillus subtilis*. *American Journal of Botany* 34(6):345-348.

11. Aguilar C, Vlamakis H, Losick R, & Kolter R (2007) Thinking about *Bacillus subtilis* as a multicellular organism. *Current Opinion in Microbiology* 10(6):638-643.

12. Auchtung JM, Lee CA, Monson RE, Lehman AP, & Grossman AD (2005) Regulation of a *Bacillus subtilis* mobile genetic element by intercellular signaling and the global DNA damage response. *Proceedings of the National Academy of Sciences* 102(35):12554-12559.

13. Youngman P, Perkins JB, & Losick R (1984) Construction of a cloning site near one end of Tn917 into which foreign DNA may be inserted without affecting transposition in *Bacillus subtilis* or expression of the transposon-borne *erm* gene. *Plasmid* 12(1):1-9.

14. Nicolas P, Mader U, Dervyn E, Rochat T, Leduc A *et al.* (2012) Condition-dependent transcriptome reveals high-level regulatory architecture in *Bacillus subtilis*. *Science* 335(6072):1103-1106.

15. Newton A & Ohta N (1990) Regulation of the cell division cycle and differentiation in bacteria. *Annual Review of Microbiology* 44(1):689-719.

16. Lemon KP & Grossman AD (2001) The extrusion-capture model for chromosome partitioning in bacteria. *Genes & Development* 15(16):2031-2041.

17. Errington J (2003) Regulation of endospore formation in *Bacillus subtilis*. *Nature Review of Microbiology* 1(2):117-126.

18. Errington J (1996) Determination of cell fate in *Bacillus subtilis*. *Trends in Genetics* 12(1):31-34.

19. Bylund JE, Haines MA, Piggot PJ, & Higgins ML (1993) Axial filament formation in *Bacillus subtilis*: induction of nucleoids of increasing length after addition of chloramphenicol to exponential-phase cultures approaching stationary phase. *Journal of Bacteriology* 175(7):1886-1890.

20. Ben-Yehuda S, Rudner DZ, & Losick R (2003) RacA, a bacterial protein that anchors chromosomes to the cell poles. *Science* 299(5606):532-536.

21. Pogliano J, Sharp MD, & Pogliano K (2002) Partitioning of chromosomal DNA during establishment of cellular asymmetry in *Bacillus subtilis*. *Journal of Bacteriology* 184(6):1743-1749.

22. Becker EC & Pogliano K (2007) Cell-specific SpoIIIE assembly and DNA translocation polarity are dictated by chromosome orientation. *Molecular Microbiology* 66(5):1066-1079.

23. Burton BM, Marquis KA, Sullivan NL, Rapoport TA, & Rudner DZ (2007) The ATPase SpoIIIE transports DNA across fused septal membranes during sporulation in *Bacillus subtilis. Cell* 131(7):1301-1312.

24. Piggot PJ & Hilbert DW (2004) Sporulation of *Bacillus subtilis*. *Current Opinion in Microbiology* 7(6):579-586.

25. Popham DL, Helin J, Costello CE, & Setlow P (1996) Analysis of the peptidoglycan structure of *Bacillus subtilis* endospores. *Journal of Bacteriology* 178(22):6451-6458.

26. Driks A (1999) *Bacillus subtilis* Spore coat. *Microbiology and Molecular Biology Reviews* 63(1):1-20.

27. Errington J (1993) *Bacillus subtilis* sporulation: regulation of gene expression and control of morphogenesis. *Microbiological Reviews* 57(1):1-33.

28. Hilbert DW & Piggot PJ (2004) Compartmentalization of gene expression during *Bacillus subtilis* spore formation. *Microbiology and Molecular Biology Reviews* 68(2):234-262.

29. Higgins D & Dworkin J (2012) Recent progress in *Bacillus subtilis* sporulation. *FEMS Microbiology Reviews* 36(1):131-148.

30. Parker GF, Daniel RA, & Errington J (1996) Timing and genetic regulation of commitment to sporulation in *Bacillus subtilis*. *Microbiology* 142(12):3445-3452.

31. Dworkin J & Losick R (2005) Developmental commitment in a bacterium. *Cell* 121(3):401-409.

32. Britton RA, Eichenberger P, Gonzalez-Pastor JE, Fawcett P, Monson R *et al.* (2002) Genome-wide analysis of the stationary-phase sigma factor (Sigma-H) regulon of *Bacillus subtilis*. *Journal of Bacteriology* 184(17):4881-4890.

33. Phillips ZE & Strauch MA (2002) *Bacillus subtilis* sporulation and stationary phase gene expression. *Cell Molecular Life Sciences* 59(3):392-402.

34. Jiang M, Shao W, Perego M, & Hoch JA (2000) Multiple histidine kinases regulate entry into stationary phase and sporulation in *Bacillus subtilis*. *Molecular Microbiology* 38(3):535-542.

35. Burbulys D, Trach KA, & Hoch JA (1991) Initiation of sporulation in *B. subtilis* is controlled by a multicomponent phosphorelay. *Cell* 64(3):545-552.

36. Molle V, Fujita M, Jensen ST, Eichenberger P, Gonzalez-Pastor JE *et al.* (2003) The Spo0A regulon of *Bacillus subtilis*. *Molecular Microbiology* 50(5):1683-1701.

37. Predich M, Nair G, & Smith I (1992) *Bacillus subtilis* early sporulation genes *kinA*, *spo0F*, and *spo0A* are transcribed by the RNA polymerase containing sigma H. *Journal of Bacteriology* 174(9):2771-2778.

38. Strauch MA, Trach KA, Day J, & Hoch JA (1992) Spo0A activates and represses its own synthesis by binding at its dual promoters. *Biochimie* 74(7-8):619-626.

39. Zaitseva E, Yang S-T, Melikov K, Pourmal S, & Chernomordik LV (2010) Dengue virus ensures its fusion in late endosomes using compartment-specific lipids. *PLoS Pathogenesis* 6(10):e1001131.

40. Fawcett P, Eichenberger P, Losick R, & Youngman P (2000) The transcriptional profile of early to middle sporulation in *Bacillus subtilis*. *Proceedings of the National Academy of Sciences* 97(14):8063-8068.

41. Ben-Yehuda S & Losick R (2002) Asymmetric cell division in *B. subtilis* involves a spiral-like intermediate of the cytokinetic protein FtsZ. *Cell* 109(2):257-266.

42. Levin PA & Losick R (1996) Transcription factor Spo0A switches the localization of the cell division protein FtsZ from a medial to a bipolar pattern in *Bacillus subtilis*. *Genes & Development* 10(4):478-488.

43. Wagner-Herman JK, Bernard R, Dunne R, Bisson-Filho AW, Kumar K *et al.* (2012) RefZ facilitates the switch from medial to polar division during spore formation in *Bacillus subtilis*. *Journal of Bacteriology* 194(17):4608-4618.

44. Fujita M & Losick R (2003) The master regulator for entry into sporulation in *Bacillus subtilis* becomes a cell-specific transcription factor after asymmetric division. *Genes & Development* 17(9):1166-1174.

45. Fujita M & Sadaie Y (1998) Feedback loops involving Spo0A and AbrB in in vitro transcription of the genes involved in the initiation of sporulation in *Bacillus subtilis*. *Journal of Biochemistry* 124(1):98-104.

46. Leonard AC & Grimwade JE (2011) Regulation of DnaA assembly and activity: taking directions from the genome. *Annual Review of Microbiology* 65(1):19-35.

47. Huberman JA & Riggs AD (1968) On the mechanism of DNA replication in mammalian chromosomes. *Journal of Molecular Biology* 32(2):327-341.

48. McCulloch SD & Kunkel TA (2008) The fidelity of DNA synthesis by eukaryotic replicative and translesion synthesis polymerases. *Cell Research* 18(1):148-161.

49. Meister P, Taddei A, & Gasser SM (2006) In and out of the replication factory. *Cell* 125(7):1233-1235.

50. Araki H (2011) Initiation of chromosomal DNA replication in eukaryotic cells; contribution of yeast genetics to the elucidation. *Genes & Genetic Systems* 86(3):141-149.

51. Diffley JF (1996) Once and only once upon a time: specifying and regulating origins of DNA replication in eukaryotic cells. *Genes & Development* 10(22):2819-2830.

52. Leatherwood J (1998) Emerging mechanisms of eukaryotic DNA replication initiation. *Current Opinion in Cell Biology* 10(6):742-748.

53. Tanaka S & Araki H (2010) Regulation of the initiation step of DNA replication by cyclin-dependent kinases. *Chromosoma* 119(6):565-574.

54. Yoshida K, Poveda A, & Pasero P (2013) Time to be versatile: regulation of the replication timing program in budding yeast. *Journal of Molecular Biology* 425(23):4696-4705.

55. Sclafani RA & Holzen TM (2007) Cell cycle regulation of DNA replication. *Annual Review of Genetics* 41(1):237-280.

56. Diffley JFX (2004) Regulation of early events in chromosome replication. *Current Biology* 14(18):R778-R786.

57. Drury LS, Perkins G, & Diffley JFX (1997) The Cdc4/34/53 pathway targets Cdc6p for proteolysis in budding yeast. *The EMBO Journal* 16(19):5966-5976.

58. Labib K, Diffley JFX, & Kearsey SE (1999) G1-phase and B-type cyclins exclude the DNA-replication factor Mcm4 from the nucleus. *Nature Cell Biology* 1(7):415-422.

59. Liku ME, Nguyen VQ, Rosales AW, Irie K, & Li JJ (2005) CDK phosphorylation of a novel NLS-NES module distributed between two subunits of the Mcm2-7 complex prevents chromosomal rereplication. *Molecular Biology of the Cell* 16(10):5026-5039.

60. Bell SP & Dutta A (2002) DNA replication in eukaryotic cells. *Annual Review of Biochemistry* 71(1):333-374.

61. Mimura S & Takisawa H (1998) *Xenopus* Cdc45-dependent loading of DNA polymerase α onto chromatin under the control of S-phase cdk. *The EMBO Journal* 17(19):5699-5707.

62. Tabata S, Oka A, Sugimoto K, Takanami M, Yasuda S *et al.* (1983) The 245 base-pair *oriC* sequence of the *E. coli* chromosome directs bidirectional replication at an adjacent region. *Nucleic Acids Research* 11(9):2617-2626.

63. Schaper S & Messer W (1995) Interaction of the initiator protein DnaA of *Escherichia coli* with its DNA target. *Journal of Biological Chemistry* 270(29):17622-17626.

64. Fuller RS, Funnell BE, & Kornberg A (1984) The DnaA protein complex with the *E. coli* chromosomal replication origin (*oriC*) and other DNA sites. *Cell* 38(3):889-900.

65. Fujikawa N, *et al.* (2003) Structural basis of replication origin recognition by the DnaA protein. *Nucleic Acids Research* 31(8):2077-2086.

66. Marszalek J & Kaguni JM (1994) DnaA protein directs the binding of DnaB protein in initiation of DNA replication in *Escherichia coli. Journal of Biological Chemistry* 269(7):4883-4890.

67. Kobori JA & Kornberg A (1982) The *Escherichia coli dnaC* gene product. III. Properties of the DnaB-DnaC protein complex. *Journal of Biological Chemistry* 257(22):13770-13775.

68. Kaguni JM (2006) DnaA: Controlling the initiation of bacterial DNA replication and more. *Annual Review of Microbiology* 60(1):351-371.

69. Heller RC & Marians KJ (2006) Replisome assembly and the direct restart of stalled replication forks. *Nature Review of Molecular Cell Biology* 7(12):932-943.

70. Indiani C & O'Donnell M (2006) The replication clamp-loading machine at work in the three domains of life. *Nature Review of Molecular Cell Biology* 7(10):751-761.

71. Smits WK, Goranov AI, & Grossman AD (2010) Ordered association of helicase loader proteins with the *Bacillus subtilis* origin of replication in vivo. *Molecular Microbiology* 75(2):452-461.

72. Smits WK, Merrikh H, Bonilla CY, & Grossman AD (2011) Primosomal proteins DnaD and DnaB are recruited to chromosomal regions bound by DnaA in *Bacillus subtilis*. *Journal of Bacteriology* 193(3):640-648.

73. Ioannou C, Schaeffer PM, Dixon NE, & Soultanas P (2006) Helicase binding to DnaI exposes a cryptic DNA-binding site during helicase loading in *Bacillus subtilis*. *Nucleic Acids Research* 34(18):5247-5258.

74. Ozaki S & Katayama T (2009) DnaA structure, function, and dynamics in the initiation at the chromosomal origin. *Plasmid* 62(2):71-82.

75. Abe Y, Jo T, Matsuda Y, Matsunaga C, Katayama T *et al.* (2007) Structure and function of DnaA N-terminal Domains: specific sites and mechanisms in inter-DnaA interaction and in DnaB helicase loading on *oriC*. *Journal of Biological Chemistry* 282(24):17816-17827.

76. Felczak MM, Simmons LA, & Kaguni JM (2005) An essential tryptophan of *Escherichia coli* DnaA protein functions in oligomerization at the *E. coli* replication origin. *Journal of Biological Chemistry* 280(26):24627-24633.

77. Duan Y, Huey JD, & Herman JK (2016) The DnaA inhibitor SirA acts in the same pathway as Soj (ParA) to facilitate oriC segregation during *Bacillus subtilis* sporulation. *Molecular Microbiology* 102(3):530-544.

78. Ishida T, Akimitsu N, Kashioka T, Hatano M, Kubota T *et al.* (2004) DiaA, a novel DnaA-binding protein, ensures the timely initiation of *Escherichia coli* chromosome replication. *Journal of Biological Chemistry* 279(44):45546-45555.

79. Jameson KH, Rostami N, Fogg MJ, Turkenburg JP, Grahl A *et al.* (2014) Structure and interactions of the *Bacillus subtilis* sporulation inhibitor of DNA replication, SirA, with domain I of DnaA. *Molecular Microbiology* 93(5):975-991.

80. Keyamura K, Fujikawa N, Ishida T, Ozaki S, Su'etsugu M *et al.* (2007) The interaction of DiaA and DnaA regulates the replication cycle in *E. coli* by directly promoting ATP–DnaA-specific initiation complexes. *Genes & Development* 21(16):2083-2099.

81. Rahn-Lee L, Merrikh H, Grossman AD, & Losick R (2011) The sporulation protein SirA inhibits the binding of DnaA to the origin of replication by contacting a patch of clustered amino acids. *Journal of Bacteriology* 193(6):1302-1307.

82. Simmons LA, Felczak M, & Kaguni JM (2003) DnaA protein of *Escherichia coli*: oligomerization at the *E. coli* chromosomal origin is required for initiation and involves specific N-terminal amino acids. *Molecular Microbiology* 49(3):849-858.

83. Weigel C, Schmidt A, Seitz H, Tungler D, Welzeck M *et al.* (1999) The N-terminus promotes oligomerization of the *Escherichia coli* initiator protein DnaA. *Molecular Microbiology* 34(1):53-66.

84. Nozaki S & Ogawa T (2008) Determination of the minimum domain II size of *Escherichia coli* DnaA protein essential for cell viability. *Microbiology* 154(11):3379-3384.

85. Sekimizu K, Bramhill D, & Kornberg A (1987) ATP activates DnaA protein in initiating replication of plasmids bearing the origin of the *E. coli* chromosome. *Cell* 50(2):259-265.

86. Erzberger JP, Pirruccello MM, & Berger JM (2002) The structure of bacterial DnaA: implications for general mechanisms underlying DNA replication initiation. *The EMBO Journal* 21(18):4763-4773.

87. Leonard AC & Grimwade JE (2010) Regulating DnaA complex assembly: it is time to fill the gaps. *Current Opinion in Microbiology* 13(6):766-772.

88. Ozaki S & Katayama T (2012) Highly organized DnaA-*oriC* complexes recruit the single-stranded DNA for replication initiation. *Nucleic Acids Research* 40(4):1648-1665.

89. Ishikawa S, Ogura Y, Yoshimura M, Okumura H, Cho E *et al.* (2007) Distribution of stable DnaA-binding sites on the *Bacillus subtilis* genome detected using a modified ChIP-chip method. *DNA Research* 14(4):155-168.

90. Goranov AI, Katz L, Breier AM, Burge CB, & Grossman AD (2005) A transcriptional response to replication status mediated by the conserved bacterial replication protein DnaA. *Proceedings of the National Academy of Sciences* 102(36):12932-12937.

91. Messer W & Weigel C (1997) DnaA initiator-also a transcription factor. *Molecular Microbiology* 24(1):1-6.

92. Burkholder WF, Kurtser I, & Grossman AD (2001) Replication initiation proteins regulate a developmental checkpoint in *Bacillus subtilis*. *Cell* 104(2):269-279.

93. Collier J, Murray SR, & Shapiro L (2006) DnaA couples DNA replication and the expression of two cell cycle master regulators. *The EMBO Journal* 25(2):346-356.

94. Gon S, Camara JE, Klungsoyr HK, Crooke E, Skarstad K *et al.* (2006) A novel regulatory mechanism couples deoxyribonucleotide synthesis and DNA replication in *Escherichia coli*. *The EMBO Journal* 25(5):1137-1147.

95. Hoover SE, Xu W, Xiao W, & Burkholder WF (2010) Changes in DnaA-dependent gene expression contribute to the transcriptional and developmental response of *Bacillus subtilis* to manganese limitation in Luria-Bertani medium. *Journal of Bacteriology* 192(15):3915-3924.

96. Veening J-W, Murray H, & Errington J (2009) A mechanism for cell cycle regulation of sporulation initiation in *Bacillus subtilis*. *Genes & Development* 23(16):1959-1970.

97. Braun RE, O'Day K, & Wright A (1985) Autoregulation of the DNA replication gene *dnaA* in *E. coli* K-12. *Cell* 40(1):159-169.

98. Katayama T, Ozaki S, Keyamura K, & Fujimitsu K (2010) Regulation of the replication cycle: conserved and diverse regulatory systems for DnaA and *oriC*. *Nature Review of Microbiology* 8(3):163-170.

99. Geier GE & Modrich P (1979) Recognition sequence of the dam methylase of *Escherichia coli* K12 and mode of cleavage of Dpn I endonuclease. *Journal of Biological Chemistry* 254(4):1408-1413.

100. Zyskind JW & Smith DW (1986) The bacterial origin of replication, *oriC*. *Cell* 46(4):489-490.

101. Rasmussen KV & Schaechter M (1994) SeqA limits DnaA activity in replication from *oriC* in *Escherichia coli*. *Molecular Microbiology* 14(4):763-772.

102. Brendler T, Abeles A, & Austin S (1995) A protein that binds to the P1 origin core and the *oriC* 13mer region in a methylation-specific fashion is the product of the host *seqA* gene. *The EMBO Journal* 14(16):4083-4089.

103. Brendler T & Austin S (1999) Binding of SeqA protein to DNA requires interaction between two or more complexes bound to separate hemimethylated GATC sequences. *The EMBO Journal* 18(8):2304-2310.

104. Russell DW & Zinder ND (1987) Hemimethylation prevents DNA replication in *E. coli*. *Cell* 50(7):1071-1079.

105. Taghbalout A, Landoulsi A, Kern R, Yamazoe M, Hiraga S *et al.* (2000) Competition between the replication initiator DnaA and the sequestration factor SeqA for binding to the hemimethylated chromosomal origin of *E. coli* in vitro. *Genes to Cells* 5(11):873-884.

106. Lu M, Campbell JL, Boye E, & Kleckner N (1994) SeqA: A negative modulator of replication initiation in *E. coli. Cell* 77(3):413-426.

107. Nievera C, Torgue JJC, Grimwade Julia E, & Leonard AC (2006) SeqA blocking of DnaA-*oriC* interactions ensures staged assembly of the *E. coli* pre-RC. *Molecular Cell* 24(4):581-592.

108. Katayama T, Kubota T, Kurokawa K, Crooke E, & Sekimizu K (1998) The initiator function of DnaA protein is negatively regulated by the sliding clamp of the *E. coli* chromosomal replicase. *Cell* 94(1):61-71.

109. Kato Ji & Katayama T (2001) Hda, a novel DnaA-related protein, regulates the replication cycle in *Escherichia coli*. *The EMBO Journal* 20(15):4253-4262.

110. Kurz M, Dalrymple B, Wijffels G, & Kongsuwan K (2004) Interaction of the sliding clamp β-subunit and Hda, a DnaA-related protein. *Journal of Bacteriology* 186(11):3508-3515.

111. Su'etsugu M, Shimuta T-r, Ishida T, Kawakami H, & Katayama T (2005) Protein associations in DnaA-ATP hydrolysis mediated by the Hda-replicase clamp complex. *Journal of Biological Chemistry* 280(8):6528-6536.

112. Nishida S, Fujimitsu K, Sekimizu K, Ohmura T, Ueda T *et al.* (2002) A nucleotide switch in the *Escherichia coli* DnaA protein initiates chromosomal replication: evidence from a mutant DnaA protein defective in regulatory ATP hydrolysis in vitro and in vivo. *Journal of Biological Chemistry* 277(17):14986-14995.

113. Su'etsugu M, Takata M, Kubota T, Matsuda Y, & Katayama T (2004) Molecular mechanism of DNA replication-coupled inactivation of the initiator protein in *Escherichia coli*: interaction of DnaA with the sliding clamp-loaded DNA and the sliding clamp-Hda complex. *Genes to Cells* 9(6):509-522.

114. Collier J & Shapiro L (2009) Feedback control of DnaA-mediated replication initiation by replisome-associated HdaA protein in *Caulobacter*. *Journal of Bacteriology* 191(18):5706-5716.

115. Kitagawa R, Mitsuki H, Okazaki T, & Ogawa T (1996) A novel DnaA protein-binding site at 94.7 min on the *Escherichia coli* chromosome. *Molecular Microbiology* 19(5):1137-1147.

116. Kitagawa R, Ozaki T, Moriya S, & Ogawa T (1998) Negative control of replication initiation by a novel chromosomal locus exhibiting exceptional affinity for *Escherichia coli* DnaA protein. *Genes & Development* 12(19):3032-3043.

117. Ogawa T, Yamada Y, Kuroda T, Kishi T, & Moriya S (2002) The *datA* locus predominantly contributes to the initiator titration mechanism in the control of replication initiation in *Escherichia coli*. *Molecular Microbiology* 44(5):1367-1375.

118. Morigen, Molina F, & Skarstad K (2005) Deletion of the *datA* Site does not affect once-per-cell-cycle timing but induces rifampin-resistant replication. *Journal of Bacteriology* 187(12):3913-3920.

119. Kasho K & Katayama T (2013) DnaA binding locus *datA* promotes DnaA-ATP hydrolysis to enable cell cycle-coordinated replication initiation. *Proceedings of the National Academy of Sciences* 110(3):936-941.

120. Fujimitsu K & Katayama T (2004) Reactivation of DnaA by DNA sequence-specific nucleotide exchange in vitro. *Biochemical and Biophysical Research Communications* 322(2):411-419.

121. Fujimitsu K, Senriuchi T, & Katayama T (2009) Specific genomic sequences of *E. coli* promote replicational initiation by directly reactivating ADP-DnaA. *Genes & Development* 23(10):1221-1233.

122. Keyamura K, Abe Y, Higashi M, Ueda T, & Katayama T (2009) DiaA dynamics are coupled with changes in initial origin complexes leading to helicase loading. *Journal of Biological Chemistry* 284(37):25038-25050.

123. Zawilak-Pawlik A, Donczew R, Szafranski S, Mackiewicz P, Terradot L *et al.* (2011) DiaA/HobA and DnaA: a pair of proteins co-evolved to cooperate during bacterial orisome assembly. *Journal of Molecular Biology* 408(2):238-251.

124. Terradot L & Zawilak-Pawlik A (2010) Structural insight into *Helicobacter pylori* DNA replication initiation. *Gut Microbes* 1(5):330-334.

125. Natrajan G, Hall DR, Thompson AC, Gutsche I, & Terradot L (2007) Structural similarity between the DnaA-binding proteins HobA (HP1230) from

Helicobacter pylori and DiaA from *Escherichia coli*. *Molecular Microbiology* 65(4):995-1005.

126. Natrajan G, Noirot-Gros MF, Zawilak-Pawlik A, Kapp U, & Terradot L (2009) The structure of a DnaA/HobA complex from *Helicobacter pylori* provides insight into regulation of DNA replication in bacteria. *Proceedings of the National Academy of Sciences* 106(50):21115-21120.

127. Scholefield G & Murray H (2013) YabA and DnaD inhibit helix assembly of the DNA replication initiation protein DnaA. *Molecular Microbiology* 90(1):147-159.

128. Kurokawa K, Mizumura H, Takaki T, Ishii Y, Ichihashi N *et al.* (2009) Rapid exchange of bound ADP on the *Staphylococcus aureus* replication initiation protein DnaA. *Journal of Biological Chemistry* 284(49):34201-34210.

129. Flatten I, Fossum-Raunehaug S, Taipale R, Martinsen S, & Skarstad K (2015) The DnaA protein is not the limiting factor for initiation of replication in *Escherichia coli*. *PLoS Genetics* 11(6):e1005276.

130. Noirot-Gros M-F, Dervyn E, Wu LJ, Mervelet P, Errington J *et al.* (2002) An expanded view of bacterial DNA replication. *Proceedings of the National Academy of Sciences* 99(12):8342-8347.

131. Goranov AI, Breier AM, Merrikh H, & Grossman AD (2009) YabA of *Bacillus subtilis* controls DnaA-mediated replication initiation but not the transcriptional response to replication stress. *Molecular Microbiology* 74(2):454-466.

132. Hayashi M, Ogura Y, Harry EJ, Ogasawara N, & Moriya S (2005) *Bacillus subtilis* YabA is involved in determining the timing and synchrony of replication initiation. *FEMS Microbiology Letters* 247(1):73-79.

133. Merrikh H & Grossman AD (2011) Control of the replication initiator DnaA by an anti-cooperativity factor. *Molecular Microbiology* 82(2):434-446.

134. Gruber S & Errington J (2009) Recruitment of condensin to replication origin regions by ParB/Spo0J promotes chromosome segregation in *B. subtilis. Cell* 137(4):685-696.

135. Abeles AL, Friedman SA, & Austin SJ (1985) Partition of unit-copy miniplasmids to daughter cells. *Journal of Molecular Biology* 185(2):261-272.

136. Livny J, Yamaichi Y, & Waldor MK (2007) Distribution of centromere-like *parS* sites in bacteria: insights from comparative genomics. *Journal of Bacteriology* 189(23):8693-8703.

137. Gerdes K, Møller-Jensen J, & Jensen RB (2000) Plasmid and chromosome partitioning: surprises from phylogeny. *Molecular Microbiology* 37(3):455-466.

138. Wu LJ & Errington J (2003) RacA and the Soj-Spo0J system combine to effect polar chromosome segregation in sporulating *Bacillus subtilis*. *Molecular Microbiology* 49(6):1463-1475.

139. Lee PS & Grossman AD (2006) The chromosome partitioning proteins Soj (ParA) and Spo0J (ParB) contribute to accurate chromosome partitioning, separation of replicated sister origins, and regulation of replication initiation in *Bacillus subtilis*. *Molecular Microbiology* 60(4):853-869.

140. Murray H & Errington J (2008) Dynamic control of the DNA replication initiation protein DnaA by Soj/ParA. *Cell* 135(1):74-84.

141. Ogura Y, Ogasawara N, Harry EJ, & Moriya S (2003) Increasing the ratio of Soj to Spo0J promotes replication initiation in *Bacillus subtilis*. *Journal of Bacteriology* 185(21):6316-6324.

142. Scholefield G, Whiting R, Errington J, & Murray H (2011) Spo0J regulates the oligomeric state of Soj to trigger its switch from an activator to an inhibitor of DNA replication initiation. *Molecular Microbiology* 79(4):1089-1100.

143. Scholefield G, Errington J, & Murray H (2012) Soj/ParA stalls DNA replication by inhibiting helix formation of the initiator protein DnaA. *The EMBO Journal* 31(6):1542-1555.

144. Kloosterman TG, *et al.* (2016) Complex polar machinery required for proper chromosome segregation in vegetative and sporulating cells of *Bacillus subtilis*. *Molecular Microbiology* 101(2):333-350.

145. Patel SS & Donmez I (2006) Mechanisms of helicases. *Journal of Biological Chemistry* 281(27):18265-18268.

146. Griep MA (1995) Primase structure and function. *Indian Journal of Biochemistry & Biophysics* 32(4):171-178.

147. Kelman Z & O'Donnell M (1995) DNA Polymerase III holoenzyme: structure and function of a chromosomal replicating machine. *Annual Review of Biochemistry* 64(1):171-200.

148. Edwards S, Li CM, Levy DL, Brown J, Snow PM *et al.* (2003) *Saccharomyces cerevisiae* DNA Polymerase ε and Polymerase σ interact physically and functionally, suggesting a role for polymerase ε in sister chromatid cohesion. *Molecular and Cellular Biology* 23(8):2733-2748.

149. Johnson RE, Klassen R, Prakash L, & Prakash S (2015) A major role of DNA Polymerase δ in replication of both the leading and lagging DNA strands. *Molecular Cell* 59(2):163-175.

150. Sakabe K & Okazaki R (1966) A unique property of the replicating region of chromosomal DNA. *Biochimica et Biophysica Acta* 129(3):651-654.

151. Okazaki R, Okazaki T, Sakabe K, & Sugimoto K (1967) Mechanism of DNA replication possible discontinuity of DNA chain growth. *Japanese Journal of Medical Science & Biology* 20(3):255-260.

152. Jin YH, Obert R, Burgers PM, Kunkel TA, Resnick MA *et al.* (2001) The 3'→5' exonuclease of DNA polymerase δ can substitute for the 5' flap endonuclease Rad27/Fen1 in processing Okazaki fragments and preventing genome instability. *Proceedings of the National Academy of Sciences* 98(9):5122-5127.

153. Jin YH, Ayyagari R, Resnick MA, Gordenin DA, & Burgers PMJ (2003) Okazaki fragment maturation in yeast: II. cooperation between the polymerase and 3'-5'-exonuclease activities of Pol δ in the creation of a ligatable nick. *Journal of Biological Chemistry* 278(3):1626-1633.

154. Levin DS, Bai W, Yao N, O'Donnell M, & Tomkinson AE (1997) An interaction between DNA ligase I and proliferating cell nuclear antigen: implications for Okazaki fragment synthesis and joining. *Proceedings of the National Academy of Sciences* 94(24):12863-12868.

155. Levin DS, McKenna AE, Motycka TA, Matsumoto Y, & Tomkinson AE (2000) Interaction between PCNA and DNA ligase I is critical for joining of Okazaki fragments and long-patch base-excision repair. *Current Biology* 10(15):919-S912.

156. Dewar JM, Budzowska M, & Walter JC (2015) The mechanism of DNA replication termination in vertebrates. *Nature* 525(7569):345-350.

157. Mulugu S, Potnis A, Shamsuzzaman, Taylor J, Alexander K *et al.* (2001) Mechanism of termination of DNA replication of *Escherichia coli* involves helicase-contrahelicase interaction. *Proceedings of the National Academy of Sciences* 98(17):9569-9574.

158. Kamada K, Horiuchi T, Ohsumi K, Shimamoto N, & Morikawa K (1996) Structure of a replication-terminator protein complexed with DNA. *Nature* 383(6601):598-603.

159. Hill TM, Pelletier AJ, Tecklenburg ML, & Kuempel PL (1988) Identification of the DNA sequence from the *E. coli* terminus region that halts replication forks. *Cell* 55(3):459-466.

160. Bussiere DE & Bastia D (1999) Termination of DNA replication of bacterial and plasmid chromosomes. *Molecular Microbiology* 31(6):1611-1618.

161. Hiasa H & Marians KJ (1992) Differential inhibition of the DNA translocation and DNA unwinding activities of DNA helicases by the *Escherichia coli* Tus protein. *Journal of Biological Chemistry* 267(16):11379-11385.

162. Horiuchi T & Hidaka M (1988) Core sequence of two separable terminus sites of the R6K plasmid that exhibit polar inhibition of replication is a 20 bp inverted repeat. *Cell* 54(4):515-523.

163. McGuffee SR, Smith DJ, & Whitehouse I (2013) Quantitative, genome-wide analysis of eukaryotic replication initiation and termination. *Molecular Cell* 50(1):123-135.

164. Santamaria D, Viguera E, Martinez-Robles ML, Hyrien O, Hernandez P *et al.* (2000) Bi-directional replication and random termination. *Nucleic Acids Research* 28(10):2099-2107.

165. Marston AL (2014) Chromosome segregation in budding yeast: sister chromatid cohesion and related mechanisms. *Genetics* 196(1):31-63.

166. Michaelis C, Ciosk R, & Nasmyth K (1997) Cohesins: chromosomal proteins that prevent premature separation of sister chromatids. *Cell* 91(1):35-45.

167. Haering CH, Lowe J, Hochwagen A, & Nasmyth K (2002) Molecular architecture of SMC proteins and the yeast cohesin complex. *Molecular Cell* 9(4):773-788.

168. Britton RA, Lin DC-H, & Grossman AD (1998) Characterization of a prokaryotic SMC protein involved in chromosome partitioning. *Genes & Development* 12(9):1254-1259.

169. Losada A, Hirano M, & Hirano T (1998) Identification of Xenopus SMC protein complexes required for sister chromatid cohesion. *Genes & Development* 12(13):1986-1997.

170. Fousteri MI & Lehmann AR (2000) A novel SMC protein complex in *Schizosaccharomyces pombe* contains the Rad18 DNA repair protein. *The EMBO Journal* 19(7):1691-1702.

171. Nasmyth K & Haering CH (2005) The structure and function of SMC and kleisin complexes. *Annual Review of Biochemistry* 74(1):595-648.

172. Hirano M & Hirano T (2002) Hinge-mediated dimerization of SMC protein is essential for its dynamic interaction with DNA. *The EMBO Journal* 21(21):5733-5744.

173. Maiato H, DeLuca J, Salmon ED, & Earnshaw WC (2004) The dynamic kinetochore-microtubule interface. *Journal of Cell Science* 117(23):5461-5477.

174. Winey M, Mamay CL, O'Toole ET, Mastronarde DN, Giddings TH Jr *et al.* (1995) Three-dimensional ultrastructural analysis of the *Saccharomyces cerevisiae* mitotic spindle. *The Journal of Cell Biology* 129(6):1601-1615.

175. Indjeian VB & Murray AW (2007) Budding yeast mitotic chromosomes have an intrinsic bias to biorient on the spindle. *Current Biology* 17(21):1837-1846.

176. Biggins S, Severin FF, Bhalla N, Sassoon I, Hyman AA *et al.* (1999) The conserved protein kinase Ipl1 regulates microtubule binding to kinetochores in budding yeast. *Genes & Development* 13(5):532-544.

177. Tanaka TU (2010) Kinetochore-microtubule interactions: steps towards bi-orientation. *The EMBO Journal* 29(24):4070-4082.

178. Irniger S, Piatti S, Michaelis C, & Nasmyth K (1995) Genes involved in sister chromatid separation are needed for b-type cyclin proteolysis in budding yeast. *Cell* 81(2):269-277.

179. Peters JM (2006) The anaphase promoting complex/cyclosome: a machine designed to destroy. *Nature Review of Molecular Cell Biology* 7(9):644-656.

180. Ciosk R, Zachariae W, Michaelis C, Shevchenko A, Mann M *et al.* (1998) An ESP1/PDS1 complex regulates loss of sister chromatid cohesion at the metaphase to anaphase transition in yeast. *Cell* 93(6):1067-1076.

181. Uhlmann F, Lottspeich F, & Nasmyth K (1999) Sister-chromatid separation at anaphase onset is promoted by cleavage of the cohesin subunit Scc1. *Nature* 400(6739):37-42.

182. Viollier PH, Thanbichler M, McGrath PT, West L, Meewan M *et al.* (2004) Rapid and sequential movement of individual chromosomal loci to specific subcellular locations during bacterial DNA replication. *Proceedings of the National Academy of Sciences* 101(25):9257-9262.

183. Sharpe ME & Errington J (1998) A fixed distance for separation of newly replicated copies of oriC in *Bacillus subtilis*: implications for co-ordination of chromosome segregation and cell division. *Molecular Microbiology* 28(5):981-990.

184. Possoz C, Junier I, & Espeli O (2012) Bacterial chromosome segregation. *Frontiers in Bioscience (Landmark edition)* 17:1020-1034.

185. Woldringh CL & Nanninga N (2006) Structural and physical aspects of bacterial chromosome segregation. *Journal of Structural Biology* 156(2):273-283.

186. Reyes-Lamothe R, Nicolas E, & Sherratt DJ (2012) Chromosome replication and segregation in bacteria. *Annual Review of Genetics* 46(1):121-143.

187. Sullivan NL, Marquis KA, & Rudner DZ (2009) Recruitment of SMC by ParB-*parS* organizes the origin region and promotes efficient chromosome segregation. *Cell* 137(4):697-707.

188. Yamaichi Y, Fogel MA, & Waldor MK (2007) *par* genes and the pathology of chromosome loss in *Vibrio cholerae*. *Proceedings of the National Academy of Sciences* 104(2):630-635.

189. Toro E & Shapiro L (2010) Bacterial chromosome organization and segregation. *Cold Spring Harbor Perspectives in Biology* 2(2).

190. Lin DC-H & Grossman AD (1998) Identification and characterization of a bacterial chromosome partitioning site. *Cell* 92(5):675-685.

191. Lee MJ, Liu CH, Wang SY, Huang CT, & Huang H (2006) Characterization of the Soj/Spo0J chromosome segregation proteins and identification of putative parS sequences in *Helicobacter pylori*. *Biochemical and Biophysical Research Communications* 342(3):744-750.

192. Yamaichi Y, Fogel MA, McLeod SM, Hui MP, & Waldor MK (2007) Distinct centromere-like *parS* sites on the two chromosomes of *Vibrio spp*. *Journal of Bacteriology* 189(14):5314-5324.

193. Bartosik AA, Lasocki K, Mierzejewska J, Thomas CM, & Jagura-Burdzy G (2004) ParB of *Pseudomonas aeruginosa*: interactions with its partner ParA and its target *parS* and specific effects on bacterial growth. *Journal of Bacteriology* 186(20):6983-6998.

194. Kim HJ, Calcutt MJ, Schmidt FJ, & Chater KF (2000) Partitioning of the linear chromosome during sporulation of *Streptomyces coelicolor* A3(2) involves an *oriC*-linked *parAB* Locus. *Journal of Bacteriology* 182(5):1313-1320.

195. Mohl DA, Easter J, & Gober JW (2001) The chromosome partitioning protein, ParB, is required for cytokinesis in *Caulobacter crescentus*. *Molecular Microbiology* 42(3):741-755.

196. Sharpe ME & Errington J (1996) The *Bacillus subtilis soj-spo0J* locus is required for a centromere-like function involved in prespore chromosome partitioning. *Molecular Microbiology* 21(3):501-509.

197. Fogel MA & Waldor MK (2006) A dynamic, mitotic-like mechanism for bacterial chromosome segregation. *Genes & Development* 20(23):3269-3282.

198. Ptacin JL, Lee SF, Garner EC, Toro E, Eckart M *et al.* (2010) A spindle-like apparatus guides bacterial chromosome segregation. *Nature Cell Biology* 12(8):791-798.

199. Lim HC, Surovtsev IV, Beltran BG, Huang F, Bewersdorf J *et al.* (2014) Evidence for a DNA-relay mechanism in ParABS-mediated chromosome segregation. *eLife* 3:e02758.

200. Cunha S, Woldringh CL, & Odijk T (2005) Restricted diffusion of DNA segments within the isolated *Escherichia coli* nucleoid. *Journal of Structural Biology* 150(2):226-232.

201. Wiggins PA, Cheveralls KC, Martin JS, Lintner R, & Kondev J (2010) Strong intranucleoid interactions organize the *Escherichia coli* chromosome into a nucleoid filament. *Proceedings of the National Academy of Sciences* 107(11):4991-4995.

202. Ireton K, Gunther NW, & Grossman AD (1994) *spo0J* is required for normal chromosome segregation as well as the initiation of sporulation in *Bacillus subtilis. Journal of Bacteriology* 176(17):5320-5329.

203. Leonard TA, Butler PJ, & Lowe J (2005) Bacterial chromosome segregation: structure and DNA binding of the Soj dimer---a conserved biological switch. *The EMBO Journal* 24(2):270-282.

204. Graumann PL, Losick R, & Strunnikov AV (1998) Subcellular localization of *Bacillus subtilis* SMC, a protein involved in chromosome condensation and segregation. *Journal of Bacteriology* 180(21):5749-5755.

205. Graumann PL (2000) *Bacillus subtilis* SMC is required for proper arrangement of the chromosome and for efficient segregation of replication termini but not for bipolar movement of newly duplicated origin regions. *Journal of Bacteriology* 182(22):6463-6471.

206. Moriya S, Tsujikawa E, Hassan AK, Asai K, Kodama T *et al.* (1998) A *Bacillus subtilis* gene-encoding protein homologous to eukaryotic SMC motor protein is necessary for chromosome partition. *Molecular Microbiology* 29(1):179-187.

207. Jensen RB & Shapiro L (1999) The *Caulobacter crescentus smc* gene is required for cell cycle progression and chromosome segregation. *Proceedings of the National Academy of Sciences* 96(19):10661-10666.

208. Niki H, Imamura R, Kitaoka M, Yamanaka K, Ogura T *et al.* (1992) *E.coli* MukB protein involved in chromosome partition forms a homodimer with a rod-and-hinge structure having DNA binding and ATP/GTP binding activities. *The EMBO Journal* 11(13):5101-5109.

209. Yamanaka K, Ogura T, Niki H, & Hiraga S (1996) Identification of two new genes, *mukE* and *mukF*, involved in chromosome partitioning in *Escherichia coli. Molecular & General Genetics : MGG* 250(3):241-251.

210. Benoist C, Guerin C, Noirot P, & Dervyn E (2015) Constitutive stringent response restores viability of *Bacillus subtilis* lacking structural maintenance of chromosome protein. *PLoS ONE* 10(11):e0142308.

211. Danilova O, Reyes-Lamothe R, Pinskaya M, Sherratt D, & Possoz C (2007) MukB colocalizes with the *oriC* region and is required for organization of the two *Escherichia coli* chromosome arms into separate cell halves. *Molecular Microbiology* 65(6):1485-1492.

212. Nolivos S, Upton AL, Badrinarayanan A, Muller J, Zawadzka K *et al.* (2016) MatP regulates the coordinated action of topoisomerase IV and MukBEF in chromosome segregation. *Nature Communications* 7:10466.

213. Wang X, Tang OW, Riley EP, & Rudner DZ (2014) The SMC condensin complex is required for origin segregation in *Bacillus subtilis*. *Current Biology* 24(3):287-292.

214. Bigot S, Sivanathan V, Possoz C, Barre FX, & Cornet F (2007) FtsK, a literate chromosome segregation machine. *Molecular Microbiology* 64(6):1434-1441.

215. Grainge I, Bregu M, Vazgues M, Sivanathan V, Ip SC *et al.* (2007) Unlinking chromosome catenanes *in vivo* by site-specific recombination. *The EMBO Journal* 26(19):4228-4238.

216. Lesterlin C, Barre FX, & Cornet F (2004) Genetic recombination and the cell cycle: what we have learned from chromosome dimers. *Molecular Microbiology* 54(5):1151-1160.

217. Lesterlin C, Pages C, Dubarry N, Dasgupta S, & Cornet F (2008) Asymmetry of chromosome replichores renders the DNA translocase activity of FtsK essential for cell division and cell shape maintenance in *Escherichia coli*. *PLoS Genetics* 4(12):e1000288.

218. Flardh K & Buttner MJ (2009) *Streptomyces* morphogenetics: dissecting differentiation in a filamentous bacterium. *Nature Review of Microbiology* 7(1):36-49.

219. Chaconas G & Kobryn K (2010) Structure, function, and evolution of linear replicons in *Borrelia*. *Annual Review of Microbiology* 64(1):185-202.

220. Kaimer C, Gonzalez-Pastor JE, & Graumann PL (2009) SpoIIIE and a novel type of DNA translocase, SftA, couple chromosome segregation with cell division in *Bacillus subtilis*. *Molecular Microbiology* 74(4):810-825.

221. Kaimer C, Schenk K, & Graumann PL (2011) Two DNA translocases synergistically affect chromosome dimer resolution in *Bacillus subtilis*. *Journal of Bacteriology* 193(6):1334-1340.

222. Biller SJ & Burkholder WF (2009) The *Bacillus subtilis* SftA (YtpS) and SpoIIIE DNA translocases play distinct roles in growing cells to ensure faithful chromosome partitioning. *Molecular Microbiology* 74(4):790-809.

223. Wu LJ & Errington J (1997) Septal localization of the SpoIIIE chromosome partitioning protein in *Bacillus subtilis*. *The EMBO Journal* 16(8):2161-2169.

224. Ben-Yehuda S, Rudner DZ, & Losick R (2003) Assembly of the SpoIIIE DNA translocase depends on chromosome trapping in *Bacillus subtilis*. *Current Biology* 13(24):2196-2200.

225. Bath J, Wu LJ, Errington J, & Wang JC (2000) Role of *Bacillus subtilis* SpoIIIE in DNA transport across the mother cell-prespore division septum. *Science* 290(5493):995-997.

226. Ptacin JL, Nollmann M, Becker EC, Cozzarelli NR, Pogliano K *et al.* (2008) Sequence-directed DNA export guides chromosome translocation during sporulation in *Bacillus subtilis*. *Nature Structure Molecular Biology* 15(5):485-493.

227. Rahn-Lee L, Gorbatyuk B, Skovgaard O, & Losick R (2009) The conserved sporulation protein YneE inhibits DNA replication in *Bacillus subtilis*. *Journal of Bacteriology* 191(11):3736-3739.

228. Mera PE, Kalogeraki VS, & Shapiro L (2014) Replication initiator DnaA binds at the *Caulobacter centromere* and enables chromosome segregation. *Proceedings of the National Academy of Sciences* 111(45):16100-16105.

229. Niki H, Yamaichi Y, & Hiraga S (2000) Dynamic organization of chromosomal DNA in *Escherichia coli*. *Genes & Development* 14(2):212-223.

230. Hirano T (2016) Condensin-based chromosome organization from bacteria to vertebrates. *Cell* 164(5):847-857.

231. Wang X, Le TB, Lajoie BR, Dekker J, Laub MT *et al.* (2015) Condensin promotes the juxtaposition of DNA flanking its loading site in *Bacillus subtilis*. *Genes & Development* 29(15):1661-1675.

232. Miller AK, Brown EE, Mercado BT, & Herman JK (2016) A DNA-binding protein defines the precise region of chromosome capture during *Bacillus* sporulation. *Molecular Microbiology* 99(1):111-122.

233. Ben-Yehuda S, Fujita M, Liu XS, Gorbatyak B, Skoko D *et al.* (2005) Defining a centromere-like element in *Bacillus subtilis* by identifying the binding sites for the chromosome-anchoring protein RacA. *Molecular Cell* 17(6):773-782.

234. Bramkamp M, Emmins R, Weston L, Donovan C, Daniel RA *et al.* (2008) A novel component of the division-site selection system of *Bacillus subtilis* and a new mode of action for the division inhibitor MinCD. *Molecular Microbiology* 70(6):1556-1569.

235. Patrick JE & Kearns DB (2008) MinJ (YvjD) is a topological determinant of cell division in *Bacillus subtilis*. *Molecular Microbiology* 70(5):1166-1179.

236. dos Santos VT, Bisson-Filho AW, & Gueiros-Filho FJ (2012) DivIVA-mediated polar localization of ComN, a posttranscriptional regulator of *Bacillus subtilis*. *Journal of Bacteriology* 194(14):3661-3669.

237. Harwood CR & Cutting SM (1990) *Molecular biological methods for Bacillus.* (Wiley, New York, NY).

238. Youngman PJ, Perkins JB, & Losick R (1983) Genetic transposition and insertional mutagenesis in *Bacillus subtilis* with *Streptococcus faecalis* transposon Tn917. *Proceedings of the National Academy of Sciences* 80(8):2305-2309.

239. Kearns DB & Losick R (2005) Cell population heterogeneity during growth of *Bacillus subtilis*. *Genes & Development* 19(24):3083-3094.

240. Rasband W (1997-2015) ImageJ (U.S. National Institutes of Health, Bethesda, Maryland).

241. Karimova G, Pidoux J, Ullmann A, & Ladant D (1998) A bacterial two-hybrid system based on a reconstituted signal transduction pathway. *Proceedings of the National Academy of Sciences* 95(10):5752-5756.

242. Ozaki S, Kawakami H, Nakamura K, Fujikawa N, Kagawa W *et al.* (2008) A common mechanism for the ATP-DnaA-dependent formation of open complexes at the replication origin. *Journal of Biological Chemistry* 283(13):8351-8362.

243. Badrinarayanan A, Le TB, & Laub MT (2015) Bacterial chromosome organization and segregation. *Annual Review of Cell and Developmental Biology* 31(1):171-199.

244. Mohl DA & Gober JW (1997) Cell cycle-dependent polar localization of chromosome partitioning proteins in *Caulobacter crescentus. Cell* 88(5):675-684.

245. Eswaramoorthy P, Winter PW, Wawrzusin P, York AG, Shroff H *et al.* (2014) Asymmetric division and differential gene expression during a bacterial developmental program requires DivIVA. *PLoS Genetics* 10(8):e1004526.

246. Lenarcic R, Halbedel S, Visser L, Shaw M, Wu LJ *et al.* (2009) Localisation of DivIVA by targeting to negatively curved membranes. *The EMBO Journal* 28(15):2272-2282.

247. Marston AL, Thomaides HB, Edwards DH, Sharpe ME, & Errington J (1998) Polar localization of the MinD protein of *Bacillus subtilis* and its role in selection of the mid-cell division site. *Genes & Development* 12(21):3419-3430.

248. Autret S & Errington J (2003) A role for division-site-selection protein MinD in regulation of internucleoid jumping of Soj (ParA) protein in *Bacillus subtilis*. *Molecular Microbiology* 47(1):159-169.

249. Cho E, Ogasawara N, & Ishikawa S (2008) The functional analysis of YabA, which interacts with DnaA and regulates initiation of chromosome replication in *Bacillus subtils*. *Genes & Genetic Systems* 83(2):111-125.

250. Bonilla CY & Grossman AD (2012) The primosomal protein DnaD inhibits cooperative DNA binding by the replication initiator DnaA in *Bacillus subtilis.* *Journal of Bacteriology* 194(18):5110-5117.

251. Jacob F, Brenner S, & Cuzin F (1963) On the regulation of DNA replication in bacteria. *Cold Spring Harbor Symposia on Quantitative Biology* 28:329-348.

252. Leaver M, Dominguez-Cuevas P, Coxhead JM, Daniel RA, & Errington J (2009) Life without a wall or division machine in *Bacillus subtilis*. *Nature* 457(7231):849-853.

253. Ogura Y, Imai Y, Ogasawara N, & Moriya S (2001) Autoregulation of the *dnaA-dnaN* operon and effects of DnaA protein levels on replication initiation in *Bacillus subtilis*. *Journal of Bacteriology* 183(13):3833-3841.

254. Molt KL, Sutera VA, Moore KK, & Lovett ST (2009) A role for nonessential Domain II of initiator protein, DnaA, in replication control. *Genetics* 183(1):39-49.

255. Ruvolo MV, Mach KE, & Burkholder WF (2006) Proteolysis of the replication checkpoint protein Sda is necessary for the efficient initiation of sporulation after transient replication stress in *Bacillus subtilis*. *Molecular Microbiology* 60(6):1490-1508.

256. Duan Y, Sperber AM, & Herman JK (2016) YodL and YisK possess shape-modifying activities that are suppressed by mutations in *Bacillus subtilis mreB* and *mbl*. *Journal of Bacteriology* 198(15):2074-2088.

257. Bunk B, Schulz A, Stammen S, Munch R, Warren MJ *et al.* (2010) A short story about a big magic bug. *Bioengineered Bugs* 1(2):85-91.

258. Bruand C, Velten M, McGovern S, Marsin S, Serena C *et al.* (2005) Functional interplay between the *Bacillus subtilis* DnaD and DnaB proteins essential for initiation and re-initiation of DNA replication. *Molecular Microbiology* 55(4):1138-1150.

259. Hu J, O'Shea E, Kim P, & Sauer R (1990) Sequence requirements for coiled-coils: analysis with lambda repressor-GCN4 leucine zipper fusions. *Science* 250(4986):1400-1403.

260. Sutton MD, Carr KM, Vicente M, & Kaguni JM (1998) *Escherichia coli* DnaA Protein: the N-terminal domain and loading of DnaB helicase at the *E. coli* chromosomal origin. *Journal of Biological Chemistry* 273(51):34255-34262.

261. Seitz H, Weigel C, & Messer W (2000) The interaction domains of the DnaA and DnaB replication proteins of *Escherichia coli*. *Molecular Microbiology* 37(5):1270-1279.

262. Jacob F, Brenner S, & Cuzin F (1963) On the regulation of DNA replication in bacteria. *Cold Spring Harbor Symposia on Quantitative Biology* 23:329.

263. Young KD (2010) Bacterial shape: two-dimensional questions and possibilities. *Annual Review of Microbiology* 64:223-240.

264. Silhavy TJ, Kahne D, & Walker S (2010) The bacterial cell envelope. *Cold Spring Harbor Perspectives in Biology* 2(5):a000414.

265. Holtje JV (1998) Growth of the stress-bearing and shape-maintaining murein sacculus of *Escherichia coli*. *Microbiology and Molecular Biology Reviews : MMBR* 62(1):181-203.

266. Young KD (2006) The selective value of bacterial shape. *Microbiology and Molecular Biology Reviews : MMBR* 70(3):660-703.

267. Young KD (2007) Bacterial morphology: why have different shapes? *Current Opinion in Microbiology* 10(6):596-600.

268. Randich AM & Brun YV (2015) Molecular mechanisms for the evolution of bacterial morphologies and growth modes. *Frontiers in Microbiology* 6:580.

269. Fenton AK & Gerdes K (2013) Direct interaction of FtsZ and MreB is required for septum synthesis and cell division in *Escherichia coli*. *The EMBO Journal* 32(13):1953-1965.

270. Figge RM, Divakaruni AV, & Gober JW (2004) MreB, the cell shape-determining bacterial actin homologue, co-ordinates cell wall morphogenesis in *Caulobacter crescentus*. *Molecular Microbiology* 51(5):1321-1332.

271. Ouellette SP, Karimova G, Subtil A, & Ladant D (2012) Chlamydia co-opts the rod shape-determining proteins MreB and Pbp2 for cell division. *Molecular Microbiology* 85(1):164-178.

272. Salje J, van den Ent F, de Boer P, & Lowe J (2011) Direct membrane binding by bacterial actin MreB. *Molecular Cell* 43(3):478-487.

273. Colavin A, Hsin J, & Huang KC (2014) Effects of polymerization and nucleotide identity on the conformational dynamics of the bacterial actin homolog MreB. *Proceedings of the National Academy of Sciences* 111(9):3585-3590.

274. Gitai Z, Dye NA, Reisenauer A, Wachi M, & Shapiro L (2005) MreB actin-mediated segregation of a specific region of a bacterial chromosome. *Cell* 120(3):329-341.

275. Iwai N, Nagai K, & Wachi M (2002) Novel S-benzylisothiourea compound that induces spherical cells in *Escherichia coli* probably by acting on a rod-shape-determining protein(s) other than penicillin-binding protein 2. *Bioscience, Biotechnology, and Biochemistry* 66(12):2658-2662.

276. Bean GJ, Flickinger ST, Westler WM, McCully ME, Sept D *et al.* (2009) A22 disrupts the bacterial actin cytoskeleton by directly binding and inducing a low-affinity state in MreB. *Biochemistry* 48(22):4852-4857.

277. Takacs CN, Poggio S, Charbon G, Pucheault M, Vollmer W *et al.* (2010) MreB drives de novo rod morphogenesis in *Caulobacter crescentus* via remodeling of the cell wall. *Journal of Bacteriology* 192(6):1671-1684.

278. Bendezu FO & de Boer PA (2008) Conditional lethality, division defects, membrane involution, and endocytosis in mre and mrd shape mutants of *Escherichia coli*. *Journal of Bacteriology* 190(5):1792-1811.

279. van den Ent F, Johnson CM, Persons L, de Boer P, & Lowe J (2010) Bacterial actin MreB assembles in complex with cell shape protein RodZ. *The EMBO Journal* 29(6):1081-1090.

280. Kruse T, Bork-Jensen J, & Gerdes K (2005) The morphogenetic MreBCD proteins of *Escherichia coli* form an essential membrane-bound complex. *Molecular Microbiology* 55(1):78-89.

281. Varma A & Young KD (2009) In *Escherichia coli*, MreB and FtsZ direct the synthesis of lateral cell wall via independent pathways that require PBP 2. *Journal of Bacteriology* 191(11):3526-3533.

282. Kawai Y, Daniel RA, & Errington J (2009) Regulation of cell wall morphogenesis in *Bacillus subtilis* by recruitment of PBP1 to the MreB helix. *Molecular Microbiology* 71(5):1131-1144.

283. Bendezu FO, Hale CA, Bernhardt TG, & de Boer PA (2009) RodZ (YfgA) is required for proper assembly of the MreB actin cytoskeleton and cell shape in *E. coli*. *The EMBO Journal* 28(3):193-204.

284. Muchova K, Chromikova Z, & Barak I (2013) Control of *Bacillus subtilis* cell shape by RodZ. *Environmental Microbiology* 15(12):3259-3271.

285. Alyahya SA, Alexander R, Costa T, Henrigues AO, Emonet T *et al.* (2009) RodZ, a component of the bacterial core morphogenic apparatus. *Proceedings of the National Academy of Sciences* 106(4):1239-1244.

286. Niba ET, Li G, Aoki K, & Kitakawa M (2010) Characterization of *rodZ* mutants: RodZ is not absolutely required for the cell shape and motility. *FEMS Microbiology Letters* 309(1):35-42.

287. Shiomi D, Toyoda A, Aizu T, Ejima F, Fujiyama A *et al.* (2013) Mutations in cell elongation genes *mreB*, *mrdA* and *mrdB* suppress the shape defect of RodZ-deficient cells. *Molecular Microbiology* 87(5):1029-1044.

288. Morgenstein RM, Bratton BP, Nguyen JP, Ouzounov N, Shaevitz JW *et al.* (2015) RodZ links MreB to cell wall synthesis to mediate MreB rotation and robust morphogenesis. *Proceedings of the National Academy of Sciences* 112(40):12510-12515.

289. Cabeen MT & Jacobs-Wagner C (2010) The bacterial cytoskeleton. *Annual Review of Genetics* 44:365-392.

290. Carballido-Lopez R, Formstone A, Li Y, Ehrlich SD, Noirot P *et al.* (2006) Actin homolog MreBH governs cell morphogenesis by localization of the cell wall hydrolase LytE. *Developmental Cell* 11(3):399-409.

291. Formstone A & Errington J (2005) A magnesium-dependent *mreB* null mutant: implications for the role of *mreB* in *Bacillus subtilis*. *Molecular Microbiology* 55(6):1646-1657.

292. Schirner K & Errington J (2009) The cell wall regulator {sigma}I specifically suppresses the lethal phenotype of mbl mutants in *Bacillus subtilis*. *Journal of Bacteriology* 191(5):1404-1413.

293. Kawai Y, Asai K, & Errington J (2009) Partial functional redundancy of MreB isoforms, MreB, Mbl and MreBH, in cell morphogenesis of *Bacillus subtilis*. *Molecular Microbiology* 73(4):719-731.

294. Defeu Soufo HJ & Graumann PL (2006) Dynamic localization and interaction with other *Bacillus subtilis* actin-like proteins are important for the function of MreB. *Molecular Microbiology* 62(5):1340-1356.

295. Mirouze N, Ferret C, Yao Z, Chastanet A, & Carballido-Lopez R (2015) MreB-dependent inhibition of cell elongation during the escape from competence in *Bacillus subtilis*. *PLoS Genetics* 11(6):e1005299.

296. Tseng CL & Shaw GC (2008) Genetic evidence for the actin homolog gene *mreBH* and the bacitracin resistance gene *bcrC* as targets of the alternative sigma factor SigI of *Bacillus subtilis*. *Journal of Bacteriology* 190(5):1561-1567.

297. Dominguez-Cuevas P, Porcelli I, Daniel RA, & Errington J (2013) Differentiated roles for MreB-actin isologues and autolytic enzymes in *Bacillus subtilis* morphogenesis. *Molecular Microbiology* 89(6):1084-1098.

298. Masuda H, Tan Q, Awano N, Wu KP, & Inouye M (2012) YeeU enhances the bundling of cytoskeletal polymers of MreB and FtsZ, antagonizing the CbtA (YeeV) toxicity in *Escherichia coli*. *Molecular Microbiology* 84(5):979-989.

299. Tan Q, Awano N, & Inouye M (2011) YeeV is an *Escherichia coli* toxin that inhibits cell division by targeting the cytoskeleton proteins, FtsZ and MreB. *Molecular Microbiology* 79(1):109-118.

300. Masuda H, Tan Q, Awano N, Yamaguchi Y, & Inouye M (2012) A novel membrane-bound toxin for cell division, CptA (YgfX), inhibits polymerization of cytoskeleton proteins, FtsZ and MreB, in *Escherichia coli*. *FEMS Microbiology Letters* 328(2):174-181.

301. Yakhnina AA & Gitai Z (2012) The small protein MbiA interacts with MreB and modulates cell shape in *Caulobacter crescentus*. *Molecular Microbiology* 85(6):1090-1104.

302. Ababneh QO & Herman JK (2015) CodY regulates SigD levels and activity by binding to three sites in the *fla/che* operon. *Journal of Bacteriology* 197(18):2999-3006.

303. Branda SS, Gonzalez-Pastor JE, Ben-Yehuda S, Losick R, & Kolter R (2001) Fruiting body formation by *Bacillus subtilis*. *Proceedings of the National Academy of Sciences* 98(20):11621-11626.

304. Schaeffer P, Millet J, & Aubert JP (1965) Catabolic repression of bacterial sporulation. *Proceedings of the National Academy of Sciences* 54(3):704-711.

305. Ababneh QO & Herman JK (2015) RelA inhibits *Bacillus subtilis* motility and chaining. *Journal of Bacteriology* 197(1):128-137.

306. Abhayawardhane Y & Stewart GC (1995) *Bacillus subtilis* possesses a second determinant with extensive sequence similarity to the *Escherichia coli mreB* morphogene. *Journal of Bacteriology* 177(3):765-773.

307. Leaver M & Errington J (2005) Roles for MreC and MreD proteins in helical growth of the cylindrical cell wall in *Bacillus subtilis*. *Molecular Microbiology* 57(5):1196-1209.

308. Arrieta-Ortiz ML, Hafemeister C, Bate AR, Chu T, Greenfield A *et al.* (2015) An experimentally supported model of the *Bacillus subtilis* global transcriptional regulatory network. *Molecular Systems Biology* 11(11):839.

309. Caspi R, Altman T, Billington R, Dreher K, Foerster H *et al.* (2014) The MetaCyc database of metabolic pathways and enzymes and the BioCyc collection of pathway/genome databases. *Nucleic Acids Research* 42(Database issue):D459-471.

310. Antoniewski C, Savelli B, & Stragier P (1990) The *spoIIJ* gene, which regulates early developmental steps in *Bacillus subtilis*, belongs to a class of environmentally responsive genes. *Journal of Bacteriology* 172(1):86-93.

311. Fujita M & Sadaie Y (1998) Promoter selectivity of the *Bacillus subtilis* RNA polymerase σ^A and σ^H holoenzymes. *Journal of Biochemistry* 124(1):89-97.

312. Chastanet A, Vitkup D, Yuan GC, Norman TM, Liu JS *et al.* (2010) Broadly heterogeneous activation of the master regulator for sporulation in *Bacillus subtilis*. *Proceedings of the National Academy of Sciences* 107(18):8486-8491.

313. de Jong IG, Veening JW, & Kuipers OP (2010) Heterochronic phosphorelay gene expression as a source of heterogeneity in *Bacillus subtilis* spore formation. *Journal of Bacteriology* 192(8):2053-2067.

314. Sterlini JM & Mandelstam J (1969) Commitment to sporulation in *Bacillus subtilis* and its relationship to development of actinomycin resistance. *Biochemistry Journal* 113(1):29-37.

315. Pan Q & Losick R (2003) Unique degradation signal for ClpCP in *Bacillus subtilis*. *Journal of Bacteriology* 185(17):5275-5278.

316. Fujita M, Gonzalez-Pastor JE, & Losick R (2005) High- and low-threshold genes in the Spo0A regulon of *Bacillus subtilis*. *Journal of Bacteriology* 187(4):1357-1368.

317. Dye NA, Pincus Z, Fisher IC, Shapiro L, & Theriot JA (2011) Mutations in the nucleotide binding pocket of MreB can alter cell curvature and polar morphology in *Caulobacter*. *Molecular Microbiology* 81(2):368-394.

318. Gitai Z, Dye N, & Shapiro L (2004) An actin-like gene can determine cell polarity in bacteria. *Proceedings of the National Academy of Sciences* 101(23):8643-8648.

319. Srivastava P, Demarre G, Karpova TS, McNally J, & Chattoraj DK (2007) Changes in nucleoid morphology and origin localization upon inhibition or alteration of the actin homolog, MreB, of *Vibrio cholerae*. *Journal of Bacteriology* 189(20):7450-7463.

320. van den Ent F, Amos LA, & Lowe J (2001) Prokaryotic origin of the actin cytoskeleton. *Nature* 413(6851):39-44.

321. Yang J, Yan R, Roy A, Xu D, Poisson J *et al.* (2015) The I-TASSER Suite: protein structure and function prediction. *Nature Methods* 12(1):7-8.

322. van den Ent F, Izore T, Bharat TA, Johnson CM, & Lowe J (2014) Bacterial actin MreB forms antiparallel double filaments. *eLife* 3:e02634.

323. Murray T, Popham DL, & Setlow P (1998) *Bacillus subtilis* cells lacking Penicillin-Binding Protein 1 require increased levels of divalent cations for growth. *Journal of Bacteriology* 180(17):4555-4563.

324. Popham DL & Setlow P (1996) Phenotypes of *Bacillus subtilis* mutants lacking multiple class A high-molecular-weight penicillin-binding proteins. *Journal of Bacteriology* 178(7):2079-2085.

325. Schirner K & Errington J (2009) The cell wall regulator σ^I specifically suppresses the lethal phenotype of mbl mutants in *Bacillus subtilis*. *Journal of Bacteriology* 191(5):1404-1413.

326. Meisner J, Montero Llopis P, Sham LT, Garner E, Bernhardt TG *et al.* (2013) FtsEX is required for CwlO peptidoglycan hydrolase activity during cell wall elongation in *Bacillus subtilis. Molecular Microbiology* 89(6):1069-1083.

327. Dubnau EJ, Cabane K, & Smith I (1987) Regulation of *spo0H*, an early sporulation gene in bacilli. *Journal of Bacteriology* 169(3):1182-1191.

328. Weir J, Predich M, Dubnau E, Nair G, & Smith I (1991) Regulation of *spo0H*, a gene coding for the *Bacillus subtilis sigma H* factor. *Journal of Bacteriology* 173(2):521-529.

329. Perego M, Spiegelman GB, & Hoch JA (1988) Structure of the gene for the transition state regulator, *abrB*: regulator synthesis is controlled by the *spo0A* sporulation gene in *Bacillus subtilis*. *Molecular Microbiology* 2(6):689-699.

330. Strauch M, Webb V, Spiegelman G, & Hoch JA (1990) The Spo0A protein of *Bacillus subtilis* is a repressor of the *abrB* gene. *Proceedings of the National Academy of Sciences* 87(5):1801-1805.

331. Wiser MJ & Lenski RE (2015) A comparison of methods to measure fitness in *Escherichia coli*. *PLoS ONE* 10(5):e0126210.

332. Typas A, Banzhaf M, Gross CA, & Vollmer W (2012) From the regulation of peptidoglycan synthesis to bacterial growth and morphology. *Nature Review of Microbiology* 10(2):123-136.

333. White CL, Kitich A, & Gober JW (2010) Positioning cell wall synthetic complexes by the bacterial morphogenetic proteins MreB and MreD. *Molecular Microbiology* 76(3):616-633.

334. Favini-Stabile S, Contreras-Martel C, Thielens N, & Dessen A (2013) MreB and MurG as scaffolds for the cytoplasmic steps of peptidoglycan biosynthesis. *Environmental Microbiology* 15(12):3218-3228.

335. Jones LJF, Carballido-Lopez R, & Errington J (2001) Control of cell shape in bacteria: helical, actin-like filaments in *Bacillus subtilis*. *Cell* 104(6):913-922.

336. Mohammadi T, Karczmarek A, Crouviosier M, Bouhss A, Mengin-Lecreulx A *et al.* (2007) The essential peptidoglycan glycosyltransferase MurG forms a complex with proteins involved in lateral envelope growth as well as with proteins involved in cell division in *Escherichia coli. Molecular Microbiology* 65(4):1106-1121.

337. Tseng HC, Harwell CL, Martin CH, & Prather KL (2010) Biosynthesis of chiral 3-hydroxyvalerate from single propionate-unrelated carbon sources in metabolically engineered *E. coli*. *Microbial Cell Factories* 9(1):1-12.

338. Gardner KAJA, Moore DA, & Erickson HP (2013) The C-terminal linker of *Escherichia coli* FtsZ functions as an intrinsically disordered peptide. *Molecular Microbiology* 89(2):264-275.

339. Shen B & Lutkenhaus J (2009) The conserved C-terminal tail of FtsZ is required for the septal localization and division inhibitory activity of MinC(C)/MinD. *Molecular Microbiology* 72(2):410-424.

340. Huang KH, Mychack A, Tchorzewski L, & Janakiraman A (2016) Characterization of the FtsZ C-terminal variable (CTV) region in Z-ring assembly and interaction with the Z-ring stabilizer ZapD in *E. coli* cytokinesis. *PLoS ONE* 11(4):e0153337.

341. Buske PJ & Levin PA (2012) Extreme C-terminus of bacterial cytoskeletal protein FtsZ plays fundamental role in assembly independent of modulatory proteins. *Journal of Biological Chemistry* 287(14):10945-10957.

342. Szwedziak P, Wang Q, Freund SM, & Lowe J (2012) FtsA forms actin-like protofilaments. *The EMBO Journal* 31(10):2249-2260.

343. Mosyak L, Zhang Y, Glasfeld E, Haney S, Stahl M *et al.* (2000) The bacterial cell-division protein ZipA and its interaction with an FtsZ fragment revealed by X-ray crystallography. *The EMBO Journal* 19(13):3179-3191.

344. Shen B & Lutkenhaus J (2010) Examination of the interaction between FtsZ and MinCN in *E. coli* suggests how MinC disrupts Z rings. *Molecular Microbiology* 75(5):1285-1298.

345. Bramhill D & Thompson CM (1994) GTP-dependent polymerization of *Escherichia coli* FtsZ protein to form tubules. *Proceedings of the National Academy of Sciences* 91(13):5813-5817.

346. Weiss DS (2004) Bacterial cell division and the septal ring. *Molecular Microbiology* 54(3):588-597.

347. Camberg JL, Viola MG, Rea L, Hoskins JR, & Wickner S (2014) Location of dual sites in *E. coli* FtsZ important for degradation by ClpXP; one at the C-terminus and one in the disordered linker. *PLoS ONE* 9(4):e94964.

348. Camberg JL, Hoskins JR, & Wickner S (2009) ClpXP protease degrades the cytoskeletal protein, FtsZ, and modulates FtsZ polymer dynamics. *Proceedings of the National Academy of Sciences* 106(26):10614-10619.

349. Le Breton Y, Mohapatra NP, & Haldenwang WG (2006) In vivo random mutagenesis of *Bacillus subtilis* by use of TnYLB-1, a mariner-based transposon. *Applied and Environmental Microbiology* 72(1):327-333.

350. Kunst F, Ogasawara N, Moszer I, Albertini AM, Alloni G *et al.* (1997) The complete genome sequence of the Gram-positive bacterium *Bacillus subtilis*. *Nature* 390(6657):249-256.

351. Ludwig H, Homuth G, Schmalisch M, Dyka FM, Hecker M *et al.* (2001) Transcription of glycolytic genes and operons in *Bacillus subtilis*: evidence for the presence of multiple levels of control of the *gapA* operon. *Molecular Microbiology* 41(2):409-422.

352. Fujita Y (2009) Carbon catabolite control of the metabolic network in *Bacillus subtilis*. *Bioscience, Biotechnology, and Biochemistry* 73(2):245-259.

353. Gorke B, Foulquier E, & Galinier A (2005) YvcK of *Bacillus subtilis* is required for a normal cell shape and for growth on Krebs cycle intermediates and substrates of the pentose phosphate pathway. *Microbiology* 151(11):3777-3791.

354. Akanuma G, Nanamiya H, Natori Y, Yano K, Suzuki S *et al.* (2012) Inactivation of ribosomal protein genes in *Bacillus subtilis* reveals importance of each ribosomal protein for cell proliferation and cell differentiation. *Journal of Bacteriology* 194(22):6282-6291.

355. Takada H, Morita M, Shiwa Y, Sugimoto R, Suzuki S *et al.* (2014) Cell motility and biofilm formation in *Bacillus subtilis* are affected by the ribosomal proteins, S11 and S21. *Bioscience, Biotechnology, and Biochemistry* 78(5):898-907.

356. Lei Y, Oshima T, Ogasawara N, & Ishikawa S (2013) Functional analysis of the protein Veg, which stimulates biofilm formation in *Bacillus subtilis*. *Journal of Bacteriology* 195(8):1697-1705.

357. Jorgenson MA, Kannan S, Laubacher ME, & Young KD (2016) Dead-end intermediates in the enterobacterial common antigen pathway induce morphological defects in *Escherichia coli* by competing for undecaprenyl phosphate. *Molecular Microbiology* 100(1):1-14.

358. Abe T, Sakaki K, Fujihara A, Ujiie H, Ushida C *et al.* (2008) tmRNA-dependent trans-translation is required for sporulation in *Bacillus subtilis*. *Molecular Microbiology* 69(6):1491-1498.

359. D'Elia MA, Millar KE, Bhavsar AP, Tomljenovic AM, Hutter B *et al.* (2009) Probing teichoic acid genetics with bioactive molecules reveals new interactions among diverse processes in bacterial cell wall biogenesis. *Chemistry & Biology* 16(5):548-556.

360. Farha MA, Czarny TL, Myers CL, Worrall LJ, French S *et al.* (2015) Antagonism screen for inhibitors of bacterial cell wall biogenesis uncovers an inhibitor of undecaprenyl diphosphate synthase. *Proceedings of the National Academy of Sciences* 112(35):11048-11053.

361. Schirner K, Eun YJ, Dion M, Luo Y, Helmann JD *et al.* (2015) Lipid-linked cell wall precursors regulate membrane association of bacterial actin MreB. *Nature Chemical Biology* 11(1):38-45.

362. Jorgenson MA & Young KD (2016) Interrupting biosynthesis of O-antigen or the lipopolysaccharide core produces morphological defects in *Escherichia coli* by sequestering undecaprenyl phosphate. *Journal of Bacteriology* 198(22):3070-3079.

363. Oknin H, Steinberg D, & Shemesh M (2015) Magnesium ions mitigate biofilm formation of *Bacillus* species via downregulation of matrix genes expression. *Frontiers in Microbiology* 6:907.

364. Lambert PA, Hancock IC, & Baddiley J (1975) The interaction of magnesium ions with teichoic acid. *Biochemistry Journal* 149(3):519-524.

365. Popham DL & Bernhards CB (2015) Spore peptidoglycan. *Microbiology Spectrum* 3(6):TBS-0005-2012.

366. Peters JM, Colavin A, Shi H, Czarny TL, Larson MH *et al.* (2016) A comprehensive, CRISPR-based functional analysis of essential genes in bacteria. *Cell* 165(6):1493-1506.

367. Kobayashi K, Ehrlich SD, Albertini A, Amati G, Andersen KK *et al.* (2003) Essential *Bacillus subtilis* genes. *Proceedings of the National Academy of Sciences* 100(8):4678-4683.

368. Beeby M, Gumbart JC, Roux B, & Jensen GJ (2013) Architecture and assembly of the Gram-positive cell wall. *Molecular Microbiology* 88(4):664-672.

369. Gan L, Chen S, & Jensen GJ (2008) Molecular organization of Gram-negative peptidoglycan. *Proceedings of the National Academy of Sciences* 105(48):18953-18957.

370. Weidel W & Pelzer H (1964) Bagshaped macromolecules---a new outlook on bacterial cell walls. *Advances in Enzymology and Related Areas of Molecular Biology* 26:193-232.

371. Holtje JV (1996) Molecular interplay of murein synthases and murein hydrolases in *Escherichia coli*. *Microbial Drug Resistance* 2(1):99-103.

372. Priyadarshini R, de Pedro MA, & Young KD (2007) Role of peptidoglycan amidases in the development and morphology of the division septum in *Escherichia coli*. *Journal of Bacteriology* 189(14):5334-5347.

373. Heidrich C, Ursinus A, Berger J, Schwarz H, & Holtje JV (2002) Effects of multiple deletions of murein hydrolases on viability, septum cleavage, and sensitivity to large toxic molecules in *Escherichia coli*. *Journal of Bacteriology* 184(22):6093-6099.

374. Uehara T, Parzych KR, Dinh T, & Bernhardt TG (2010) Daughter cell separation is controlled by cytokinetic ring-activated cell wall hydrolysis. *The EMBO Journal* 29(8):1412-1422.

375. Yang DC, Tan K, Joachimiak A, & Bernhardt TG (2012) A conformational switch controls cell wall-remodelling enzymes required for bacterial cell division. *Molecular Microbiology* 85(4):768-781.

376. Yang DC, Peters NT, Parzych KR, Uehara T, Markovski M *et al.* (2011) An ATP-binding cassette transporter-like complex governs cell-wall hydrolysis at the bacterial cytokinetic ring. *Proceedings of the National Academy of Sciences* 108(45):E1052–E1060.

377. Dominguez-Cuevas P, Porcelli I, Daniel RA, & Errington J (2013) Differentiated roles for MreB-actin isologues and autolytic enzymes in *Bacillus subtilis* morphogenesis. *Molecular Microbiology* 89(6):1084-1098.

378. Hashimoto M, Ooiwa S, & Sekiguchi J (2012) Synthetic lethality of the *lytE cwlO* genotype in *Bacillus subtilis* is caused by lack of d,l-endopeptidase activity at the lateral cell wall. *Journal of Bacteriology* 194(4):796-803.

379. Bisicchia P, Noone D, Lioliou E, Howell A, Quigley S *et al.* (2007) The essential YycFG two-component system controls cell wall metabolism in *Bacillus subtilis*. *Molecular Microbiology* 65(1):180-200.

380. Garti-Levi S, Hazan R, Kain J, Fujita M, & Ben-Yehuda S (2008) The FtsEX ABC transporter directs cellular differentiation in *Bacillus subtilis*. *Molecular Microbiology* 69(4):1018-1028.

APPENDIX I

YodL AND YisK POSSESS SHAPE-MODIFYING ACTIVITIES THAT ARE SUPPRESSED BY MUTATIONS IN *Bacillus subtilis* MreB AND Mbl*

Introduction

Bacterial cell growth requires that the machineries directing enlargement and division of the bacterial cell envelope be coordinated in both time and space (263). The cell envelope is comprised of membranes and a macromolecular mesh of peptidoglycan (PG) that possesses both rigid and elastic properties (264, 265). PG is highly cross-linked, allowing bacteria to maintain shapes and avoid lysis, even in the presence of several atmospheres of internal turgor pressure. PG rearrangements are required during the inward redirection of growth that occurs at the time of cell division, but are also necessary when cells insert new PG and dynamically modify their morphologies in response to developmental or environmental signals (266, 267). To avoid lysis during PG rearrangements, bacteria must carefully regulate the making and breaking of glycan strands and peptide crosslinks (265). In rod-shaped bacteria, PG enlargement during steady-state growth is constrained in one dimension along the cell's long-axis and can either occur through polar growth, as is the case in *Agrobacterium tumefaciens* and *Streptomyces coelicolor,* or through incorporation of new cell wall material along the length of the cell cylinder, as observed in *Escherichia coli, Bacillus subtilis,* and *Caulobacter crescentus* (268).

To control cell diameter and create osmotically stable PG, bacteria that exhibit

---

*Reprinted with permission from "YodL and YisK possess shape-modifying activities that are suppressed by mutations in *Bacillus subtilis* MreB and Mbl" by Duan, Y., Sperber, A.M. and Herman, J.K., 2016. *Journal of Bacteriology,* 198(15):2074-2088. Copyright 2016 by American Society for Microbiology.

non-polar growth require the activity of the highly conserved actin-like protein MreB. Biochemical, genetic, and cell biological data suggest that MreB likely directs PG synthesis during cell elongation and in some bacteria, MreB may also function during cell division (269-271). MreB possesses ATPase activity, and polymerizes at sites along the cytoplasmic side of the inner membrane (272). ATP binding and hydrolysis is required for MreB polymerization and activity (273) and two S-benzylisothiourea derivatives, A22 and MP265, target the ATPase domain of MreB in Gram negative organisms, possibly preventing nucleotide hydrolysis and/or release (274-277). Depletion or inactivation of MreB is lethal except in some conditional backgrounds (278), so organisms sensitive to A22 and/or MP265 lose shape and eventually lyse (274-277).

MreB has been found to interact with several other proteins involved in PG synthesis, including the bitopic membrane protein RodZ (270, 279-282). RodZ interacts directly with MreB through a cytoplasmic helix-turn-helix motif located at its N-terminus (279). A co-crystal structure of RodZ and MreB shows the N-terminus of RodZ extending into a conserved hydrophobic pocket located in subdomain IIA of MreB (279). Depletion of RodZ also leads to loss of cell shape and cell death (283-285). However, in various mutant backgrounds, *rodZ* can be deleted without loss of rod shape or viability, indicating that RodZ is not absolutely required for MreB's function in maintaining shape (286-288). Based on these observations and others, it has been proposed that MreB-RodZ interactions may regulate some aspect of MreB activity (272, 288).

Gram-positives often encode multiple paralogs (289). *B. subtilis* possesses three *mreB* family genes: *mreB, mbl,* and *mreBH*. *mreB* is distinguished from *mbl* and *mreBH* by its location within the highly conserved *mreBCD* operon. Although *mreB, mbl,* and

mreBH are essential, it has been reported that each can be deleted under conditions in which cells are provided sufficient magnesium (290-292), or in strain backgrounds lacking *ponA*, the gene encoding penicillin binding protein 1 (PBP1)(282). In addition, all three genes can be deleted in a single background with only minor effects on cell shape if any one of the paralogs is artificially overexpressed in *trans* from an inducible promoter (293). The ability of any one of the paralogs to compensate for the loss of the others, at least under some growth conditions, strongly suggests that MreB, Mbl, and MreBH share significant functional redundancy (293, 294).

At the same time, several lines of evidence suggest that the paralogs possess non-overlapping functions. The genes themselves exhibit different patterns of transcriptional regulation, suggesting that each likely possesses specialized activities that are important in different growth contexts. For example, *mreB* and *mbl* are maximally expressed at the end of exponential growth, but expression falls off sharply during stationary phase (295), whereas *mreBH* is part of the SigI heat-shock regulon (296). There is also evidence suggesting that each protein may possess specialized activities. For example, MreBH interacts with the lytic transglycosylase LytE, and is required for LytE localization (297), whereas the lytic transglycosylase CwlO, depends on Mbl for wild-type function (297). More recently MreB (but not Mbl or MreBH) was shown to aid in escape from the competent cell state (295).

Aside from RodZ (272, 288), only a handful of proteins targeting MreB activity in vivo have been identified. In *E. coli*, the YeeU-YeeV prophage toxin-antitoxin system is comprised of a negative regulator of MreB polymerization, CbtA (298), and a positive regulator of MreB bundling, CbeA (299). Another *E. coli* prophage toxin, CptA, is also reported to inhibit MreB polymerization (300). The MbiA protein of *C. crescentus* appears to regulate MreB in vivo, however, its physiological role is unknown (301).

Given the importance of PG synthesis to cell viability and in cell shape control, it is likely that many undiscovered factors exist that modulate the activity of MreB and its paralogs.

In the present work we describe the identification of YodL and YisK, modulators of MreB and Mbl activity that are expressed during early stages of *B. subtilis* sporulation. Misexpression of either *yodL* or *yisK* during vegetative growth results in loss of cell width control and cell death. Genetic evidence indicates that YodL targets and inhibits MreB activity, whereas YisK targets and inhibits Mbl. Our data also show that YisK activity affects cell length control through an Mbl and MreBH-independent pathway.

Materials and Methods

General methods.

All *B. subtilis* strains were derived from *B. subtilis* 168. *E. coli* and *B. subtilis* strains utilized in this study are listed in Table A1.1. Plasmids are listed in Table A1.2. Oligonucleotide primers are listed in Table A1.3.

Table A1.1. Strains used in Appendix I.

Strain	Description	Reference
Parental		
B. subtilis 168	*Bacillus subtilis* laboratory strain 168 *trpC2*	BGSC (1A866)
B. subtilis 3610	*spo0H::cat (sigH::cat)*	(303)
B. subtilis PY79	*Bacillus subtilis* laboratory strain	(238)
E. coli DH5α	*F⁻ endA1 glnV44 thi-1 recA1 relA1 gyrA96 deoR nupG Φ80dlacZΔM15 Δ(lacZYA-argF)U169, hsdR17(r_K^- m_K^+), λ–*	
***B. subtilis* 168**		
BAS040	*amyE::*P_{hy}*-yodL (spec)*	This study
BAS041	*amyE::*P_{hy}*-yisK (spec)*	This study
BAS146	*ponA::erm, kanΩΔmreB*	This study
BAS147	*ponA::erm, kanΩΔmbl*	This study
BAS170	*amyE::*P_{yodL}*-lacZ (spec)*	This study
BAS171	*amyE::*P_{yodL}*-gfp (spec)*	This study
BAS191	*amyE::*P_{hy}*-yodL (spec), yhdG::*P_{hy}*-yodL (phleo)*	This study
BAS192	*amyE::*P_{yisK}*-lacZ (spec)*	This study
BAS193	*amyE::*P_{yisK}*-gfp (spec)*	This study
BAS205	*amyE::*P_{empty}*-gfp (spec)*	This study
BAS248	*ponA::erm, kanΩΔmbl, catΩΔmreBH, amyE::*P_{hy}*-yisK (spec), yhdG::*P_{hy}*-yisK (phleo)*	This study
BAS249	*ponA::erm, kanΩΔmbl, catΩΔmreBH, amyE::*P_{hy}*-yodL (spec), yhdG::*P_{hy}*-yodL (phleo)*	This study
BAS265	*spo0A::erm*	This study
BAS266	*amyE::*P_{yodL}*-gfp (spec), spo0A::erm*	This study
BAS267	*amyE::*P_{yisK}*-gfp (spec), spo0A::erm*	This study
BAS282	*sigH::cat*	This study
BAS301	*amyE::*P_{yodL}*-lacZ (spec), spo0A::erm*	This study
BAS302	*amyE::*P_{yisK}*-lacZ (spec), spo0A::erm*	This study
BAS303	*amyE::*P_{yodL}*-lacZ (spec), sigH::cat*	This study
BAS304	*amyE::*P_{yisK}*-lacZ (spec), sigH::cat*	This study
BAS305	*amyE::*P_{yodL}*-lacZ (spec), spo0A::erm, sigH::cat*	This study
BAS306	*amyE::*P_{yisK}*-lacZ (spec), spo0A::erm, sigH::cat*	This study
BDR992	*amyE::*P_{hy}*-lacZ (spec)*	David Z. Rudner
BKE10750	*yisK::erm*	BGSC

Table A1.1. Continued.

Strain	Description	Reference
BKE19640	*yodL::erm*	BGSC
BKE22320	*ponA::erm*	BGSC
BYD048	*amyE::*P$_{hy}$*-yodL (spec), ycgO::*P$_{hy}$*-yodL (tet), yhdG::*P$_{hy}$*-yodL (phleo), sacA::*P$_{hy}$*-lacZ (erm)*	This study
BYD074	*amyE::*P$_{hy}$*-yisK (spec), yhdG::*P$_{hy}$*-yisK (phleo)*	This study
BYD076	*amyE::*P$_{hy}$*-yisK (spec), yhdG::*P$_{hy}$*-yisK (phleo), yycR::*P$_{hy}$*-yisK (cat), sacA::*P$_{hy}$*-lacZ (erm)*	This study
BYD175	*ponA::erm, amyE::* P$_{hy}$*-yisK (spec), yhdG::*P$_{hy}$*-yisK (phleo)*	This study
BYD176	*ponA::erm, amyE::* P$_{hy}$*-yodL (spec), yhdG::*P$_{hy}$*-yodL (phleo)*	This study
BYD177	*kanΩmreB*$_{G323E}$*, amyE::P$_{hy}$-yisK (spec), yhdG::P$_{hy}$-yisK (phleo), yycR::P$_{hy}$-yisK (cat)*	This study
BYD178	*kanΩmreB*$_{P147R}$*, amyE::P$_{hy}$-yisK (spec), yhdG::P$_{hy}$-yisK (phleo), yycR::P$_{hy}$-yisK (cat)*	This study
BYD179	*kanΩmreB*$_{R282S}$*, amyE::P$_{hy}$-yisK (spec), yhdG::P$_{hy}$-yisK (phleo), yycR::P$_{hy}$-yisK (cat)*	This study
BYD180	*kanΩmreB*$_{G143A}$*, amyE::P$_{hy}$-yisK (spec), yhdG::P$_{hy}$-yisK (phleo), yycR::P$_{hy}$-yisK (cat)*	This study
BYD184	*kanΩmreB*$_{R117G}$*, amyE::P$_{hy}$-yisK (spec), yhdG::P$_{hy}$-yisK (phleo), yycR::P$_{hy}$-yisK (cat)*	This study
BYD258	*ponA::erm, kanΩΔmbl, amyE::*P$_{hy}$*-yisK (spec), yhdG::*P$_{hy}$*-yisK (phleo)*	This study
BYD259	*ponA::erm, kanΩΔmbl, amyE::*P$_{hy}$*-yodL (spec), yhdG::*P$_{hy}$*-yodL (phleo)*	This study
BYD262	*ponA::erm, kanΩΔmreB, amyE::P$_{hy}$-yisK (spec), yhdG::P$_{hy}$-yisK (phleo)*	This study
BYD263	*ponA::erm, kanΩΔmreB, amyE::P$_{hy}$-yodL (spec), yhdG::P$_{hy}$-yodL (phleo)*	This study
BYD276	*ΔyodL*	This study
BYD278	*ΔyisK*	This study
BYD279	*ΔyodL, ΔyisK*	This study
BYD281	*amyE::P$_{hy}$-yisK (spec), ycgO::P$_{hy}$-yisK (tet), yhdG::P$_{hy}$-yodL (phleo), yycR::P$_{hy}$-yodL (cat)*	This study
BYD327	*kanΩmreB*$_{G323E}$*, amyE::P$_{hy}$-yodL (spec), yhdG::P$_{hy}$-yodL (phleo), yycR::P$_{hy}$-yodL (cat)*	This study
BYD328	*kanΩmreB*$_{R117G}$*, amyE::P$_{hy}$-yodL (spec), yhdG::P$_{hy}$-yodL (phleo), yycR::P$_{hy}$-yodL (cat)*	This study
BYD329	*kanΩmreB*$_{N145D}$*, amyE::P$_{hy}$-yodL (spec), yhdG::P$_{hy}$-yodL (phleo), yycR::P$_{hy}$-yodL (cat)*	This study

Table A1.1. Continued.

Strain	Description	Reference
BYD330	*kanΩmreB*$_{P147R}$, *amyE::*P$_{hy}$*-yodL (spec), yhdG::*P$_{hy}$*-yodL (phleo), yycR::*P$_{hy}$*-yodL (cat)*	This study
BYD332	*kanΩmreB*$_{S154R,R230C}$, *amyE::*P$_{hy}$*-yodL (spec), yhdG::*P$_{hy}$*-yodL (phleo), yycR::*P$_{hy}$*-yodL (cat)*	This study
BYD333	*kanΩmreB*$_{G143A}$, *amyE::*P$_{hy}$*-yodL (spec), yhdG::*P$_{hy}$*-yodL (phleo), yycR::*P$_{hy}$*-yodL (cat)*	This study
BYD334	*kanΩmbl*$_{E250K}$, *amyE::P$_{hy}$-yisK (spec), yhdG::P$_{hy}$-yisK (phleo), yycR::P$_{hy}$-yisK (cat)*	This study
BYD335	*kanΩmbl*$_{T317I}$, *amyE::*P$_{hy}$*-yodL (spec), yhdG::*P$_{hy}$*-yodL (phleo), yycR::*P$_{hy}$*-yodL (cat)*	This study
BYD336	*kanΩmbl*$_{T158M}$, *amyE::*P$_{hy}$*-yodL (spec), yhdG::*P$_{hy}$*-yodL (phleo), yycR::*P$_{hy}$*-yodL (cat)*	This study
BYD337	*kanΩmbl*$_{\Delta S251}$, *amyE::P$_{hy}$-yisK (spec), yhdG::P$_{hy}$-yisK (phleo), yycR::P$_{hy}$-yisK (cat)*	This study
BYD338	*kanΩmbl*$_{P309L}$, *amyE::P$_{hy}$-yisK (spec), yhdG::P$_{hy}$-yisK (phleo), yycR::P$_{hy}$-yisK (cat)*	This study
BYD339	*kanΩmbl*$_{G156D}$, *amyE::P$_{hy}$-yisK (spec), yhdG::P$_{hy}$-yisK (phleo), yycR::P$_{hy}$-yisK (cat)*	This study
BYD340	*kanΩmbl$_{T158A}$, amyE::P$_{hy}$-yisK (spec), yhdG::P$_{hy}$-yisK (phleo), yycR::P$_{hy}$-yisK (cat)*	This study
BYD341	*kanΩmbl$_{D153N}$, amyE::P$_{hy}$-yisK (spec), yhdG::P$_{hy}$-yisK (phleo), yycR::P$_{hy}$-yisK (cat)*	This study
BYD342	*kanΩmbl$_{R63C}$, amyE::P$_{hy}$-yisK (spec), yhdG::P$_{hy}$-yisK (phleo), yycR::P$_{hy}$-yisK (cat)*	This study
BYD343	*kanΩmbl$_{M51I}$, amyE::P$_{hy}$-yisK (spec), yhdG::P$_{hy}$-yisK (phleo), yycR::P$_{hy}$-yisK (cat)*	This study
BYD344	*kanΩmbl$_{A314T}$, amyE::P$_{hy}$-yisK (spec), yhdG::P$_{hy}$-yisK (phleo), yycR::P$_{hy}$-yisK (cat)*	This study
BYD345	*kanΩmbl$_{E204G}$, amyE::P$_{hy}$-yisK (spec), yhdG::P$_{hy}$-yisK (phleo), yycR::P$_{hy}$-yisK (cat)*	This study
BYD346	*kanΩmbl$_{E250K}$, amyE::P$_{hy}$-yodL (spec), yhdG::P$_{hy}$-yodL (phleo), yycR::P$_{hy}$-yodL (cat)*	This study
BYD348	*kanΩmbl$_{T158A}$, amyE::P$_{hy}$-yodL (spec), yhdG::P$_{hy}$-yodL (phleo), yycR::P$_{hy}$-yodL (cat)*	This study
BYD349	*kanΩmbl$_{G156D}$, amyE::P$_{hy}$-yodL (spec), yhdG::P$_{hy}$-yodL (phleo), yycR::P$_{hy}$-yodL (cat)*	This study
BYD351	*kanΩmbl$_{D153N}$, amyE::P$_{hy}$-yodL (spec), yhdG::P$_{hy}$-yodL (phleo), yycR::P$_{hy}$-yodL (cat)*	This study
BYD352	*kanΩmbl$_{M51I}$, amyE::P$_{hy}$-yodL (spec), yhdG::P$_{hy}$-yodL (phleo), yycR::P$_{hy}$-yodL (cat)*	This study

Table A1.1. Continued.

Strain	Description	Reference
BYD353	*kanΩmbl*$_{A314T}$, *amyE::*P$_{hy}$*-yodL (spec)*, *yhdG::*P$_{hy}$*-yodL (phleo)*, *yycR::*P$_{hy}$*-yodL (cat)*	This study
BYD354	*kanΩmbl*$_{E204G}$, *amyE::*P$_{hy}$*-yodL (spec)*, *yhdG::*P$_{hy}$*-yodL (phleo)*, *yycR::*P$_{hy}$*-yodL (cat)*	This study
BYD361	*amyE::*P$_{hy}$*-yisK (spec)*, *yhdG::*P$_{hy}$*-yodL (phleo)*	This study
BYD363	*kanΩmreB*$_{S154R,R230C}$, *amyE::P$_{hy}$-yisK (spec)*, *yhdG::P$_{hy}$-yisK (phleo)*, *yycR::P$_{hy}$-yisK (cat)*	This study
BYD365	*kanΩmreB*$_{R282S}$, *amyE::*P$_{hy}$*-yodL (spec)*, *yhdG::*P$_{hy}$*-yodL (phleo)*, *yycR::*P$_{hy}$*-yodL (cat)*	This study
BYD404	*kanΩmreB*$_{N145D}$, *amyE::P$_{hy}$-yisK (spec)*, *yhdG::Phy-yisK (phleo)*, *yycR::P$_{hy}$-yisK (cat)*	This study
BYD405	*kanΩmbl*$_{R63C}$, *amyE::*P$_{hy}$*-yodL (spec)*, *yhdG::*P$_{hy}$*-yodL (phleo)*, *yycR::*P$_{hy}$*-yodL (cat)*	This study
BYD406	*kanΩmbl*$_{\Delta S251}$, *amyE::*P$_{hy}$*-yodL (spec)*, *yhdG::*P$_{hy}$*-yodL (phleo)*, *yycR::*P$_{hy}$*-yodL (cat)*	This study
BYD407	*kanΩmbl*$_{P309L}$, *amyE::*P$_{hy}$*-yodL (spec)*, *yhdG::*P$_{hy}$*-yodL (phleo)*, *yycR::*P$_{hy}$*-yodL (cat)*	This study
BYD510	*ΔyodL, ΔyisK, amyE::*P$_{yisK}$*-yisK (spec)*	This study

Table A1.2. Plasmids used in Appendix I.

Plasmid	**Description**	**Reference**
pAS015	*yhdG::*P_{hy}*-yisK (amp)*	This study
pAS040	*amyE::*P_{yodL}*-lacZ (amp)*	This study
pAS041	*amyE::*P_{yodL}*-gfp (amp)*	This study
pAS044	*amyE::*P_{yisK}*-lacZ (amp)*	This study
pAS045	*amyE::*P_{yisK}*-gfp (amp)*	This study
pAS047	*amyE::gfp (amp)*	This study
pAS067	*amyE::*P_{yisK}*-yisK (amp)*	This study
pDR111	*amyE::*P_{hy} *(amp)*	David Z. Rudner
pDR244	Temperature sensitive Cre recombinase plasmid (*amp*)(*spec*)	David Z. Rudner
pJH036	*sacA::*P_{hy}*-lacZ (amp)*	This study
pJW004	*yhdG::*P_{hy} *(amp)*	This study
pJW006	*amyE::*P_{hy}*-sirA-gfp (amp)*	(7)
pJW033	*ycgO::*P_{hy} *(amp)*	This study
pJW034	*yycR::*P_{hy} *(amp)(cat)*	This study
pKM062	*sacA::erm (amp)*	David Z. Rudner
pWX114	*yrvN::*P_{hy} *(amp)(kan)*	David Z. Rudner
pYD073	*yhdG::*P_{hy}*-yodL (amp)*	This study
pYD155	*yycR::*P_{hy}*-yodL (amp)*	This study
pYD156	*ycgO::*P_{hy}*-yisK (amp)*	This study

Table A1.3. Oligonucleotides used in Appendix I.

Oligo	Sequence 5' to 3'
OAM001	AGAAGCGTTAGCGGCAGCAAGTGAT
OAM002	CCATGTCTGCCCGTATTTCGCGTAAGGAAATCCATTATGTACT ATTTCGATCAGACCAG
OAM009	GAAAACAATAAACCCTTGCATAGGGGGATCGGGCAAGGCTAG ACGGGACTTACC
OAM010	ATGGACACAACAACAGCAAAACAGGC
OAM011	TAATGGATTTCCTTACGCGAAATA
OAM013	AGTAGTTCCTCCTTATGTAAGC
OAS064	TCCTCCTTTTCAAAAGAAAAAAAC
OAS067	TGTTACATATTGCTGCTTTTTGGT
OAS078	GGATCCCAGCGAACCATTTGA
OAS079	GTCGACAAATTCCTCGTAGGC
OAS080	CCTATCACCTCAAATGGTTCGCTGGGATCCAAAGCAAAAATA CCCTAAAGGGAA
OAS081	GTCCCGAGCGCCTACGAGGAATTTGTCGACACACTTTTTTTTT CGTCGAATTAAG
OAS086	CGAATACATACGATCCTACAGC
OAS087	CCTATCACCTCAAATGGTTCGCTGGGATCCAAAAAGTTGGAA GCACAATAAGTT
OAS088	GTCCCGAGCGCCTACGAGGAATTTGTCGACATCACCTGGCATT GCCTTCTT
OAS089	ATTAATGGTGATATTCTTCATTGA
OAS091	AGATGGATGTGCTCCAGTGCTCCAAGATCTATACCAAGGTCT
OAS092	AGACCTTGGTATAGATCTTGGAGCACTGGAGCACATCCATCT
OAS095	GGAAGCTTGTCCATATTATCAAGATTTGCAGTACCGAGGTCAA TA
OAS096	TATTGACCTCGGTACTGCAAATCTTGATAATATGGACAAGCTT CC
OAS114	TCTAAGGAATTCCTGTTTTAGTCGGCATAAGCAG
OAS116	GTAATCTTACGTCAGTAACTTCCACCAAGATCCCCTCCCTTTT ATTT
OAS117	AAGAAATAAAAGGGAGGGGATCTTGGTGGAAGTTACTGACGT AAGAT
OAS118	ACTTAGGGATCCTTATTTTTGACACCAGACCAACT
OAS119	TGAAAAGTTCTTCTCCTTTACTCATCAAGATCCCCTCCCTTTTA TTT
OAS120	AAGAAATAAAAGGGAGGGGATCTTGATGAGTAAAGGAGAAG AACTTTTC
OAS121	ACTTAGGGATCCTTATTTGTATAGTTCATCCATGCCAT
OAS134	TCTAAGGAATTCTCCTTTTCAGCTGCTCCCGAT

Table A1.3. Continued.

Oligo	Sequence 5' to 3'
OAS135	GTAATCTTACGTCAGTAACTTCCACGTTATTCCTCCATCATCTTTTAAA
OAS136	ATTTAAAAGATGATGGAGGAATAACGTGGAAGTTACTGACGTAAGAT
OAS137	TGAAAAGTTCTTCTCCTTTACTCATGTTATTCCTCCATCATCTTTTAAA
OAS138	ATTTAAAAGATGATGGAGGAATAACATGAGTAAAGGAGAAGAACTTTTC
OAS148	TCTAAGGAATTCATGAGTAAAGGAGAAGAACTTTTC
OAS149	ACTTAGGGATCCTTATTTGTATAGTTCATCCATGCC
OAS274	TCTAAGGAATTCTCCTTTTCAGCTGCTCCCGA
OAS275	ACTTAGGGATCCTCAGCCAATTTGGTTTGACAG
OEA035	GGATAACAATTAAGCTTACATAAGGAGGAACTACTATGAAATTTGCGACAGGGGAACTT
OEA036	TTCCACCGAATTAGCTTGCATGCGGCTAGCCCAGTTTTATTCAGCCAATTTGGT
OEA275	GGATAACAATTAAGCTTACATAAGGAGGAACTACTATGATGTTATCCGTGTTTAAAAAG
OEA276	TTCCACCGAATTAGCTTGCATGCGGCTAGCTTTCTTTTCATTATGTCGTTTGTA
OJH159	CTGCAGGAATTCGACTCTCTA
OJH160	TAGCTTGCATGCGGCTAGC
OJH185	CAGGAATTCGACTCTCTAGC
OJH186	CTCAGCTAGCTAACTCACATTAATTGCGTTGC

Escherichia coli DH5α was used for cloning. All *E. coli* strains were grown in LB-Lennox medium supplemented with 100 µg/ml ampicillin. The following concentrations of antibiotics were used for generating *B. subtilis* strains: 100 µg/ml spectinomycin, 7.5 µg/ml chloramphenicol, 0.8 mg/ml phleomycin, 10 µg/ml tetracycline, 10 µg/ml kanamycin. To select for erythromycin resistance, plates were supplemented with 1 µg/ml erythromycin (erm) and 25 µg/ml lincomycin. *B. subtilis* transformations were carried out as described previously (302). When indicated, the LB in the *B. subtilis* microscopy experiments was LB-Lennox broth. Sporulation by resuspension was carried out at 37°C according to the Sterlini-Mandelstam method (237). Penassay broth (PAB) is composed of 5 g peptone, 1.5 g beef extract, 1.5 g yeast extract, 1.0 g D-glucose (dextrose), 3.5 g NaCl, 3.68 g dipotassium phosphate, and 1.32 g monopotassium phosphate per liter of distilled water. To make solid media, the relevant media was supplemented with 1.5% (w/v) bacto-agar.

Microscopy

For microscopy experiments, all strains were grown in the indicated medium in volumes of 25 ml in 250 ml baffled flasks, and placed in a shaking waterbath set at 37°C and 280 rpm. Unless stated otherwise, misexpression was performed by inducing samples with 1.0 mM isopropyl-beta-D-thiogalactopyranoside (IPTG) and imaging samples 90 min post-induction. Fluorescence microscopy was performed with a Nikon Ti-E microscope equipped with a CFI Plan Apo lambda DM 100X objective, Prior Scientific Lumen 200 Illumination system, C-FL UV-2E/C DAPI and C-FL GFP HC HISN Zero Shift filter cubes, and a CoolSNAP HQ2 monochrome camera. Membranes were stained with TMA-DPH [1-(4-trimethylammoniumphenyl)-6-phenyl-1,3,5-

hexatriene *p* -toluenesulfonate] (0.02 mM) and imaged with exposure times of 1 sec with a neutral density filter in place to reduce cytoplasmic background. All GFP images were captured with a 1 sec exposure time. All images were captured with NIS Elements Advanced Research (version 4.10), and processed with NIS Elements Advanced Research (version 4.10) and ImageJ64 (240). Cells were mounted on glass slides with 1% agarose pads or polylysine-treated coverslips prior to imaging. To quantitate cell lengths for Fig A1.11, the cell lengths for 500 cells were determined for each population. The statistical significance of cell length differences between populations was determined using an unpaired student's t-test.

Plate growth assay

B. subtilis strains were streaked on LB-Lennox plates containing 100 µg/ml spectinomycin and 1 mM IPTG. The plates were supplemented with the indicated concentrations of $MgCl_2$ when indicated. Plates were incubated at 37°C overnight and images were captured on a ScanJet G4050 flatbed scanner (Hewlett Packard).

Heat kill

Spore formation was quantified by growing cells in Difco sporulation medium (DSM)(304). A freshly grown single colony of each strain was inoculated into 2 mL of DSM media and placed in a roller drum at 37°C, 60 rpm for 36 hrs. To determine colony forming units/ml, an aliquot of each culture was serially diluted and plated on DSM agar plates. To enumerate heat resistant spores/ml, the serial diluted cultures were subjected to a 20 min heat treatment at 80°C and plated on DSM agar plates. The plates were

incubated at 37°C overnight and the next day colony counts were determined. The relative sporulation frequency compared to wildtype was determined by calculating the spores/CFU of each experimental and dividing it by the spores/CFU of wildtype. The reported statistical significance was determined using an unpaired student's t-test.

Transcription fusions

Transcriptional fusions were constructed by fusing a ~200 bp region up to the start codon of either *yodL* or *yisK* to *gfp* or *lacZ* and integrating the fusions into the *B. subtilis* chromosome at the *amyE* locus (for more details, see strain construction in the supplemental text). Microscopy was conducted on each strain over a timecourse in sporulation by resuspension media (see general methods) or in a nutrient exhaustion timecourse in CH (237). Beta-galactosidase assays were performed as described (305), except all samples were frozen at -80°C before processing. All experiments were performed on at least three independent biological replicates.

Suppressor selections

Single colonies of BYD048 (3X P_{hy}-*yodL*, P_{hy}-*lacZ*) or BYD076 (3X P_{hy}-*yisK*, P_{hy}-*lacZ*) were used to inoculate independent 5 ml LB-Lennox cultures. Six independent cultures were grown for each strain. The cultures were grown for 6 hrs at 37°C and 0.3 µl of each culture was diluted in 100 µl LB and plated on an LB-Lennox agar plate containing 100 µg/ml spectinomycin and 1 mM IPTG. After overnight growth, suppressors that arose were patched on both LB-Lennox agar plates supplemented with 100 µg/ml spectinomycin and LB-Lennox agar plates supplemented with 100 µg/ml

spectinomycin, 1.0 mM IPTG, and 40 μg/ml X-Gal and grown at 37°C overnight. Only blue colonies were selected for further analysis; this screen eliminated mutants unable to derepress P_{hy} in the presence of IPTG. In addition, each P_{hy}-*yodL* or P_{hy}-*yisK* construct was transformed into a wildtype background to ensure that the construct remained fully functional with respect to preventing cell growth on LB-Lennox agar plates supplemented with the relevant antibiotic and 1 mM IPTG.

Whole-genome sequencing and analysis

Genomic DNA was isolated from six YodL-resistant suppressors obtained from independent cultures as well as the parent strain (BYD048) by inoculating a single colony in 6 ml LB-Lennox media and growing at 37°C for 4 hr in a roller drum. Cells were collected by spinning at 21,130 x g for 2 min at room temperature, resuspending the pellets in lysis buffer [20 mM Tris-HCl pH 7.5, 50 mM EDTA pH 8, 100 mM NaCl, and 2 mg/ml lysozyme] and incubating at 37°C for 30 min. Sarkosyl was added to a final concentration of 1% (w/v). Protein was removed by extracting with 600 μl phenol, centrifuging at 21,130 x g for 5 min at room temperature, and transferring the top (aqueous layer) to a new microcentrifuge tube. This was followed by an extraction with 600 μl phenol-saturated chloroform and centrifugation at 21,130 x g for 5 min at room temperature. After transferring the aqueous layer to a new microcentrifuge tube, a final extraction was performed with 100% chloroform, followed by centrifugation at 21,130 x g for 5 min at room temperature. The aqueous layer was transferred to a new microcentrifuge tube, being careful to avoid the interphase material. To precipitate the genomic DNA, a $1/10^{th}$ volume of 3.0 M Na-acetate and 1 ml of 100% ethanol was added, and the tube was inverted multiple times. The sample was centrifuged at 21,130 x

g for 1 min at room temperature in a microcentrifuge. The pellet was washed with 150 µl 70% ethanol and resuspended in 500 µl TE [10 mM Tris pH 7.5, 1 mM EDTA, pH 8.0]. To eliminate potential RNA contamination, RNase was added to a final concentration of 200 µg/ml and the sample was incubated at 55°C for 1 hr. To remove the RNase, the genomic DNA was re-purified by phenol-chloroform extraction and ethanol precipitation as described above. The final pellet was resuspended in 100 µl TE. Bar-coded libraries were prepared from each genomic DNA sample using a TruSeq DNA kit according to manufacture specifications (Illumina), and the samples were subjected to Illumina-based whole-genome sequencing using a MiSeq 250 paired-end run (Illumina). CLC Genomics Workbench (Qiagen) was used to map the sequence reads against the *Bs*168 reference genome and to identify single nucleotide polymorphisms, insertions, and deletions. Mutations associated with the P_{hy} integration contructs and those in which less than 40% of the reads differed from the reference genome were excluded as candidate changes responsible for suppression in our initial analysis (Table A1.5). The remaining suppressors mutations were identified by PCR amplifying *mreB* (using primer set OAS044 and OAS045) and *mbl* (using primer set OAS046 and OAS047), and sequencing with the same primers. To determine if the candidate suppressors alleles identified were sufficient to confer resistance to the original selective pressure, each was linked to a kanamycin resistance cassette and moved by transformation into a clean genetic background.

Results

YodL and YisK affect cell width

To identify novel factors involved in cellular morphogenesis, we created an ordered gene misexpression library comprising over 800 previously uncharacterized genes from *B. subtilis*. Each gene was placed under the control of an IPTG-inducible promoter (P_{hy}) and integrated in single copy (1X) at *amyE*, a non-essential locus in the *B. subtilis* chromosome. The library (called the BEIGEL for *Bacillus* Ectopic Inducible Gene Expression Library), was screened for misexpression phenotypes that perturbed growth on solid media, and also resulted in obvious defects in nucleoid morphology, changes in cell division frequency, and/or perturbations in overall cell shape in liquid cultures. Two strains, one harboring P_{hy}-*yodL* and one harboring P_{hy}-*yisK*, were unable to form colonies on plates containing inducer (Fig A1.1A) and also produced wide, irregular cells with slightly tapered poles following misexpression in LB liquid media (Fig A1.1B). Cell lysis and aberrant cell divisions were also observed. Introducing a second copy (2X) of each P_{hy} misexpression construct into the chromosome did not appreciably enhance cell widening at the 90 min post-induction timepoint, although cell lysis was more readily observed (Fig A1.1B). P_{hy}-*yisK* (2X) misexpression also led to a drop in optical density over time (Fig A1.2A), consistent with the cell lysis observed microscopically. We conclude that the activities of *yodL* and *yisK* target one or more processes integral to width control during cell elongation.

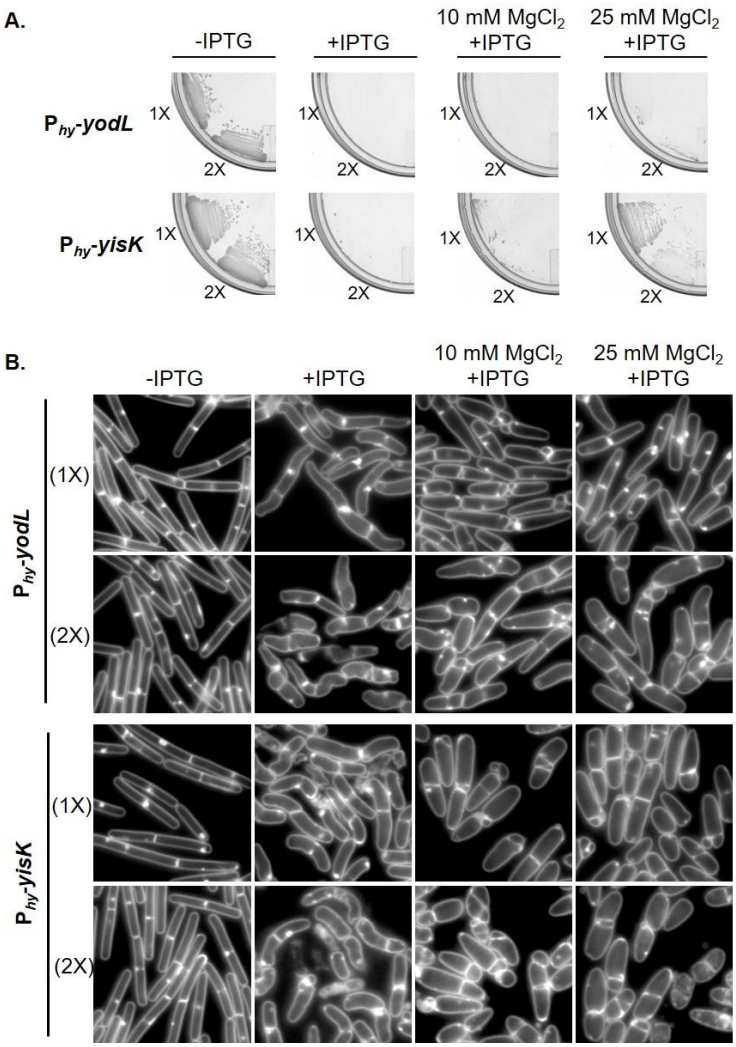

Fig. A1.1. Misexpression of YodL and YisK prevents cell growth on solid media and causes loss of cell shape in liquid media. (A) Cells harboring one (1X) or two (2X) copies of P_{hy}-*yodL* (BAS040 and BAS191) or P_{hy}-*yisK* (BAS041 and BYD074) were streaked on an LB plate supplemented with 100 µg/ml spectinomycin and, when indicated, 1 mM IPTG or 1 mM IPTG and the denoted concentration of $MgCl_2$. Plates were incubated for ~16 hrs at 37°C before image capture (top). (B) The strains described above were grown in LB-Lennox media at 37°C to mid-exponential and back-diluted to an OD_{600} of ~0.02. When indicated, 1 mM IPTG or 1 mM IPTG and the denoted concentration of $MgCl_2$ was added. Cells were grown for 1.5 hrs at 37°C before image capture. Membranes were stained with TMA-DPH. All images were scaled identically.

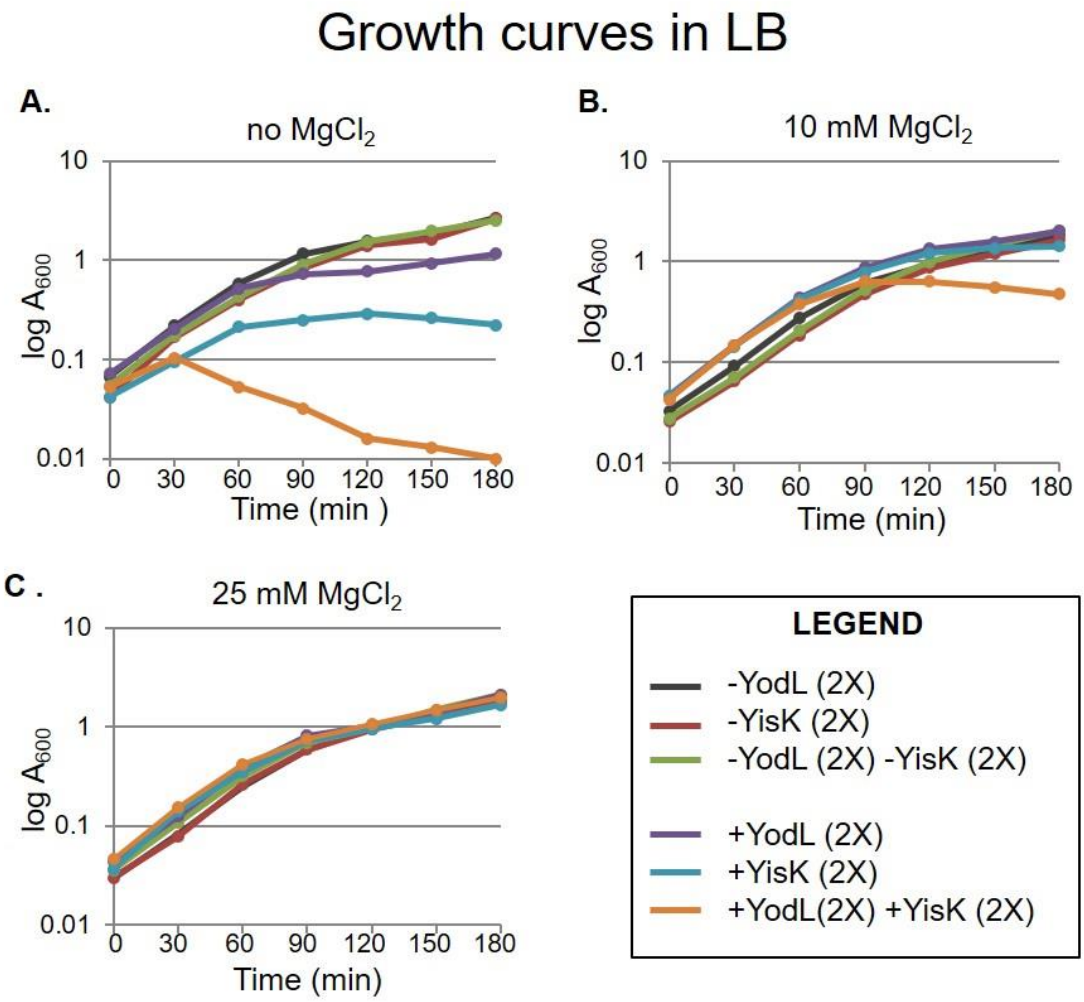

Fig. A1.2. Growth curves in LB following misexpression of YodL and/or YisK. 2X *P*$_{hy}$-*yodL* (BAS191), 2X *P*$_{hy}$-*yisK* (BYD074) and 2X *P*$_{hy}$-*yodL*, 2X *P*$_{hy}$-*yisK* (BYD281) were grown in LB media at 37°C to mid-exponential diluted to an OD_{600} of <0.02. At time 0, 1 mM IPTG or 1 mM IPTG and the indicated concentration of $MgCl_2$ was added.

The *yodL* and *yisK* misexpression phenotypes are similar to those observed when proteins involved in cell elongation are perturbed in *B. subtilis* (282, 293, 306). Since the addition of magnesium was previously reported to suppress the lethality and/or morphological phenotypes associated with depletion or deletion of some proteins important for cell elongation in *B. subtilis* (280, 282, 291, 293, 307), we assessed if the P_{hy}-*yodL* and P_{hy}-*yisK* misexpression phenotypes could be rescued by growing cells with media supplemented with two different concentrations of $MgCl_2$. The YodL-producing cells failed to grow on any LB media containing inducer, regardless of $MgCl_2$ concentration (Fig A1.1A). In contrast, LB supplemented with 25 mM $MgCl_2$ restored viability to the strain producing YisK (Fig A1.1A). Interestingly, even 25 mM $MgCl_2$ was not sufficient to suppress the cell-widening effect associated with YodL and YisK misexpression (Fig A1.1B), although these cells did not lyse (Fig A1.2C). Since PAB medium was often used in the prior studies showing $MgCl_2$ supplementation rescued cell shape (280, 282, 291, 293, 307), we also assayed for growth on PAB following YodL and YisK expression. PAB supplemented with 25 mM $MgCl_2$ rescued growth on plates (Fig A1.3A), but still did not rescue morphology in liquid culture (Fig A1.3B).

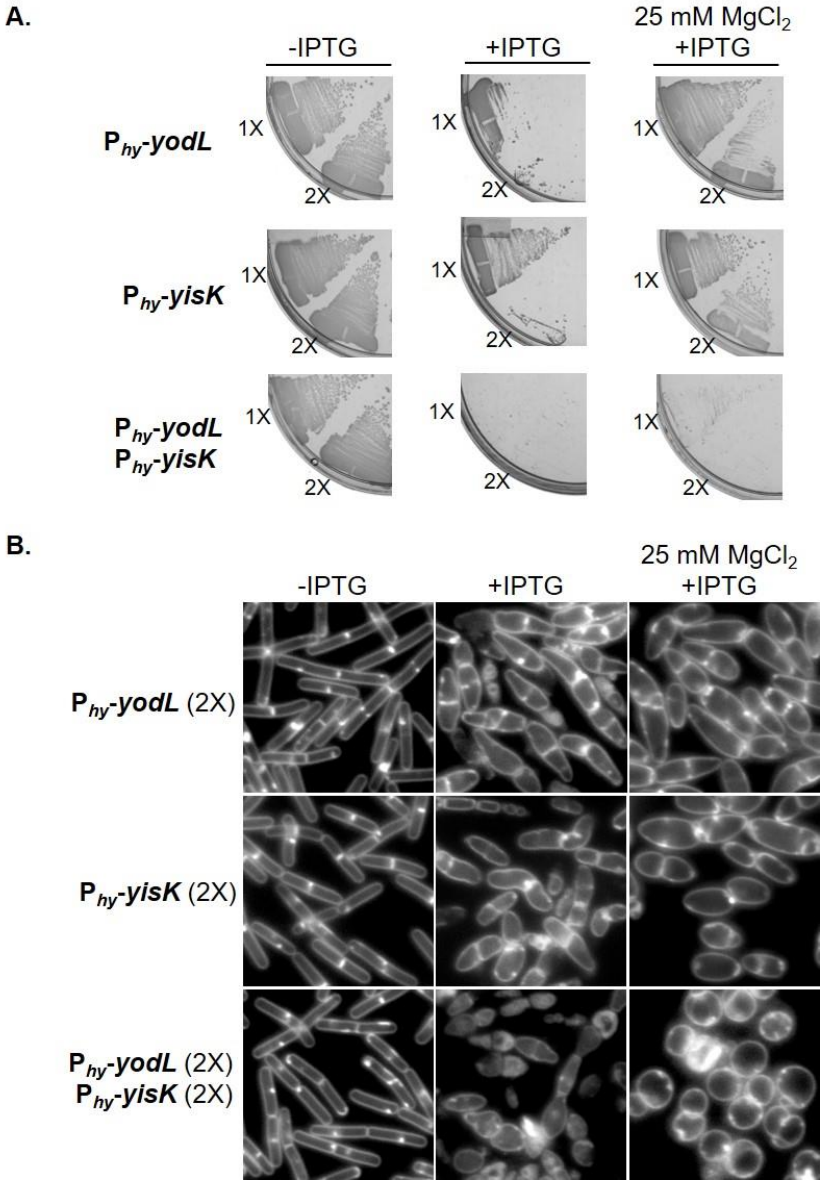

Fig. A1.3. Misexpression of YodL and YisK on PAB media. (A) Cells were streaked on PAB solid media supplemented with 100 µg/ml spectinomycin and, when indicated, 1 mM IPTG and the denoted concentration of $MgCl_2$. Plates were incubated for ~16 hr at 37°C before image capture. (B) Cells were grown in PAB liquid media at 37°C to mid-exponential and back-diluted to an OD_{600} of <0.02. When indicated, 1 mM IPTG and the denoted concentration of $MgCl_2$ was added. Cells were then grown for 1.5 hrs at 37°C before image capture. Membranes are stained with TMA-DPH (white). All images are shown at the same magnification.

yodL and *yisK* expression

To better understand the possible physiological functions of the *yodL* and *yisK* gene products, we analyzed the genes and their genetic contexts bioinformatically. *yodL* is predicted to encode a 12.5 kDa hypothetical protein which, based on amino acid similarity, is conserved in the *Bacillus* genus. In data from a global microarray study analyzing conditional gene expression in *B. subtilis*, *yodL* is expressed as a monocistronic mRNA, exhibiting peak expression ~2 hrs after entry into sporulation (14). *yodL* expression is most strongly correlated with expression of *racA* and *refZ* (*yttP*)(14), genes directly regulated by Spo0A (36). *yodL* was not previously identified as a member of the Spo0A regulon controlling early sporulation gene expression (32, 36), however a more recent study found that *yodL* expression during sporulation is reduced in a Δ*spo0A* mutant (308). Consistent with this observation, we identified a putative Spo0A box approximately ~75 bp upstream of the annotated *yodL* start codon (Fig A1.4A). *yisK* is predicted to encode a 33 kDa protein and is annotated as a putative catabolic enzyme based on its similarity to proteins involved in the degradation of aromatic amino acids (309). *yisK* was previously identified as a member of the SigH regulon, and possesses a SigH -35/-10 motif (Fig A1.4B)(32). Expression of *yisK* peaks ~2 hrs after entry into sporulation (301) and is most strongly correlated with expression of *kinA* (14), a gene regulated by both SigH (the stationary phase sigma factor)(32, 37, 310, 311) and Spo0A (36, 311). As with *yodL*, we identified a putative Spo0A box in the regulatory region upstream of the *yisK* start codon (Fig A1.4B).

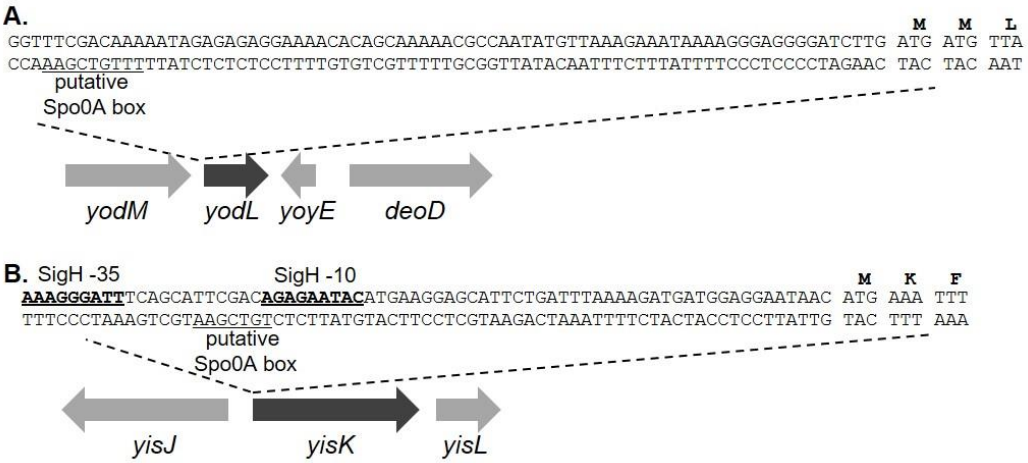

Fig. A1.4. DNA sequence upstream of *yodL* and *yisK*. (A) Putative Spo0A box (underlined) upstream of the *yodL* start codon. (B) SigH binding motifs (double underline) and putative Spo0A box (underlined) upstream of *yisK* start codon.

To independently test if *yodL* and *yisK* expression are consistent with Spo0A-dependent regulation, we fused the putative regulatory regions upstream of each gene to a *gfp* reporter gene, and integrated the fusions into the *amyE* locus. We then followed expression from the promoter fusions over a timecourse in CH liquid broth, a rich medium in which the cells first grow exponentially, transition to stationary phase, and finally gradually enter sporulation (Fig A1.5A-C). In this timecourse, GFP signal from P_{yisK}-*gfp* increased dramatically from time 0 (OD_{600} ~0.6) to time 1 hr (OD_{600} ~1.6) (Fig A1.5C), consistent with *yisK*'s prior characterization as a SigH-regulated gene (32). In contrast, GFP fluorescence from P_{yodL}-*gfp* became evident at a later timepoint (120 min) and was more heterogeneous (Fig A1.5C), consistent with expression patterns previously observed for other Spo0A-P regulated genes (312, 313).

To quantitate expression from the promoters, we generated P_{yodL}-*lacZ* and P_{yisK}-*lacZ* reporter strains and collected samples over a CH timecourse beginning with early exponential (OD_{600} = 0.2). Expression from P_{yodL}-*lacZ* rose steadily beginning about 2 hrs after exit from exponential growth, and continued to rise at least until the final timepoint taken (Fig A1.5D). In contrast, expression from P_{yisK}-*lacZ* rose as cells transitioned from early to late exponential growth, reached peak levels shortly after exit from exponential growth, and remained steady for the remainder of the timepoints (Fig A1.5E). Wild-type expression from both P_{yodL}-*lacZ* and P_{yisK}-*lacZ* required both SigH and Spo0A, and was largely eliminated in the absence of both regulators (Fig A1.5D and Ap1.5E). We did not attempt to draw further conclusions from this data, since Spo0A and SigH each require the other for wildtype levels of expression (see discussion).

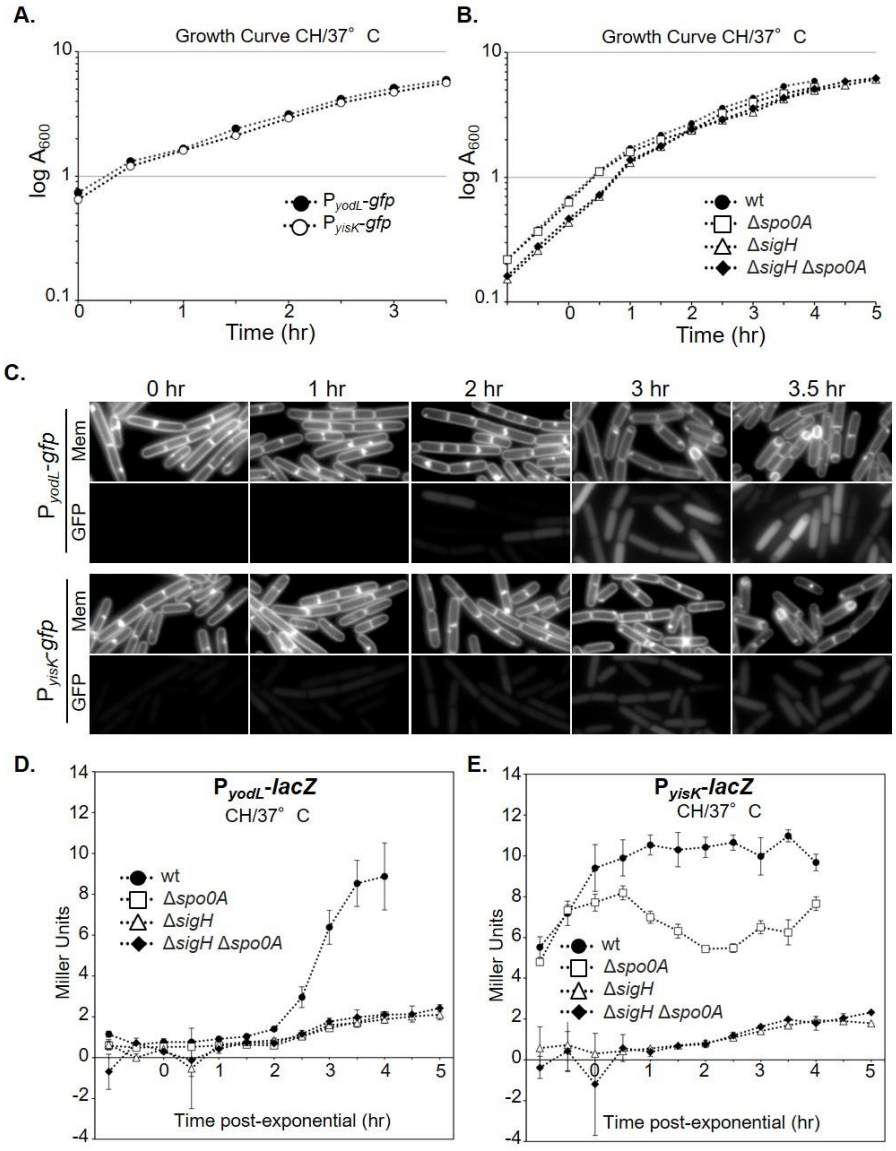

Fig. A1.5. Expression from *yodL* and *yisK* promoters during a CH timecourse. Expression from the putative *yodL* and *yisK* promoter regions was monitored in CH medium at 37°C over a timecourse. The OD_{600} (A and B) and production of either GFP (C) or beta-galactosidase (D and E) was monitored at 30 min intervals. Membranes were stained with TMA-DPH. All GFP channel images were captured with 1 sec exposures and scaled identically to allow for direct comparison. In this media, time 0 represents the last exponential timepoint, not the initiation of sporulation.

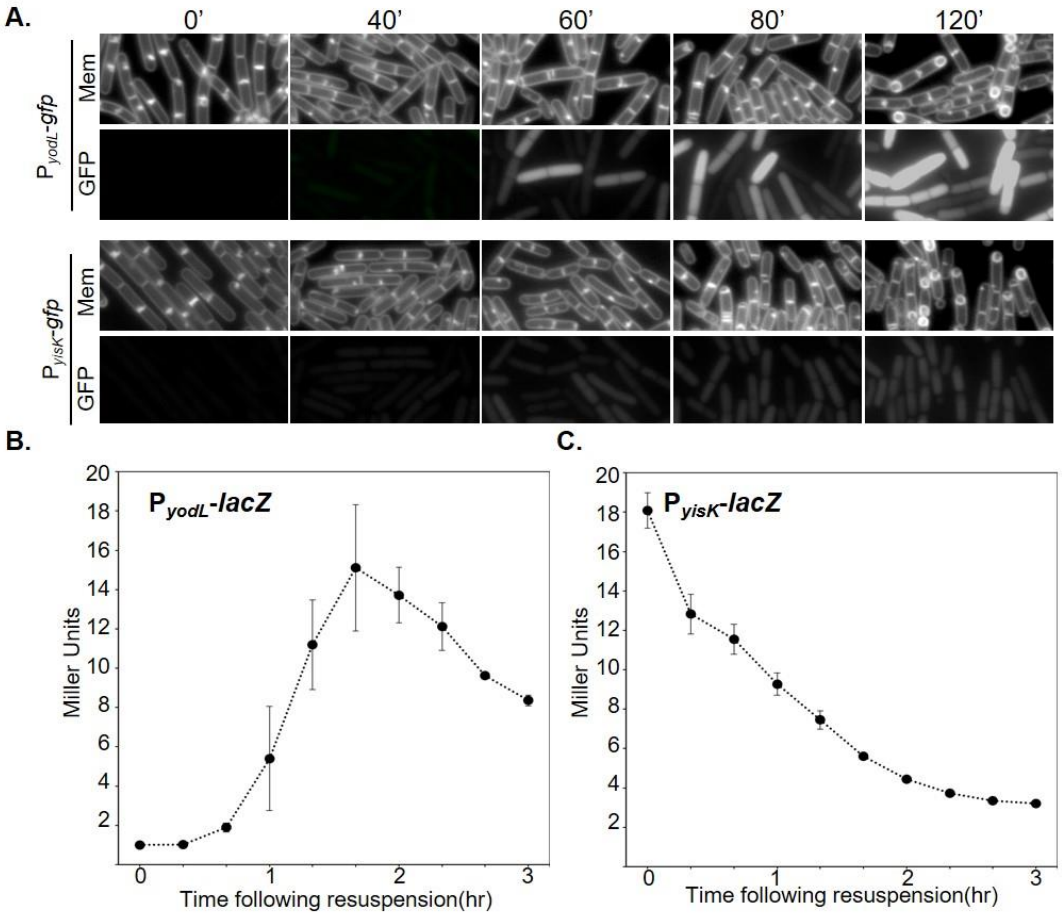

Fig. A1.6. Expression from *yodL* and *yisK* promoters following sporulation by resuspension. Expression from the putative *yodL* and *yisK* promoter regions was monitored in resuspension medium. The production of either GFP (A) or beta-galactosidase (B and C) was monitored at 20 min intervals. Membranes were stained with TMA-DPH. All GFP channel images were captured with 1 sec exposures and scaled identically to allow for direct comparison.

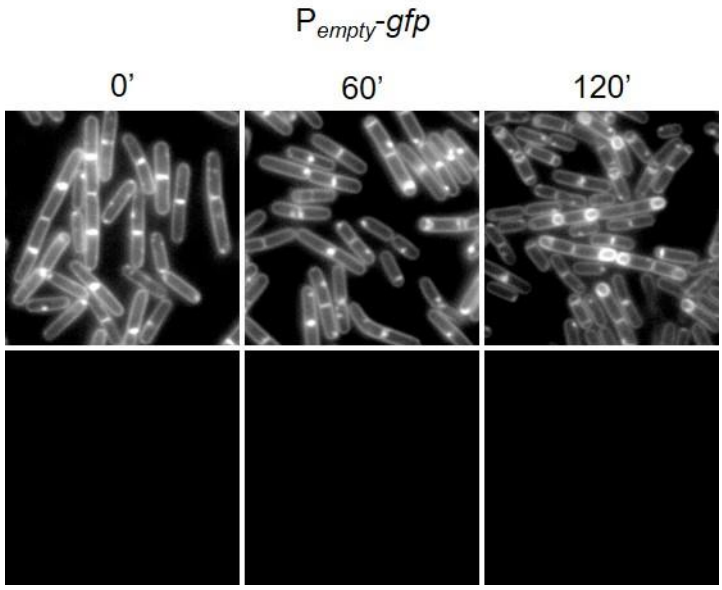

Fig. A1.7. A strain harboring a GFP reporter without a promoter during a sporulation timecourse. BAS205 (P_{empty}-*gfp*) was induced to sporulate via resuspension, and membranes are stained with TMA (white). Signal from GFP was scaled identically for all images and pseudocolored green. All images are shown at the same magnification.

We then followed expression from the promoter fusions over a time-course following the sporulation by resuspension method, which generates a more synchronous entry into sporulation (314). At time 0, neither the strain harboring P_{yodL}-*gfp*, nor the strain harboring P_{yisK}-*gfp* showed appreciable levels of fluorescence (Fig A1.6A), appearing similar to a negative control harboring *gfp* without a promoter (Fig A1.7). Between 0 and 40 min, both strains showed detectable increases in fluorescence. At 60 min, when the first polar division characteristic of sporulation begins to manifest, both strains were more strongly fluorescent (Fig A1.6A). GFP fluorescence from P_{yodL} was qualitatively more intense than fluorescence produced from P_{yisK} (all images were captured and scaled with identical parameters to allow for direct comparison). Moreover, the GFP signal continued to accumulate in the strain harboring P_{yodL}-*gfp* for at least two hrs (Fig A1.6A) and was heterogenous, consistent with activation by Spo0A. In contrast, the fluorescence signal produced from P_{yisK}-*gfp* was similar across the population and appeared similar at the 60 and 120 min timepoints (Fig A1.6A), consistent with SigH regulation.

To quantitate expression from the promoters during a sporulation by resuspension timecourse, we collected timepoints from strains harboring either the P_{yodL}-*lacZ* or P_{yisK}-*lacZ* reporter constructs and performed beta-galactosidase assays. Expression from P_{yodL}-*lacZ* rose rapidly between the 40 min and 100 min timepoints, and steadily declined thereafter (Fig A1.6B). The decline in signal was not observed for the GFP reporter, likely because the GFP is stable once synthesized (315). In contrast, expression from P_{yisK}-*lacZ* was highest at the time of resuspension (T0) and declined up until the final timepoint (Fig A1.6C).

Collectively, the patterns expression we observe for *yodL* are consistent with those observed for genes activated by high-threshold levels of Spo0A during sporulation,

including *racA*, *spoIIG*, and *spoIIA* (316). In contrast, *yisK*'s expression pattern is similar to that observed for *kinA* (14, 34, 310), with expression increasing in late exponential and stationary phase and early sporulation in a SigH-dependent manner (Fig A1.5), but decreasing during a sporulation by resuspension timecourse (Fig A1.6). We do not exclude the possibility that YodL and YisK might also function in other growth contexts.

A Δ*yodL* Δ*yisK* mutant is defective in sporulation

Since *yodL* and *yisK* expression correlates with other early sporulation genes, we next investigated if the gene products influenced the production of heat-resistant spores. To determine the number of heat-resistant spores in a sporulation culture, we quantified the number of colony forming units (CFU) present in cultures before (total CFU) and after (heat-resistant CFU) a heat treatment that kills vegetative cells. These values were normalized to display the sporulation efficiency of the mutants relative to wildtype. Single mutants in which either *yodL* or *yisK* were deleted displayed only mild (97% and 94%, respectively) reductions in relative sporulation efficiency (Table A1.4). Although the single mutants always sporulated less efficiently than wildtype in each experimental replicate, the differences were not statistically significant with only six experimental replicates. In contrast, the Δ*yodL* Δ*yisK* double mutant produced ~20% less heat-resistant spores than wildtype ($P<0.0006$)(Table A1.4). No decrease in total CFU was observed for any of the mutants compared to wildtype, indicating that the reduction in heat-resistant spores in the Δ*yodL* Δ*yisK* mutant was not due to reduced cell viability before heat treatment (Table A1.4). The gene downstream of *yisK*, *yisL*, is transcribed in the same direction as *yisK*. To determine if the reduction in sporulation we observed

might be partially attributable to polar effects of the *yisK* deletion on *yisL* expression, we introduced P_{yisK}-*yisK* at an ectopic locus (*amyE*) in the Δ*yodL* Δ*yisK* mutant and repeated the heat-kill assay. The ectopic copy of P_{yisK}-*yisK* restored sporulation in the Δ*yodL* Δ*yisK* to levels statistically indistinguishable from the Δ*yodL* single mutant (Table A1.4). These results lend support to the idea that YodL and YisK function during early sporulation and possess activities that, directly or indirectly, affect the production of viable spores. We do not exclude the possibility that YodL and YisK might also function outside the context of sporulation.

Given that *yisK* and *yodL* expression during vegetative growth leads to cell widening, we hypothesized that *yisK* and *yodL* mutants might produce thinner cells or spores during sporulation. However, no qualitative differences in cell or spore width were observed for the Δ*yodL*, Δ*yisK*, or Δ*yodL* Δ*yisK* mutant populations compared to wildtype during a sporulation timecourse (Fig A1.8). We also observed no qualitative differences in the shapes of germinating cells (data not shown). Thus, although YodL and YisK contribute to the production of heat-resistant spores, they do not appear to be required to generate any of the major morphological changes required for spore production.

Table A1.4. Sporulation efficiency of *yodL* and *yisK* mutants. Sporulation efficiency is the number of spores/ml divided by the total cfu/ml × 100%. Relative sporulation efficiency is sporulation efficiency normalized to wildtype × 100%. The data shown is the average of three independent biological replicates. The difference in sporulation efficiency between wildtype and the Δ*yodL* Δ*yisK* double mutant is statistically significant (P<0.0006).

Strain	Strain #	Total cfu	Heat-resistant cfu	Sporulation efficiency	Relative sporulation efficiency
wildtype	*B. subtilis* 168	2.8×10^8 ($\pm4.7\times10^7$)	1.9×10^8 ($\pm4.5\times10^7$)	66.9% (±5)	100%
Δ*yodL*	BYD276	2.6×10^8 ($\pm3.9\times10^7$)	1.7×10^8 ($\pm2.8\times10^7$)	65.2% (±7)	97%
Δ*yisK*	BYD278	2.7×10^8 ($\pm4.6\times10^7$)	2.4×10^8 ($\pm2.7\times10^7$)	63.1% (±6)	94%
Δ*yodL* Δ*yisK*	BYD279	3.1×10^8 ($\pm6.5\times10^7$)	1.7×10^8 ($\pm4.1\times10^7$)	54.1% (±4)	81%
Δ*yodL* Δ*yisK* P_{yisK}-*yisK*	BYD510	3.4×10^8 ($\pm3.3\times10^7$)	2.3×10^8 ($\pm4.1\times10^7$)	66.2% (±7)	99%

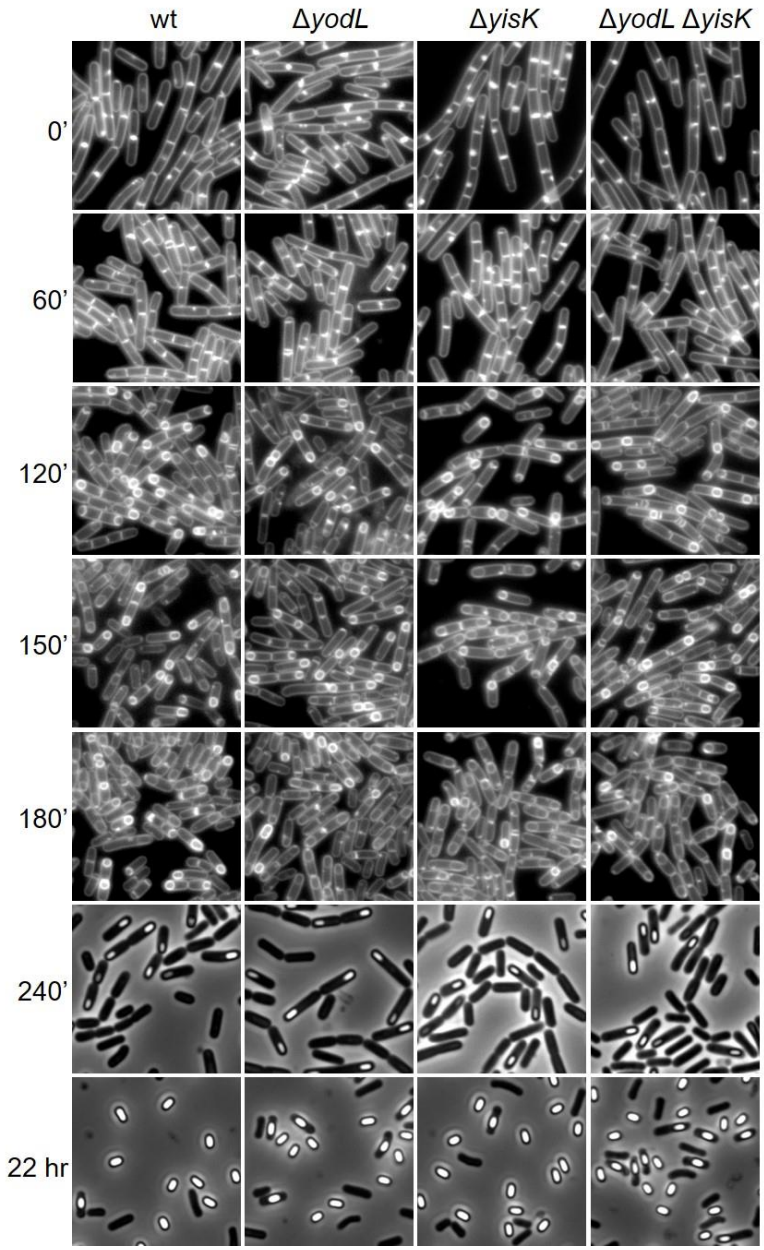

Fig. A1.8. Strains lacking *yodL* and/or *yisK* appear morphologically similar to wildtype during a sporulation timecourse. *B. subtilis* 168 (wt), BYD276 (*ΔyodL*), BYD278 (*ΔyisK*) and BYD279 (*ΔyodL ΔyisK*) were grown induced to sporulate via resuspension, and cells were grown for the indicated amount of time at 37°C before image capture. Membranes are stained with TMA-DPH (white). All images are shown at the same magnification.

MreB and Mbl are genetic targets of YodL and YisK activity

To identify genetic targets associated with YodL and YisK activity, we took advantage of the fact that misexpression of the proteins during vegetative growth prevents colony formation on plates and performed suppressor selection analysis. Strains harboring three copies of each misexpression cassette were utilized to reduce the chances of obtaining trivial suppressors in the misexpression cassette itself. In addition, P_{hy}-*lacZ* was used as a reporter to eliminate suppressors unable to release LacI repression following addition of inducer. In total, we obtained 14 suppressors resistant to YodL expression and 13 suppressors resistant to YisK expression. Six of the suppressors resistant to YodL were subjected to whole-genome sequencing. The results of the sequencing are shown in Table A1.5. All of the suppressors possessed mutations in either *mreB* or *mbl*, genes previously shown to be important in regulating cell width (Table A1.5). Using targeted sequencing, we determined that the remaining suppressor strains resistant to YodL also harbored mutations in *mreB* or *mbl*. Since the phenotypes of YodL and YisK expression were similar, we also performed targeted sequencing of the *mreB* and *mbl* chromosomal regions in the YisK-resistant suppressors. All but one of the YisK-resistant suppressors possessed mutations in *mbl*; the remaining suppressor harbored a mutation in *mreB.*

Table A1.5. Whole-genome sequencing analysis of genomic DNA from six YodL-resistant suppressors. BYD048 (three copies of P_{hy}-*yodL*) was used for suppressor selection. Candidates were analyzed by whole-genome sequencing as described in the materials and methods.

Suppressors of YodL	GENE	COORDINATE	REFERENCE	SAMPLE	DISTRIBUTION	VARIANT
SYL#1	*lmrB*	289144	C	A	50% C, 50% A	G317C
	yigA	1284721	C	G	61% C, 39% G	G17R
	mreB	2860903	T	A	100% A	R282S
	bioI	3089273	G	T	50% G, 50% T	R381I
	yvaC-parB	4205543	A	T	47% A, 53% T	intergenic
SYL#3	*mreB*	2861400	G	C	100% C	R117G
SYL#7	*mbl*	3747508	C	T	97% T	E250K
SYL#8	*mreB*	2861287	G	T	98% T	S154R
SYL#10	*mreB*	2861309	G	C	99% C	P147R
SYL#14	*mreB*	2860781	C	T	99% T	G323E
	folC	2866565	C	A	100% A	G14W

To determine if the point mutations we identified were sufficient to confer resistance to YodL or YisK misexpression, we generated the mutant alleles in clean genetic backgrounds and assayed for resistance to three copies (3X) of each misexpression construct (Table A1.6). In all cases but one, the engineered strains were resistant to the same selective pressure applied in the original selections (either 3X *yodL* or 3X *yisK*)(Table A1.6), indicating that the *mreB* or *mbl* mutations identified through sequencing were sufficient to confer resistance. When we attempted to engineer a strain harboring only $MreB_{S154R}$, all but one of the strains also possessed a second substitution, $MreB_{R230C}$. Although the remaining strain possessed only the $MreB_{S154R}$ substitution in MreB, unlike the original suppressor identified by whole genome sequencing (Table A1.5), the $MreB_{S154R}$ harboring strain was also sensitive to YodL expression. Based on these data, we suspect that the strain harboring $MreB_{S154R}$ might be unstable, and possibly predisposed to the accumulation of second-site mutations.

The YodL-resistant strains generally possessed mutations resulting in amino acid substitutions with charge changes (Table A1.6). When mapped to the *T. maritima* MreB structure, 5/7 of the unique suppressor strains possessed amino acid substitutions in a region important for mediating the interaction between MreB and the bitopic membrane protein RodZ ($MreB_{G143A}$, $MreB_{N145D}$, $MreB_{P147R}$, $MreB_{S154R}$, and $MreB_{R282S}$)(Table A1.6 and Fig A1.9)(279, 320); three of these substitutions occur in residues that make up the RodZ-MreB binding surface ($MreB_{N140}$, $MreB_{P142}$, and $MreB_{R279}$ in *T. maritima*)(279).

Table A1.6. Analysis of suppressor strains resistant to YodL and/or YisK. The suppressor selections are described in detail in materials and methods. Candidate mutations were introduced into clean genetic backgrounds harboring three copies of P_{hy}-*yodL* or three copies of P_{hy}-*yisK*, and the resultant strains were assessed for resistance (R) or sensitivity (S) to either *yodL* or *yisK* expression as judged by ability to grow on LB plates supplemented with 1 mM IPTG and 100 μg/ml spectinomycin. [1]Originally identified using whole-genome sequencing (Table S1). [2]Residues previously implicated in the RodZ-MreB interaction (279). [3]Residues previously implicated in resistance to A22 (317-319). The (*) indicates that two suppressors possessing the same nucleotide change were obtained in original selection. The underlined residues displayed specificity in resistance to YodL over YisK (top) or YisK over YodL (bottom).

Variants obtained following **YodL** misexpression			
mreB	**MreB Variants**	**+YodL**	**+YisK**
CGC→GGC	R117G[1]	R	R
GGA→GCA	G143A	R	R
AAT→GAT*	N145D[2]	R	S
CCA→CGA*	P147R[1,2]	R	S
AGC→AGA	S154R[1,2]	---	---
AGC→AGA	S154R[1]	R	R
CGC→TGC	R230C		
AGA→AGT*	R282S[1,2]	R	S
GGG→GAG	G323E[1]	R	R
mbl	**Mbl Variants**	**+YodL**	**+YisK**
ACG→ATG	T158M	R	R
GAA→AAA*	E250K[1]	R	R
ACA→ATA	T317I	R	R
Variants obtained following **YisK** misexpression			
mreB	**MreB Variants**	**+YisK**	**+YodL**
CGC→TGC	R117G	R	R
mbl	**Mbl Variants**	**+YisK**	**+YodL**
ATG→ATA	M51I[3]	R	R
CGC→TGC	R63C[3]	R	S
GAC→AAC*	D153N[3]	R	R
GGC→GAC	G156D[3]	R	R
ACG→GCG*	T158A[3]	R	R
GAG→GGG	E204G[3]	R	R
GAA→AAA	E250K	R	R
TCT→ΔΔΔ	ΔS251	R	S
CCT→CTT	P309L[3]	R	S
GCC→ACC	A314T[3]	R	R

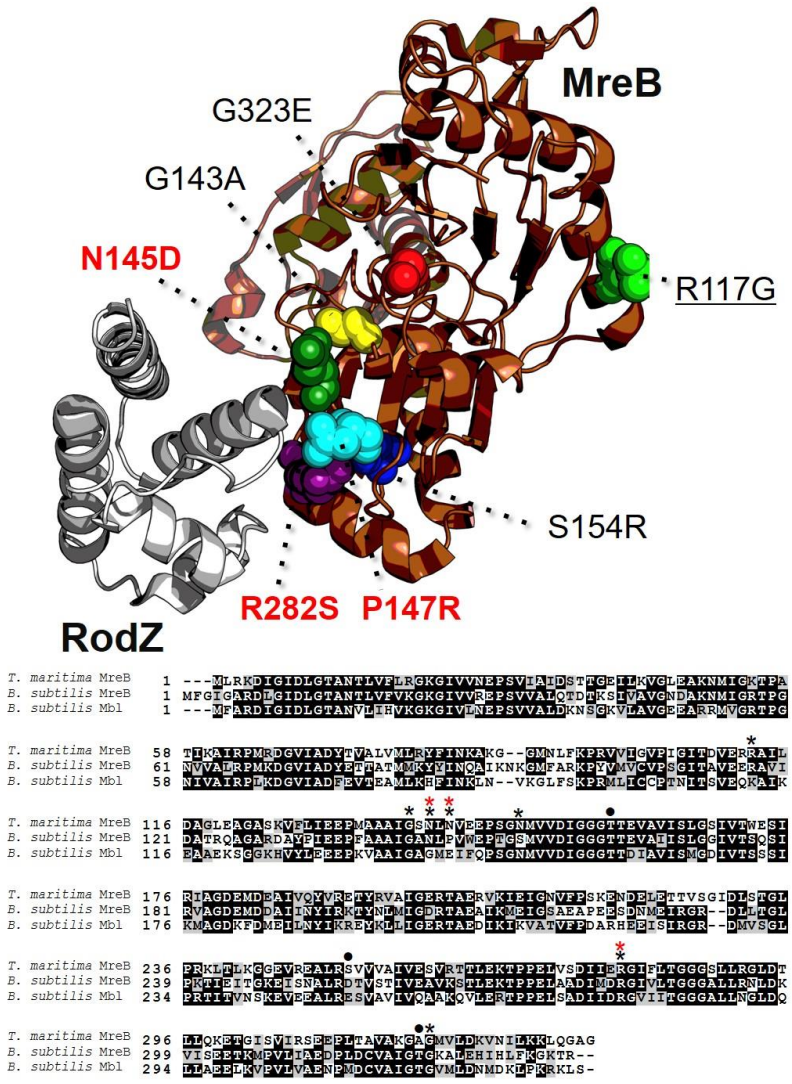

Fig. A1.9. Location of MreB residues conferring resistance to YodL. The co-crystal structure of RodZ-MreB (2WUS)(279) was extracted from the Protein Data Bank. MreB is labeled in brown and RodZ is labeled in grey. The identity and locations of the amino acid substitutions obtained from the YodL spontaneous suppressor selections are indicated on the structure, marked by a black asterisk above the relevant amino acid on the sequence alignment. Substitutions that confer resistance to YodL over YisK are shown in bold. Residues previously implicated in the MreB-RodZ interaction interface (279) are indicated by red asterisks. The filled circles indicate the location of the substitutions in Mbl conferring resistance to YodL misexpression. $MreB_{R117G}$ (underlined) was identified in a suppressor selections conferring resistance to YodL as well as in suppressor selections conferring resistance to YisK.

A majority of the YisK-resistant Mbl variants clustered in regions of Mbl that are predicted to make up the ATP-binding pocket (Table A1.6 and Fig A1.10). Moreover, seven of the substitutions occurred in amino acids previously associated with resistance to the MreB inhibitor A22 in *C. crescentus* and *Vibrio cholerae* (Fig A1.10)(274, 317, 319).

$MreB_{R117G}$ and Mbl_{E250K} were independently isolated in both the YodL and YisK suppressor selections, raising the possibility that at least some of the other MreB and Mbl variants might exhibit cross-resistance to YodL and YisK misexpression. To test for cross-resistance, we generated the mutant alleles in clean genetic backgrounds, and then introduced 3X copies of P_{hy}-*yisK* into the YodL-resistant suppressors, and 3X copies P_{hy}-*yodL* into the YisK-resistant suppressors. We then assayed for the ability of the misexpression strains to grow on media in the presence of inducer. The results, summarized in Table A1.6, show that several of the variants exhibited resistance to both YodL and YisK. Three MreB variants, $MreB_{N145D,}$ $MreB_{P147R}$ and $MreB_{R282S}$, exhibited specificity in their resistance to YodL compared to YisK. Three Mbl variants, Mbl_{R63C}, $Mbl_{\Delta S251}$, and Mbl_{P309L}, showed specificity in their resistance to YisK over YodL. These results suggest that the alleles exhibiting cross-resistance to both YisK and YodL are likely to be general, possibly conferring gain-of-function to either MreB or Mbl activity.

B. subtilis Mbl

Threaded to *T. maritima* MreB (PDB:1JCG)

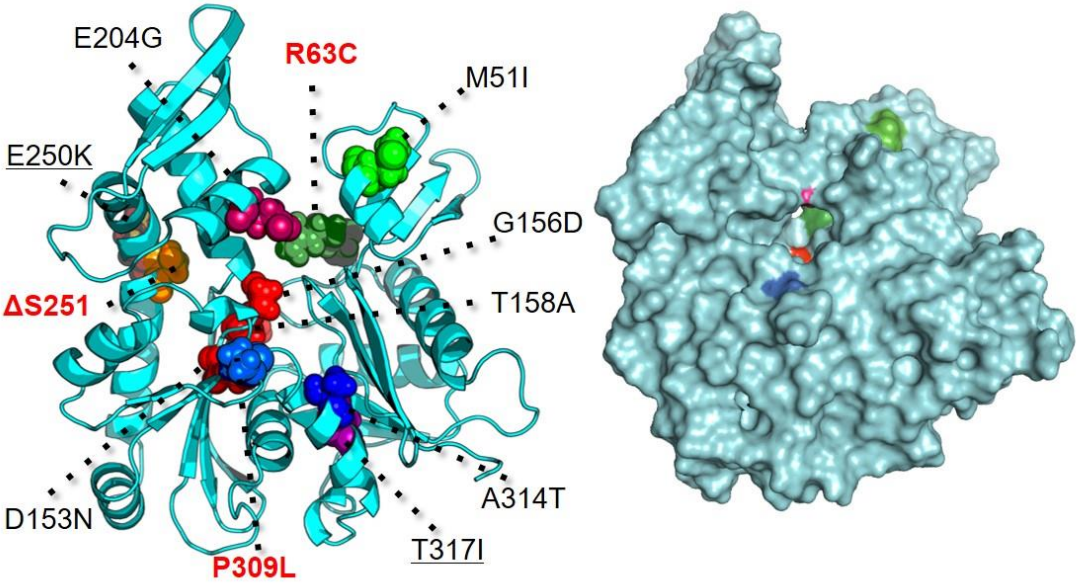


```
T. maritima MreB      1 -------MLRKDIGIDLGTANTLVFLRGKGIVVNEPSVIAIDSTTG-----EILKVGLEAK
B. subtilis MreB      1 ----MFGIGARDLGIDLGTANTLVFVKGKGIVVREPSVVALQTDT-----KSIVAVGNDAK
B. subtilis Mbl        1 -------MFARDIGIDLGTANVLIHVKGKGIVLNEPSVVALDKNSG----KVLAVGEEAR
C. crescentus MreB    1 MFSSLFGVISNDIAIDLGTANTLIYQKGKGIVLNEPSVVALRN--VGGRKVVHAVGIEAK
E. coli MreB          1 MLKKFRGMFSNDLSIDLGTANTLIYVKGQGIVLNEPSVVAIRQDRAGSPKSVAAVGHDAK
V. cholerae MreB      1 MFKKLRGMFSNDLSIDLGTANTLIYVKGQGIVLDEPSVVAIRQDKGRGGKTVAAVGHAAK

T. maritima MreB     50 NMIGKTPATIKAIRPMRDGVIADYTVALVMIRYFINKAKGG--MNLFKPRVVIGVPIGIT
B. subtilis MreB      53 NMIGRTPGNVVAIRPMKDGVIADYEITATMMKYVINQAIKNKKGMFARKPVVMVCVPSGIT
B. subtilis Mbl        50 RMVGRTPGNIVAIRPLKDGVIADFEVTEAMLKHFINKLNVKG--LFSKPRMLICCPTNIT
C. crescentus MreB    59 QMLGRTPGHMEAIRPMRDGVIADFEVAEEMEKYFIRKVHNRK-GFVN-PKVIVCVPSGAT
E. coli MreB          61 QMLGRTPGNIAAIRPMKDGVIADFEVTEKMLQHFIKQVHSNS-FMRPSPRVLVCVPVGAT
V. cholerae MreB      61 QMLGRTPGNISAIRPMKDGVIADFEVTEKMLQHFIRQVHDNS-VLKPSPRVLVCVPCGST

T. maritima MreB    108 DVERRAILDAGLEAGASKVFLIEEPMAAAIGSNLNVEEPSGNMVVDIGGGTTEVAVISLG
B. subtilis MreB     113 AVEERAVIDATRQAGARDAYPIEEPFAAAIGANLPVEEPTGSMVVDIGGGTTEVAIISLG
B. subtilis Mbl       108 SVEQKATKEAAEKSGGKHVYLEEEPKVAAIGAGMEIFQPSGNMVVDIGGGTTDIAVISMG
C. crescentus MreB   117 AVERRAINDSCLNAGARRVGLIDEPMAAAIGAGLPIHEPTGSMVVDIGGGTTEVAVLSLS
E. coli MreB         120 QVERRAIRESAQGAGAREVFLIEEPMAAAIGAGLPVSEATGSMVVDIGGGTTEVAVISLN
V. cholerae MreB     120 QVERRAIRESALGAGAREVYLIDEPMAAAIGAGLRVSEPTGSMVIDIGGGTTEVAVISLN

T. maritima MreB    168 SIVTWESIRIAGDEMDEAIVQYVRETYRVAIGERTAERVKIEIGNVFPSKENDELETTVS
B. subtilis MreB     173 GIVTSQSIRVAGDEMDDAIINYIRKTYNLMIGDRTAEAIKMEIGSAEAP--EESDNMEIR
B. subtilis Mbl       168 DIVTSSSIKMAGDKFDMEILNYIKREYKLLIGERTAEDIKIKVATVFP--DARHEEISIR
C. crescentus MreB   177 GIVYSRSVRVGGDKMDEAIISYMRRHHNLLIGETTAERIKKEIGTARAPADGEGLSIDVK
E. coli MreB         180 GVVYSSSVRIGGDRFDEAIINYVRRNYGSLIGEATAERIKHEIGSAWP--GDEVREIEVR
V. cholerae MreB     180 GVVYSSSVRIGGDRFDEAIINYVRRNYGSLIGEATAERIKHEIGSAWP--GDDVQEIEVR

T. maritima MreB    228 GIDLSTGLPRKLTLKGGEVREALRSVVAIVESVRTTLEKTPPELVSDIIERGIPLTGGG
B. subtilis MreB     231 GRDLLTGLPKTIEITGKEISNALRDTVSTIVEAVKSTLEKTPPELAADIMDRGIVLTGGG
B. subtilis Mbl       226 GRDMVSGLPRTIFVNSKEVEEALRESVAVIVQAAKQVLERTPPELSADIIDRGVIITGGG
C. crescentus MreB   237 GRDLMQGVPREVRISEKQAADALAEPVGQIVEAVKVALEATPPELASDIADKGIMLTGGG
E. coli MreB         238 GRNLAEGVPRGFTLNSNEILEALQEPLTGIVSAVMVALEQCPPELASDISERGMVLTGGG
V. cholerae MreB     238 GRNLAEGVPRSFTLNSNEILEALQEPLTGIVSAVMVALEQCPPELASDISENGMVLTGGG

T. maritima MreB    288 SLLRGLDTLLQKETGISVIRSEEPLTAVAKGAGMVLDKVNILKKLQGAG--
B. subtilis MreB     291 ALLRNLDKVISEETKMPVLIAEDPLDCVAIGTGKALEHIHLFKGKTR----
B. subtilis Mbl       286 ALLNGLDQLLAEELKVPVLVAENPMDCVAIGTGVMLDNMDKLPRRKLS----
C. crescentus MreB   297 ALLRGLDAEIRDHTGLPVTVADDPLSCVALGCGKVLEHPKWMKGVLFSTLA
E. coli MreB         298 ALLRNLDRLLMEETGIPVVVADDPLTCVARGGGKALEMIDMHGGDLFSEE-
V. cholerae MreB     298 ALLKDLDRLLMEETGIPVVIADDPLTCVARGGGKALEMIDMHGGDLFSEE-
```

Fig. A1.10. Location of Mbl residues conferring resistance to YisK. The structure of *B. subtilis* Mbl, as predicted by I-TASSER (321), threaded to *T. maritima* MreB (1JCG)(279). The structure on the right is a surface prediction model. The identity and locations of the amino acid substitutions obtained from the YisK spontaneous suppressor selections are indicated on the structure, with substitutions conferring resistance to YisK over YodL in bold. The sequence alignment is of MreB from *T. maritima*, *B. subtilis* 168, *C. crescentus* NA1000, *E. coli* MG1655, and *V. cholera* N16961. The location of amino acid substitutions conferring YisK resistance are indicated by black asterisks. Residues also previously shown to confer resistance to A22 in *C. crescentus* NA1000 (274, 317) and *V. cholera* N16961 (319) are indicated by red and blue asterisks, respectively. The filled triangle corresponds to a residue shown by in vivo crosslinking to be important for the formation of antiparallel MreB protofilaments (322). The filled circle denotes the location of $MreB_{R117G}$, which was identified in spontaneous suppressor selections conferring resistance to both YodL and YisK. Mbl_{T317I} (underlined) was only identified in a spontaneous suppressor selection conferring resistance to YodL, although it exhibits cross-resistance to YisK (see Fig A1.5).

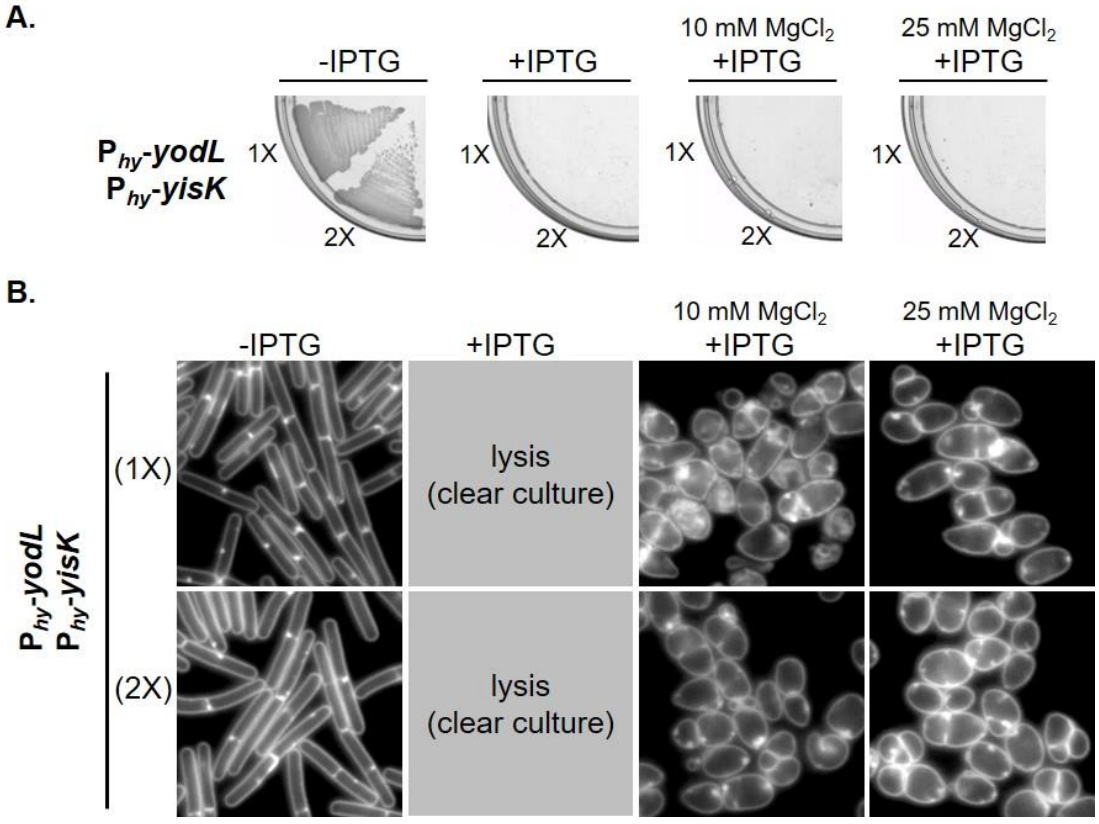

Fig. A1.11. YodL and YisK co-misexpression causes cell lysis. (A) BYD361 (P_{hy}-*yodL*, P_{hy}-*yisK*) and BYD281 (2X P_{hy}-*yodL*, 2X P_{hy}-*yisK*) were streaked on an LB plate with 100 µg/ml spectinomycin and, when indicated 1 mM IPTG or 1 mM IPTG and the denoted concentration of $MgCl_2$. (B) Cells were grown in LB-Lennox media at 37°C to mid-exponential and back-diluted to an OD_{600} of ~0.02. When indicated 1 mM IPTG or 1 mM IPTG and the denoted concentration of $MgCl_2$ were added. Cells were then grown for 1.5 hrs at 37°C before image capture. Membranes are stained with TMA-DPH. All images are shown at the same magnification.

YodL and YisK's cell-widening activities require MreB and Mbl, respectively

The phenotypic consequences of YodL and YisK misexpression are similar but not identical (Fig A1.1B), suggesting that YodL and YisK might have distinct targets. Consistent with this idea, YodL and YisK coexpression resulted in phenotypes distinct from misexpression of either YodL or YisK alone. More specifically, cells co-expressing YodL and YisK did not grow on plates, regardless of media or $MgCl_2$ concentration (Fig A1.3A and Fig A1.11A) and growth without lysis in liquid media required the presence of $MgCl_2$ (Fig A1.2, Fig A1.3B, and Fig A1.11B). Importantly, the co-expressing cells displayed a round morphology that strongly contrasted with strains expressing either YodL or YisK alone (Fig A1.3B and Fig A1.11B). The round morphology was unlikely due to higher expression of gene products (1X P_{hy}-*yodL* plus 1X P_{hy}-*yisK*), since cells harboring two copies (2X) of either P_{hy}-*yodL* or P_{hy}-*yisK* did not become round (Fig A1.1B and Fig A1.3B).

Based on the observation that YodL and YisK coexpression yields distinct phenotypes, and the fact that all of the YodL-specific suppressor mutations occurred in *mreB* ($MreB_{N145D,}$ $MreB_{P147R}$ and $MreB_{R282S}$), while all of the YisK-specific suppressor mutations occurred in *mbl* (Mbl_{R63C}, $Mbl_{\Delta S251}$, and Mbl_{P309L}), we hypothesized that YodL targets MreB, whereas YisK targets Mbl. To test these hypotheses, we assessed if MreB and Mbl are specifically required for YodL and YisK function by taking advantage of the fact that *mreB* and *mbl* can be deleted in a Δ*ponA* background with only minor changes in cell shape (282, 293). The Δ*ponA* strain, which does not make PBP1, produces slightly longer and thinner cells than the parent strain, and requires $MgCl_2$ supplementation for normal growth (323, 324). We generated Δ*ponA* Δ*mreB* and Δ*ponA* Δ*mbl* strains and then introduced either two copies of P_{hy}-*yodL* or two copies of P_{hy}-*yisK*

into each background. We reasoned that 2X expression would provide a more stringent test for specificity than 1X expression, as off-target effects (if any), would be easier to detect. To assess the requirement of either *mreB* or *mbl* for YodL and YisK activity, cells were grown to exponential phase in LB media supplemented with 10 mM $MgCl_2$, back-diluted to a low optical density, and induced for 90 min before images were captured for microscopy. Uninduced controls all appeared as regular rods, although Δ*ponA* deletion strains were noticeably thinner than wildtype parents (Fig A1.12). The Δ*ponA* cells became wider following YodL expression, indicating that PBP1 is not required for YodL activity. We also observed that the poles of the Δ*ponA* mutant were less elongated and tapered than the wild-type control following YodL expression, suggesting that this particular effect of YodL expression is PBP1-dependent (Fig A1.12A). A Δ*ponA* Δ*mbl* mutant phenocopied the Δ*ponA* parent following YodL expression (Fig A1.12A), indicating that Mbl is not required for YodL's activity. In contrast, the Δ*ponA* Δ*mreB* strain did not show morphological changes following YodL expression, and instead appeared similar to the uninduced control. We conclude that YodL requires MreB for its cell-widening activity.

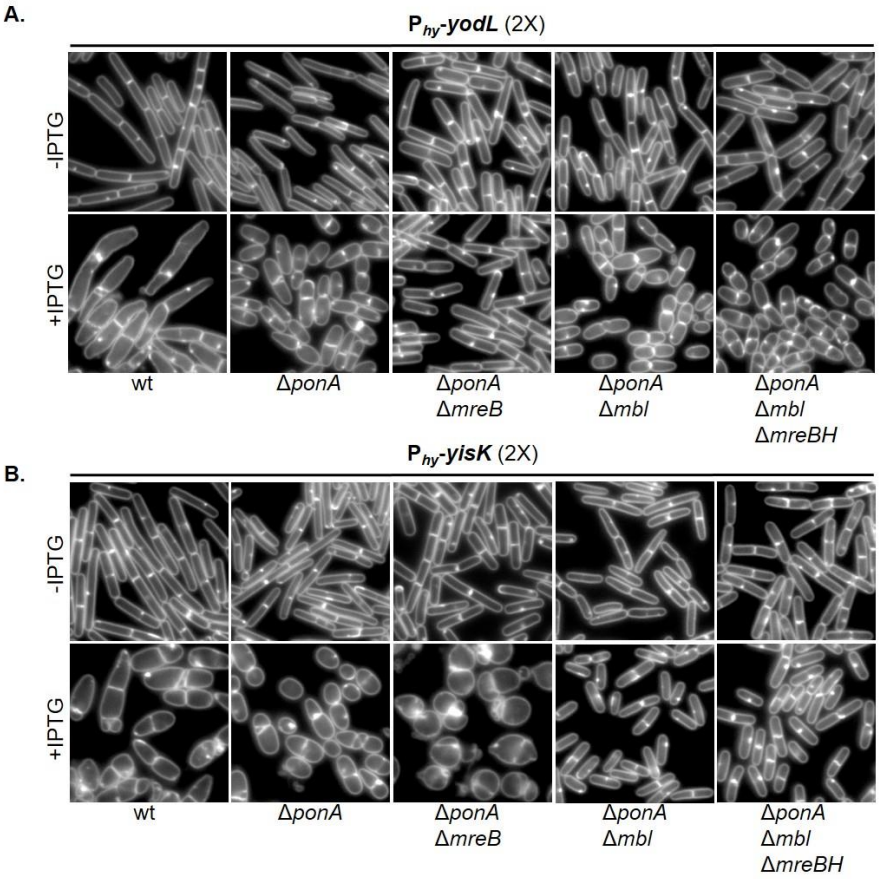

Fig. A1.12. YodL and YisK's cell-widening activities require MreB and Mbl, respectively. (A) Cells harboring 2X copies of P_{hy}-*yodL* in a wildtype (BAS191), Δ*ponA* (BYD176), Δ*ponA* Δ*mreB* (BYD263), Δ*ponA* Δ*mbl* (BYD259) or Δ*ponA* Δ*mbl* Δ*mreBH* (BAS249) background were grown at 37°C in LB supplemented with 10 mM $MgCl_2$ to mid-exponential. To induce *yodL* expression, cells were back-diluted to an OD_{600} of ~0.02 in LB with 10 mM $MgCl_2$, and IPTG (1 mM) was added. Cells were grown for 1.5 hrs at 37°C before image capture. Membranes are stained with TMA-DPH. All images are shown at the same magnification. (B) Cells harboring 2X copies of P_{hy}-*yisK* in a wildtype (BYD074), Δ*ponA* (BYD175), Δ*ponA* Δ*mreB* (BYD262), Δ*ponA* Δ*mbl* (BYD258) or Δ*ponA* Δ*mbl* Δ*mreBH* (BAS248) background were grown at 37°C in LB supplemented with 10 mM $MgCl_2$ to mid-exponential. To induce *yisK* expression, cells were back-diluted to an OD_{600} of ~0.02 in LB with 10 mM $MgCl_2$, and IPTG (1 mM) was added. Cells were grown for 1.5 hrs at 37°C before image capture. Membranes are stained with TMA-DPH. All images are shown at the same magnification.

We performed a similar series of experiments for YisK misexpression. The Δ*ponA* mutant was sensitive to YisK expression, indicating that PBP1 is not required for YisK-dependent cell-widening. Similarly, expression of YisK in a Δ*ponA* Δ*mreB* mutant also resulted in loss of cell width control (Fig A1.12B), indicating that MreB is not required for YisK activity; however, unlike YisK expression in a wildtype or Δ*ponA* background, the cells became round (Fig A1.12B), more similar to the YodL and YisK co-expressing cells (Fig A1.3B and Fig A1.11). In contrast, a Δ*ponA* Δ*mbl* mutant did not lose control over cell width following YisK expression (Fig A1.12B), indicating that YisK activity requires Mbl for its cell-widening activity. We conclude that YodL requires MreB, but not Mbl for its cell-widening activity, whereas YisK requires Mbl, but not MreB.

YisK possesses at least one additional target

Although YisK expression in a Δ*ponA* Δ*mbl* mutant did not result in cell-widening, we observed that the induced cells appeared qualitatively shorter than the uninduced control, suggesting that YisK might possess a second activity (Fig A1.12B). Quantitation of cell lengths in a Δ*ponA* Δ*mbl* mutant following YisK expression revealed that the YisK-induced cells were ~20% shorter than the uninduced cells (Fig A1.13A). In contrast, YodL expression did not result in a change in cell length in a Δ*ponA* Δ*mreB* mutant (Fig A1.13B), suggesting the the cell shortening effect is specific to YisK. We hypothesized that MreBH, the third and final *B. subtilis* MreB family member, might be YisK's additional target. We hypothesized that if MreBH is the additional target, then the cell shortening observed upon YisK expression in a Δ*ponA* Δ*mbl* mutant strain should be lost in a Δ*ponA* Δ*mbl* Δ*mreBH* mutant background.

However, we found that even when *mreBH* was additionally deleted, YisK expression still resulted in cell shortening (Fig A1.13C). We conclude that YisK likely has at least one additional target that is not MreB or Mbl dependent, and that this additional target regulates some aspect of cell length.

Discussion

YodL and YisK's functional targets

Misexpression of YodL during vegetative growth results in cell-widening and lysis, and spontaneous suppressor mutations conferring resistance to YodL occur primarily in *mreB*. MreB is also required for YodL's cell-widening activity, whereas Mbl is not. By comparison, expression of YisK during vegetative growth also results in cell-widening and lysis, however, spontaneous suppressor mutations conferring resistance to YisK occur primarily in *mbl*. YisK's cell-widening activity requires Mbl, but not MreB. The simplest interpretation of these results is that YodL targets MreB function, while YisK targets Mbl function. Alternatively, YodL and YisK could target other factors that affect cell shape and simply require MreB and Mbl for their respective functions.

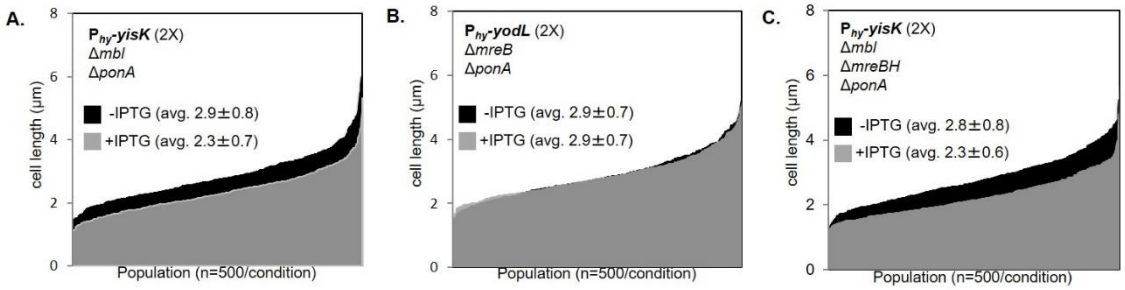

Fig. A1.13. YisK expression results in cell shortening. (A) Cells harboring 2X copies of P$_{hy}$-*yisK* in a Δ*ponA* Δ*mbl* background (BYD262) were grown at 37°C in LB supplemented with 10 mM $MgCl_2$ to mid-exponential. To induce *yisK* expression, cells were back-diluted to an OD_{600} of ~0.02 in LB with 10 mM $MgCl_2$ and IPTG (1 mM) was added. Cells were grown for 1.5 hrs at 37°C before image capture. Membranes are stained with TMA-DPH. Cell lengths (n=500/condition) were measured before and after *yisK* expression and rank-ordered from smallest to largest along the x-axis so the entire population could be visualized without binning. The uninduced population (black) is juxtaposed behind the induced population (semi-transparent, gray). The difference in average cell length before and after P$_{hy}$-*yisK* induction were statistically significant ($P<0.0001$). (B) Cells harboring 2X copies of P$_{hy}$-*yodL* in a Δ*ponA* Δ*mreB* background (BYD263) were grown, quantitated, and plotted as described above. The difference in average cell length before and after P$_{hy}$-*yodL* induction were not statistically significant. (C) Cells harboring 2X copies of P$_{hy}$-*yisK* in a Δ*ponA* Δ*mbl* Δ*mreBH* background (BAS248) were grown, quantitated, and plotted as described above. The difference in average cell length before and after P$_{hy}$-*yisK* induction were statistically significant ($P<0.0001$).

MreB variants specifically resistant to YodL activity, $MreB_{N145D,}$ $MreB_{P147R}$ and $MreB_{R282S,}$ all result in charge change substitutions in residues previously shown to constitute the RodZ-MreB interaction surface (equivalent *T. maritima* residues are: $MreB_{N140,}$ $MreB_{N142}$ and $MreB_{R279}$)(279). $MreB_{G143A}$, which exhibits cross-resistance to YisK, also maps near the RodZ-MreB interaction interface. The two remaining YodL-resistant MreB variants occur in ($MreB_{R117G}$) or near ($MreB_{G323E}$) residues previously associated with bypass of RodZ essentiality in *E. coli* (Fig A1.9)(287). A simple model explaining both the nature of the MreB variants we obtained in the suppressor selections, and YodL's MreB-dependent effect on cell shape, is that YodL acts by disrupting the interaction between RodZ and MreB. In this model, MreB's RodZ-independent activities would remain functional, and several observations are consistent with this idea. If YodL were to completely inactivate MreB function, then we would expect that expressing YodL in a Δ*ponA* Δ*mbl* Δ*mreBH* background would generate round cells, similar to the phenotype observed when MreB is depleted in a Δ*mbl* Δ*mreBH* mutant background (293), or when *mreB*, *mbl*, and *mreBH* are deleted in backgrounds with upregulated *sigI* expression (the triple mutant is otherwise lethal)(325). However, we observe that cells expressing YodL in a Δ*ponA* Δ*mbl* Δ*mreBH* mutant instead form wide rods (Fig A1.12A). If YodL does specifically target MreB activity, then these results suggest that MreB likely retains at least some of its width-maintenance function. Morgenstein et al. recently found that the interaction between RodZ and MreB in *E. coli* is required for MreB rotation, but that MreB rotation was not required for rod shape or cell viability under standard laboratory conditions (288). This study is consistent with prior findings indicating that RodZ is not absolutely required for maintenance of rod shape (287).

We hypothesize that the substitutions obtained in residues near the RodZ-MreB interface either enhance RodZ-MreB interaction, or decrease the ability of YodL to

disrupt the RodZ-MreB interface. Although we did not identify YodL-resistant suppressor mutations in *rodZ*, it is possible that the requisite *rodZ* mutations are rare or lethal for the cell, thus we cannot rule out the possibility that YodL could target RodZ function. Similarly, although we found that MreB is required for YodL activity, we can envision a scenario in which a YodL-MreB interaction may be necessary to localize YodL to a cellular location where it can be effective against RodZ or some other cellular component. We think this possibility is less likely, as cells expressing YodL have a distinct phenotype from RodZ depletion in *B. subtilis*. More specifically, YodL expression results in cell widening and tapered poles (Fig A1.1B), whereas RodZ-depleted cells generate wide rods (284), similar to the phenotype we observed following YodL expression in a Δ*ponA* Δ*mbl* Δ*mreBH* mutant (Fig A1.12A). These results argue against the idea that YodL could work by inactivating RodZ function completely. Future work aimed at characterizing the nature of the YodL resistant suppressors and the effect of YodL on MreB function will shed light on the mechanism underlying YodL's observed activity.

Only three Mbl variants, Mbl_{R63C}, $Mbl_{\Delta S251}$, and Mbl_{P309L}, showed specificity in resistance to YisK over YodL. $Mbl_{R63C,}$ Mbl_{D153N}, Mbl_{G156D}, Mbl_{T158A}, Mbl_{E204G}, $MreB_{P309L}$ and Mbl_{A314T} occur in residues that form Mbl's predicted ATP-binding pocket (Fig A1.10), and substitutions in all seven of these residues have been previously implicated in A22 resistance (Fig A1.10)(274, 317, 319). We speculate that most, if not all of the substitutions in Mbl's ATP-binding pocket are gain-of-function with respect to Mbl polymerization, a hypothesis that can ultimately be tested in vitro. Similarly, we hypothesize that the Mbl_{M51I} substitution, located at the MreB head-tail polymerization interface (320), may overcome YisK activity by promoting Mbl polymerization. $MreB_{E262}$ of *C. crescentus*, equivalent to *B. subtilis* Mbl_{E250} (Fig A1.10), is located at the

interaction interface of antiparallel MreB protofilament bundles (322). If *B. subtilis* Mbl_{E250} is also present at this interface (this has not been tested to our knowledge), then Mbl_{E250K} could promote resistance to YodL and YisK by enhancing Mbl bundling. How might YisK exert its activity? One idea is that YisK disrupts Mbl bundling, possibly by competing for sites required for protofilament formation. An alternative possibility is that YisK somehow prevents Mbl from effectively binding or hydrolyzing ATP. It is also possible that Mbl is simply required for YisK to target one or more other factors involved in cell-width control.

In addition to Mbl-dependent cell widening, YisK expression resulted in cell shortening, an effect that only became apparent in a Δ*ponA* Δ*mbl* mutant background (Fig A1.12B and Ap1.13A). Given the similarities of MreB, Mbl, and MreBH to each other, we initially hypothesized that YisK-dependent effects on MreB and/or MreBH might be responsible for the decrease in cell length we observed; however, we found that *mreBH* was not required for cell shortening (Fig A1.12B and Fig A1.13C). Since YisK expression results in a dramatic loss of cell shape in Δ*mreB* mutant backgrounds (Fig A1.12A), we were unable to confidently assess cell length changes to determine if there is a requirement for MreB in the cell-shortening phenotype. It is unlikely that YisK's additional activity affects MreB's role in maintaining cell width (at least not without Mbl), as YisK-expressing cells retain rod shape when *mbl* and *mreBH* are both deleted (Fig A1.12B). An exciting alternative possibility is that YisK activity affects another factor involved in cell length control. One attractive candidate is the cell wall hydrolase CwlO, a known modulator of cell length in *B. subtilis* (326) which recent genetic data also suggests depends at least in part on Mbl (297). Future experiments aimed at determining the identity and function of YisK's additional target should shed light on how cells regulate both cell length and cell width.

We performed a similar series of experiments for YisK misexpression. The Δ*ponA* mutant was sensitive to YisK expression, indicating that PBP1 is not required for YisK-dependent cell-widening. Similarly, expression of YisK in a Δ*ponA* Δ*mreB* mutant also resulted in loss of cell width control (Fig A1.12B), indicating that MreB is not required for YisK activity; however, unlike YisK expression in a wildtype or Δ*ponA* background, the cells became round (Fig A1.12B), more similar to the YodL and YisK co-expressing cells (Fig A1.3B and Fig A1.11). In contrast, a Δ*ponA* Δ*mbl* mutant did not lose control over cell width following YisK expression (Fig A1.12B), indicating that YisK activity requires Mbl for its cell-widening activity. We conclude that YodL requires MreB, but not Mbl for its cell-widening activity, whereas YisK requires Mbl, but not MreB.

Identification of genes involved in cellular organization through a novel gene discovery pipeline

To systematically identify and characterize novel genes involved in cellular organization, we developed a gene discovery pipeline that combines known regulatory information (14), phenotypes obtained from misexpression screening, and suppressor selection analysis. The ability to identify genetic targets associated with the unknown genes provides a key parameter beyond phenotype from which to formulate testable hypotheses regarding each gene's possible function. The misexpression constructs we generated are inducible and present in single copy on the chromosome. We have found that to obtain phenotypes, our strategy works best when the unknown genes are expressed outside of their native regulatory context. Thus far, we have restricted our

gene function discovery pipeline to *B. subtilis*; however, the general approach should be broadly applicable to other organisms and diverse screening strategies.

In this work, we describe the use of the pipeline to identify and characterize two *B. subtilis* genes, *yodL* and *yisK*, that produce proteins capable of targeting activities intrinsic to cell width control. Although *yodL* and *yisK* were not previously recognized as members of the Spo0A regulon, both genes have putative Spo0A boxes and possess promoters that exhibit expression patterns consistent with other Spo0A-regulated genes (Fig A1.4-1.6). YisK is also a member of the SigH regulon (32), and our expression analysis is also consistent with expression of *yisK* during stationary phase (Fig A1.5). If the putative Spo0A box we identified is utilized in vivo, then we would predict based on our expression profiling that *yisK* is transcribed during exponential and early stationary phase via SigH, and then repressed as Spo0A-P accumulates during early sporulation. Such a pattern is similar to the regulation that has been proposed for *kinA* (45, 316). We also observe expression from P_{yodL} and P_{yisK} is reduced in the absence of Spo0A and SigH (Fig A1.5D-E). The specific contributions of these global regulators to *yodL* and *yisK* regulation cannot be determined by analyzing the expression profiles of the *sigH* and *spo0A* deletion strains alone, since *spo0A* depends on SigH for upregulation during the early stages of sporulation (37, 45). Moreover, since Spo0A inhibits expression of the *sigH* repressor AbrB (327-330), a *spo0A* mutant is also down for *sigH* expression.

A Δ*yodL* Δ*yisK* double mutant reproducibly produces ~20% less heat-stable spores than wildtype, suggesting that the YodL and YisK have functions that affect spore development (either directly or indirectly). Most studies on sporulation genes are biased toward factors that reduce sporulation efficiency by an order of magnitude or more in a standard heat-kill assay. However, even small differences in fitness (if reproducible) can contribute significantly to the ability of an organism to persist,

especially in competitive environments (331). The 20% reduction in heat-resistant spores we observe in cells lacking YisK and YodL would likely result in a substantial fitness disadvantage to cells in the environment. We do not currently understand how YodL and YisK might function in spore development, but the identification of MreB and Mbl as genetic targets suggests the proteins likely regulate some aspect of PG synthesis. Future studies will be aimed at understanding the molecular and biochemical basis of YodL and YisK activity.

In this study, the morphological phenotypes associated with YodL and YisK occurred when the genes were expressed during vegetative growth. Consequently, it is formally possible (although we think unlikely), that the targeting of MreB and Mbl is simply a coincidence that is unrelated to the potential functions of the proteins during stationary phase or sporulation. Regardless of what YodL and YisK's physiological roles turn out to be, we have already been able to utilize misexpression of the proteins to obtain interesting variants of both MreB and Mbl that can now be used to generate testable predictions regarding how MreB and Mbl function in *B. subtilis*. Moreover, the apparent specificity with which YodL and YisK appear to target MreB and Mbl, respectively, make them potentially powerful tools to differentially target the activities of these two highly similar paralogs in vivo. Of course, more studies will be required to determine if YodL and YisK interact directly or indirectly to modulate MreB and Mbl activity. In the meantime, it is exciting to speculate that many undiscovered modulators of MreB and MreB-like proteins exist, and that we have only just begun to scratch the surface regarding regulation of this important class of proteins. The identification and characterization of such modulators could go a long way toward addressing the significant gaps in our knowledge that exist regarding the regulation of PG synthesis in bacteria.

APPENDIX II

CHARACTERIZATION OF THE EFFECTS OF *B. subtilis* YodL AND YisK ON *E. coli*

Introduction

Bacterial actin-like proteins play important roles in bacterial peptidoglycan (PG) synthesis (290, 332). One such protein, MreB, is conserved and essential across the majority of non-coccoid bacteria (269, 270). Gram negative bacteria like *Escherichia coli* often encodes only one MreB-like protein, while Gram positives often encode more than one paralog. *B. subtilis* possesses three MreB-like proteins: MreB, Mbl, and MreBH (289, 293). MreB interacts with other components of the elongation system including MreC/MreD (encoded by the genes downstream of *mreB* in the same operon)(333), penicillin binding proteins (PBPs) such as PBP1, PBP2a and PBP2b (282), the membrane associated cytosolic enzyme MurG (334), and the bitopic membrane protein RodZ (288). Depletion or inactivation of MreB leads to rounding up of rod-shaped cells (335), consistent with its proposed role in directing assembly of peptidoglycan-synthesizing cell elongation complexes (270, 336). However, in several organisms including *E. coli*, MreB has also been shown to be involved in cell division, interacting directly with the tubulin-like protein FtsZ (269, 270). Although MreB-like proteins are recognized as central players in both cell growth and cell shape maintenance, relatively little is known about how cells regulate MreB activity.

In a prior study we identified two previously uncharacterized gene products YodL and YisK, that appear to target MreB and Mbl activity in *Bacillus subtilis* (Appenidix I)(256). Misexpression of YodL or YisK prevents colony formation on

plates and leads to a cell-widening phenotype (Fig A1.1) that is suppressed by specific point mutations in *mreB* and *mbl* respectively (Table A1.6). Moreover, we showed using conditionally permissive deletion strains that to elicit cell-widening effects, YodL specifically requires MreB while YisK requires Mbl (Fig A1.2). The purpose of this study was to investigate the effects of YodL and YisK overexpression in an unrelated Gram negative organism, *E. coli*. Expression of YisK in *E. coli* did not affect overall cell shape. Since current data suggest YisK affects some aspect of Mbl function (Appendix I)(256) and *E. coli* does not encode *mbl*, this result was expected. In contrast, expression of YodL in *E. coli* did not result in cell widening as it does in *B. subtilis*. Instead, cells filamented, consistent with an inhibition of cell division. To identify possible functional targets associated with YodL activity in *E. coli*, suppressor selections were performed, and several mutants resistant to YodL expression were obtained. One of these mutants possessed a T376A substitution in *E. coli* FtsZ, suggesting that in *E. coli* YodL perturbs some aspect of FtsZ function.

Materials and Methods

General methods.

E. coli strains utilized in the study are listed in Table A2.1. Plasmids are listed in Table A2.2. Oligonucleotide primers are listed in Table A2.3. *Escherichia coli* DH5α was used for cloning. The expression studies and suppressor selection analysis were performed with *E. coli* MG1655 (DE3). All *E. coli* strains were grown in LB-Lennox medium supplemented with 100 µg/ml ampicillin and/or 25 µg/ml kanamycin.

Table A2.1. Strains used in Appendix II.

Strain	Description	Reference
Parental		
E. coli DH5α	*F- endA1 glnV44 thi-1 recA1 relA1 gyrA96 deoR nupG Φ80dlacZΔM15 Δ(lacZYA-argF)U169, hsdR17(r_K^- m_K^+), λ–*	
E. coli MG1655	K-12 F– λ– *ilvG– rfb-50 rph-1*	
E. coli MG1655 (DE3)	K-12 F– λ– *ilvG– rfb-50 rph-1 endA recA* λ(DE3 [*lacI lacUV5-T7p07 ind1 sam7 nin5*])	Addgene (337)
***E. coli* MG1655**		
CYD642	*yisK-pBAD24 (amp)*	This study
CYD643	*yodL-pBAD24 (amp)*	This study
***E. coli* MG1655 (DE3)**		
CYD694	*yodL-pBAD24 (amp), yodL-pET24b+ (kan)*	This study

Table A2.2. Plasmids used in Appendix II.

Plasmid	**Description**	**Reference**
pYD093	*yodL-pBAD24 (amp)*	This study
pYD095	*yodL-pET24b+ (kan)*	This study
pYD187	*yisK-pBAD24 (amp)*	This study

Table A2.3. Oligonucleotides used in Appendix II.

Oligo	**Sequence 5' to 3'**
OAS029	GTCAATGTCGACTGTCGTTTGTACA
OYD209	GCATGAATTCTTATGTCGTTTGTACAATCAGACG
OYD332	GATCGAATTCACCATGAAATTTGCGACAGGGGAAC
OYD333	GATCCTGCAGTCAGCCAATTTGGTTTGACAGC
OYD334	GATCGAATTCACCATGATGTTATCCGTGTTTAAAAAG
OYD335	GATCCTGCAGTTATGTCGTTTGTACAATCAGAC
OYD355	CTTACGCGGTTGCAAACAGG
OYD356	GGCGGTATCCATATAAGTACG
OYD357	ATTCGACGGCGGTGGGATTG
OYD358	AGGGCGTAACGTCAGGGTGA
OYD371	GAATGCTGCTGATGCATTAAG
OYD372	ATTTCACGGACTTCATCGCC
OYD385	AAAGATTTGGGTATCCTGACC
OYD386	CCGTGATGTTAACCAGCACG

Plate growth assay

E. coli strains harboring relevant plasmids were streaked on LB-Lennox agar plates supplemented with 100 µg/ml ampicillin and/or 25 µg/ml kanamycin. When indicated, inducer was added at the following concentrations: 1mM IPTG and/or 0.2% arabinose (w/v). Plates were incubated at 37°C overnight and images were captured on a ScanJet G4050 flatbed scanner (Hewlett Packard).

Microscopy

1 ng of pYD093 (*yodL-pBAD24*) or pYD187 (*yisK-pBAD24)* was transformed into *E. coli* MG1655 cells and plated on LB-Lennox agar (1.5% w/v) plates containing 100 µg/ml ampicillin. For microscopy experiments, all strains were inoculated in 25 ml LB-Lennox medium with 100 µg/ml ampicillin in 250 ml baffled flasks and placed in a shaking waterbath set at.37°C and 280 rpm. At low OD_{600} (~0.08), 0.2% arabinose was added to the induced cultures. Images were captured 90 min post-induction. 1 ml culture was pelleted by centrifugation at 6,010 x g for 1 minute at room temperature, then pellets were resuspended in ~5 µl TMA-DPH (0.02 mM) before mounting on glass slides with polylysine-treated coverslips. Images were taken with 1 sec exposure time using a Nikon Ti-E microscope equipped with a CFI Plan Apo lambda DM 100X objective, Prior Scientific Lumen 200 Illumination system, C-FL UV-2E/C DAPI and C-FL GFP HC HISN Zero Shift filter cubes, and a CoolSNAP HQ2 monochrome camera.

Suppressor selections

To reduce the chances of obtaining suppressors arising as the result of changes in *yodL* expression, two different compatible plasmids with different induction systems were utilized. Single colonies of *E. coli* harboring the IPTG-inducible plasmid P_{T7}-*yodL* and the arabinose inducible plasmid P_{BAD}-*yodL* (CYD694) were used to inoculate six independent 5 ml LB-Lennox cultures with 100 µg/ml ampicillin and 25 µg/ml kanamycin. Cultures were grown for eight hrs at 37°C and 0.3 µl of each culture was diluted in 100 µl LB. The entire dilution was plated on an LB-Lennox agar plate supplemented with 100 µg/ml ampicillin, 25 µg/ml kanamycin and 1 mM IPTG. After overnight growth, suppressors that arose were patched on all four plates mentioned below at once: (1) LB-Lennox agar plates supplemented with 100 µg/ml ampicillin and 25 µg/ml kanamycin; (2) LB-Lennox agar plates supplemented with 100 µg/ml ampicillin, 25 µg/ml kanamycin and 1 mM IPTG; (3) LB-Lennox agar plates supplemented with 100 µg/ml ampicillin, 25 µg/ml kanamycin and 0.2% arabinose; (4) LB-Lennox agar plates supplemented with 100 µg/ml ampicillin, 25 µg/ml kanamycin, 1 mM IPTG and 0.2% arabinose. The ones did not grow by patching on IPTG plates were excluded as false positives from the initial selection. Mutants unable to grow in the presence of the arabinose were eliminated to reduce the chances of obtaining mutations specifically associated with the P_{T7}-*yodL* plasmid (eg. *yodL* truncations). By patching variants on plates with both inducers, candidates would fall into different classes because increasing amount of YodL could make some of them sicker than others, although in this round, all the candidates grew well on double-inducer plates. Genomic DNA was then extracted from each candidate (see Appendix I) and used as template to PCR amplify *E. coli mreB* (primer pair OYD355 and OYD356) and *ftsZ* (primer pair OYD357 and

OYD358). The PCR products were then used to as template to Sanger sequence the *mreB* and *ftsZ* regions from each of the suppressor. *mreB* was sequenced using OYD371 and OYD372, while *ftsZ* was sequenced using OYD385 and OYD386.

Results

Overexpression YodL, but not YisK, in *E. coli* prevents colony formation on plates

In *B. subtilis*, misexpression of YodL or YisK prevented colony formation on plates and produced irregularly shaped cells in liquid culture through targeting (directly or indirectly) of MreB and Mbl, respectively (Appendix I, Table A1.6, Fig A1.1, Fig A1.12)(256). Since MreB is a highly conserved protein, we hypothesized that YodL's mechanism of action might be conserved in a heterologous system, specifically in *E. coli*. To test this idea, we expressed *yodL* on a plasmid from an inducible promoter in *E. coli* MG1655. Cells growing in the presence of inducer were unable to form colonies on plates (Fig A2.1), similar to observations with *B. subtilis*. We hypothesized that since *E. coli* does not encode *mbl*, YisK would not affect *E. coli* growth. Consistent with our hypothesis, YisK expression had no observable effect on *E. coli* cell growth (Fig A2.1).

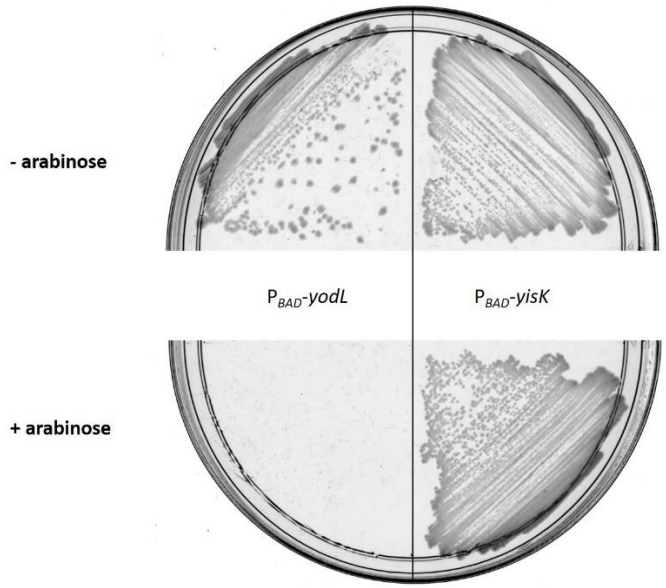

Fig. A2.1. Overexpression YodL, but not YisK, in *E. coli* prevents colony formation on plates. P$_{BAD}$-*yodL* (CYD643) and P$_{BAD}$-*yisK* (CYD642) were streaked on LB-Lennox plates supplemented with 100 µg/ml ampicillin and incubated at 37°C overnight. When indicated, 0.2% arabinose was added onto the plate to induce protein expression.

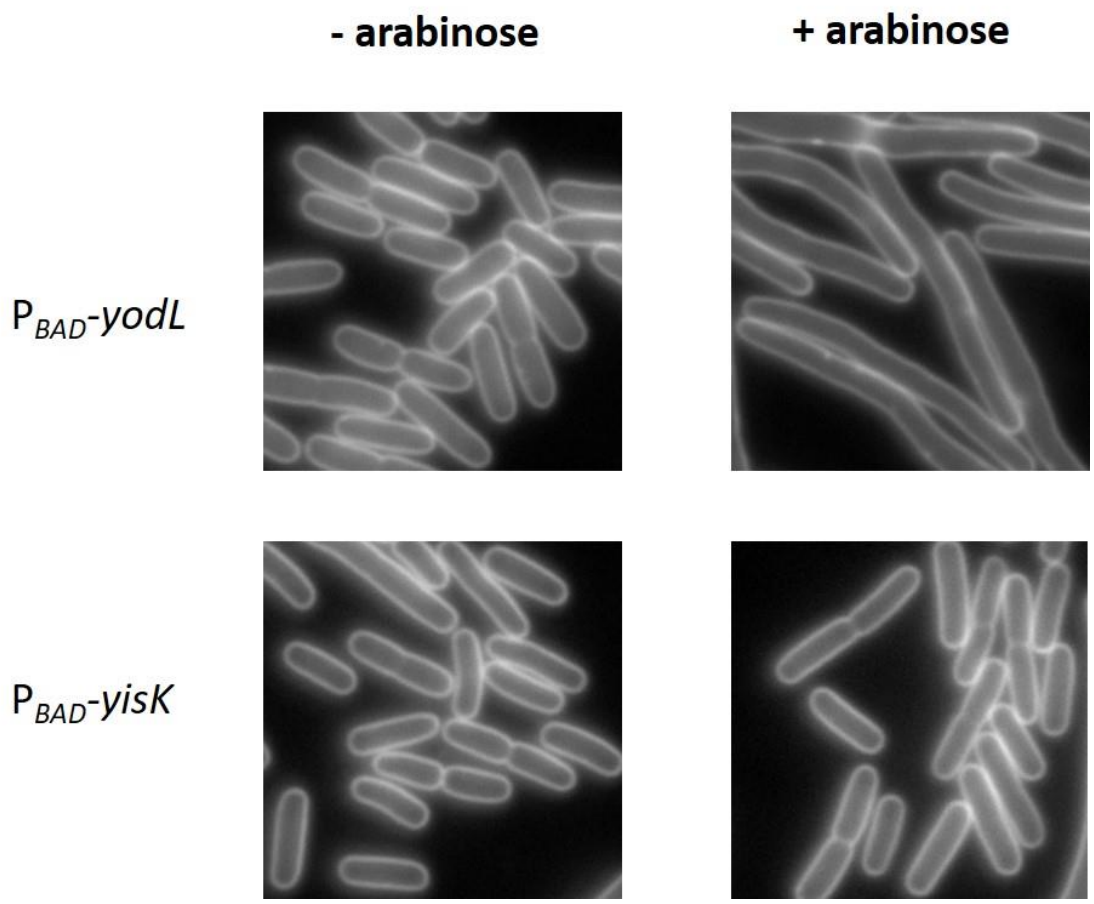

Fig. A2.2. YodL inhibits *E. coli* cell division. P$_{BAD}$-*yodL* (CYD643) and P$_{BAD}$-*yisK* (CYD642) were grown in LB-Lennox media at 37°C to mid-exponential and back-diluted to an OD_{600} of ~0.08. When indicated, 0.2% arabinose was added to induce protein expression. Cells were grown for 1.5 hrs at 37°C before image capture. Membranes were stained with TMA-DPH. All images were scaled identically.

YodL inhibits *E. coli* cell division

To further characterize the effect of YodL on *E. coli* growth, epi-fluorescence microscopy was performed on *E. coli* cultures before and after YodL induction. Unexpectedly expression of YodL in *E. coli* resulted in cell filamentation (Fig A2.2) rather than the cell-widening that was observed in *B. subtilis* (Fig A1.1B). In contrast, YisK expression had no obvious effect on *E. coli* morphology (Fig A2.2), consistent with the lack of phenotype observed on plates (Fig A2.1).

FtsZ is the genetic target of YodL in *E. coli*

Overexpression of YodL in *E. coli* results in filamentous cells. To better understand the mechanism behind this phenotype, we took advantage of the fact that overexpression YodL prevents colony formation on plates (Fig A2.1) and performed suppressor selection analysis. Two YodL overexpression plasmids with different promoters (one IPTG-inducible and one arabinose-inducible) and different antibiotic resistance cassettes were transformed into *E. coli*. Cells were plated in the presence of single inducer (IPTG) and both antibiotics, and patched onto LB plates supplemented with antibiotics and each of the following: no inducer, IPTG (the original selective pressure), arabinose (the alternate inducer), and IPTG plus arabinose. This step allowed us to eliminate suppressors that grew due to an inability to express functional YodL in the presence of IPTG because they were unable to take up inducer or derepress the promoter, as well as those producing non-functional forms of YodL. After patching, 12 suppressor strains were identified that were resistant following selection in the presence of arabinose or arabinose and IPTG. In *B. subtilis*, mutations in *mreB* confer resistance

to YodL (Appendix I, Table A1.6, Fig A1.12)(256), so we sequenced the *mreB* locus in each YodL-resistant suppressor strain. In addition, since the cells filamented and a prior relationship between MreB and FtsZ activity has been observed (269, 270), we also sequenced *ftsZ*. Eleven of the twelve YodL-resistant strains encoded wild-type versions of both *mreB* and *ftsZ*, indicating that the resistance was associated with a mutation elsewhere in the genome. One YodL-resistant suppressor encoded a substitution in the FtsZ, T376A. *E. coli* FtsZ has 383 residues, and T376 is located in the flexible C-terminal tail (338), a region of FtsZ previously shown to be important for septum localization (339), regulation of Z-ring assembly (340, 341), and interaction of FtsZ with other cell division proteins such including FtsA (342), ZipA (343) and MinC (344).

Discussion

Overexpression of YodL in *E. coli* prevents colony formation on plates (Fig A2.1), suggesting that YodL is somehow toxic to *E. coli* cells. Consistent with this observation, prior attempts to overexpress and purify YodL from *E. coli* have been problematic due to very low expression levels (data not shown). The toxicity is unlikely to be attributable to the protein overexpression itself since the protein could be overexpressed successfully in a strain background harboring $FtsZ_{T376A}$.

Using epi-fluorescence microscopy, it was observed that YodL expression results in filamentation (Fig A2.2), suggesting that in *E. coli*, YodL perturbs some aspect of cell division. Consistent with this hypothesis, the $FtsZ_{T376A}$ variant is resistant to YodL. FtsZ polymerizes at the incipient cell division site (345), and recruits additional factors required for cell division (346). Our results suggest that in *E. coli*, YodL activity is disrupting FtsZ activity. In contrast, in *B. subtilis*, YodL expression results in cell-widening through

disruption of MreB activity, but does not affect cell division (Appendix I, Fig A1.1, Fig A1.12)(256).

We propose that the distinctive phenotypes observed in *E. coli* and *B. subtilis* can be attributed to differences in the way MreB functions in these two organisms. In *E. coli*, MreB-FtsZ interaction is important for cell division (269, 270) and expression of a non-interacting variant, $MreB_{D285A}$ inhibits cell division by locking FtsZ rings into a non-constrictive state (269). This phenotype can be overcome by specific substitutions in FtsZ (269). Intriguingly, most of the YodL resistant suppressors identified in *B. subtilis* map to a region of MreB that interacts directly with RodZ (279). RodZ is broadly conserved in bacteria with MreB, and has been shown to regulate MreB's dynamic behavior (288). Based on these observations, it was hypothesized that in *B. subtilis*, YodL leads to cell widening by changing the interaction between RodZ and MreB (256). Interestingly, the region of MreB possessing substitutions resistant to YodL function is the same region of MreB shown to interact directly with FtsZ in *E. coli* (Appendix I, Table A1.6, Fig A1.9)(256, 269). Based on these data, we propose that in *E. coli*, YodL binds MreB and prevents MreB interaction with FtsZ. This possibility could be investigated by determining if YodL expression in *E. coli* leads to disruption or "locking" of FtsZ rings as was observed following expression of $MreB_{D285A}$ (269). Another prediction of this model is that *ftsZ* alleles that allow bypass of $MreB_{D285A}$ (269) would also make cells more resistant to YodL.

So far we have isolated one *E. coli* suppressor resistant to the effects of YodL, $FtsZ_{T376A}$, located in a region important for ClpXP-dependent degradation of FtsZ protein (347, 348). Thus it is possible that $FtsZ_{T376A}$ overcomes the killing effects of YodL activity by increasing overall FtsZ levels. Determining the nature of the mutations in the other 11

E. coli YodL-resistant suppressors should provide additional clues regarding how YodL functions.

APPENDIX III

INVESTIGATION OF THE ROLES OF YodL AND YisK DURING *Bacillus subtilis* SPORULATION

Introduction

The actin-like protein MreB is critical to bacterial peptidoglycan (PG) synthesis during cell elongation (269, 270). *Bacillus subtilis* possesses three genes encoding MreB-like proteins: *mreB*, *mbl*, and *mreBH* (290, 293). All three genes are essential during vegetative growth, although they exhibit different patterns of transcription (291, 293). Peak expression of *mreB* and *mbl* occurs during transition state that occurs at the end of exponential phase (295). In contrast, *mreBH* is maximally induced during cell stress by the alternative sigma factor SigI (296). To our knowledge, the roles of MreB, Mbl, and MreBH during *B. subtilis* sporulation have not been investigated.

We recently identified two proteins, YodL and YisK, that affect aspects of MreB and Mbl activity, respectively (Appendix I)(256). Both genes are induced in Spo0A-dependent manner during the early phases of sporulation. *yodL* exhibits peak expression at ~2 hrs after entry into sporulation, whereas peak *yisK* expression is earlier (Appendix I, Fig A1.6)(256), consistent with its prior characterization as a member of the SigH stationary phase regulon (32). *yisK* and *yodL* knockout strains exhibit minor reductions in laboratory sporulation efficiency; a double knockout strain possesses an ~20% reduction in production of heat-resistant spores (Appendix I, Table A1.4)(256). Based on these data, it was hypothesized that YodL and YisK likely function to modify some aspect of MreB and Mbl function during sporulation.

In this study, we found that overexpression of YodL, which we previously hypothesized perturbs the interaction between MreB and RodZ (See Appendix II)(256), has no obvious effect on cell shape during sporulation. In contrast, overexpression of YisK during sporulation results in production of round cells. During vegetative growth, YisK requires Mbl to produce its cell-widening effects (Appendix I, Fig A1.12)(256), therefore we hypothesized that YisK affects Mbl function during sporulation as well. Surprisingly, strains lacking Mbl appeared relatively normal during sporulation, while strains lacking MreB were round, more similar to the YisK misexpression phenotype. Although YisK requires a functioning Mbl to elicit cell-widening during vegetative growth, in the context of sporulation, Mbl does not appear to play an essential role in cell-shape control. These data provide the first evidence that YisK's activity may also affect some aspect of MreB function (directly or indirectly). The specific activities of YodL and YisK during sporulation remain unknown. To better understand how YodL and YisK function, a screen was developed to identify additional factors that act redundantly with YodL and YisK to support sporulation.

Materials and Methods

General methods.

All *B. subtilis* strains were derived from *B. subtilis* 168. *B. subtilis* strains utilized in this study are listed in Table A3.1. Plasmids are listed in Table A3.2. Oligonucleotide primers are listed in Table A3.3. The following concentrations of antibiotics were used for generating *B. subtilis* strains: 100 µg/ml spectinomycin, 7.5 µg/ml chloramphenicol, 0.8 mg/ml phleomycin, 10 µg/ml tetracycline, 10 µg/ml kanamycin. To select for

erythromycin resistance, plates were supplemented with 1 µg/ml erythromycin (erm) and 25 µg/ml lincomycin. *B. subtilis* transformations were carried out as described previously (302).

Microscopy

All samples were grown in CH media overnight at room temperature to mid-exponential, back-diluted to OD_{600} = 0.05 in 25 ml CH (237) in 250 ml baffled flasks, and grown at 37°C in a shaking waterbath set at 280 rpm for 1.5 hrs. Sporulation was induced by resuspension at 37°C according to the Sterlini-Mandelstam method (237). When indicated, 1 mM IPTG was added together with resuspension. 10mM $MgCl_2$ was added into all the media when indicated. All the samples were imaged 24 hrs post-induction and exposed. 1 ml culture was centrifuged at 6,010 x g for 1 minute at room temperature. The pellets were then resuspended with 5 µl TMA-DPH (0.02 mM). Cells were mounted on glass slides with polylysine-treated coverslips prior to imaging. The phase images were exposed for 0.2 sec, whereas for the membrane stain, the exposure time is 1 sec.

Table A3.1. Strains used in Appendix III.

Strain	Description	Reference
Parental		
B. subtilis 168	*Bacillus subtilis* laboratory strain 168 *trpC2*	BGSC (1A866)
E. coli DH5α	*F- endA1 glnV44 thi-1 recA1 relA1 gyrA96 deoR nupG Φ80dlacZΔM15 Δ(lacZYA-argF)U169, hsdR17(r_K^- m_K^+), λ–*	
E. coli TG1	*glnV44 thi-1* Δ*(lac-proAB)* Δ*(mcrB-hsdSM)5,* ($r_K^-m_K^-$) F′ [*traD36 proAB+ lacIq lacZΔM15*]	
***B. subtilis* 168**		
CYD642	*yisK-pBAD24 (amp)*	This study
CYD643	*yodL-pBAD24 (amp)*	This study
BAS146	*ponA::erm, kanΩΔmreB*	This study
BAS147	*ponA::erm, kanΩΔmbl*	This study
BAS191	*amyE::*P_{hy}*-yodL (spec), yhdG::*P_{hy}*-yodL (phleo),*	(256)
BAS271	*kanΩrpsU*$_{K34stop}$*, amyE::*P_{hy}*-yodL (spec)*	This study
BAS272	*kanΩrpsU*$_{K34stop}$*, amyE::*P_{hy}*-yodL (spec), yhdG::*P_{hy}*-yodL (phleo)*	This study
BAS273	*kanΩrpsU*$_{K34stop}$*, amyE::*P_{hy}*-yodL (spec), yhdG::*P_{hy}*-yodL (phleo), yycR::*P_{hy}*-yodL (cat)*	This study
BAS274	*kanΩrpsU*$_{K34stop}$*, amyE::*P_{hy}*-yisK (spec)*	This study
BAS275	*kanΩrpsU*$_{K34stop}$*, amyE::*P_{hy}*-yisK (spec), yhdG::*P_{hy}*-yisK (phleo)*	This study
BAS276	*kanΩrpsU*$_{K34stop}$*, amyE::*P_{hy}*-yisK (spec), yhdG::*P_{hy}*-yisK (phleo), yycR::*P_{hy}*-yisK (cat)*	This study
BYD074	*amyE::*P_{hy}*-yisK (spec), yhdG::*P_{hy}*-yisK (phleo)*	(256)
BYD099	*yvbJ::*P_{cotD}*-lacZ (cat)*	This study
BYD172	*ponA::erm*	This study
BYD258	*ponA::erm, kanΩΔmbl, amyE::*P_{hy}*-yisK (spec), yhdG::*P_{hy}*-yisK (phleo)*	(256)
BYD281	*amyE::*P_{hy}*-yisK (spec), ycgO::*P_{hy}*-yisK (tet), yhdG::*P_{hy}*-yodL (phleo), yycR::*P_{hy}*-yodL (cat)*	(256)
BYD359	*ΔyodL, ΔyisK, yvbJ::*P_{cotD}*-lacZ (cat)*	This study
BYD376	*kanΩrpsU*$_{Tn}$*, amyE::*P_{hy}*-yisK (spec)*	This study
BYD379	*kanΩrpsU*$_{Tn}$*, amyE::*P_{hy}*-yisK (spec), yhdG::*P_{hy}*-yisK (phleo)*	This study
BYD382	*kanΩrpsU*$_{Tn}$*, amyE::*P_{hy}*-yisK (spec), yhdG::*P_{hy}*-yisK (phleo), yycR::*P_{hy}*-yisK (cat)*	This study
BYD384	*kanΩrpsU*$_{Tn}$*, amyE::*P_{hy}*-yodL (spec)*	This study

Table A3.1. Continued.

Strain	Description	Reference
BYD386	*kanΩrpsU$_{Tn}$, amyE::P$_{hy}$-yodL (spec), yhdG::P$_{hy}$-yodL (phleo)*	This study
BYD388	*kanΩrpsU$_{Tn}$, amyE::P$_{hy}$-yodL (spec), yhdG::P$_{hy}$-yodL (phleo), yycR::P$_{hy}$-yodL (cat)*	This study

Table A3.2. Plasmids used in Appendix III.

Plasmid	**Description**	**Reference**
pMarA	*TnYLB-1 (kan), mariner-Himar1 (erm) (amp)*	(349)

Table A3.3. Oligonucleotides used in Appendix III.

Oligo	**Sequence 5' to 3'**
OAS200	TTTCTTCAATCGAAGCCAGCC
OAS201	CCTATCACCTCAAATGGTTCGCTGGGATCCTCTCTTTCCCTCCC TCCGAAT
OAS202	GTCCCGAGCGCCTACGAGGAATTTGTCGACGAGCAGTAAAGC TAATCAGAATT
OAS203	AAGAAAAATCTCAAGCAGAATGAG

Heat kills

The formation of heat-resistant spores was quantified by growing cells in CH medium and performing sporulation by resuspension as described above (237). After 24 hrs, samples were collected and the number of both total viable cells and heat-resistant units were enumerated. To determine colony forming units/ml, an aliquot of each culture was serially diluted and plated on Difco sporulation medium (DSM)(304) agar plates. To enumerate heat resistant spores/ml, the serial diluted cultures were subjected to a 20 min heat treatment at 80°C and plated on DSM agar plates. The plates were incubated at 37°C overnight and the next day colony counts were determined. The relative sporulation frequency compared to wild-type was determined by calculating the spores/CFU of each experimental and dividing it by the spores/CFU of wild-type. The reported statistical significance was determined using an unpaired student's t-test.

Making the Spo+ transposon library

To induce mariner-based transposon mutagenesis, 500 ng of pMarA plasmid (encoding a mariner transposase and the mariner transposon on a temperature sensitive vector) was transformed into *B. subtilis* 168 strain, selected on an LB-Lennox plate containing 10 µg/ml kanamycin, and incubated overnight at room temperature. The next day, a single colony was used to inoculate 2 ml LB-Lennox medium supplemented with 10 µg/ml kanamycin. The culture was grown overnight at room temperature and 200 µl was used to inoculate 1.8 ml fresh LB-Lennox medium supplemented with 10 µg/ml kanamycin. After 6 hrs growth at room temperature, cells were pelleted by centrifugation at 6,010 x g for 1 min at room temperature, and resuspended in 25 mL

DSM liquid medium supplemented with 10 µg/ml kanamycin. Cells were grown for additional 36 hrs at 42°C to induce sporulation and loss of the plasmid harboring the transposase. The culture was subjected to a 20 min heat treatment at 80°C to kill cells that failed to sporulate. 5.5 ml of heat-treated culture was mixed with 3.5 ml 50% glycerol, and distributed into 100 µl aliquots before freezing at -80°C. It was determined that ~22,000 colonies would be sufficient to generate a sporulation proficient mariner transposon genomic library with greater than 99% coverage using the following formula:

$$N = \frac{\ln(1-P)}{\ln(1-f)}$$

N= number of mutants needed

P = coverage (0.99 = 99%)

f = average gene size (890 bp)/genome size (4,214,810 bp)(350).

To obtain genomic DNA from 22,000 independent transposon mutants, three 100 µl aliquots of library were thawed on ice and 900 µl LB-Lennox medium was then added into each tube and mixed. 100 µl of the resuspended cells were plated on each of 30 LB-Lennox agar plates containing 10 µg/ml kanamycin, then incubated overnight at 37°C. Plating yielded ~30,000 colonies (~1,000 colonies/plate). Each plate was flooded with 2 ml LB-Lennox media, crudely resuspended with a sterilized inoculating loop, and transferred to six independent test tubes, each containing ~5 ml of the resuspension culture. The cultures were then grown in a roller drum at 37°C for 2 hrs. For unknown reasons, this growth step was important to obtain good yields of genomic DNA (see below). After 2 hrs, the cultures were split into two 50 ml Falcon tubes and the cells were pelleted at 2,576 x g for 10 min at room temperature. The supernatants were discarded and each pellet was then resuspended into 20 ml lysis buffer [20 mM Tris-HCl pH 7.5, 50 mM EDTA pH 8, 100 mM NaCl, and 2 mg/ml lysozyme] and combined. The

suspension was aliquoted into 1.7 ml centrifuge tubes (550 µl/tube) and placed in a 37°C waterbath for 30 minutes to lyse the cells. Due to the high cell density, this initial lysis step was not sufficient to lyse all the cells, thus a second round lysis was performed. 50 µl lysed culture (after the initial lysis) was added into 500 µl lysis buffer and incubated at 37°C for 30 min. Genomic DNA was then extracted (See Appendix I for more details on genomic DNA purification). The aliquots of genomic DNA were frozen at -80°C until use. For unknown reasons, the genomic DNA prepared from the pooled mariner library routinely resulted in ~10-fold fewer colonies following transformation into competent *B. subtilis* than genomic DNA prepared from a strain harboring a single transposon insertion.

Redundant factor screen

To introduce the library of *mariner* transposon insertions, 200 ng of genomic DNA was used to transform a strain harboring Δ*yodL* Δ*yisK* as well as a reporter of a late stage in sporulation, P_{cotD}-*lacZ* (BYD359). Transformations were plated on DSM agar plates supplemented with 10 µg/ml kanamycin to select for the transposon and 40 µg/ml 5-bromo-4-chloro-3-indolyl-β-D-galactopyranoside (X-Gal), to detect production of beta-galactosidase. Cells that were able to reach the late stage of sporulation expressed *lacZ* and were able to cleave the X-gal substrate, producing blue colonies. The plates were incubated at 37°C for 36 hrs and then at room temperature for another 36 hrs. Cells that produced white or light blue colonies (compared to the non-mutagenized BYD359 control) were considered delayed or reduced in sporulation and streaked for isolation; each strain was labeled as RFL (Redundant Factors of YodL and YisK). Genomic DNA was then extracted from each candidate. This genomic DNA was used to

transform a clean genetic background of BYD359 by selecting on LB-Lennox plates supplemented with 10 μg/ml kanamycin. The new strains were labelled as RFL_K.

To determine if the reduced sporulation could be attributed to the transposon as opposed to an unlinked mutation in the original isolate, individual colonies from the original RFL isolate and its corresponding RFL_K counterpart were used to inoculate 3 ml LB-Lennox medium, and the cells were grown to exponential phase (OD_{600} between 0.3 and 0.7). Samples were normalized by OD_{600} and five μl of each culture was spotted on a DSM agar plate supplemented with 40 μg/ml X-Gal. Plates were incubated at 30°C for 20 hrs. For each pair, the color of RFL and its corresponding RFL_K were compared. If the colors were consistent (both light blue or both white compared to the BYD359 control), then the genomic DNA from the RFL genomic was used to transform BYD99 (P_{cotD}-*lacZ*) to determine if the transposon itself was responsible for the observed sporulation defect, or if the delay required both Δ*yodL* Δ*yisK* and the *mariner* insertion. These new strains were labelled as RFL_C. Using the spot test described above, each RFL_K and its corresponding RFL_C strain were then compared. Only RFL_K strains that appeared white or light blue compared to the BYD359 control, and also had a corresponding blue RFL_C strain were selected for further analysis.

Inverse PCR

To determine the location of the *mariner* insertion associated with reduced sporulation in the Δ*yodL/*Δ*yisK* background, inverse PCR was performed. 1 μg of genomic DNA isolated from the RFL strain was digested with Sau3AI (New England BioLabs) for 60 min at 37°C. The enzyme was inactivated by heating to 65°C for 30 min. To circularize the genomic DNA fragments, 200 units of T4 DNA ligase were

added to 200 ng of the digested DNA, and the reaction was placed at room temperature for 60 min. 100 ng of the ligated DNA was then used in a 31-cycle PCR reaction (98°C for 10 sec, 56°C for 30 sec, 72°C for 2 min) using 0.4 μM OJH232 and OJH233 as the primers. The cleaned PCR product was then Sanger sequenced using primer OJH233. The locations of the transposon insertions were determined by Blast of the BsubCyc database.

Plate growth assay

B. subtilis strains were streaked on LB-Lennox plates supplemented with 100 μg/ml spectinomycin (for uninduced samples), or 100 μg/ml spectinomycin and 1 mM IPTG (for induced samples). Plates were incubated at 37°C overnight and images were captured on a ScanJet G4050 flatbed scanner (Hewlett Packard).

Results

Overexpression of YisK, but not YodL, during *B. subtilis* sporulation produced round-shaped cells

Knocking-out *yodL* and *yisK* did not result in an obvious morphological phenotype during sporulation (Appendix I, Fig A1.8)(256). We also tested if overexpression of either *yodL* or *yisK* during sporulation would affect cell or spore morphology. Cells harboring either the P_{hy}-*yodL* or P_{hy}-*yisK* misexpression constructs were sporulated by resuspension. Inducer was added at the time of resuspension and the morphology of the cells was monitored over a timecourse using microscopy. Expression

of *yodL* did not result in any obvious changes in morphology compared to wild-type, even after 24 hrs of growth (Fig A3.1). In contrast, expression of *yisK* resulted in cell-widening, which first became evident at 2.5 hrs of resuspension and eventually produced round cells (Fig A3.1). These results suggest that during sporulation, *B. subtilis* morphology is sensitive to the effects of YisK but not YodL.

During sporulation, Δ*mreB*, but not Δ*mbl*, produced round-shaped cells

Cells are sensitive to the effects of YisK overexpression during sporulation, as evidenced by the production of round cells (Fig A3.1). Since YisK is proposed to target Mbl activity and YodL is proposed to target some aspect of MreB function (Appendix I, Table A1.6, Fig A1.12)(256), we hypothesized that the YisK and YodL overexpression phenotypes observed would mimic those of deleting *mbl* and *mreB* respectively. We generated *mbl* and *mreB* deletion strains in a Δ*ponA* background (see Appendix I for details). In this background, deletion of either gene results in minimal effects on cell shape as long as cultures are also supplemented with excess Mg^{2+}.

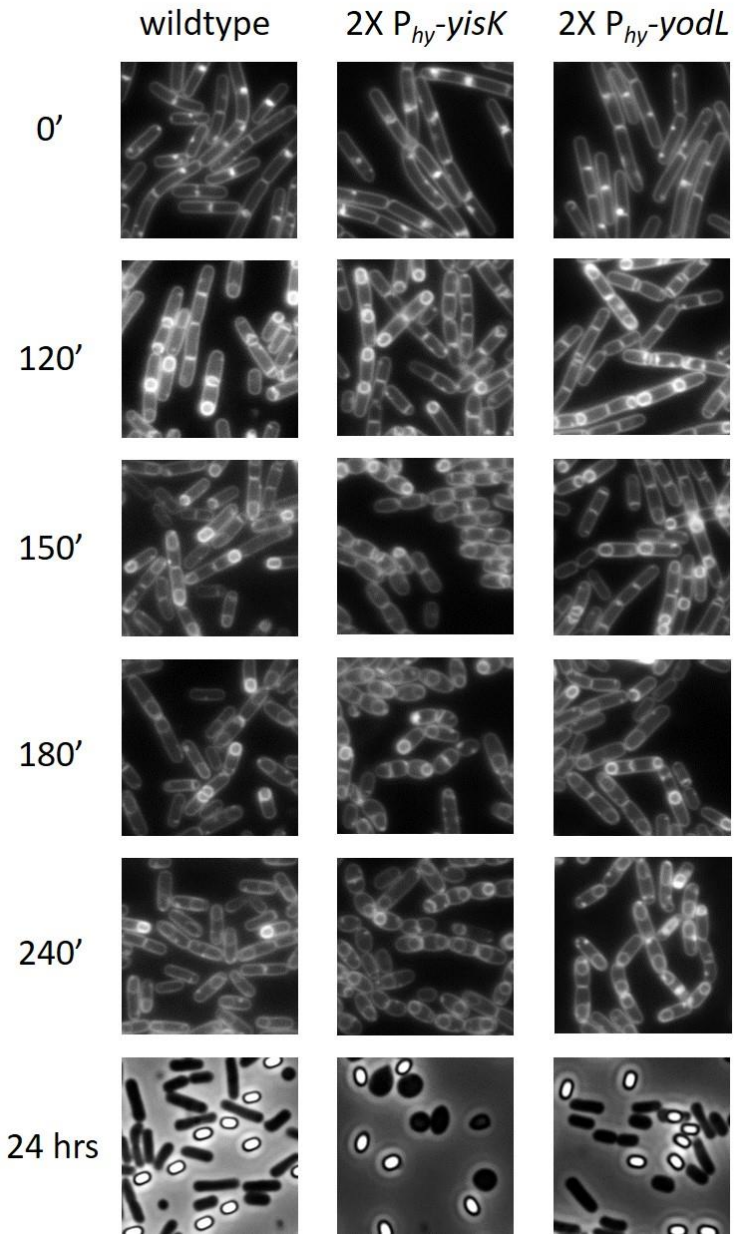

Fig. A3.1. YisK overexpression produces round cells during a *B. subtilis* sporulation timecourse. *B. subtilis* 168 (wildtype), BYD074 (2X P$_{hy}$-*yisK*) and BAS191 (2X P$_{hy}$-*yodL*) were sporulated by resuspension (237). 1 mM IPTG was added at the time of resuspension (T = 0 min) to induce expression of either *yisK* or *yodL*. Cells were grown for the indicated amount of time at 37°C before image capture. Membranes were stained with TMA-DPH. All images are shown at the same magnification.

Cells were grown to mid-exponential phase in the presence of 10 mM $MgCl_2$ and sporulated by resuspension in both regular resuspension media (237), and resusepnsion media supplemented with 10 mM $MgCl_2$. At the time of resuspension both the Δ*mbl* and Δ*mreB* strains appeared similar in overall morphology (Fig A3.2). Unexpectedly, the Δ*mbl* strain possessed no obvious morphological differences compared to the wild-type strain during sporulation (Fig A3.1 – A3.2). In contrast, the Δ*mreB* strain became round (Fig A3.2), similar to the phenotype observed upon YisK induction (Fig A3.1). These results suggest that during sporulation, MreB but not Mbl appears to function in cell shape maintenance. Moreover, these observations are consistent with the idea that YisK may perturb not only Mbl, but also some aspect of MreB activity.

Deleting *mbl* rescues the round-cell phenotype produced by YisK overexpression

In vegetative growth, YisK overexpression results in cell widening (Appendix I, Fig A1.1)(256), and this phenotype specifically depends on Mbl (Appendix I, Fig A1.12), suggesting that either YisK specifically targets Mbl, or that YisK's cell-widening activity depends on the presence of Mbl (256). To test if the cell-widening effects of YisK overexpression during sporulation were also dependent on Mbl, YisK was overexpressed during sporulation in a Δ*mbl* background. Consistent with prior observations during vegetative growth, YisK overexpression required the presence of Mbl to produce its cell-widening activity (Fig A3.3).

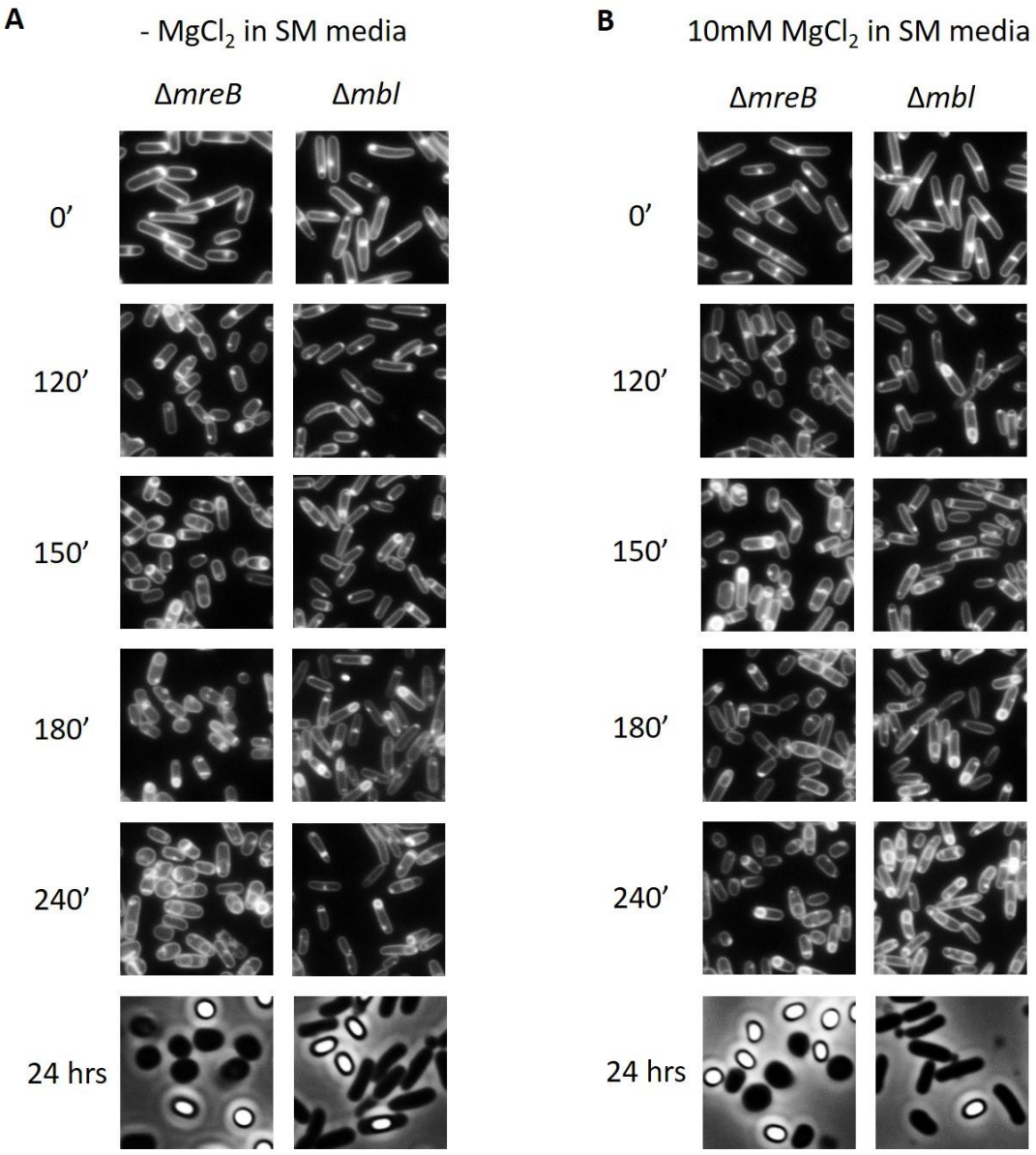

Fig. A3.2. Deletion of *mreB*, but not *mbl*, results in the production of round cells during a sporulation timecourse. BAS146 (Δ*ponA*/Δ*mreB*) and BAS147 (Δ*ponA*/Δ*mbl*) were grown in CH media (237) supplemented with 10 mM $MgCl_2$ at 37°C to mid-exponential phase growth. Sporulation was induced by resuspension at 37°C according to the Sterlini-Mandelstam method (237). When indicated, 10 mM $MgCl_2$ was added into the resuspension media (SM media). Images were captured at the indicated time, where resuspension = 0'. Membranes were stained with TMA-DPH. All images are shown at the magnification.

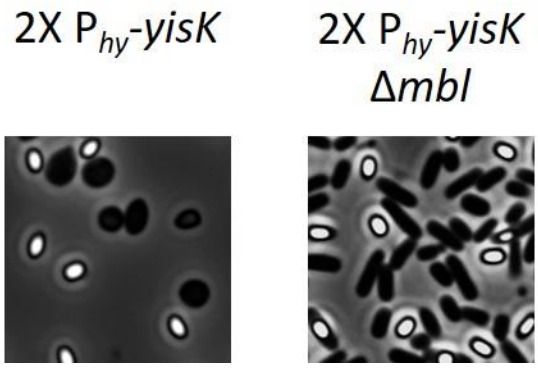

Fig. A3.3. Mbl is required for YisK to induce cell rounding during sporulation. BYD258 (2X P_{hy}-*yisK*, Δ*ponA*/Δ*mbl*) was grown in CH media (237) supplemented with 10 mM $MgCl_2$ at 37°C to mid-exponential phase growth. Sporulation was induced by resuspension at 37°C according to the Sterlini-Mandelstam method (237). 1 mM IPTG was used to induce *yisK* expression at the time of resuspension (T = 0 min). Images were captured 24 hrs after resuspension. All images are shown at the same magnification. The image of the *yisK* overexpression in wild-type background is the same one shown in Fig A3.1, and is repeated here to facilitate comparison.

Overexpression YodL and YisK affect sporulation efficiency

In addition to testing the morphological changes associated with YodL and YisK overexpression during sporulation, we also investigated the effect of overexpression on the production of heat-resistant spores. To determine the number of heat-resistant spores in a sporulation culture, we quantified the number of colony forming units (CFU) present in cultures before (total CFU) and after a heat treatment that kills vegetative cells (heat-resistant CFU). These values were normalized to display the sporulation efficiency of the mutants relative to wildtype. Overexpression of YodL increased the relative sporulation efficiency by ~20% (Table A3.4), whereas overexpression of YisK decreased the efficiency by ~20% (Table A3.4). Overexpression of both YodL and YisK resulted no significant difference in relative sporulation efficiency compared to wild-type cells (Table A3.4). No significant difference in total CFU was observed for any of the overexpression strains compared to wildtype, indicating that the changes in heat-resistant spores produced were not due to changes in germination efficiency or cell viability before heat treatment (Table A3.4)

Table A3.4. Sporulation efficiency following *yodL* and *yisK* overexpression. Sporulation efficiency is the number of spores/ml divided by the total cfu/ml × 100%. Relative sporulation efficiency is sporulation efficiency normalized to wildtype × 100%. The data shown is the average of three independent biological replicates. The difference in sporulation efficiency for wildtype compared to following YodL overexpression or YisK overexpression is statistically significant by an unpaired students t-test($P<0.05$).

Strain	Strain #	Total cfu	Heat-resistant cfu	Sporulation efficiency	Relative sporulation efficiency
wildtype	*B. subtilis* 168	2.9×10^8 ($\pm7.4\times10^7$)	2.2×10^8 ($\pm5.9\times10^7$)	75.6% (±3)	100%
2X P_{hy}-*yodL*	BAS191	2.5×10^8 ($\pm2.9\times10^7$)	2.3×10^8 ($\pm2.4\times10^7$)	92.4% (±6)	122%
2X P_{hy}-*yisK*	BYD74	2.8×10^8 ($\pm3.3\times10^7$)	1.7×10^8 ($\pm4.2\times10^7$)	61.8% (±10)	81%
2X P_{hy}-*yodL* 2X P_{hy}-*yisK*	BYD281	3.2×10^8 ($\pm1.1\times10^8$)	2.3×10^8 ($\pm6.2\times10^7$)	74.7% (±8)	99%

Δ*mreB* and Δ*mbl* had severe defects in sporulation efficiency

Overexpression of YodL slightly increases the relative sporulation efficiency while overexpression of YisK slightly reduces it (Table A3.4). Since current models suggest YodL and YisK inhibit MreB and Mbl activity respectively (Appendix I)(256), we next sought to determine if the conditionally viable Δ*mreB* and Δ*mbl* strains also showed differences in sporulation efficiency. Unexpectedly, the Δ*mbl* strain exhibited no significant difference in sporulation efficiency (97%) compared to wildtype, whereas the Δ*mreB* strain was reduced to ~40% of wildtype (Table A3.5). The total CFU for the Δ*mbl* strain was slightly higher than wildtype (Table A3.5). The reduced sporulation efficiency of the Δ*mreB* strain was largely attributable to a reduction in the ability of the strain to form colonies prior to heat-kill. The number of cells was reduced by approximately half (Table A3.5). This result could be attributed to a reduced ability of the Δ*mreB* strain to germinate or to reduced cell viability. Combined with the observations in the microscopy experiments (Δ*mreB* produced round-shaped cells, whereas there was no difference between wildtype and the Δ*mbl* strain)(Fig A3.2), these results suggest that during sporulation, MreB plays important roles in both cell shape maintenance as well as cell viability and/or the ability of spores to germinate.

It has been shown that magnesium supports both viability and cell shape of *mreB* and *mbl* deletion mutants on non-sporulation medium (291). Therefore, we also tested the effect of $MgCl_2$ supplementation on sporulation efficiency. Unexpectedly, the addition of 10 mM $MgCl_2$ to the sporulation medium reduced sporulation efficiency for both the Δ*mbl* and Δ*mreB* strains, (from 97% to 59%, and 40% to 18%, respectively) (Table A3.5). The total CFU of both strains showed no difference regardless of $MgCl_2$ addition, indicating that the reduction in sporulation efficiency was not due to lower cell

viability (Table A3.5). We have not yet tested the effect of $MgCl_2$ on wild-type sporulation, so it is not currently possible to know if the effect observed is attributable to the $MgCl_2$ itself.

Identification of factors that act redundantly with YodL and/or YisK during sporulation

yodL and *yisK* are expressed during early sporulation (Fig A1.4 - A1.6). However, even a Δ*yodL*/Δ*yisK* strain only reduced sporulation efficiency by ~20% (Table A1.4). We hypothesized that the modest defects might be due to the presence of other factors that act redundantly with YodL and YisK during sporulation. To identify such factors, we designed a genetic screen for *mariner* transposon insertions that, in a Δ*yodL* Δ*yisK* strain background, result in an observable block or delay in sporulation (for details, See Materials and Methods). The candidates identified were called RFLs for Redundant Factors of YodL and YisK.

In a screen of more than 5,000 colonies containing transposon insertions, 92 were perturbed in sporulation. Of these, only 36 retained the sporulation defect when the transposon was introduced into a clean Δ*yodL* Δ*yisK* strain background. Candidates that exhibited sporulation defects when the transposon was introduced into a wild-type background were eliminated, as these sporulation defects did not require the absence of *yodL* and/or *yisK*. The remaining 12 candidates exhibited sporulation defects only when introduced into the Δ*yodL* Δ*yisK* strain and thus were deemed more likely to contribute to sporulation in a redundant manner. The location of the transposon insertions in these mutants were determined using inverse PCR (Table A3.6).

Table A3.5. Sporulation efficiency of *mreB* and *mbl* mutants. Sporulation efficiency is the number of spores/ml divided by the total cfu/ml × 100%. Relative sporulation efficiency is sporulation efficiency normalized to wildtype × 100%. The data shown is the average of three independent biological replicates.

Strain	Strain #	Total cfu	Heat-resistant cfu	Sporulation efficiency	Relative sporulation efficiency
wildtype	*B. subtilis* 168	2.8×10^8 ($\pm7.4\times10^7$)	2.2×10^8 ($\pm5.9\times10^7$)	77.4% (±3)	100%
ΔponA	BYD172	2.8×10^8 ($\pm2.9\times10^7$)	2.1×10^8 ($\pm2.4\times10^7$)	76% (±6)	98%
ΔponA Δmbl - $MgCl_2$	BAS147	3.4×10^8 ($\pm3.3\times10^7$)	2.6×10^8 ($\pm4.2\times10^7$)	74.9% (±10)	97%
ΔponA ΔmreB - $MgCl_2$	BAS146	1.4×10^8 ($\pm3.3\times10^7$)	4.4×10^7 ($\pm4.2\times10^7$)	30.9% (±10)	40%
ΔponA Δmbl 10mM $MgCl_2$	BAS147	3.6×10^8 ($\pm1.1\times10^8$)	1.6×10^8 ($\pm6.2\times10^7$)	44.3% (±8)	59%
ΔponA ΔmreB 10mM $MgCl_2$	BAS146	1.5×10^8 ($\pm3.3\times10^7$)	2×10^7 ($\pm4.2\times10^7$)	13.5% (±10)	18%

Table A3.6. Identification of *mariner* transposon insertion sites that result in a sporulation defect in the Δ*yodL* Δ*yisK* background. The site of transposon was determined using inverse PCR.

Strain (RFL #)	Transposon insertion site
6	after the 23rd bp in ***engD***
20	after the 101th bp in ***veg***
30 & 81	4 bp upstream of ***ssrA***
49, 62 & 89	60 bp upstream of ***rpsU***
59	genes encoding **16S rRNA**
61	90 bp upstream of ***dnaD***
64 & 84	genes encoding **23S rRNA**
90	32 bp upstream of ***pgk***

***rpsU* is associated with resistance to YisK misexpression**

In a selection for spontaneous suppressors resistant to YisK misexpression during vegetative growth, we identified an *rpsU* mutant containing a non-sense mutation that resulted in a K34→stop truncation for ribosomal protein S21 (encoded by *rpsU*)(for details about the suppressor selection, see Appendix I). To test whether this mutant was also resistant to YodL, we generated the mutant in a clean genetic background, and introduced 1X, 2X or 3X copies of P_{hy}-*yodL*. We observed that in the presence of inducer, the *rpsU* mutant was resistant to one copy of P_{hy}-*yodL*, but not to additional copies. In contrast, the *rpsU* was resistant to 1X, 2X and 3X copies of P_{hy}-*yisK* (Fig A3.4)(see below for further discussion).

Since we identified a transposon insertion upstream of *rpsU* in the redundant factor screen, we hypothesized that this mutant might also be resistant to YisK and/or YodL misexpression during vegetative growth. To test this, 1X, 2X and 3X copies of P_{hy}-*yisK* and 1X, 2X and 3X copies of P_{hy}-*yodL* were introduced into a genetic background otherwise harboring only the transposon insertion upstream of *rpsU*. In the presence of inducer, the strain was resistant to one copy of P_{hy}-*yisK*, but not multiple copies (Fig A3.5). In contrast, the transposon did not confer any resistance to YodL (Fig A3.5). These results suggest that the transposon confers specific resistance to YisK.

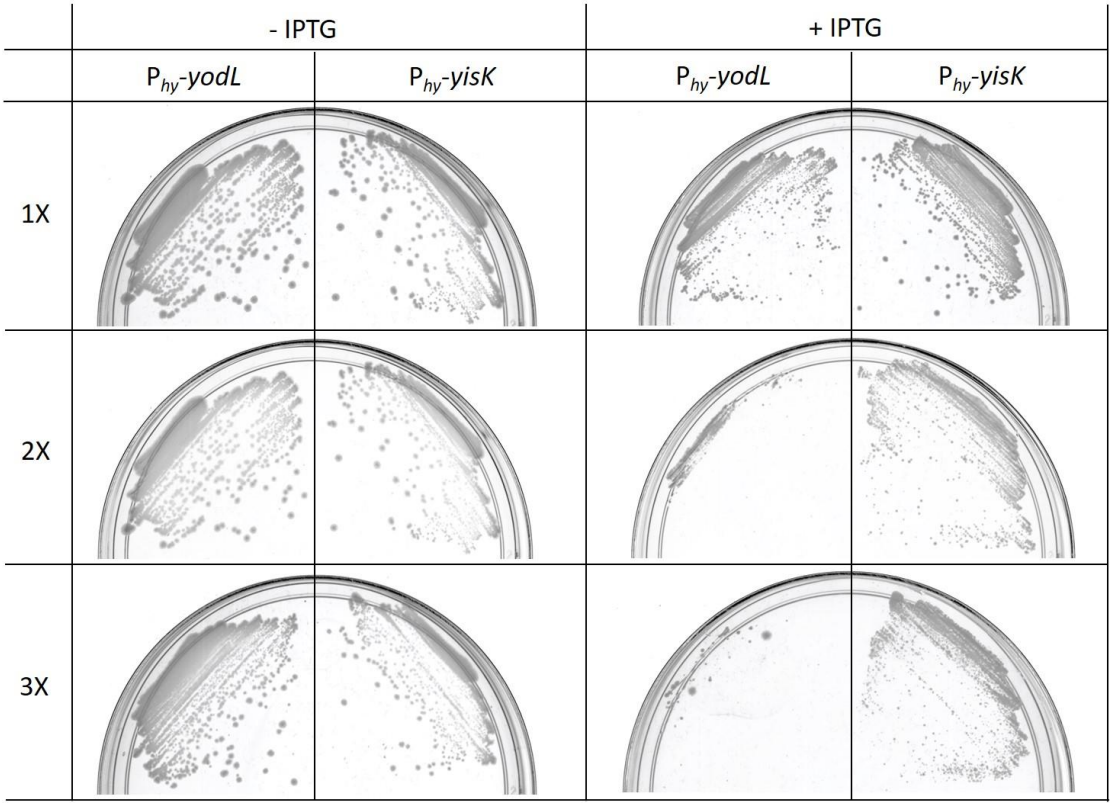

Fig. A3.4. An *rpsU* truncation mutant generating S21$_{K34\rightarrow STOP}$ is resistant to YisK misexpression. 1X, 2X and 3X copies of P$_{hy}$-*yodL* and 1X, 2X and 3X copies of P$_{hy}$-*yisK* were introduced into *rpsU* mutant background (BAS271 – BAS276, repectively). Each strain was streaked on LB-Lennox plates containing 100 µg/ml spectinomycin (left columns), or 100 µg/ml spectinomycin and 1 mM IPTG (right columns).

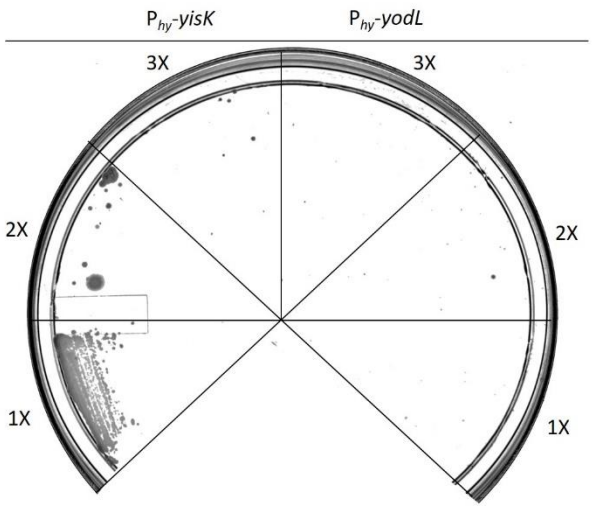

Fig. A3.5. A mutant with a transposon insertion upstream of *rpsU* is resistant to 1X P_{hy}-*yisK* misexpression. 1X, 2X and 3X copies of P_{hy}-*yisK* and 1X, 2X and 3X copies of P_{hy}-*yodL* were introduced into *rpsU* mutant background (BYD376, BYD379, BYD382, BYD384, BYD386, BYD388, repectively). Each strain was streaked on an LB-Lennox plate containing 100 µg/ml spectinomycin and 1 mM IPTG. Plate was incubated at 37°C overnight before image was captured.

Discussion

Overexpression of YisK during sporulation produced round cells (Fig A3.1) and decreased the relative sporulation efficiency by ~20% (Table A3.4), whereas a *yisK* knockout has no obvious morphological defects during sporulation (Fig A1.8). These results suggest that the presence of too much YisK protein is detrimental for sporulating cells. These results are consistent with the idea that *yisK* is expressed during stationary phase and early sporulation, but might actually be repressed by higher levels of Spo0A-P as sporulation proceeds (256). In contrast, overexpression of YodL, which the previous data suggested is induced to maximal levels in a Spo0A-dependent manner (256, 308), did not result in any obvious morphological changes (Fig A3.1) and actually increased the relative sporulation efficiency by ~20% (Table A3.4).

Previous genetic data showed that YodL depends on MreB to perturb cell shape (Fig A1.12), and suppressor selection analysis are consistent with MreB being YodL's primary target (Table A1.6). Similarly, YisK requires Mbl to elicit its cell-widening effects (Fig A1.12), and YisK-resistant suppressors arise primarily in *mbl* (Table A1.6)(256). Based on these observations, we hypothesized that during sporulation, a Δ*mreB* strain would phenocopy the YodL overexpression phenotype, whereas a Δ*mbl* strain would phenocopy the YisK overexpression phenotype. To our surprise, we observed that the Δ*mreB* mutant produced round-shaped cells (Fig A3.2), similar to YisK overexpression (Fig A3.1), while the Δ*mbl* mutant displayed no differences compared to wildtype (Fig A3.2), more similar to YodL overexpression (Fig A3.1). At the same time, overexpression of YisK in a Δ*mbl* background did not result in round cells (Fig A3.3), suggesting that even during sporulation, YisK requires the presence of Mbl to perform its activity. The simplest explanation of these results is that YisK is

capable of inhibiting some aspect of MreB or MreB and Mbl function as long as Mbl is present. It is also possible that the round-cell phenotype is due to YisK affecting one or more other factors or processes that are required for maintenance of rod-shape during sporulation. For example, YisK could affect the pool of PG precursors available to PG synthesizing proteins.

To gain better insight regarding how YodL and YisK might function during sporulation, we performed a screen for factors that act redundantly with YodL and YisK to support sporulation. The transposon insertions identified occur both within genes and upstream of the genes; in the future it will be necessary to carry out further analyses to determine which genes are specifically responsible for the observed sporulation defects. Interestingly, one of the transposon insertions occurred 32 bp upstream of *pgk* (Table A3.6), an essential gene which product is involved in regulation of carbon flux through the glycolytic and gluconeogenic pathways (351, 352). Of note, *pgk* is the first gene in an operon that includes *eno*, *pgm*, and *tpiA*, other genes required for the pathway converting phosphenolpyruvate (PEP) to glucose-6-phosphate during gluconeogenesis. The first dedicated step in PG synthesis (carried out by the enzyme MurA), is the condensation of PEP with the PG precursor UDP-GlcNAc to generate UDP-GlcNAc-enolpyruvate. Previous researchers have associated bypass of MreB essentiality with changes in flux through the gluconeogenic pathway, possibly due to a changes in the pools of available PG precursors (353). We do not know if the expression of *pgk*, *pgm*, *eno*, and *tpiA* is increased or decreased in the strain we isolated, but this could be determined by examining mRNA levels. Since YodL and YisK appear to negatively regulate MreB and/or Mbl activity, we predict that the sporulation defect we observe is due to upregulation of PG synthesis. One exciting possibility is that YisK regulates Mbl and possibly MreB activity by limiting the availability of a substrate feeding into the

synthesis of UDP-GlcNAc-enolpyruvate. Future investigation will be aimed at probing this specific hypothesis.

Another transposon we identified in the redundant factor screen inserted 60 bp upstream of *rpsU*. We have not investigated if the insertion results in increased or decreased expression of *rpsU* since this mutant has pleotropic effects on the cell (354) that will likely complicate its analysis. Prior work suggested that *rpsU* (the gene encoding ribosomal protein S21) null mutant results in an enhancement of biofilms and the upregulation of exopolysaccharide (EPS) production (355). However, the *rpsU* mutation also suppresses defects in phospholipid synthesis (354), so multiple processes are likely effected. Interestingly, before obtaining this mutant, we had already observed a genetic link between YisK and *rpsU*. In a suppressor selection for mutants spontaneously resistant to YisK activity (see Appendix I for details), we identified an *rpsU* truncation mutant (Fig A3.4) which, based on phenotype, is loss-of-function (355). We also identified a transposon in the open reading frame of *veg* in the redundant factor screen (Table A3.6). A *veg* knockout strain exhibits a biofilm-down phenotype, producing less EPS (356). We hypothesize that transposon insertion in *veg* inactivates the gene and represses EPS production. Since EPS and PG compete for the same Und-P precursor (357), we suspect this strain exhibits more robust PG synthesis. Similar to the situation with the *pgk* mutant, we hypothesize increased and/or disregulated PG synthesis is detrimental during sporulation.

It is possible that one or more of the transposons have subtle effects on sporulation that are unrelated to either YodL or YisK activity, but that become evident in the Δ*yodL* Δ*yisK* background (which itself has a subtle sporulation defect)(Table A1.4)(256). For example, the *ssrA* transposon could affect sporulation subtly, as *ssrA* has previously been shown to affect sporulation (358). We currently do not have

hypotheses to be tested regarding the remaining insertions. Future experiments will be aimed at further characterization of the mutants identified, including determining if the sporulation phenotypes can be recapitulated in backgrounds in which the transposon is present and only *yodL* or *yisK* have been deleted.

We also observed that addition of excess Mg^{2+} to sporulating cultures decreased cell viability in both Δ*mreB* and Δ*mbl* strains. This result is interesting because during vegetative growth, increasing Mg^{2+} levels in media has been shown to have a stabilizing effect on mutants with perturbations in PG synthesis (290, 291, 325). Although the reasons for this stabilization are unclear, we would like to propose based on our current data that Mg^{2+} addition somehow leads to an increase in the availability of precursors available for PG synthesis. In bacteria, the sugar precursors required for synthesizing various cell wall glycan polymers, including those required for production of EPS, lipopolysaccharide, techoic acid, and PG synthesis, are conjugated to a single common lipid carrier called Und-P (359-361). The pool of Und-P is limiting, thus fluxes toward one pathway result in a corresponding depletion of Und-P available for another pathway (357, 362). Mg^{2+} is known to downregulate EPS production in *Bacillus* (363), so one idea is that the decreased EPS production increases the availability of Und-P available for PG synthesis (362). Similarly, in *B. subtilis*, low Mg^{2+} levels result in an increase in synthesis of techoic acid (364); although it has not been investigated specifically, such a shift would be expected to shift Und-P towards to techoic acid synthesis, and would therefore deplete PG precursors. Reciprocally, excess Mg^{2+} would be predicted to lead to a downregulation in techoic acid biosynthesis, and a corresponding increase in the Und-P available for PG synthesis.

The excess Mg^{2+} provided during sporulation in cells lacking either *mreB* or *mbl* could lead to an increase in the availability of precursors for PG synthesis at a time that

they are actually detrimental for spore development. Since the spore cortex is largely composed of PG (365), it is not clear why such a defect would occur, but it is possible that the ability of cells to generate the cortex-specific modifications to the PG, such as removal of peptide side chains and conversion of N-acetyl muramic acid to muramic-delta-lactam (365) may be perturbed in the absence of MreB and/or Mbl. Although these modifications have not been shown to affect the heat-stability of spores produced, they have a major impact on the ability of spores to germinate successfully (365). Future investigations will be aimed at testing these different hypotheses.

APPENDIX IV

YodL DISRUPTS CELL SHAPE INDEPENDENT OF RodZ

Introduction

The bacterial actin-like protein MreB is critical to peptidoglycan (PG) synthesis in a large number of rod-shaped bacteria, including the important model organisms *Escherichia coli* and *Bacillus subtilis* (269, 270). MreB interacts with several other proteins involved in PG synthesis, including the bitopic membrane protein RodZ (279, 283, 288). RodZ has been shown to be important for cell shape maintenance both in *E. coli* and in *B. subtilis* (283, 284) and a co-crystal structure of RodZ-MreB is available showing the N-terminus of RodZ extending into a conserved hydrophobic pocket located in subdomain IIA of MreB (279). Recently, Morgenstein et al. showed that RodZ couples MreB to PG synthesis by mediating MreB's dynamic rotational behavior in *E. coli* (288). In *E. coli*, MreB rotation is required for the robustness of rod shape, but is also dispensable for rod-like shape determination under standard laboratory conditions (288).

Current data suggest that in *B. subtilis*, YodL affects MreB activity (Appendix I, Table A1.6, Fig A1.12)(256). During vegetative growth, misexpression of YodL prevents colony formation on plates and results in cell widening (Fig A1.1); these phenotypes can be rescued by substitutions in MreB at the RodZ-MreB interface, as well as in residues at/near those previously associated with bypass of RodZ essentiality (Table A1.6, Fig A1.9). Based on these results and the fact that MreB is required for YodL to induce cell widening (Fig A1.12), it was hypothesized that in its native context

of sporulation, YodL may function by regulating the interaction between RodZ and MreB.

Here, we showed that *B. subtilis* MreB interacts with RodZ in a bacterial two-hybrid (B2H) assay. This assay was then used to show that the YodL resistant MreB variants identified previously (256) can be divided into at least two classes: those that show loss of interaction with RodZ and those that show gain of interaction with RodZ. Furthermore, we found that contrary to prior reports (284), RodZ is non-essential in *B. subtilis* 168. The gene can be deleted with only minor effects on cell shape as long as expression of the essential downstream gene, *pgsA,* is not disrupted (366). Using the Δ*rodZ* strain, it was observed that RodZ is not required for YodL-dependent killing or cell shape perturbations, suggesting that YodL does not act by targeting RodZ specifically.

Materials and Methods

General methods.

All *B. subtilis* strains were derived from *B. subtilis* 168. *E. coli* and *B. subtilis* strains utilized in this study are listed in Table A4.1. Plasmids are listed in Table A4.2. Oligonucleotide primers are listed in Table A4.3. *Escherichia coli* DH5α was used for cloning. All *E. coli* strains were grown in LB-Lennox medium supplemented with 100 µg/ml ampicillin and/or 25 µg/ml kanamycin. The following concentrations of antibiotics were used for generating *B. subtilis* strains: 100 µg/ml spectinomycin, 7.5 µg/ml chloramphenicol, 0.8 mg/ml phleomycin, 10 µg/ml tetracycline, 10 µg/ml kanamycin. To select for erythromycin resistance, plates were supplemented with 1

µg/ml erythromycin (erm) and 25 µg/ml lincomycin. *B. subtilis* transformations were carried out as described previously (302).

Bacterial two-hybrid assay

Bacterial two hybrids were performed essentially as described (241). For more details, see Materials and Methods in Chapter II.

Plate growth assay

B. subtilis strains were streaked on LB-Lennox plates containing 100 µg/ml spectinomycin and 1 mM IPTG. Plates were incubated at 37°C overnight and images were captured on a ScanJet G4050 flatbed scanner (Hewlett Packard).

Microscopy

All strains were grown in 25 ml LB-Lennox medium in 250 ml baffled flasks at 37°C in a shaking waterbath set at 280 rpm for 1.5 hrs. When indicated, 1 mM IPTG was added to induce protein misexpression and all the samples were imaged 1.5 hrs post-induction. 1 ml samples were spun down at 6,010 x g for 1 minute at room temperature. The pellets were resuspended in 5 µl TMA-DPH (0.02 mM) to stain the membrane and exposed for 1 sec. Cells were mounted on glass slides with polylysine-treated coverslips prior to imaging.

Table A4.1. Strains used in Appendix IV.

Strain	Description	Reference
Parental		
B. subtilis 168	*Bacillus subtilis* laboratory strain 168 *trpC2*	BGSC (1A866)
E. coli DH5α	*F^- endA1 glnV44 thi-1 recA1 relA1 gyrA96 deoR nupG Φ80dlacZΔM15 Δ(lacZYA-argF)U169, hsdR17(r_K^- m_K^+), λ–*	
E. coli DHP1	*F-, cya-99, araD139, galE15, galK16, rpsL1 (Strr), hsdR2, mcrA1,mcrB1;*	Tom Bernhardt
***B. subtilis* 168**		
BAS191	*amyE::*P_{hy}*-yodL (spec), yhdG::*P_{hy}*-yodL (phleo)*	(256)
BAS316	*rodZ::tet*	This study
BAS321	*rodZ::tet*, *amyE::*P_{hy}*-yodL (spec), yhdG::*P_{hy}*-yodL (phleo)*	This study
***E. coli* DHP1**		
CYD217	*T25-yodL (kan), T18-mreB (amp)*	This study
CYD218	*T25-yodL (kan), mreB-T18 (amp)*	This study
CYD219	*yodL-T25 (kan), T18-mreB (amp)*	This study
CYD220	*yodL-T25 (kan), mreB-T18 (amp)*	This study
CYD221	*T25-mreB (kan), T18-yodL (amp)*	This study
CYD222	*mreB-T25 (kan), T18-yodL (amp)*	This study
CYD223	*T25-mreB (kan), yodL-T18 (amp)*	This study
CYD224	*mreB-T25 (kan), yodL-T18 (amp)*	This study
CYD340	*yodL-T25 (kan), rodZ-T18 (amp)*	This study
CYD341	*yodL-T25 (kan), T18-rodZ (amp)*	This study
CYD342	*T25-yodL (kan), rodZ-T18 (amp)*	This study
CYD343	*T25-yodL (kan), T18-rodZ (amp)*	This study
CYD344	*rodZ-T25 (kan), yodL-T18 (amp)*	This study
CYD345	*T25-rodZ (kan), yodL-T18 (amp)*	This study
CYD346	*rodZ-T25 (kan), T18-yodL (amp)*	This study
CYD347	*T25-rodZ (kan), T18-yodL (amp)*	This study
CYD394	*T25-rodZ (kan), mreB-T18 (amp)*	This study
CYD421	*T25-empty (kan), mreB-T18 (amp)*	This study
CYD422	*T25-rodZ (kan), empty-T18 (amp)*	This study
CYD439	*T25-rodZ (kan),* $mreB_{G143A}$*-T18 (amp)*	This study
CYD440	*T25-rodZ (kan),* $mreB_{R282S}$*-T18 (amp)*	This study
CYD441	*T25-rodZ (kan),* $mreB_{S154R}$*-T18 (amp)*	This study
CYD442	*T25-rodZ (kan),* $mreB_{P147R}$*-T18 (amp)*	This study
CYD443	*T25-rodZ (kan),* $mreB_{N145D}$*-T18 (amp)*	This study

Table A4.1. Continued.

Strain	Description	Reference
CYD444	*T25-empty (kan), mreB$_{G143A}$-T18 (amp)*	This study
CYD445	*T25-empty (kan), mreB$_{R282S}$-T18 (amp)*	This study
CYD446	*T25-empty (kan), mreB$_{S154R}$-T18 (amp)*	This study
CYD447	*T25-empty (kan), mreB$_{P147R}$-T18 (amp)*	This study
CYD448	*T25-empty (kan), mreB$_{N145D}$-T18 (amp)*	This study

Table A4.2. Plasmids used in Appendix IV.

Plasmid	**Description**	**Reference**
pKT25	*T25-empty (kan)*	Tom Bernhardt
pCH363	*empty-T18 (amp)*	Tom Bernhardt
pYD199	*T25-yodL (kan)*	This study
pYD200	*yodL-T25 (kan)*	This study
pYD201	*T18-yodL (amp)*	This study
pYD202	*yodL-T18 (amp)*	This study
pYD203	*T25-mreB (kan)*	This study
pYD204	*mreB-T25 (kan)*	This study
pYD205	*T18-mreB (amp)*	This study
pYD206	*mreB-T18 (amp)*	This study
pYD207	*rodZ-T18 (amp)*	This study
pYD208	*T18-rodZ (amp)*	This study
pYD209	*rodZ-T25 (kan)*	This study
pYD210	*T25-rodZ (kan)*	This study
pYD211	*mreB*$_{G143A}$*-T18 (amp)*	This study
pYD212	*mreB*$_{R282S}$*-T18 (amp)*	This study
pYD213	*mreB*$_{S154R}$*-T18 (amp)*	This study
pYD214	*mreB*$_{P147R}$*-T18 (amp)*	This study
pYD215	*mreB*$_{N145D}$*-T18 (amp)*	This study

Table A4.3. Oligonucleotides used in Appendix IV.

Oligo	**Sequence 5' to 3'**
OYD206	CATTGCATGCGTAACACACAGGAAACAGCTATGATGTTATCCGTGTTTAAAAAG
OYD207	GCATGGATCCGAACCGCTACCTGTCGTTTGTACAATCAGACG
OYD208	GCATGGATCCGGGCAGCGGTATGATGTTATCCGTGTTTAAAAAG
OYD209	GCATGAATTCTTATGTCGTTTGTACAATCAGACG
OYD210	CATTGCATGCGTAACACACAGGAAACAGCTATGTTTGGAATTGGTGCTAGAG
OYD211	GCATGGATCCGAACCGCTACCTCTAGTTTTCCCTTTGAAAAGATG
OYD212	GCATGGATCCGGGCAGCGGTATGTTTGGAATTGGTGCTAGAG
OYD213	GCATGAATTCTTATCTAGTTTTCCCTTTGAAAAG
OYD266	GCATGGATCCGTAACACACAGGAAACAGCTATGTCATTGGATGATCTCCAAG
OYD267	GCATGAATTCGAACCGCTACCAGATGACTTTTCTTCCTTTTTATTT
OYD268	GCATGGATCCGGGCAGCGGTATGTCATTGGATGATCTCCAAG
OYD269	GCATGAATTCTTAAGATGACTTTTCTTCCTTTTTATTT

Results

B. subtilis MreB interacts with RodZ in a B2H assay

Muchova et al. showed that in *B. subtilis*, the cytosolic portion of RodZ interacts with MreB in a pull-down assay (284). We independently tested the interaction between RodZ and MreB using a bacterial two-hybrid assay. A positive interaction between RodZ and MreB was detected that was absent in the negative controls, consistent with the idea that the two proteins interact (Fig A4.1).

Amino acid substitutions in MreB that suppress YodL's cell widening and killing effects influence MreB-RodZ interaction

Misexpression of YodL during vegetative growth results in cell-widening and prevents colony formation on plates (Appendix I, Fig A1.1). To identify genetic targets associated with YodL activity, we performed suppressor selection analysis and found out that most YodL-resistant strains possessed point mutations in *mreB* (Appendix I, Table A1.6)(256). Interestingly, five of the MreB variants identified, $MreB_{G143A}$, $MreB_{N145D}$, $MreB_{P147R}$, $MreB_{S154R}$, and $MreB_{R282S}$, possessed amino acid substitutions in a region important for mediating MreB-RodZ interaction in *E. coli* (Appendix I, Table A1.6 and Fig A1.9)(256); three of these substitutions ($MreB_{N145D}$, $MreB_{P147R}$, and $MreB_{R282S}$) occur in residues that interact directly in the *T. maritima* MreB-RodZ structure. Each of these later substitutions are resistant toYodL but not YisK, and thus are less likely to be general MreB gain-of-function suppressors (256).

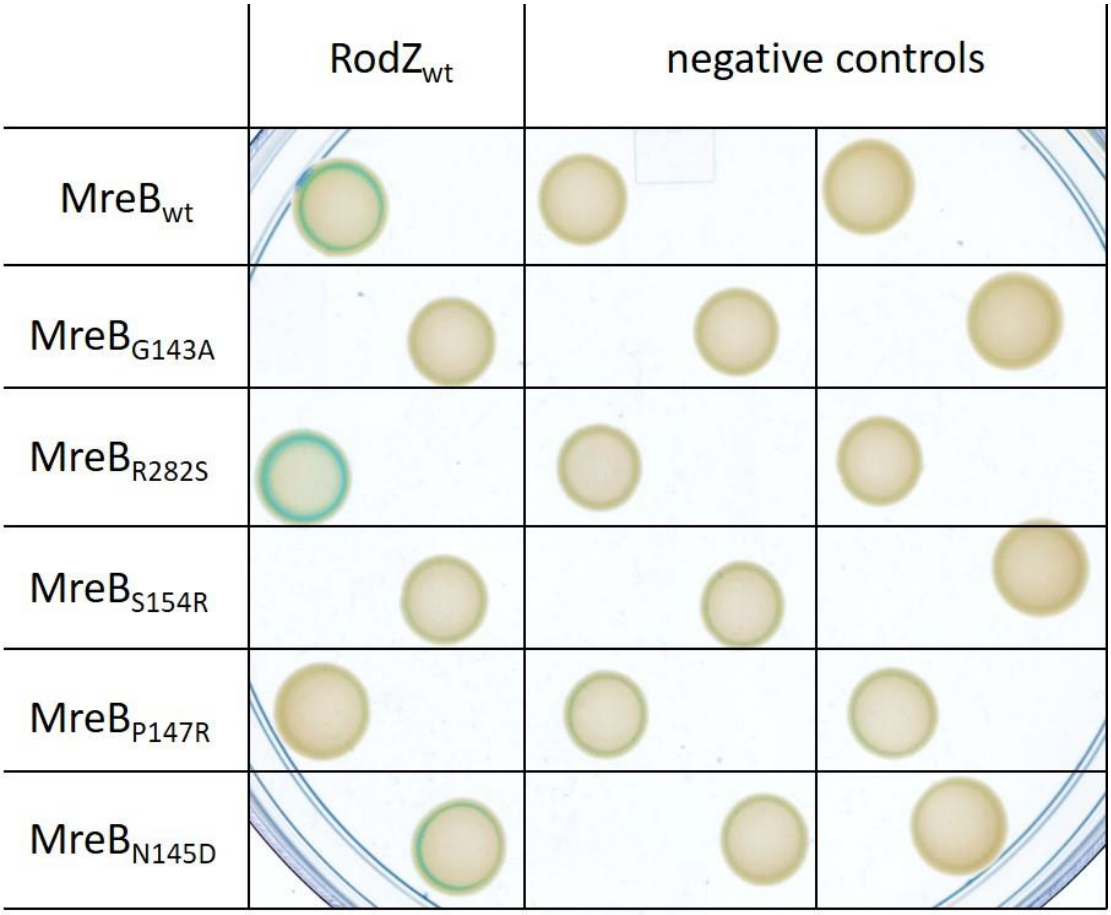

Fig. A4.1. MreB interacts with RodZ by bacterial two-hybrid assay. B2H between RodZ and MreB (CYD394) or RodZ and each of the following MreB variants: $MreB_{G143A}$ (CYD439), $MreB_{R282S}$ (CYD440), $MreB_{S154R}$ (CYD441), $MreB_{P147R}$ (CYD442) and $MreB_{N145D}$ (CYD443). Negative controls: empty partner vector with wild-type MreB or the indicated MreB variant (left) or RodZ with the empty partner vector (right).

To test if the amino acid substitutions in MreB indeed affected MreB-RodZ interaction, we performed B2H using wild-type RodZ and each of the MreB variants. In the assay, interaction between RodZ and $MreB_{G143A}$, $MreB_{P147R}$ and $MreB_{S154R}$ were not detectable, whereas $MreB_{N145D}$ exhibited a slightly weaker interaction compared to wild-type MreB (Fig A4.1). In contrast, $MreB_{R282S}$ appeared to interact more strongly with RodZ in the B2H (Fig A4.1). These results suggest that, analogous to what was observed in the *T. maritima* RodZ-MreB co-crystal (279), $MreB_{G143}$, $MreB_{N145}$, $MreB_{P147}$, $MreB_{S154}$, and $MreB_{R282}$ facilitate the MreB-RodZ interaction in *B. subtilis*.

YodL-MreB and YodL-RodZ interactions are not detectable in a B2H assay

We hypothesized that YodL might perturb MreB function by interacting directly with either MreB and/or RodZ. To test this idea, we tested for interaction between YodL and MreB and YodL and RodZ in a B2H assay. None of the combinations tested resulted in a positive interaction in the assay (Fig A4.2). However, based on this negative data, we do not exclude the possibility that YodL and MreB could interact directly.

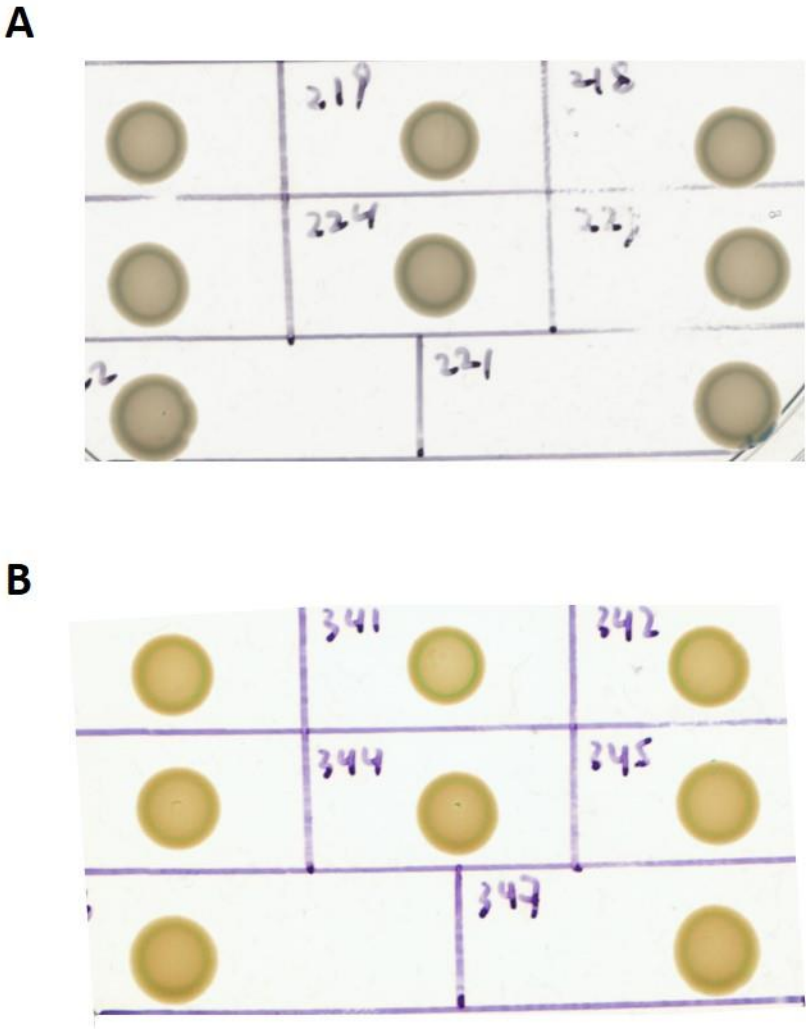

Fig. A4.2. YodL-MreB interaction and YodL-RodZ interaction were not detected in a B2H assay. (A) B2H between YodL and MreB (CYD217-224). (B) B2H between YodL and RodZ (CYD340-347). The plates were incubated at room temperature for 96 hrs.

RodZ is not required for YodL activity

We hypothesized that if YodL's cell-widening and cell-killing effects were due to targeting of RodZ (as opposed to MreB), then YodL would no longer be functional in a strain lacking RodZ. To test this idea, we constructed a Δ*rodZ* strain. Although prior reports indicated that *rodZ* was essential, the knockout strains were not designed to avoid polar effects on the downstream gene, *pgsA*, which is known to be essential (366, 367). In addition, genetic complementation was not performed to show that the loss of viability was attributable to RodZ. Therefore, a knockout construct was designed to introduce a kanamycin-resistant linked *rodZ* deletion into the *B. subtilis* chromosome while minimizing the possibility of polar effects on *pgsA*. Using this strategy, *rodZ* deletion mutants were readily obtained. The Δ*rodZ* strain occasionally produced slightly twisted cells and bent or curled poles, and phenotype that was ameliorated by the addition of 10 mM $MgCl_2$ (Fig A4.3). However, even in the presence of 10 mM $MgCl_2$, some small membrane-bound structures were observed, reminiscent of minicells (Fig A4.3). To test if YodL required RodZ for its cell-widening and cell-killing misexpression phenotypes, P_{hy}-*yodL* was introduced into the Δ*rodZ* background. Neither wildtype nor the Δ*rodZ* strain could form colonies on plates containing inducer, suggesting that RodZ was not required for YodL activity (Fig A4.4A). Similarly, RodZ was not required for the cell-widening, as cells expressing YodL in the Δ*rodZ* background readily rounded up and lysed (Fig A4.4B). Moreover, the Δ*rodZ* strain appeared sensitized to the presence of YodL. Taken together, these results suggest that RodZ is not required for YodL activity.

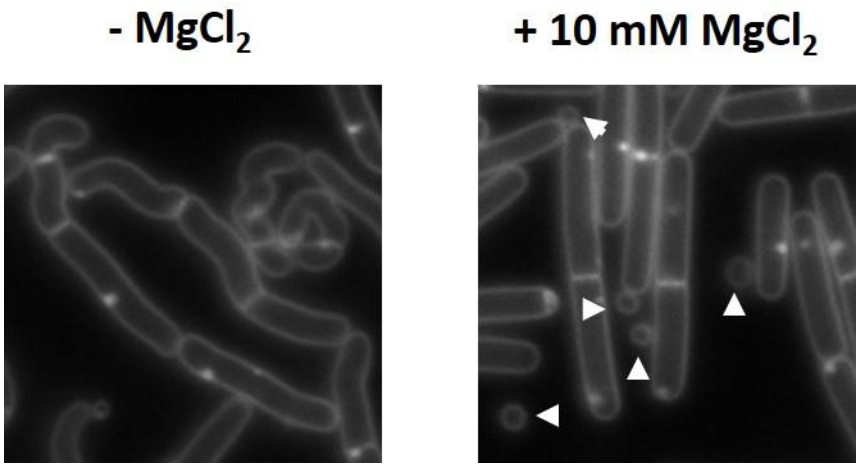

Fig. A4.3. Phenotypic characterization of a Δ*rodZ* mutant grown in liquid culture. BAS316 (Δ*rodZ*) was grown in LB-Lennox media at 37°C to mid-exponential and back-diluted to an OD_{600} of ~0.02. When indicated, 10 mM $MgCl_2$ was added. Cells were grown for 1.5 hrs at 37°C before image capture. Membranes were stained with TMA-DPH. All images are shown at the same magnification. White arrows indicate the "minicells" (see text above).

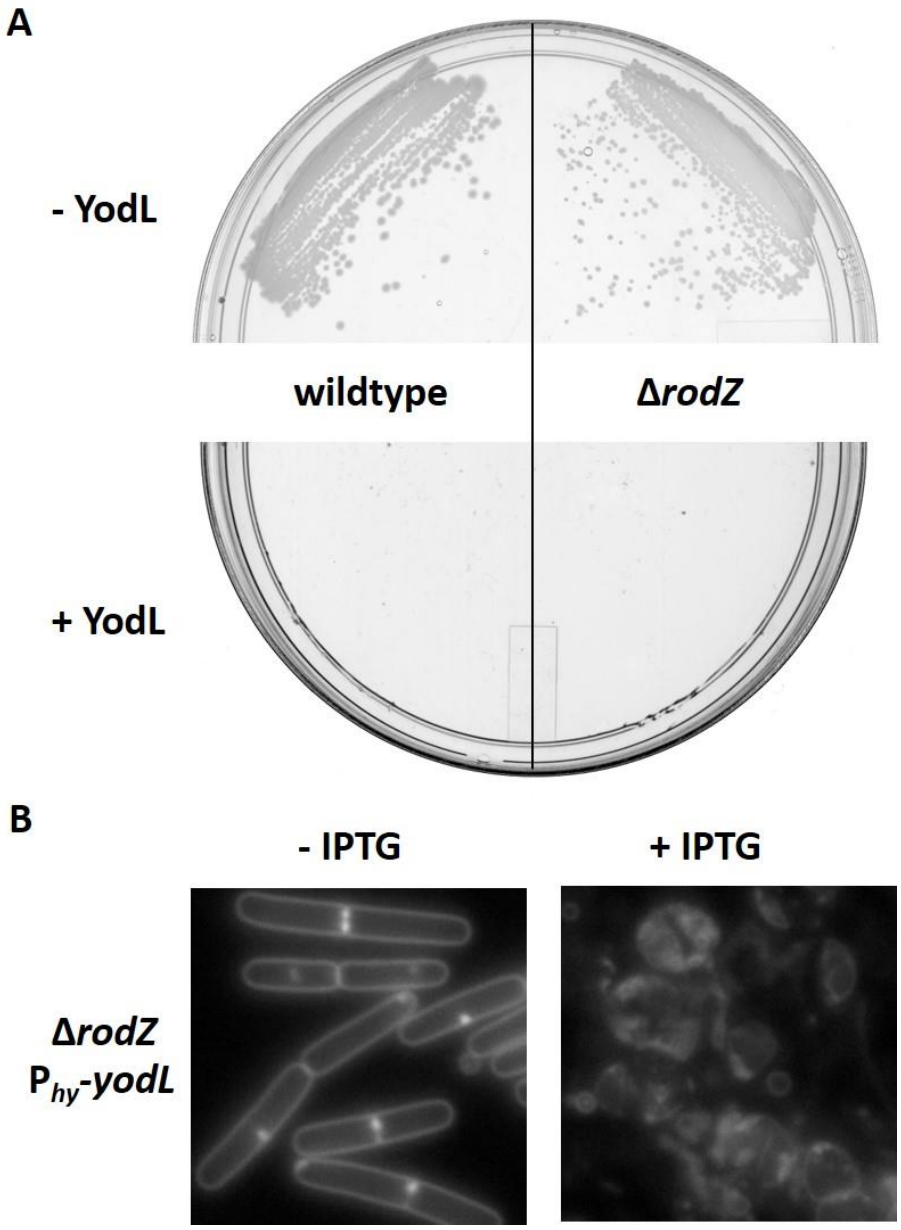

Fig. A4.4. RodZ is not required for YodL activity. (A) BAS191 (2X P_{hy}-*yodL*) and BAS321 (2X P_{hy}-*yodL*, Δ*rodZ*) were streaked on an LB plate supplemented with 100 µg/ml spectinomycin and, when indicated, 1 mM IPTG. Plates were incubated at 37°C overnight before image capture. (B) BAS321 was grown in LB-Lennox media at 37°C to mid-exponential and back-diluted to an OD_{600} of ~0.02. When indicated, 1 mM IPTG was added. Cells were grown for 1.5 hrs at 37°C before image capture. Membranes were stained with TMA-DPH. All images were scaled in size identically.

Discussion

Current data suggest that YodL disrupts cell shape in a manner that requires MreB (Appendix I, Fig A1.12)(256). Moreover, YodL-resistant suppressor mutations primarily result in MreB substitutions at the interaction interface between RodZ and MreB (Appendix I, Table A1.6, Fig A1.9)(256). We developed a B2H assay to test if the YodL-resistant MreB substitutions resulted in a change of interaction between RodZ and MreB. $MreB_{G143A}$, $MreB_{P147R}$ and $MreB_{S154R}$ appear to reduce RodZ-MreB interaction by B2H while $MreB_{R282S}$ results in stronger interaction Fig A4.1. Based on these data, we hypothesize that YodL directly targets MreB at the RodZ-MreB interaction interface, and that the loss of interaction substitutions prevent YodL from interacting with MreB but also disrupt the native RodZ-MreB interaction. Similarly, we propose that $MreB_{R282S}$ leads to a stronger RodZ-MreB interaction, thereby overcoming the inhibitory effects of YodL.

YodL-MreB interaction was not detected in a B2H assay (Fig A4.2). We also did not detect an interaction between YodL and RodZ by B2H (Fig A4.2). The lack of interaction in the B2H may indicate that YodL does not interact directly with either RodZ or MreB. It is also possible that the interactions are below the level of detection in the assay. Alternatively, YodL may require the formation of a RodZ-MreB complex to create its interaction site. It is also possible that the tagged YodL expressed in the B2H is titrated away from forming a complex through interactions with native *E. coli* proteins. This later possibility is supported by preliminary evidence suggesting that in *E. coli*, YodL disrupts the interaction between MreB and FtsZ (see Appendix II). This last possibility could be tested by performing the two-hybrid analysis in yeast, a eukaryote that does not encode *mreB, ftsZ*, or *rodZ*.

When YodL is misexpressed in a Δ*rodZ* background, the cells appear to be sensitized to the cell-altering effects of YodL, producing round cells that readily lyse (Fig A4.4B). These results suggest that cells lacking *rodZ* produce less robust peptidoglycan, similar to what has been shown in *E. coli* (288). We hypothesize that this reduced robustness is what sensitizes the cells to YodL activity. Interestingly, the MreB variants we identified that showed loss of interaction with RodZ, $MreB_{G143A}$, $MreB_{P147R}$ and $MreB_{S154R}$ were less, not more sensitive to YodL activity (Appendix I, Table A1.6)(256). We can envision three possibilities to explain this result. The first and simplest model is that YodL is no longer able to target MreB activity when these substitutions are present, and that the loss-of-interaction with RodZ is simply a byproduct of the fact that the proteins interact with the same region of MreB. A second possibility is that RodZ bound at MreB creates the site for YodL interaction, thus the loss of interaction variants would be less susceptible to YodL activity. Both of these results are consistent with prior observations that YodL requires MreB for activity (Appendix I, Fig A1.12)(256). However, if YodL's function is simply to interfere with the interaction between RodZ and MreB by binding to both proteins, the misexpression phenotype should be similar to the RodZ-MreB loss of interaction variants and these variants appear relatively normal (data not shown). The third possibility is that RodZ has additional functions in maintaining rod shape that become favored when the interaction between RodZ and MreB is perturbed. For example, it is possible that RodZ also regulates Mbl function (this has not been tested formally) and that some of the MreB variants may shift RodZ toward interaction with Mbl. $MreB_{G143A}$ is a good candidate for this class because, although it is located at the RodZ-MreB interaction interface, it is also highly resistant to YisK, a protein hypothesized to target Mbl (Appendix I, Table A1.6,

Fig A1.12)(256). Future experiments will be aimed at testing these different possibilities with the ultimate goal of determining YodL's mechanism of action.

APPENDIX V

MISEXPRESSION OF YisK CAUSES FtsEX-DEPENDENT CELL SHORTENING

Introduction

Bacterial cells have an external cell wall composed of peptidoglycan (PG) that provides structural rigidity to the cell, maintaining shape and protecting cells from osmotic lysis. PG is a macromolecular meshwork assembled from the glycan strands cross-linked to each other by short peptides (368, 369). In order for the cells to grow or divide or for cell the existing glycan bonds need to be broken (PG hydrolysis), thus allowing newly synthesized glycan strands to be inserted into the covalently network (PG synthesis)(332, 370, 371). Numerous studies have been performed to investigate the mechanisms of PG synthesis; however, the mechanisms underlying PG hydrolysis and its regulation remain largely mysterious.

In the Gram negative model organism *Escherichia coli*, PG hydrolases have been shown to be particularly important during cell division, and are required for septal PG splitting (372-374). It has been shown that the ABC transporter protein complex FtsEX regulates the PG binding protein EnvC. In turn, EnvC activates the PG amidases AmiA and AmiB, leading to the hydrolysis of the PG crosslinks and septal splitting during cell division (375, 376). In the Gram positive bacterium *Bacillus subtilis*, FtsEX complex also plays an important role in PG hydrolysis, somehow regulating the activity of the cell wall hydrolase CwlO (a DL-endopeptidase)(326, 377-379). However, in contrast to *E. coli*, an *ftsEX* mutant exhibits no defects in cell division; instead, the mutant is shorter than wildtype, phenocopying a *cwlO* knockout (326, 377). These results indicate that

FtsEX/CwlO complex plays an important role in the regulation of cell elongation. In the complex, FtsE is the cytoplasmic ATPase and FtsX is the transmembrane component, which associates with the PG hydrolase CwlO (326, 377). The ATP binding and hydrolysis activity of FtsE is required for CwlO function (326). FtsX is also needed for CwlO function, although it is unclear if FtsX is required for association of CwlO with the cell membrane (326, 377).

In addition to CwlO, *B. subtilis* has another DL-endopeptidase called LytE (378, 379). LytE interacts with the actin-like protein MreBH and that this interaction is required for LytE's localization around the cell periphery (290). Moreover, Dominguez-Cuevas et al. demonstrated genetically that another actin-like protein, Mbl, is crucial for FtsEX/CwlO function (377). Although neither LytE nor CwlO are essential, a double mutant is non-viable (326, 377), suggesting that these factors act redundantly to carry out essential functions activity during cell growth.

We have shown that Mbl is a genetic target of YisK activity (Appendix I, Table A1.6, Fig A1.12)(256). Misexpression of YisK during vegetative growth causes cell widening and this phenotype is dependent on Mbl (Appendix I, Fig A1.1, Fig A1.12)(256). In addition, YisK misexpression also leads to cell shortening in a manner that is independent of both Mbl and MreBH (Appendix I, Fig A1.13)(256). Here we show that YisK interacts with FtsE directly in a bacterial two-hybrid. Moreover, we observe that the cell-shortening but not the cell-widening phenotypes associated with YisK activity are dependent on the FtsEX complex. Our results support the idea that YisK activity targets not only Mbl, but also the Mbl-dependent FtsEX complex.

Materials and Methods

General methods.

All *B. subtilis* strains were derived from *B. subtilis* 168. *E. coli* and *B. subtilis* strains utilized in this study are listed in Table A5.1. Plasmids are listed in Table A5.2. Oligonucleotide primers are listed in Table A5.3. *Escherichia coli* DH5α was used for cloning. All *E. coli* strains were grown in LB-Lennox medium supplemented with 100 µg/ml ampicillin and/or 25 µg/ml kanamycin. The following concentrations of antibiotics were used for generating *B. subtilis* strains: 100 µg/ml spectinomycin, 7.5 µg/ml chloramphenicol, 0.8 mg/ml phleomycin, 10 µg/ml tetracycline, 10 µg/ml kanamycin. To select for erythromycin resistance, plates were supplemented with 1 µg/ml erythromycin (erm) and 25 µg/ml lincomycin. *B. subtilis* transformations were carried out as described previously (302).

Bacterial two-hybrid assay

Bacterial two hybrids were performed essentially as described (241). For more details, see Materials and Methods in Chapter II.

Table A5.1. Strains used in Appendix V.

Strain	Description	Reference
Parental		
B. subtilis 168	*Bacillus subtilis* laboratory strain 168 *trpC2*	BGSC (1A866)
E. coli DH5α	*F^- endA1 glnV44 thi-1 recA1 relA1 gyrA96 deoR nupG Φ80dlacZΔM15 Δ(lacZYA-argF)U169, hsdR17(r_K^- m_K^+), λ–*	
E. coli DHP1	*F-, cya-99, araD139, galE15, galK16, rpsL1 (Strr), hsdR2, mcrA1,mcrB1;*	Tom Bernhardt
***B. subtilis* 168**		
BAS319	*ftsEX::tet*	This study
BJH407	*lytE::cat*	David Z. Rudner
BJH408	*kanΩmbl$_{D153N}$, lytE::cat*	This study
BJH410	*kanΩmbl$_{D153N}$, lytE::cat, amyE::P_{hy}-yisK (spec)*	This study
BJH412	*kanΩmbl$_{D153N}$, lytE::cat, amyE::P_{hy}-yisK (spec), yhdG::P_{hy}-yisK (phleo)*	This study
BJH413	*kanΩmbl$_{R63C}$, lytE::cat*	This study
BJH415	*kanΩmbl$_{R63C}$, lytE::cat, amyE::P_{hy}-yisK (spec), yhdG::P_{hy}-yisK (phleo)*	This study
BJH416	*kanΩmbl$_{R63C}$, lytE::cat, amyE::P_{hy}-yisK (spec), yhdG::P_{hy}-yisK (phleo), ycgO::P_{hy}-yisK (tet)*	This study
BJH417	*kanΩmbl$_{R63C}$, lytE::cat, amyE::P_{hy}-yisK (spec)*	This study
BJH418	*kanΩmbl$_{D153N}$, lytE::cat, amyE::P_{hy}-yisK (spec), yhdG::P_{hy}-yisK (phleo), ycgO::P_{hy}-yisK (tet)*	This study
BYD074	*amyE::P_{hy}-yisK (spec), yhdG::P_{hy}-yisK (phleo)*	(256)
BYD262	*ponA::erm, kanΩΔmreB, amyE::P_{hy}-yisK (spec), yhdG::P_{hy}-yisK (phleo)*	(256)
BYD468	*cwlO::cat, amyE::P_{hy}-yisK (spec), yhdG::P_{hy}-yisK (phleo)*	This study
BYD476	*ftsEX::tet, amyE::P_{hy}-yisK (spec), yhdG::P_{hy}-yisK (phleo)*	This study
BYD480	*ponA::erm, kanΩΔmreB, ftsEX::tet, amyE::P_{hy}-yisK (spec), yhdG::P_{hy}-yisK (phleo)*	This study
***E. coli* DHP1**		
CYD962	*ftsE-T25 (kan), yisK-T18 (amp)*	This study
CYD966	*yisK-T25 (kan), ftsX-T18 (amp)*	This study
CYD967	*yisK-T25 (kan), T18-ftsX (amp)*	This study
CYD968	*T25-yisK (kan), ftsX-T18 (amp)*	This study

Table A5.1. Continued.

Strain	Description	Reference
***E. coli* DHP1**		
CYD969	*T25-yisK (kan), T18-ftsX (amp)*	This study
CYD970	*ftsX-T25 (kan), yisK-T18 (amp)*	This study
CYD971	*ftsX-T25 (kan), T18-yisK (amp)*	This study
CYD972	*T25-ftsX (kan), yisK-T18 (amp)*	This study
CYD973	*T25-ftsX (kan), T18-yisK (amp)*	This study
CYD974	*yisK-T25 (kan), ftsEX-T18 (amp)*	This study
CYD982	*yisK-T25 (kan), empty-T18 (amp)*	This study
CYD984	*empty-T25 (kan), yisK-T18 (amp)*	This study
CYD985	*ftsE-T25 (kan), empty-T18 (amp)*	This study
CYD986	*empty-T25 (kan), ftsEX-T18 (amp)*	This study

Table A5.2. Plasmids used in Appendix V.

Plasmid	**Description**	**Reference**
pKNT25	*empty-T25 (kan)*	Tom Bernhardt
pKT25	*T25-empty (kan)*	Tom Bernhardt
pCH363	*empty-T18 (amp)*	Tom Bernhardt
pCH364	*T18-empty (amp)*	Tom Bernhardt
pYD216	*yisK-T18 (amp)*	This study
pYD217	*T18-yisK (amp)*	This study
pYD218	*yisK-T25 (kan)*	This study
pYD219	*T25-yisK (kan)*	This study
pYD220	*ftsE-T25 (kan)*	This study
pYD221	*ftsX-T25 (kan)*	This study
pYD222	*T25-ftsX (kan)*	This study
pYD223	*ftsX-T18 (amp)*	This study
pYD224	*T18-ftsX (amp)*	This study
pYD225	*ftsEX-T18 (amp)*	This study

Table A5.3. Oligonucleotides used in Appendix V.

Oligo	**Sequence 5' to 3'**
OYD245	AGAAGCGGCCGCTTATTCTG
OYD246	CTTCGTATAATGTATGCTATACGAACGGTACTCACTTTTTATA TCCTCCCTTTTAC
OAS247	CTTCGTATAGCATACATTATACGAACGGTATAATAAATATGAC AAGGGCCTTCT
OAS248	TCATCCGTCTGAAGCACAC
OAS251	TACCGTTCGTATAGCATACATTATACGAAGTTATCATACGGCA ATAGTTACCCTTAT
OAS252	TACCGTTCGTATAATGTATGCTATACGAAGTTATGGAGCTGTA ATATAAAAACCTTC
OAS253	TACCGTTCGTATAGCATACATTATACGAAGTTATGATTTTATG ACCGATGATGAAGA
OAS254	TACCGTTCGTATAATGTATGCTATACGAAGTTATAACTCTCTC CCAAAGTTGATC
OAS255	ATCGGAGAGCATTGGAAGAAA
OAS256	ATAACTTCGTATAATGTATGCTATACGAACGGTAATCATGAAA TCACCTAATCTTTTA
OAS257	ATAACTTCGTATAGCATACATTATACGAACGGTATAAAGTGA AAAAGCCGTTCCGT
OAS258	TTTAATGTCTCTGCAGTGCGA
OYD206	CATTGCATGCGTAACACACAGGAAACAGCTATGATGTTATCC GTGTTTAAAAAG
OYD298	GCATGGATCCGTAACACACAGGAAACAGCTATGAAATTTGCG ACAGGGGAAC
OYD299	GCATGAATTCGAACCGCTACCGCCAATTTGGTTTGACAGCGTT
OYD300	GCATGGATCCGGGCAGCGGTATGAAATTTGCGACAGGGGAAC
OYD301	GCATGAATTCTTAGCCAATTTGGTTTGACAGCGTT
OYD475	GCATGGATCCGTAACACACAGGAAACAGCTATGATAGAGATG AAGGAAGTATAT
OYD476	GCATGAATTCGAACCGCTACCATCATATGAACCATACTCCCC
OYD479	GCATGGATCCGTAACACACAGGAAACAGCTATGATTAAAATT CTCGGGCGC
OYD480	GCATGAATTCGAACCGCTACCTACTCGCAGAAACTTGCGGA
OYD481	GCATGGATCCGGGCAGCGGTATGATTAAAATTCTCGGGCGC
OYD482	GCATGAATTCTTATACTCGCAGAAACTTGCGGA

Microscopy

All strains were grown in 25 ml LB-Lennox medium in 250 ml baffled flasks at 37°C in a shaking waterbath set at 280 rpm for 1.5 hrs. When indicated, 1 mM IPTG was added to induce protein misexpression and all the samples were imaged 1.5 hrs post-induction. 1 ml samples were spun down at 6,010 x g for 1 minute at room temperature. The pellets were resuspended in 5 µl TMA-DPH (0.02 mM) to stain the membranes. Cells were mounted on glass slides with polylysine-treated coverslips prior to imaging (generally 1 sec exposures). Fluorescence microscopy was performed with a Nikon Ti-E microscope equipped with a CFI Plan Apo lambda DM 100X objective, Prior Scientific Lumen 200 Illumination system, C-FL UV-2E/C DAPI and C-FL GFP HC HISN Zero Shift filter cubes, and a CoolSNAP HQ2 monochrome camera. Images were captured with NIS Elements Advanced Research (version 4.10), and processed with NIS Elements Advanced Research (version 4.10) and ImageJ64 (240).

Plate growth assay

B. subtilis strains were streaked on LB-Lennox plates containing 100 µg/ml spectinomycin and 1 mM IPTG. Plates were incubated at 37°C overnight and images were captured on a ScanJet G4050 flatbed scanner (Hewlett Packard).

Results

FtsEX is required for YisK causing cell shortening phenotype

We have shown that misexpression of YisK leads to cell shortening (Appendix I, Fig A1.13)(256). Since *ftsEX* and/or *cwlO* mutants also produced shorter cells (326, 377), we hypothesized that YisK might cause cell shortening by disrupting the function of the FtsEX/CwlO protein complex.

To test this idea, we measured cell lengths in a Δ*ponA* Δ*mbl* Δ*ftsEX* mutant before and after YisK expression. The Δ*ponA* Δ*mbl* background was used as the cell-shortening effect of YisK is more quantifiable when the cells are not additionally perturbed in overall shape as occurs when YisK is expressed in a strain expressing functional Mbl (Appendix I, Fig A1.1)(256). Even without YisK expression, the Δ*ponA* Δ*mbl* Δ*ftsEX* mutant was slightly shorter than the Δ*ponA* Δ*mbl* mutant (Fig A5.1); this result was expected, as the Δ*ftsEX* mutant itself produces shorter cells (326, 377). Following YisK induction, the Δ*ponA* Δ*mbl* Δ*ftsEX* strain showed no significant difference in cell length compared to the uninduced control (Fig A5.1B). In contrast, and as previously observed, the Δ*ponA* Δ*mbl* strain was ~20% shorter than the uninduced control when YisK was induced (Fig A1.13, Fig A5.1A)(256). These results suggest that FtsE and/or FtsX are required for mediating cell shortening via YisK.

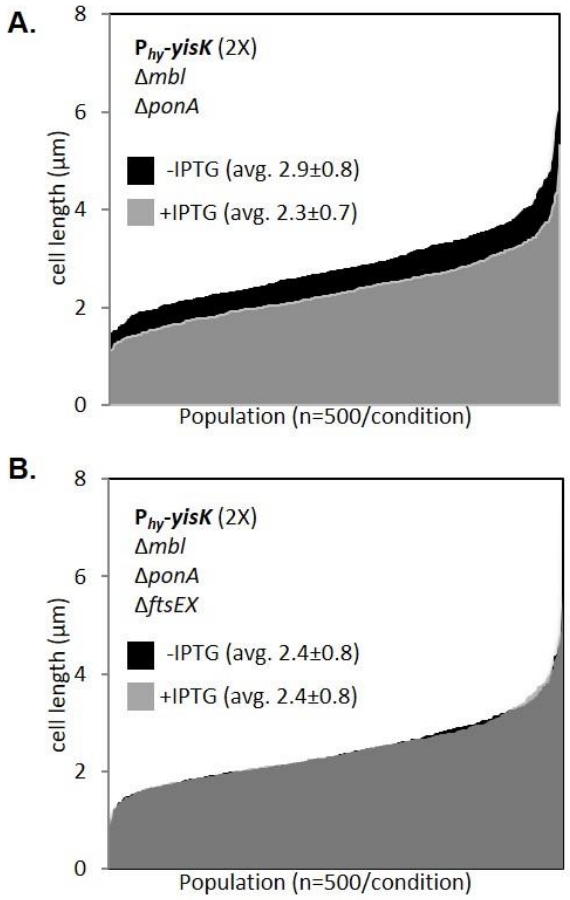

Fig. A5.1. Cell shortening phenotype by YisK misexpression is dependent on FtsEX complex. Cells harboring 2X copies of P$_{hy}$-*yisK* in a Δ*ponA* Δ*mbl* background (BYD262)(A) or a Δ*ponA* Δ*mbl* Δ*ftsEX* background (BYD480)(B) were grown at 37°C in LB supplemented with 10 mM $MgCl_2$ to mid-exponential. To induce *yisK* expression, cells were back-diluted to an OD_{600} of ~0.02 in LB with 10 mM $MgCl_2$ and IPTG (1 mM) was added. Cells were grown for 1.5 hrs at 37°C before image capture. Membranes are stained with TMA-DPH. Cell lengths (n=500/condition) were measured before and after *yisK* expression and rank-ordered from smallest to largest along the x-axis so the entire population could be visualized without binning. The uninduced population (black) is juxtaposed behind the induced population (semi-transparent, gray). The difference in average cell length before and after P$_{hy}$-*yisK* induction was only significant in the Δ*ponA* Δ*mbl* background (P<0.0001)(A). The data presented in (A) is the same as shown in Fig A1.13A.

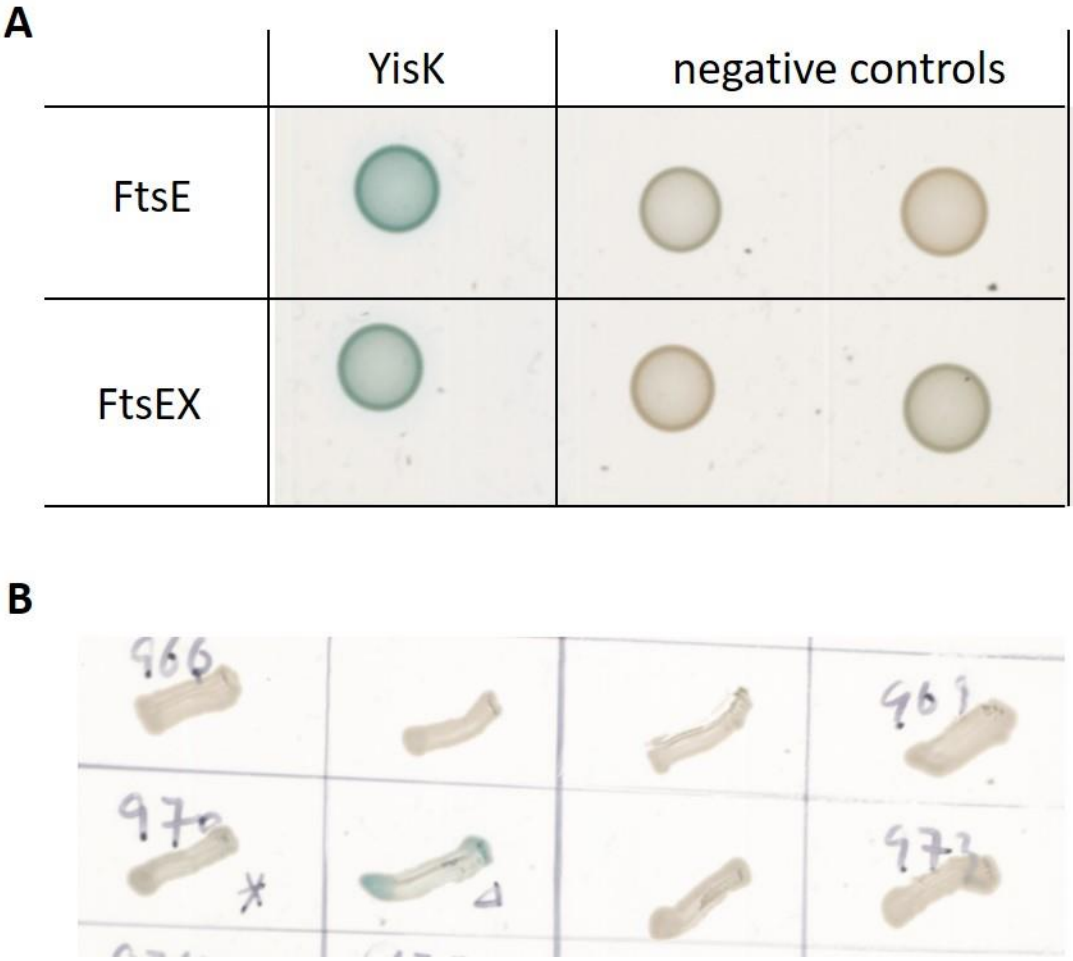

Fig. A5.2. YisK interacts with FtsEX by bacterial two-hybrid assay. (A) B2H between YisK and FtsE (CYD962) or FtsEX in which only FtsX is tagged (CYD974). Negative controls: YisK with the empty partner vector (CYD984 or CYD982) (middle column) or empty partner vector with FtsE (CYD985) or FtsEX (CYD986) (right column). (B) B2H between YisK and FtsX (CYD966---CYD973). All eight different tagged combinations are shown here.

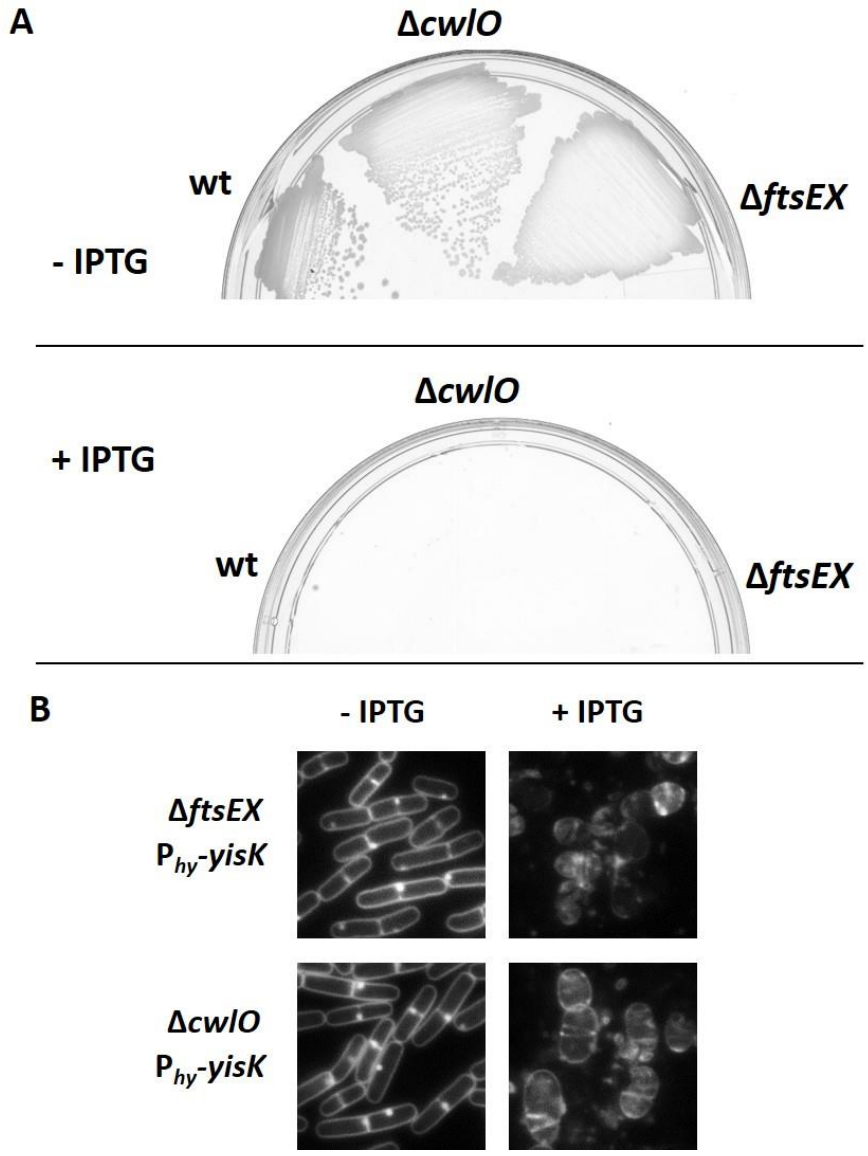

Fig. A5.3. FtsEX is not required for YisK activity. (A) BYD074 (2X P_{hy}-*yisK*), BYD476 (2X P_{hy}-*yisK*, Δ*ftsEX*) and BYD468 (2X P_{hy}-*yisK*, Δ*cwlO*) were streaked on an LB plate supplemented with 100 µg/ml spectinomycin and, when indicated, 1 mM IPTG. Plates were incubated at 37°C overnight before image capture. (B) BYD476 and BYD468 were grown in LB-Lennox media at 37°C to mid-exponential and back-diluted to an OD_{600} of ~0.02. When indicated, 1 mM IPTG was added. Cells were grown for 1.5 hrs at 37°C before image capture. Membranes were stained with TMA-DPH. All images are shown at the same magnification

YisK interacts with FtsE, but not FtsX, in a B2H assay

We have shown that FtsE and/or FtsX required for YisK-dependent cell shortening (Fig A5.1). To test if YisK might interact directly with FtsE and/or FtsX, we performed a bacterial two-hybrid (B2H) assay between YisK and FtsE, YisK and FtsX, and YisK and FtsEX.

As shown in Fig A5.2A, YisK could interact with both FtsE alone and FtsEX complex when FtsX was the tagged partner. However, no interaction between YisK and FtsX alone was detected, suggesting the interaction observed in the FtsEX complex is primarily mediated through FtsE (Fig A5.2B). Taken together, these results are consistent with they hypothesis that YisK targets FtsE activity in vivo to cause cell shortening.

FtsEX/CwlO is not required for YisK's cell widening activity

We have shown that FtsEX is required for the YisK-dependent cell shortening phenotype (Fig A5.1) and that YisK can interact directly with FtsE in a B2H assay (Fig A5.2). To test if the cell-widening and cell killing phenotypes previously observed following YisK misexpression (Appendix I, Fig A1.1)(256) also required FtsE and/or FtsX, we repeated the misexpression experiments in an Δ*ftsEX* mutant. YisK misexpression in Δ*ftsEX* mutant still prevented colony formation on plates (Fig A5.3A), similar to a wildtype background. Using epifluorescence microscopy, we also observed that YisK misexpression still resulted in the production of irregularly shaped cells (Fig A5.3B). Moreover, the Δ*ftsEX* strain appeared sensitized to the presence of YisK, as cells were more round and lysed more readily. Cells lacking CwlO, which acts in the

same genetic pathway as FtsEX (326, 377), appeared similarly to Δ*ftsEX* mutant (Fig A5.3). Taken together, these results suggest that YisK possesses two distinct activities: cell shortening mediated through FtsEX and CwlO and cell widening, which depends on the presence of Mbl.

The FtsEX complex retains some activity following YisK misexpression

It has been shown that the simultaneous inactivation of FtsEX and LytE or CwlO and LytE is synthetically lethal (326, 377). These results suggest that these proteins carry out a redundant function in the cell that is essential. Our data suggest that YisK targets FtsEX (Fig A5.1, Fig A5.2), so we hypothesized that misexpression of YisK in Δ*lytE* mutant would also result in a synthetically lethal phenotype. To test this hypothesis, we transformed genomic DNA from a Δ*ftsEX::tet* strain into a Δ*lytE* mutant. Consistent with the prior observations, we were unable to obtain viable Δ*lytE* Δ*ftsEX* transformants (Fig A5.4A). We then transformed the *ftsEX::tet* genomic into several strains harboring the YisK misexpression construct. Since misexpression of YisK in wild-type background leads to cell death (Appendix I, Fig A1.1), the strain backgrounds included allelic replacements of wildtype *mbl* with mutants encoding either the Mbl_{R63C} or Mbl_{D153N} variants (which are resistant to YisK-dependent killing)(Appendix I, Table A1.6)(256). Surprisingly, in each of these backgrounds, the Δ*lytE* strains could still grow on plates, even with multiple copies of P_{hy}-*yisK* (Fig A5.4B). To test if the non-killing phenotype we observed could be attributed to the *mbl* mutations themselves, we attempted to introduce the *ftsEX::tet* into a Δ*lytE* strain harboring either Mbl_{R63C} or Mbl_{D153N}; and no viable transformants could be obtained (Fig A5.4A). Taken together,

these results suggest that YisK either incompletely inactivates FtsEX function, or that YisK targets an FtsEX function that is not redundant with LytE.

Discussion

Our previous results showed that misexpression of YisK produced irregular shaped cells and this phenotype depends on Mbl (Appendix I, Fig A1.1, Fig A1.12)(256). In addition, we observed that YisK misexpression also led to cell shortening (Fig A1.13)(256). Since FtsEX and CwlO depend at least in part on Mbl for function (297) and the Δ*ftsEX* and Δ*cwlO* mutants are shorter than wildtype (326, 377), we hypothesized that YisK might be inhibiting the FtsEX/CwlO protein complex to cause cell shortening. Consistent with this hypothesis, we observed that YisK can no longer shorten cells in the absence of FtsEX (Fig A5.1). As we also observe that YisK and FtsE interact in a B2H assay (Fig A5.2), we hypothesize that YisK causes cell shortening by targeting and perturbing FtsE function.

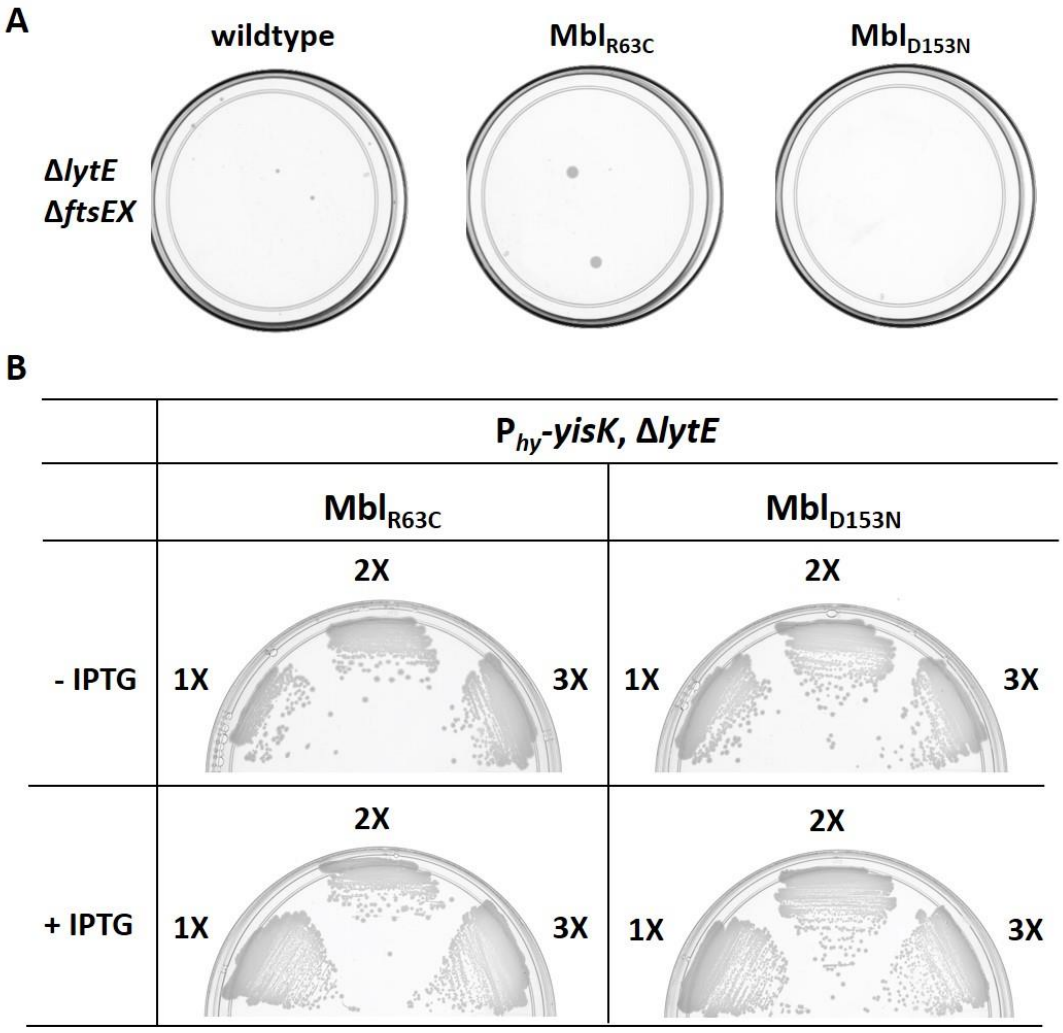

Fig. A5.4. YisK misexpression does not inhibit growth of a Δ*lytE* mutant. (A) Genomic DNA from BAS319 (*ftsEX::tet*) was used to transform BJH407 (Δ*lytE*), BJH408 (Δ*lytE*, Mbl_{D153N}) or BJH413 (Δ*lytE*, Mbl_{R63C}). Cells were plated on LB-Lennox agar plates supplemented with 10 µg/ml tetracycline and incubated at 37°C overnight before image capture. (B) BJH417 (1X P_{hy}-*yisK*, Mbl_{R63C}, Δ*lytE*), BJH415 (2X P_{hy}-*yisK*, Mbl_{R63C}, Δ*lytE*), BJH416 (3X P_{hy}-*yisK*, Mbl_{R63C}, Δ*lytE*), BJH410 (1X P_{hy}-*yisK*, Mbl_{D153N}, Δ*lytE*), BJH412 (2X P_{hy}-*yisK*, Mbl_{D153N}, Δ*lytE*) and BJH418 (3X P_{hy}-*yisK*, Mbl_{D153N}, Δ*lytE*) were streaked on LB plates supplemented with 100 µg/ml spectinomycin and, when indicated, 1 mM IPTG. Plates were incubated at 37°C overnight before image capture.

In order for bacterial cells to elongate, both PG hydrolysis and PG synthesis are essential (332, 370, 371). We have shown that YisK is mainly expressed during stationary phase and early sporulation (Appendix I, Fig A1.4 – A1.6)(256), at a time when cell growth is downregulated. Since cell elongation is expensive, we raised up an idea that as an inhibitor of cell elongation, YisK targets and prevents both PG hydrolysis and PG synthesis, in order to surely turn off cell elongation. We do not observed an obvious difference in cell length during either stationary phase or sporulation (data not shown and Appendix I)(256), therefore we propose that YisK's physiological role is not to regulate cell length. Instead, YisK may perform a more subtle function, such as fine-tuning the activities of proteins important for PG synthesis, such as Mbl, FtsEX, and CwlO.

Two sets of data suggest that YisK has the capacity to affect cell length and cell width independently. First, Mbl is not required for YisK-mediated cell shortening (Appendix I, Fig A1.13)(256). Second, neither FtsEX nor CwlO are required for YisK to disrupt cell shape (Fig A5.3).

Garti-Levi et al. showed that *ftsEX* mutants are slightly delayed for entry into sporulation (380), a result that was confirmed by others (326). Garti-Levi et. al. also showed that after overnight growth, an *ftsE* mutant produces round cells and less ovoid spores (380). We also observed this phenotype in strains deleted for *mreB* (256) as well as those expressing artificially high levels of YisK during sporulation (Fig A3.1 and Fig A3.2, Appendix III). These results suggest that during sporulation, YisK, FtsEX, CwlO, and MreB may act in a common pathway to regulate processes that effect cell width and spore morphology, and provide an avenue for future investigation.

Simultaneous inactivation of *lytE* and *ftsEX* or lytE and *cwlO* is synthetically lethal in *B. subtilis* (326, 377). Surprisingly, although our data suggest that YisK

inactivates the aspect of FtsEX function responsible for preventing cell shortening, misexpression of YisK in Δ*lytE* mutant backgrounds resistant to YisK's cell-widening function are not synthetically lethal (Fig A5.4), even when YisK is expressed at higher levels. The simplest explanation for this result is that YisK does not inactivate all functions of FtsE, only those related to cell length control. FtsE mutants that cannot bind or hydrolyze ATP are also synthetically lethal in a Δ*lytE* mutant background (326). Therefore, we think it is unlikely that YisK Affects FtsE's ATP binding and/or hydrolysis activities. Although we cannot exclude the possibility that YisK is simply a poor inhibitor of this activity, the lack of an intermediate phenotype (for instance, poor growth) following YisK misexpression in a Δ*lytE* argues against this possibility. It is also possible that YisK effects FtsE-FtsX interaction by targeting FtsE and causing some conformational changes, so that FtsE can still bind to FtsX but not as tight as before, thus YisK does not completely abolish the FtsEX/CwlO complex's function, but make it inefficient. We do not exclude any other possible mechanisms that YisK might affect FtsEX/CwlO protein complex.